Investigating aberrant cell separation in *sloughy*, an *Arabidopsis thaliana* mutant allelic to *SCHIZORIZA*

A THESIS

SUBMITTED IN PARTIAL FULFILFMENT

OF THE REQUIREMENTS FOR THE DEGREE

OF

Master of Science

in Biotechnology

at the

University of Canterbury

New Zealand

Ronan Charles Broad

2014

Contents

List of Figures

List of Tables

Acknowledgments

I would like to express my sincere gratitude to my senior supervisor, David Collings. Dave's generosity of time and commitment to his students goes far beyond the call of duty and his time and dedication to this project has been very much appreciated. Dave has always encouraged me to think creatively and critically, and has allowed me the freedom to pursuit many different lines of scientific enquiry and techniques under his supervision. I have also been fortunate to learn from Dave's expertise in writing, improving my ability to communicate ideas, including (hopefully) those presented in this thesis.

I would also like to express my sincere gratitude to my associate supervisor, Arvind Varsani. Arvind's extensive knowledge of molecular biology was crucial to the timely success of this project. His philosophy towards science and education has been enlightening, and is to be admired. Furthermore, during the course of my Masters, Arvind provided the opportunity for me to undertake research in the field of virology, broadening my skills and interests as a scientist. For that, I am very grateful.

I would like to thank the Virus group, namely Daisy Stainton, Simona Kraberger, Anisha Dayaram, Laurel Julian and Katherine van Bysterveldt for their support and guidance in molecular techniques, to Anish Malde and Kata Farkas for their advice on gene expression analysis, to Patrick Collins for the hands on guide to crossing arabidopsis, to Manfred Ingerfield for microscopy technical assistance, Matt Walters for

photography and Adobe programming support, and to Friedrich Schöffl for generously supplying the *SCHIZORIZA* over-expressing lines.

I would also like to thank the members of the Williamson group at the Australian National University who initiated the *rsw* mutant collection, and first isolated *sloughy*. These people include Professors Richard Williamson and Tobias Baskin, Drs Tony Arioli, Paul Howles, Leigh Gebbie and Andreas Betzner, and the technicians who worked with the group over many years including Rosemary Birch and Ann Cork.

A big shout out to all the students from the David Collings and Ashley Garrill lab groups, including Aliaa, Patrick, Sitara, Gonda, Steph, Alex and Wafi to name a few, for keeping me company in the lab and the Monday morning baking.

A big thanks to all my friends and family, especially my Mum for her constant support and life guidance, my outstanding flatmates at Waimairi for all the good times, and to my wonderfully intelligent girlfriend Sionainn Byrnes, who has made me far more rounded, multi-dimensional individual.

I dedicate this thesis to my Dad, Timothy Richard Maunsell Broad, who always supported me, and took great interest, in all of my endeavours. I am sure I have done him proud.

Abstract

Plant growth and development depends on controlled cell expansion. This, in itself, is determined by the plant cell wall, a structural matrix of polysaccharides encasing the plant cell. One line of investigation that has proven particularly successful in elucidating the components of the plant cell wall machinery has been the forward genetic screens of cell wall mutants. In this study, the molecular and cellular characterisation of *sloughy*, a cell separation mutant in *Arabidopsis thaliana*, was commenced. This mutant has a striking phenotype, with files of elongating epidermal cells snaking away from the adjacent epidermal cells and from the underlying cortex, loosing contact from the side walls while remaining attached at the cell ends, in a manner reminiscent of border-like cells in the root cap of arabidopsis. The *sloughy* mutation was fine mapped to a short region on chromosome I using high resolution melt point analysis. On sequencing all five genes in this region, a single nucleotide mutation, introducing a stop codon, was detected in exon 2 in the previously-described heat shock transcription factor *SCHIZORIZA* that results in a truncated protein missing several conserved domains essential for activity. SCHIZORIZA acts as a cell fate determinate in the root meristem to promote cortex fate, while suppressing epidermal and root cap fate in the mature ground tissue. Although the literature on *schizoriza* mutants has focused on the developing root meristem, with little documentation on the cell separation phenotype further up in the roots, the investigation of a collection of *schizoriza* TILLING mutants revealed that aberrant cell separation was ubiquitous to *schizoriza* mutants with a

severely truncated protein. To investigate cell identity in the mature roots, *sloughy* was crossed to GAL4-GFP enhancer trap lines that act as cell-specific markers. Epidermal identity lines revealed that *sloughy* possessed a supernumerary ground tissue layer with epidermal identity. A cortex and endodermal line revealed that these two identities are restricted to the endodermal layer and the next ground tissue layer out. There was no indication of root cap identity in the mature root with any of the root cap lines used, although partial lateral root cap identity has been previously described in the epidermal and subepidermal cell layers in the meristem of *schizoriza* mutants expressing *SOMBRERO*-GFP, a lateral root cap-specific transcription factor. Immunolabelling of cell wall epitopes revealed that the JIM13 antibody, which specifically labels arabinogalactan-proteins in wild-type root caps, often labelled the epidermal cells and surrounding mucilage further up the in the roots of *sloughy*. The aberrant cell separation present in *sloughy* is thought to be a consequence of epidermal cells possessing partial lateral root cap identity. The data on *sloughy*/*schizoriza* is sufficient to generate a model on how a meristem developmental gene can generate a cell separation phenotype in the mature roots. Loss of SCHIZORIZA causes confused cell identity in the root meristem that results in an epidermal and subepidermal layer possessing mixed epidermal and lateral root cap identity. The distinctive properties of border-like cells in the root cap of arabidopsis have been linked to unique cell wall maturation and developmental processes, implicating the cellulases CEL3 and CEL5, the pectin glycosyltransferase QUA1, the pectin methyltransferase QUA2 and other pectolytic enzymes. The ectopic expression of these cell wall enzymes in the epidermal and subepidermal layers of *sloughy* roots result in reduced adhesion along the sides of the cell, while the ends remain attached, causing the observed cell separation phenotype.

Abbreviations

ABRC	Arabidopsis Biological Resource Centre
ANOVA	Analysis of variance
bp	Base pairs
CAPS	Cleaved amplified polymorphic sequence
cDNA	Complementary DNA
CFP	Cyan fluorescent protein
Co	Cortex
Col	Columbia, an ecotype of *Arabidopsis thaliana*
Cy5	Cyanine5
dCAPS	Derived cleaved amplified polymorphic sequence
EDTA	Ethylenediaminetetraacetic acid
EMS	Ethyl methanesulfonate
En	Endodermis
Epi	Epidermis
FITC	Fluorescein isothiocyanate
Gb	Gigabase pairs (1,000,000,000 bp)
GFP	Green fluorescent protein
HRM	High resolution melt point
kb	Kilobase pairs (1,000 bp)
Lrc	Lateral root cap

L*er*	Landsberg *erecta*, an ecotype of *Arabidopsis thaliana*
NASC	Nottingham Arabidopsis Stock Centre
Mb	Megabase pairs (1,000,000 bp)
PBS	Phosphate buffered saline
PCR	Polymerase chain reaction
PME	PIPES, $MgSO_4$ and EGTA fixation solution
qPCR	Quantitative PCR
RFLP	Restriction fragment length polymorphisms
RFP	Red fluorescent protein
***SCZ*-OE**	*SCHIZORIZA* over-expressing
SEM	Standard error of the mean
slg	*sloughy*
SNP	Single nucleotide polymorphism
T-DNA	Transfer DNA
TAIR	The Arabidopsis Information Resource
TE	Tris and EDTA
TILLING	Targeting Induced Local Lesions IN Genomes
***T*m**	Melting temperature
v/v	volume/volume
w/v	weight/volume
WT	Wild-type
YFP	Yellow fluorescent protein

Arabidopsis thaliana Gene Abbreviations

ACT	*ACTIN*
AGO	*ARGONAUTE*
ANL	*ANTHOCYANINLESS*
ARAD	*ARABINAN DEFICIENT*
AtHsfB4	*Arabidopsis thaliana Heat shock factor B4*
BRN	*BEARSKIN*
CEL	*CELLULASE*
CesA	*CELLULOSE SYNTHASE A*
CRE	*CYTOKININ RESPONSE*
CSI	*CELLULOSE SYNTHASE INTERACTIVE*
CSL	*CELLULOSE-SYNTHASE-LIKE*
DRP	*DYNAMIN-RELATED PROTEIN*
EPC	*ECTOPICALLY PARTING CELLS*
GAUT	*GALACTURONOSYLTRANSFERASE*
IRX	*IRREGULAR XYLEM*
JKD	*JACKDAW*
KOR	*KORRIGAN*
MGP	*MAGPIE*
MUR	*MURUS*

PLT	*PLETHORA*
POM	*POM-POM*
PME	*PECTINMETHYLESTERASE*
QUA	*QUASIMODO*
RSW	*RADIALLY SWOLLEN*
SCR	*SCARECROW*
SCZ	*SCHIZORIZA*
SHBY	*SHRUBBY*
SHR	*SHORTROOT*
SMB	*SOMBRERO*
TRN	*TORNADO*
WER	*WEREWOLF*
WOL	*WOODENLEG*

The arabidopsis nomenclature for genes identified by mutation follows.

- Mutant gene symbols should have three letters written in italics in lower case letters (e.g. *abc*).
- The wild-type allele should be written in italics in capital letters (e.g. *ABC*).
- Wild-type protein products of genes should be written in capital letters without italics (e.g. ABC), whereas the mutated protein should be written in lowercase letters without italics (e.g. abc).
- Different genes with the same symbol are distinguished by different numbers (e.g. *abc1* and *abc2*).
- Different alleles of the same gene are distinguished with a number following a hyphen (e.g. *abc3-1* and *abc3-2*).

Chapter 1

General Introduction

"What a marvellous cooperative arrangement - plants and animals each inhaling each other's exhalations, a kind of planet-wide mutual mouth-to-stoma resuscitation, the entire elegant cycle powered by a star 150 million kilometres away."

- Carl Sagan (Cosmos: A Personal Voyage, 1980)

1.1 Overview

Plant growth and development depends on controlled cell expansion. This, in itself, is determined by the plant cell wall, a structural matrix of polysaccharides encasing the plant cell. In the root meristem of plants, cells typically have similar dimensions in all directions. However, upon leaving the meristem, and undergoing cell expansion, the length of the cells may increase ten-fold without any change in width. This phenomena of anisotropic growth (growth rates that are not equal in all directions) is based on the unique biochemical properties of the plant cell wall and its ability to form a rigid, crystalline structure capable of high tensile strength, while maintaining the flexibility and elasticity required to harness turgor pressure in order to drive cell expansion.

Due to this, emphasis has generally been placed on understanding how the cell wall allows for anisotropic cell expansion to occur and, in particular, the biochemical properties of the elongating side cell walls. By comparison, little emphasis has been placed on the end walls where expansion does not occur. Although transverse cellulose deposition is known to prevent an elongating cell expanding in a radial direction, it is not yet known what prevents the end wall from expanding. Clearly, cell wall modifications must be highly specific, with fundamental structural, biochemical and enzymatic variations between the walls. Investigating how these cell wall ends prevent expansion may also help us to further understand how plants control the elongation of cells in general. One line of investigation that has proven particularly successful in elucidating the components of the plant cell wall machinery has been the forward genetic screens of cell wall mutants in *Arabidopsis thaliana*, a plant that is hereafter referred to by its now common name arabidopsis.

A novel, cell separation mutant in arabidopsis, provisionally referred to as *sloughy*, was isolated by the Williamson group at the Australian National University in the early 1990s during a temperature-sensitive screen for *radial swelling* mutants (*rsw*) (Baskin *et al*., 1992). This mutant possesses a striking phenotype, with files of elongating epidermal cells snaking away from the root surface, separating from adjacent epidermal cells and from the underlying cortex (Figure 1.1). The epidermal cells detach along the sides of the cell wall, while remaining attached at the cell ends. This is indicative of a biochemical difference between the cell walls and reminiscent of border-like cells which detach from the root cap of arabidopsis (Vicré *et al*., 2005).

A previous attempt to map the mutation to a gene conducted about 10 years ago did not yield success. Using a new fine mapping approach that utilizes the molecular technique of high resolution melt point analysis of DNA, this study aims to elucidate the mutated gene(s) responsible for the observed cell separation phenotype. In addition to the molecular characterization of *sloughy*, in-depth phenotypic and biochemical characterization will be undertaken.

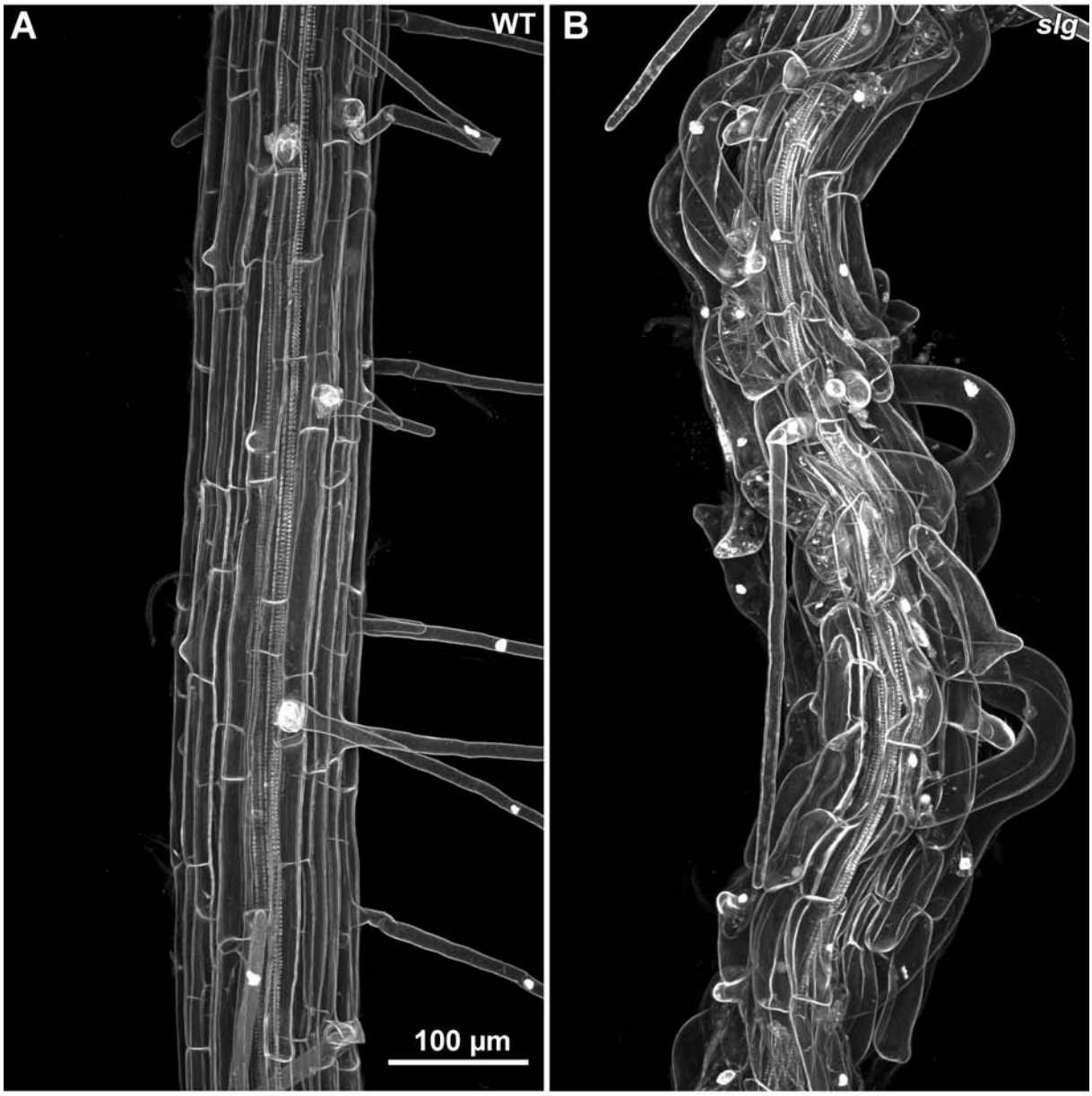

Figure 1.1 The classical *sloughy* cell separation phenotype. Confocal maximum projections of roots stained with propidium iodide. Bar in **A** = 100 µm.

A Wild-type (WT).

B *sloughy* (*slg*).

1.2 The plant cell wall

1.2.1 Biological and economical importance of the plant cell wall

The mechanically-strong cell wall is the extracellular structure of plant cells, and a defining feature distinguishing them from animal cells. The cell wall is not only critical for plant function, but is also of tremendous importance to a human economies.

The cell wall performs a myriad of essential functions for plant growth and development (Taiz and Zeiger, 2002, Roberts and Gonzalez-Carranza, 2007, Liepman *et al*., 2010, Keegstra, 2010):

- The cell wall is responsible for providing the mechanical strength to all plant cells, and holds the plant up against the force of gravity allowing many plants to grow to great heights.
- The cell wall acts as a barrier outside the plasma membrane. This allows the development and maintenance of high turgor pressure. As turgor pressure drives cell expansion, the cell wall contributes to determining cell shape, growth anisotropy, and overall plant morphogenesis.
- The cell wall acts an adhesive responsible for the attachment of plant cells to one another thereby keeping them in place. The cell wall, and the pores called plasmodesmata that penetrate through it, regulate intercellular communication between cells.
- The cell wall provides a major structural barrier essential for plant protection, and as such plays an essential role in plant-microbe and plant-pathogen interactions.

- The cell wall acts as a constraint to prevent the excessive uptake of water, and helps to the control of water balance throughout the plant.

The cell wall is also responsible for many other functions at the cellular and whole plant level. The desire to understand these fundamental functions in plant growth and development, as well as considerable economic implications, explains the extensive research in cell wall structure and biosynthesis.

In addition to its essential biological functions, the plant cell wall is also of considerable importance for human economies. Some of the products derived from the plant cell wall include natural fibres and textiles, charcoal, paper and wood products, fuels and medicines. The plant cell wall also provides the textural properties of fruits and vegetables, and plays a significant role in human health and nutrition as an important source of dietary fibre (McCann and Rose, 2010). Plant cell walls can also be modified to produce a huge range of synthetic products such as plastics, synthetic fibres, films, coatings, adhesives, gels and thickeners (Taiz and Zeiger, 2002). More recently, the plant cell wall has been an important source of renewable energy, through the fermentation of cell wall sugars into ethanol, butanol and other advanced biofuels (Keegstra, 2010, McCann and Rose, 2010). As humanity moves into the 21st century, it faces the global challenges of energy and food security. As a response to this, enhanced research into the plant cell wall for its nutritional content and quality for human consumption, as well as an important source of renewable energy, is critical (McCann and Rose, 2010). Such research should be applied to the engineering of plants for improved yield and quality, assisting in the provision of an abundant source of food, fibre, and energy for future generations.

1.2.2 Plant cell wall architecture and composition

Consistent with the diverse functions of the plant cell wall, the architecture and composition of the plant cell wall is also complex. Plant cell walls originate *de novo* during the final stages of cell division and are modified during plant growth and development. Cell walls may consist of up to three layers:

i) The middle lamella.

ii) The primary cell wall.

iii) The secondary cell wall.

The middle lamella is the first layer of the cell wall to be formed. The cell plate, formed during cytokinesis, develops into the middle lamella and thus represents the interface between cells. The middle lamella is a thin, adhesive layer sticking adjacent cells together. While the cell is still growing, the primary cell wall forms. The primary cell wall is generally a thin, extensible layer and once formed provides the main force bearing load for the plant cell. The middle lamella and the primary cell wall are present in all plant cells. After cell growth and expansion, some plant cell types may go on to develop a secondary cell wall, which is a thick, rigid layer. The secondary cell wall is formed between the plasma membrane and the primary cell wall. Since the epidermal and cortical cells in arabidopsis roots do not form secondary cell walls, emphasis will be placed on the middle lamella and the primary cell wall during the remainder of this introduction.

Although the precise biochemical composition of the primary plant cell wall varies considerably between different species, and even between different cell and tissue types within the same plant, the basic architectural properties of the plant cell wall are similar (Albersheim *et al*., 2010). Primary plant cell walls are composed of a mixture of interacting

polysaccharides, proteins, and enzymes. The structural polysaccharides themselves are categorized into three main classes (Zablackis *et al*., 1995, Liepman *et al*., 2010):

i) Cellulose

ii) Hemicellulose

iii) Pectin

The major polysaccharide component of the primary plant cell wall is cellulose, the discovery of which dates back to 1838 (Payen, 1838). Cellulose is ubiquitous and fundamental to all plant life and often contributes to roughly a third of the total mass of many plants: it is probably the most abundant biopolymer on Earth (Saxena and Brown, 2005, Somerville, 2006).

Cellulose consists of a simple linear chain of β(1-4)-linked D-glucan units (glucose molecules, the D refers to the chirality of the molecule). These chains range from 500 to 14,000 subunits and thus can be many micrometers in length, long enough to wrap around the circumference of a cell may times (Cosgrove, 2005, Somerville, 2006). These unbranched linear chains spontaneously interact with each other via hydrogen bonds in parallel arrangements to generate stiff, semi-crystalline, cable-like structures called cellulose microfibrils that have a high tensile strength, equivalent to that of steel (Taiz and Zeiger, 2002, Somerville, 2006). In the extracellular space, cellulose microfibrils are embedded in a highly-hydrated matrix of polysaccharides and proteins, and act as a scaffold that provides the main loading-bearing force of the cell well. The structure of the cell wall with cellulose embedded in a matrix has been likened to the design of steel-reinforced concrete or fibreglass (Carpita and Gibeaut, 1993).

Cellulose microfibrils are synthesized at the plasma membrane by cellulose synthase complexes. These structures, which are hexameric when viewed by electron microscopy and thus referred to as rosettes, contain 6 subunits each composed of 6 modules (Arioli *et al*., 1998, Kimura *et al*., 1999). Cellulose synthase subunits are encoded by the *Cellulose synthase A* (*CesA*) gene family. In arabidopsis, this protein family has 10 members that are differentially expressed in different tissues and cell types (Pear *et al*., 1996, Arioli *et al*., 1998, Doblin *et al*., 2002). The cellulose synthase rosette complexes secrete the long β(1-4)-linked D-glucan chains outside of the plasma membrane that crystallize into microfibrils (Doblin *et al*., 2002).

The deposition and orientation of the cellulose microfibrils is controlled by the orientation of microtubules that underlie the plasma membrane, which guide the membrane-localised cellulose synthase complexes as they synthesize the microfibrils into the extracellular space (Paredez *et al*., 2006). The implications for non-randomly orientated cellulose microfibrils on cell expansion are discussed below (section 1.2.3).

The second major group of cell wall polysaccharides are the hemicelluloses. Hemicellulosic polysaccharides are typically characterized by possessing β(1-4)-linked sugars with an equatorial configuration and the ability to hydrogen bond to cellulose (Scheller and Ulvskov, 2010, Albersheim *et al*., 2010). The primary cell walls consist of xyloglucans, glucomannans and xylans, with xyloglucan typically representing the most abundant hemicellulosic polysaccharide (Carpita and Gibeaut, 1993, Scheller and Ulvskov, 2010). In contrast to cellulose chains, hemicellulose chains are significantly shorter and can be branched or kinked, preventing the formation of crystalline microfibrils (Scheller and Ulvskov, 2010). Hemicellulosic polysaccharides are flexible structures capable of binding to the surface of cellulose microfibrils, the primary function of which is to strengthen the plant cell wall by

cross linking cellulose microfibrils to form a three-dimensional load bearing structure (Scheller and Ulvskov, 2010).

Hemicelluloses are synthesized in the Golgi membranes by glycan synthases, processive enzymes (capable of catalyzing consecutive reactions without releasing its substrate) that are responsible for the biosynthesis of the backbone, and by glycosyltransferases, non-processive enzymes that are responsible for the addition of specific monosaccharides (Keegstra, 2010, Scheller and Ulvskov, 2010). After synthesis, the hemicelluloses are transported to the extracellular space via the exocytosis of Golgi vesicles. Many of the biosynthetic enzymes involved in hemicellulose biosynthesis have been identified in arabidopsis (Scheller and Ulvskov, 2010). For example, the cellulose-synthase-like (CSL) super-family, multimembrane-spanning proteins involved in the synthesis of xyloglucan, mannan, and glucans backbones (Cocuron *et al*., 2007, Scheller and Ulvskov, 2010). However, the synthesis of xylan backbones is much more ambiguous and has yet to be functional characterized (Scheller and Ulvskov, 2010).

The third major group of polysaccharides in the primary plant cell wall is the highly complex family of pectins. The pectic polysaccharide family can be characterized by possessing a high proportion of galacturonic acid (Albersheim *et al*., 2010), and include homogalacturonan, xylogalacturonan, apiogalacturonan, and rhamnogalacturonan I and II (Harholt *et al*., 2010). Homogalacturonan, a linear homopolymer composed of 100-200 galacturonic acid subunits, represents the largest contributing member of the pectin family (Thibault *et al*., 1993). Pectic polysaccharides themselves are very large and complex molecules and are composed of a diverse range of pectic polysaccharide domains that can be linked together by both covalent and non-covalent bonds.

Pectins are the predominant component of the middle lamella, are responsible for cellular adhesion between adjacent cells, and possess a range of structural and physiological roles in plant growth and development (Roberts and Gonzalez-Carranza, 2007). For example, pectins play essential roles in strengthening the cell wall once the cell matures, controlling morphology, the abscission of organs, and are essential to plant defence and disease resistance (Vorwerk *et al*., 2004, Mohnen, 2008). Pectins also have an important part to play in the primary cell wall by providing a hydrated matrix into which the cellulose-hemicellulose network is embedded. Consequently, this matrix helps to prevent the collapse of the cellulose-hemicellulose network.

Like hemicelluloses, pectic polysaccharides are synthesized in the Golgi apparatus, during which they are subject to extensive modifications that alter their conformation and linkage. Examples of such modifications include the glycosylation, methylation and acetylation of the pectic backbone. The modified pectins are subsequently transported to the extracellular space via the exocytosis of Golgi vesicles (Sterling *et al*., 2001). Due to the considerable diversity of monosaccharide units and glycosidic linkages that constitute their biochemical make up, a large number of enzymes must be required for its synthesis (Roberts and Gonzalez-Carranza, 2007, Liepman *et al*., 2010). It has been deduced that at least 67 different transferases, including glycosyl-, methyl- and acetyl-transferases, are required for the biosynthesis of pectic polysaccharides in arabidopsis (Mohnen, 2008). However, the enzymes responsible for such modifications have not been well characterized. As of 2010, only three of these enzymes had been unambiguously characterized (Harholt *et al*., 2010). These are GAUT1, a homogalacturonan galacturonosyltransferase (Sterling *et al*., 2006, Atmodjo *et al*., 2011), QUA1, a homogalacturonan glycosyltransferase (Bouton *et al*., 2002), and ARAD1, an arabinan arabinosyltransferase (Harholt *et al*., 2006, 2010). It is evident that a considerable

number of discoveries have yet to be made in the field of pectin synthesis, modifications and function.

Plant cell walls also contain many proteins, which perform both enzymatic and structural roles. The structural proteins can be divided into families based on the predominate amino acid present in the polypeptide backbones, or on their polysaccharide side chains (Roberts and Gonzalez-Carranza, 2007). The first family includes proteins in which the backbone is particularly rich in hydroxyproline (hydroxyproline-rich protein, also known as extensins), proline (proline-rich protein) or glycine (glycine-rich protein) (Roberts and Gonzalez-Carranza, 2007). The second main family includes proteins in which the protein backbone is heavily glycosylated with arabinose and galactose-containing polysaccharides (Roberts and Gonzalez-Carranza, 2007). These proteins are aptly termed arabinogalactan proteins. Extensins and arabinogalactan proteins represent the most abundant structural proteins in the plant cell wall.

The precise biological functions of these structural proteins remain unclear. They are, however, thought to provide mechanical strength via crosslinking of cell wall polymers, facilitate the assembly of cell wall components, and play a role in responses to wounding and pathogen attack (Taiz and Zeiger, 2002). Interestingly, arabinogalactan proteins have also been implicated in cell adhesion and a wide range of other physiological roles (Showalter, 2001). For example, the fascilin-like arabinogalactan proteins, which possess a conserved cell adhesion domain (fascilin) found in proteins across various kingdoms of life, are strong candidates to act as adhesive molecules between cells (Johnson *et al*., 2003, MacMillan *et al*., 2010). Arabinogalactan proteins are found in a range of tissues throughout the plant, including the cortical, epidermal, and root hair cells of the root, and are especially abundant in the roots tips and root exudates where they are thought to play an essential role in root-microbe interactions in the rhizosphere (Nguema-Ona *et al*., 2013).

In addition to proteins and glycoproteins, plant cell walls also contain a myriad of cell wall modifying enzymes such as hydrolases, esterases, galactosidases, xylosidases, glucanases, peroxidases, laccases, and transglycosylases (Albersheim *et al*., 2010). These enzymes are implicated in a range of key cell wall processes including the modification and cross-linking of cell wall polymers, the assembly of lignin, or in the defence of plants against pathogens (Albersheim *et al*., 2010).

1.2.3 Cell expansion is controlled by the plant cell wall

In addition to its crucial structural role, the plant cell wall plays an essential role in regulating cell growth and expansion. Thus, it is necessary for the plant cell wall to possess what would appear to be two contradictory characteristics: it needs to be a rigid, crystalline structure capable of high tensile strength but it also needs to possess the flexibility and elasticity required for cell expansion.

In plant cells, an influx of water flows into the vacuole by virtue of the vacuole maintaining a higher solute concentration than outside the cell. This influx of water into the vacuole results in turgor pressure exerted upon the cell wall. Turgor pressure helps to maintain the rigidity of the plant cell but it also drives cell expansion. Since turgor pressure creates an outward force that is equal in all directions, the directionality of growth is determined primarily by the elasticity of the plant cell wall (Steudle *et al*., 1977). In elongating cells, it is the orientation of cellulose microfibrils in the plant cell wall that harness turgor pressure to control the directionality of cell expansion.

In the root meristem of plants, cells are typically isodiametric, having similar dimensions in width, length and height. If the cellulose microfibrils were randomly orientated, the outward force exerted by turgor pressure would cause the cell to expand equally in all directions, described as isotropic growth. However, if the cellulose microfibrils were to be arranged non-

randomly and in the same orientation as is typically found in most plant cell walls, then the cells would elongate perpendicular to the orientation of the reinforced cellulose microfibrils. This is referred to as anisotropic growth. The orientation of cellulose microfibrils around the circumference of the cell are similar to the steel hoops on a wooden beer barrel or a water tower, with both the cellulose and the steel restricting expansion (Taiz and Zeiger, 2002).

The ability for a cell to undergo cell expansion is limited by the rate at which cell wall polymers can creep apart from one another, controlled by pH-sensitive cell wall loosening enzymes such as expansins (Cosgrove, 2005). It is thought that plasma membrane proton pumps in the plasma membrane acidify the cell wall, thereby activating expansins and other wall loosening agents which increase cell wall flexibility by disrupting the cross links between cellulose microfibrils and hemicelluloses, a process described as the acid growth hypothesis (McQueen-Mason and Cosgrove, 1995). By carefully disrupting this polymeric network, the cell can then expand perpendicular to the orientation of the cellulose microfibrils giving anisotropic growth. To prevent the cell wall from becoming too thin and weak, new polymers are simultaneously deposited into the cell wall during expansion (Cosgrove, 2005).

It is clear that the orientation of cellulose microfibrils is an important determinant of plant growth patterns and it is the cytoplasmic microtubules that control the patterns of deposition and orientation of cellulose microfibrils. Ehrhardt and colleagues (Paredez *et al*., 2006) visualized the process of cellulose deposition in living cells through co-expression of a functional YFP:CESA6 fusion protein along with RFP-tubulin. They demonstrated that the cellulose synthase complexes moved in linear tracks that were co-aligned to the cytoplasmic microtubules. Furthermore, the disruption of the microtubule network with the microtubule-depolymerizing drug oryzalin, or microtubule reorganisation caused by blue light, caused the movement of the cellulose synthase complexes to change. This indicated a direct relationship between the cytoskeleton and the guided deposition of cellulose microfibrils by cellulose

synthase. This relationship has since been corroborated with the identification of the CELLULOSE SYNTHASE INTERACTIVE PROTEIN 1 (POM2/CSI1) which is thought to provide a scaffold between cellulose synthase complexes to the underlying cortical microtubules responsible for guiding cellulose synthesis (Li *et al*., 2012, Bringmann *et al*., 2012).

Moreover, experiments in which the cytoskeletal organisation is disrupted with drugs or by genetic defects lead to disorganized wall structure and growth. For example, when growing roots are treated with microtubule disrupting drugs such as the depolymerizing agents colchicine and oryzalin, or the microtubule stabilizing taxol, the cells in the elongation zone expand laterally (Green, 1962, Baskin *et al*., 1994, Baskin and Bivens, 1995). Since the non-random orientation of the cellulose microfibrils itself is controlled by the orientation of the underlying microtubule cytoskeleton, the cytoskeleton fundamentally controls plant growth patterns.

Although there has been considerable research into how the cell walls permit anisotropic growth and the diffuse expansion of the side wall, how the end walls of the cells prevent expansion is less well understood. In part, this deficiency is due to difficulties in imaging the ends of cells. While the sides of cells can be readily observed by light microscopy, observation of cell ends require either sectioning or optical reconstruction. In stark contrast to the side walls, the arabidopsis end walls do not grow at all, likely due to fundamental structural or enzymatic variations between the specific walls. It should be expected that changes in the physical properties of end walls of cells may be reflected in different arrangements of the underlying cytoskeleton. Indeed, Collings and Wasteneys (Collings and Wasteneys, 2005) used reconstructions of confocal optical series to demonstrate that the microtubules underlying the end walls of epidermal cells were orientated in a radial direction relative to the transverse axis of the root in arabidopsis. This microtubule orientation had also

previously been demonstrated in transmitted election microscopy sections in *Azolla pinnata* (Busby and Gunning, 1983). These results agree with the hypothesis that microtubules align in perpendicular to the direction of cell expansion, but align in a parallel orientation to the direction in which cell expansion is blocked.

Since the *sloughy* mutant has an apparent biochemical difference in the side walls from the end walls in the root epidermal cells, this mutant may be able to provide insight into the variations between the side and end walls of elongating cells. It is hypothesized that the mutated gene responsible for the *sloughy* phenotype may play a structural, biochemical, or enzymatic role in cell adhesion unique to the side walls of cells. Therefore, identifying this gene may provide a valuable clue into the fundamental difference between the cell walls.

1.2.4 Plant cell separation

Cell adhesion via the pectin-rich middle lamella is fundamental for plant growth and development. Despite the fact that consistent cell adhesion is essential for the overall mechanical strength of the plant, cell adhesion can also be highly dynamic, changing to enable the plant's growth and development (Roberts and Gonzalez-Carranza, 2007). For example, cell separation is an integral factor in developmental processes including radical emergence during germination (Sitrit *et al*., 1999), lateral roots emergence and penetration through the cortical and epidermal layers (Peretto *et al*., 1992), stoma and intercellular space formation (Stevens and Martin, 1978, Chalain and Berjak, 1979), and perhaps the two most well known examples, abscission of organs and the ripening of fleshy fruit (Rose, 2003).

The developmental modifications of cell adhesion are associated with the expression of a broad host of enzymes that modify and solubilise the components of the plant cell wall. These include the pectolytic enzymes, a family of enzymes responsible for modifying pectins, which include pectin methyl esterases, pectin lyases, pectate lyases and polygalacturonases

(Roberts and Gonzalez-Carranza, 2007). In addition to all of the pectolytic enzymes, there are a wide range of enzymes that modify other components of the cell wall such as cellulases (glucanases), galactosidases, xylosidases, and arabionofuranosidases, amongst others (Roberts and Gonzalez-Carranza, 2007).

Since the epidermal cells in the *sloughy* mutant appear to visually possess similar morphological characteristics to that of lateral root cap cells (i.e. the epidermal cells slough), the following discussion will highlight some of the insights made into the cell adhesion and separation processes during the development and function of the plant root cap.

The root caps of many plant species release large numbers of cells known as border cells that completely dissociate from the root tissue and from each other. Border cells can be identified as cells that are released into solution within seconds of root tips being placed in water (Hawes and Lin, 1990, Driouich *et al*., 2007). Border cells represent populations of individually detached, metabolically active cells and were redefined from the classical term of 'sloughed dead root cap cells' to reflect their unique morphology and patterns of gene expression (Hawes and Lin, 1990, Roberts and Gonzalez-Carranza, 2007).

Legumes have been used as a model to study border cell separation. Both the activity and expression of a range pectolytic enzymes from the root cap tissue correlate with the process of border cell separation (Hawes and Lin, 1990, Stephenson and Hawes, Wen *et al*., 1999 1994, Wen *et al*., 2008). The hydrolysis of polygalacturonic acid, for example, is detectable before the border cells dissociate, thereby implicating a polygalacturonase enzyme in border cell separation (Hawes and Lin, 1990). The role that pectin methyl esterases contribute to border cell separation has been studied in detail. Pectin methyl esterase levels and activity are strongly correlated with border cell separation (Stephenson and Hawes, 1994). Furthermore, the expression of *rcpme1*, a root cap-specific pectin methylesterase gene, is specifically

correlated with border cell separation, while in roots expressing *rcpme1* antisense mRNA border cell separation is prevented. Instead the border cells accumulate in a ball at the root cap periphery that does not separate from the root when immersed in water (Wen *et al*., 1999).

In arabidopsis and other members of the Brassicaceae family, individual border cells are not produced. Instead, files of cell attached end-on-end are released. Since the cells do not fit the strict definition of border cells, they have been termed border-like cells (Vicré *et al*., 2005). In contrast to border cells which release from root tissue and from each other individually, border-like cells disassociate along the sides of the cell walls but remain attached at the cell ends, thereby detaching in multiple files of root cap cells.

Large amounts of arabinogalactan proteins and homogalacturonan are present in the cell walls of border-like cells, two classes of cell wall molecules that are implicated in cell adhesion (Johnson *et al*., 2003, Vicré *et al*., 2005). Thus, homogalacturonan and arabinogalactan proteins may be critical for border-like cell function and separation, although the exact function that these proteins play is not understood. To investigate the adhesive properties of border-like cells, Driouich and colleagues (Durand *et al*., 2009) investigated mutants defective in the biosynthesis of cellulose, xyloglucan, and pectin to see whether any of them had any impact on the release of border-like cells. Of all the mutants investigated, only the pectin mutants *quasimodo1* (*qua1)* and *qua2*, both characterized by producing less homogalacturonan, had altered border-like cell phenotypes compared to wild-type with the border-like cells released as isolated cells. This phenotype was more pronounced in *qua1* than in *qua2*. *QUA1* encodes a pectin glycosyltransferase (Bouton *et al*., 2002, Orfila *et al*., 2005), while *QUA2* is encodes a pectin methyltransferase (Mouille *et al*., 2007). These mutants provided valuable insight into the unique cell wall biochemistry of border-like cells,

indicating that homogalacturonan is an essential component for cell adhesion at the cell ends. The *qua* mutants are discussed in greater detail in section 1.3.3.4.

It is clear that alterations in pectin levels impact root cap cell separation. In addition to pectin enzymes, however, glucanases have also been implicated in border-like cell separation in arabidopsis. The endo-1,4-β-D-glucanases CELLULASE3 (CEL3) and CEL5 that hydrolyse cellulose have been proposed to function in the sloughing of the arabidopsis root cap (del Campillo *et al*., 2004). CEL5 was shown to be exclusively expressed in the root cap and a *cel5* T-DNA mutant had an increased retention of the root cap compared to wild-type, thereby making sloughing less efficient (del Campillo *et al*., 2004), but lacked any other distinct phenotypic differences. The modest effect of abolishing *CEL5* suggested there may be multiple, redundant genes regulating the process of sloughing of the root cap. Indeed, *CEL3*, a paralog of *CEL5*, was identified in the genome of arabidopsis. Accordingly, these two glucanases may play a significant role in the sloughing of border-like cells from the root tip.

In addition to understanding the role of which developmental changes in cell adhesion play in plant function, growth, and development, manipulating the cell separation and adhesion properties of plants may be of significant worth to agricultural and horticultural industries (Roberts and Gonzalez-Carranza, 2007). Further understanding the phenomena of plant cell adhesion and separation clearly represents an important line of scientific enquiry.

1.2.5 Elucidating the genetics of the plant cell wall machinery

Despite significant progress having been made in the identification of cell wall components and their functions, significant gaps in our knowledge remain. The function of most of the proteins involved in the biosynthesis and metabolism of the plant cell wall are still relatively unknown (Liepman *et al*., 2010). An estimated 2000 genes, a staggering 10% of the total

genes in a plant genome, may be required for the task (Keegstra, 2010, McCann and Rose, 2010). The enzymes responsible for the biosynthesis and metabolism of the plant cell wall are typically members of large multi-gene families. For example, there are over 400 genes for glycosyltransferases in the arabidopsis genome (Scheible and Pauly, 2004, Cosgrove, 2005). A significant challenge for the future will be to characterize the individual function of each of these genes.

Progress made into elucidating the genetics of cell wall machinery has largely been due to the use of forward and reverse genetics. In particular, the investigation of cell wall mutants has been successful in the functional characterization of genes critical for cell wall synthesis. These genetic approaches have since been coupled with genomic tools to great effect. The availability of the arabidopsis genome has proven invaluable in assisting the identification of the candidate genes of the cell wall machinery (Arabidopsis Genome Initiative, 2000, Liepman *et al*., 2010). In addition to the genome of arabidopsis, a significant range of economically important species to forestry, horticulture, and agriculture have since had their genomes sequenced, including rice (Goff *et al*., 2002), maize (Schnable *et al*., 2009), potato (Xu *et al*., 2011), tomato (Sato *et al*., 2012), poplar (Tuskan *et al*., 2006) and loblolly pine (Zimin *et al*., 2014). This has allowed for a greater understanding of the plant cell wall machinery, and how it may be engineered to greater effect throughout the plant kingdom.

1.3 Forward genetic screens to isolate *Arabidopsis thaliana* cell wall mutants

1.3.1 *Arabidopsis thaliana*: the model plant

Arabidopsis is a small flowering plant from the Brassicaceae family, and although it is not of any agronomic importance, arabidopsis represents a popular model organism in plant biology and genetics. It is the equivalent of the lab rat for plant biologists.

Arabidopsis was chosen as a model organism more than 30 years ago because of its rapid life cycle (about 6 weeks), small size (20 - 25 cm in height), its ability to self-fertilise, and prolific seed production (up to 10,000 seeds per plant). These attributes facilitate the cultivation and rapid cycling of generations within a limited amount of space. These fundamental growth habits made arabidopsis an early favourite in mutant screens, contributing to its emergence as a model organism (Koornneef and Meinke, 2010). Although these characteristics still contribute to the popular choice of arabidopsis as a model organism, additional, unforeseen benefits have allowed arabidopsis to remain a model organism (Koornneef and Meinke, 2010). Arabidopsis has a remarkably small genome size of only 125 Mb and 5 chromosomes (Arabidopsis Genome Initiative, 2000). In comparison, the rice genome has a size of 420 Mb and 12 chromosomes (Goff *et al*., 2002), the maize genome a size of 2.3 Gb and 10 chromosomes (Schnable *et al*., 2009), and the human genome a size of 3.2 Gb and 23 chromosomes (Venter *et al*., 2001). Arabidopsis was the first plant to have its genome sequenced and the complete genome sequence is currently maintained by The Arabidopsis Information Resource (TAIR) (Arabidopsis Genome Initiative, 2000, Rhee *et al*.,

2003). One aspect of the small genome size makes arabidopsis particularly useful for mapping and sequencing (Page and Grossniklaus, 2002). An impressive catalogue of sequence polymorphisms and molecular markers are now also openly available, which can be easily exploited for fine mapping using technically simple laboratory methods (Lukowitz *et al*., 2000, Clark *et al*., 2007). As a result, it is now possible to complete mapping projects within a short period of time with relatively little physical effort (Lukowitz *et al*., 2000).

Another major advantage for the use of arabidopsis is that it is readily transformed via *Agrobacterium tumefaciens*. The floral-dip method involves dipping the flowers of arabidopsis into a suspension of *Agrobacterium*, sucrose, and a surfactant. This highly efficient method of transformation avoids the use of any plant tissue culture or regeneration, facilitating genetic modification and the generation of a large number of transformants (Clough and Bent, 1998).

A third major advantage for arabidopsis is that seedlings, and in particular the roots, are relatively translucent, which along with their small size makes them ideal for live cell imaging using light and confocal microscopy (Pawley, 2010). As such, arabidopsis is as an effective model for plant development, including the cellular organisation of the developing root (Dolan *et al*., 1993). The use of cell or tissue specific fluorescent markers, allowing the developmental stage of every cell to be inferred, has subsequently lead to a detailed developmental map of arabidopsis (Haseloff, 1999).

A further advantage is that a large collection of T-DNA insertion lines are now readily available from the online database (TAIR) that contains over 300,000 independent transgenic lines. Indeed, insertion mutants are now available for most arabidopsis genes (Alonso *et al*., 2003). The Nottingham Arabidopsis Stock Centre (NASC) and the Arabidopsis Biological Resource Centre in Ohio (ABRC) provide a large catalogue of arabidopsis lines, including

mutants, that can be readily obtained by researchers worldwide. Also available are over 750 natural accessions of arabidopsis, genetically distinct geographic variants within the species, which have been collected from around the world. The two most common accessions used in arabidopsis research are the Columbia (Col) and Landsberg *erecta* (L*er*) lines. George Rédei isolated both lines in the 1960s, Columbia from a non-irradiated Landsberg population and Landsberg *erecta* from a population of Landsberg seed that he had irradiated from X-ray mutagenesis experiments (Rédei, 1992).

Arabidopsis continues to be the most thoroughly studied plant today, and has successfully held its place as the premiere plant model organism (Koornneef and Meinke, 2010). With an ever increasing global research community and the open sharing of resources, the future of arabidopsis research continues to hold much promise. One particular goal remains to be the functional characterization of each and every gene, an estimated 27,000, in the arabidopsis genome (TAIR).

All though the complete genome sequences of many organisms have allowed for the rapid discovery of large families of candidate genes, the current challenge is to link these genes with their biochemical function and biological role (Page and Grossniklaus, 2002, Coutinho *et al*., 2003). This still largely depends on the use of well designed forward and reverse genetic screens. Coupled with the genomic information now available, both approaches have proven incredibly successful in identifying the functionality of key developmental genes within a plant. Since this project is based on the forward genetic screen of an arabidopsis mutant, emphasis will be placed on forward genetics, rather than reverse genetics, for the following discussion.

1.3.2 Forward genetics

Forward and reverse genetics (or forward and reverse genetic screens) refer to two common molecular approaches to identify and deduce the functionality of genes. In short, forward genetic screens involve starting from a mutant phenotype and working towards identifying the responsible mutated gene so that a function may be assigned (Figure 1.2). Reverse genetic screens run in the opposite direction and involve starting from a known gene and disrupting it in order to measure the phenotypic effects.

A forward genetic screen typically begins with random mutagenesis introduced into the genome of an organism (Page and Grossniklaus, 2002). In plants, this is most commonly achieved by treating a large population of seeds with ethyl methanesulfonate (EMS), a chemical mutagen that predominantly induces cytosine to thymine and guanine to adenine point mutations randomly throughout the genome (Gady *et al*., 2009). The mutated plant population is then screened under a particular set of conditions from which individuals are identified for a phenotype of interest.

A specific form of genetic screens are temperature-sensitive screens. These involve shifting a mutagenized population from one temperature range to another to enhance the mutant phenotype. The enhanced phenotypes may be due to a subtle change at the protein level that makes it unstable at higher temperatures. For example, the original temperature-sensitive screen from which *sloughy* was isolated, which involved screening mutagenized seedlings for the development of root morphologies upon being shifted to 31°C from 18°C (see section 1.3.3.1) (Baskin *et al*., 1992). The primary advantage of temperature-sensitive screens is the ability to isolate mutations that may otherwise be lethal to the embryo or seedling, allowing for the characterization of genes fundamental to plant growth and development. This may

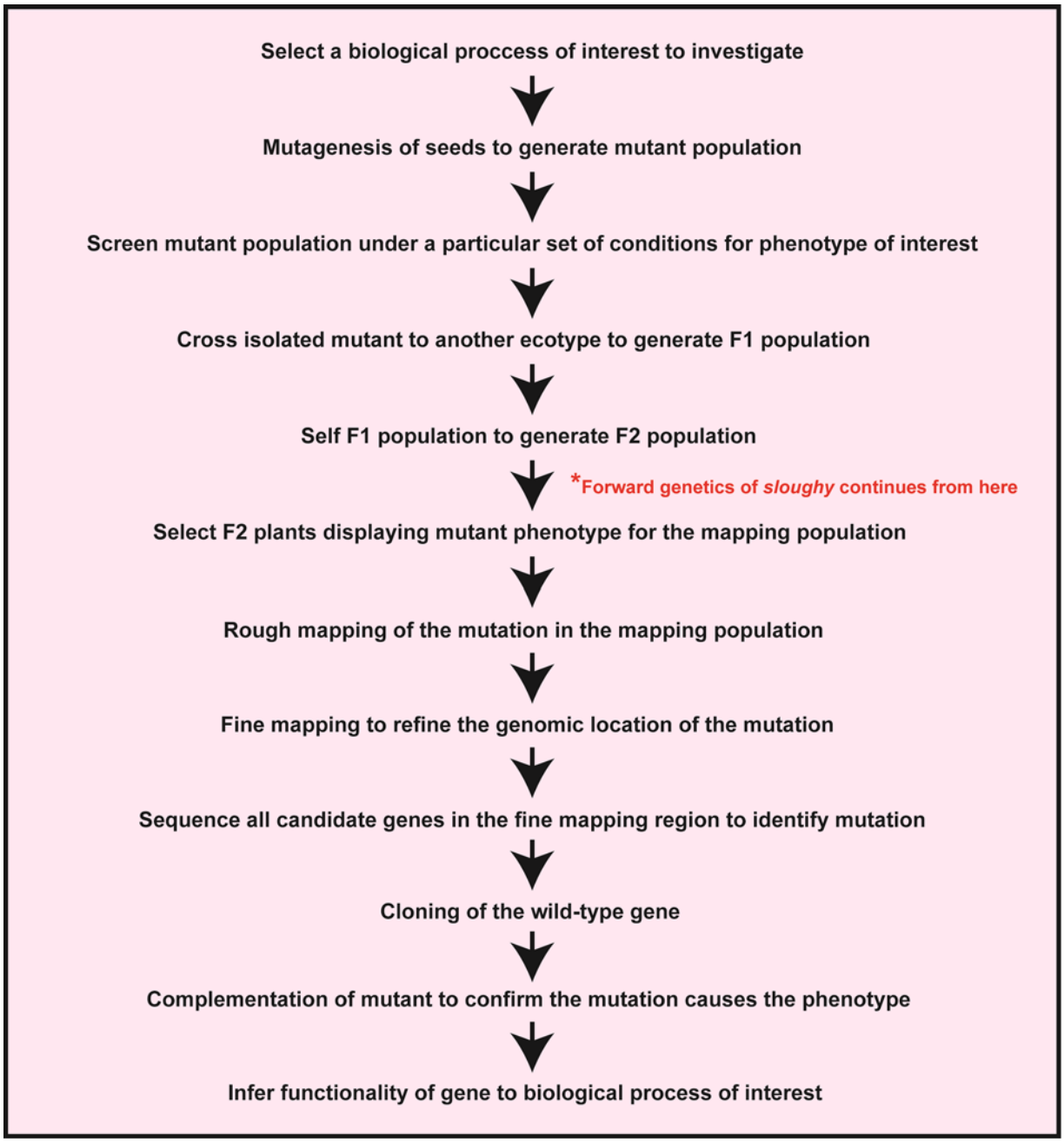

Figure 1.2 A flow diagram demonstrating the major steps involved in the forward genetics of an arabidopsis mutant. A detailed methodology for the generation and identification of arabidopsis EMS mutants was recently described (Qu and Qin, 2014). The asterisk indicates the stage from which the forward genetics of *sloughy* is commenced in this project.

otherwise be impossible using a reverse genetic approach, since reverse genetics typically relies on T-DNA insertional mutants that lead to the complete disruption genes.

Once a mutant has been isolated, the next step in forward genetics is to locate (map) the genomic location of the mutation responsible for the phenotype. This is known as map-based cloning or positional cloning. The typically involves out-crossing the mutant to generate a mapping population and calculating recombination (the exchange of DNA between homologous chromosomes during meiosis I) frequencies to test the degree of linkage of the mutation to a map of molecular markers whose location in the genome is already known (Jander *et al*., 2002). In the case of arabidopsis, the first step involves crossing the mutant to another accession. The F2 generation is collected by self-pollination of the F1 generation. A large population of individuals from the F2 population are planted from which the mapping population is selected. In the case of recessive mutation, this involves selecting and growing the homozygote mutants that demonstrate the recessive phenotype (1 in 4 individuals) for the mapping population. It is from these individuals in which the frequency of recombination is calculated. The frequency of recombination is a direct measurement of the degree of linkage between the mutation and known molecular markers. The greater the frequency of recombination, the further apart the mutation must be from the marker. Conversely, the lower the frequency of recombination between the mutation and a molecular marker, the closer the proximity must be. The iterative process of calculating recombination frequencies in F2 mapping population until no further recombinants are available is known as fine mapping.

One of the first major developments in molecular markers was the analysis of restriction fragment length polymorphisms (RFLP) (Chang *et al*., 1988). RFLP analysis is a molecular technique that exploits natural sequence variation between individuals leading to the presence or absence of different restriction enzyme sites. RFLP analysis involves treating DNA with restriction enzymes and separating the fragmented DNA via gel electrophoresis. This results

in distinct patterns of bands allowing the individuals to be distinguished. Further advances in molecular markers included the analysis of cleaved amplified polymorphic sequence (CAPS), an extension of RFLP that utilizes PCR to amplify the markers to speed up the process (Konieczny and Ausubel, 1993). If no cleavage sites are available, it is also possible to create one during PCR with suitably designed primers (dCAPS) (Neff *et al*., 1998).

Genomic sequencing has subsequently allowed the identification of single nucleotide polymorphisms (SNPs), a variation in DNA sequence in which a single nucleotide differs between two individuals of the same species. Although there are many molecular marker systems available, SNPs are now the preferred molecular marker for mapping due to their high frequency. For example, there are 349,171 SNPs between Columbia and Landsberg *erecta* allowing for extremely fine mapping resolutions (Lu *et al*., 2012). Many molecular approaches are now available for detecting SNPs. These include hybridisation-based methods, enzyme-based methods, or other post-amplification methods based on the physical properties of DNA. One example of the later is the high resolution melt point analysis of DNA, a post-PCR molecular technique that used the melting properties of double-stranded DNA to detect sequence variation (see section 3.1.2).

Once all recombinants in the mapping population have been exhausted and the fine mapping completed the genes in the mapped region are considered candidate genes and sequenced to detect any mutations. Once the mutated gene has been identified, the mutant may then be transformed with the wild-type gene in an effort to revert the mutant phenotype back to a wild-type phenotype. This is known as complementation and provides the most compelling evidence to determine whether the mutation causes the phenotype of interest (Qu and Qin, 2014).

1.3.3 *Arabidopsis thaliana* cell wall mutants

Due to the combined, recent efforts of well-designed forward and reverse genetic screens, a large cohort of arabidopsis mutants with altered cell wall properties have been characterized. These mutants have provided invaluable insight into the biosynthesis and metabolism of the plant cell wall. Of note are the collection of cellulose deficient and reduced *radially swelling* mutants (Baskin *et al*., 1992), the cellulose mutant *pom-pom2* (Hauser *et al*., 1995), the collection of altered cell wall polysaccharide *murus* mutants (Reiter *et al*., 1997), and the pectin deficient mutants *quasimodo1* and *2* (Bouton *et al*., 2002), *ectopically parting cells1* (Singh *et al*., 2005) and *arabinan deficient1* (Harholt *et al*., 2006).

1.3.3.1 The *radial swelling* collection of mutants

The first step towards identifying the molecular machinery responsible for cellulose biosynthesis came from a temperature-sensitive screen for roots with abnormal morphology, performed by the Williamson lab at the Australian Nation University (Baskin *et al*., 1992). As this is the screen in which *sloughy* was originally isolated, a more detailed history of this work is provided. The temperature-sensitive screening protocol involved plating approximately 100 seeds per agar plate, growing them at 18°C for 5 days, then transferring them to 31°C for 2 days before examination (Baskin *et al*., 1992). Mutants were then selected for the presence of abnormal root morphology. From this original temperature-sensitive screen, approximately 40 temperature-sensitive mutants with altered root morphology were recovered. The initial genetic and physiological characterisation of six of these mutants with altered root morphology were reported 1992, three of which caused extensive radial swelling of the root apex (*rsw1*, *rsw2* and *rsw3*) (Baskin *et al*., 1992). The *rsw* mutants are temperature-sensitive mutants that display a wild-type phenotype at 18°C, but upon being shifted to 31°C display radial swelling of the root apex. When returned back to 18°C from

31°C, a wild-type phenotype gradually returns. Genetic analysis placed the three *rsw* mutations at three difference loci, thus representing three unique alleles.

The Williamson lab went on to demonstrate that the *RSW1* gene encoded a catalytic subunit of the cellulose synthase complex, CesA1 (Arioli *et al*., 1998). By imaging freeze-fractured root cells in *rsw1* mutants grown at the restrictive temperature of 31°C, they were able to observe the disassembly and subsequent loss of cellulose synthase complexes in the plasma membrane. This disassembly corresponded with a significant reduction, as well as altered crystalline properties, of cellulose within the cell wall at the restrictive temperature. Consequently, widespread morphological abnormalities were observed throughout the plant (Williamson *et al*., 2001). Using a map-based cloning strategy utilizing CAPS markers, they were able to successful map and clone *rsw1* to a β-glycosyltransferase, which complemented the *rsw1* mutant, correcting any radial swelling. Cloning of the *RSW1* gene, which corresponds to the *CesA1* gene, represented a significant step towards the manipulation of the biosynthesis and physical properties of cellulose, as well as cementing the link between cellulose biosynthesis and plant morphogenesis.

The cellulose-deficient *rsw2-1* mutant was later complemented with the *KORRIGAN* (*KOR*) gene, a membrane-bound endo-β-(1–4)-glucanase (Nicol *et al*., 1998), demonstrating that *rsw2-1* is allelic for *KOR* (Lane *et al*., 2001). The *KOR* gene was identified as an extreme dwarf mutant with pronounced architectural alterations in the primary cell wall and shown to encode a plasma membrane-anchored endo-β-(1–4)-glucanase (Nicol *et al*., 1998). The mutant phenotype of *kor* (resembling the *rsw1* phenotype at the restrictive temperature) was consistent with a critical role in the biosynthesis of the cellulose network in the expanding cell wall. As was the case in *rsw1* mutants, *rsw2-1/kor* seedlings produce less cellulose with altered crystalline properties (Lane *et al*., 2001). The exact role KOR plays in cellulose production however has yet to be fully ascertained, although several functions have been

proposed (Endler and Persson, 2011). These include the processing or release of newly synthesized cellulose microfibrils from cellulose synthase complexes (Szyjanowicz *et al*., 2004), the cleavage of a primer from the growing cellulose chain (Peng *et al*., 2002), or the alteration of the crystalline properties of cellulose (Takahashi *et al*., 2009)

RSW3 was shown to be a putative glycosidase II enzyme, involved in the processing and quality control of glycan in the endoplasmic reticulum (Burn *et al*., 2002). In contrast to *rsw1* and *rsw2* that act directly at the plasma membrane to reduce cellulose synthesis, *rsw3* acts indirectly by reducing the rate of properly folded glycoprotein delivery from the endoplasmic reticulum to the plasma membrane (Burn *et al*., 2002). This model is corroborated by the fact that the *rsw3* root swelling phenotype develops more slowly than the *rsw1* and *rsw2* phenotypes when seedlings are transferred to their restrictive temperatures.

Several further mutants from the *rsw* collection have since been cloned, although their genes often played only an indirect role in the biosynthesis of the cell wall. The *rsw6* mutant has been identified to β-tubulin-3 (Collings and Baskin, Unpublished), an important component of the microtubule cytoskeleton (Benign *et al*., 2006), the *rsw9* mutant was identified as a dynamin-related protein (DRP1A) involved in endocytosis (Collings *et al*., 2008), the *rsw10* mutant was shown to encode a ribose 5-phosphate isomerase thought to be involved in many biochemical pathways (Howles *et al*., 2006), and the *rsw12* was recently confirmed to be an RNA helicase present in the nucleus (Howles *et al*., submitted).

1.3.3.2 Identifying the missing link between microtubules and cellulose

Recently, an elusive component responsible for the interaction between cellulose synthase complexes and the microtubule network was identified through the characterization of a cell elongation mutant, *pom-pom2* (*pom-2*) (Bringmann *et al*., 2012). To better understand the molecular machinery controlling cell elongation and cellulose biosynthesis, Bringmann and

colleagues (Hauser *et al*., 1995) characterized the *pom2* mutant, which displays cell elongation and microtubule related defects. Through a map-based cloning strategy, the *POM2* locus was revealed to be allelic to *CELLULOSE SYNTHASE INTERACTING1 (CSI1)*, a gene which encodes a protein that was identified through a yeast two-hybrid screen to interact with CESA isoforms (Gu *et al*., 2010). Fluorescent tagging of POM2/CSI1 demonstrated that the protein associated with cellulose synthase complexes and was essential for the sustained movement of cellulose synthase complexes along the microtubules (Bringmann *et al*., 2012, Li *et al*., 2012). It has thus been proposed that POM2/CSI1 provides a connection either directly, or in association with other proteins, between cellulose synthase complexes in the plasma membrane and the underlying cortical microtubules.

1.3.3.3 The *murus* collection of mutants

The isolation of mutants with altered cell wall polysaccharides, including hemicellulosic and pectic polysaccharides, began with a biochemical screen of EMS mutagenized-plants for altered cell wall monosaccharide content, performed by the Somerville laboratory (Reiter *et al*., 1993). This resulted in a collection of 23 mutants representing 11 unique alleles, designated *mur1* to *mur11* (from Latin *murus* meaning wall) (Reiter *et al*., 1997). The isolation of these mutants provided the groundwork to identify some of the molecular machinery responsible for the biosynthesis of diverse cell wall polysaccharides.

The *mur1* mutant was completely deficient in L-fucose, a constituent monosaccharide of hemicellulose, pectic polysaccharides and many glycoproteins (Reiter *et al*., 1993). The *mur1* mutants had a significantly dwarfed growth habit and decreased cell wall strength. The *MUR1* gene was shown encode a cytosolic GDP-D-mannose-4,6-dehydratase, responsible for catalyzing the first step in the *de novo* synthesis of L-fucose, resulting in the complete deficiency of L-fucose (Bonin *et al*., 1997).

The *mur2* and *mur3* mutants were characterized to have a 50% reduction in L-fucose levels compared to wild-type (Reiter *et al*., 1997). In contrast to *mur1* plants, *mur*2 and *mur3* plants are phenotypically normal, with a normal growth habit and cell wall strength. The *mur2* mutants contained about 1% of the wild-type amount of fucosylated xyloglucan, while the pectic polysaccharides and glycoproteins contained wild-type levels of L-fucose (Vanzin *et al*., 2002), and the *mur3* mutants had a severely altered structure of xyloglucan (Madson *et al*., 2003). Xyloglucan consists of a glucan backbone that is heavily substituted with mono-, di- or tri-saccharide side chains, and is typically the most abundant hemicellulosic polysaccharide in the primary cell wall (Hayashi, 1989). The *MUR2* gene was identified as a fucosyltransferase, AtFUT1 (Vanzin *et al*., 2002). AtFUT1 catalyzes the transfer of L-fucose to the glucan backbone of xyloglucan, thus why the *mur2* mutation results in a specific reduction in fucosylated xyloglucan. The *MUR3* gene was identified as a xyloglucan galactosyltransferase, responsible for the attachment of galactose monosaccharides to the xylosyl units within the core structure of xyloglucan (Madson *et al*., 2003). The *mur3* mutation results in the absence of a conserved L-fucosyl-D-galactosyl side chain of xyloglucan, and as a result reduced L-fucose content within the cell wall.

The *mur4*, *mur5, mur6* and *mur7* mutants have reductions in the monosaccharide arabinose (Reiter *et al*., 1997). The *mur4* mutation leads to a 50% reduction in L-arabinose content, affecting arabinose-containing pectic polysaccharides and arabinogalactan proteins (Burget and Reiter, 1999). The *MUR4* gene was shown to encode a UDP-Xyl 4-epimerase, responsible for catalyzing the final step in the *de novo* synthesis of L-arabinose in the Golgi apparatus. It is thought that the mutation leads to a only partial, rather than a complete defect, in the *de novo* synthesis of L-arabinose synthesis due to genetic redundancy (Burget and Reiter, 1999). To date, it appears that the *mur5*, *mur6* and *mur7* mutants have yet to be identified, with no further references having been made to them in the literature since 1997

(Reiter *et al*., 1997). The *mur8* mutant was characterized as having a reduction in rhamnose levels, and has also yet to be identified (Reiter *et al*., 1997).

The *mur9*, *mur10* and *mur11* mutants all have complex changes in their cell wall monosaccharide composition (Reiter *et al*., 1997). The *mur10* mutant has reduced growth, fertility, and mechanical strength, as well as complex changes in the monosaccharide content in both the primary and secondary cell walls (Bosca *et al*., 2006). The *MUR10* locus was found to be allelic with the *CesA7/IRX3* (*IRRGULAR XYLEM3*) gene, which encodes a cellulose catalytic subunit, required for cellulose synthesis in the secondary wall (Taylor *et al*., 1999, Bosca *et al*., 2006). The observed complex changes of the primary and secondary cell wall composition are thought to be a result of dynamic remodelling of the cell wall, indicating the existence of a mechanism that is able to sense cell wall integrity and control cell wall deposition. The *mur9* and *mur11* mutants have also yet to be identified, with no further references having been made to them in the literature since 1997 (Reiter *et al*., 1997).

1.3.3.4 Pectin-related cell wall mutants

In contrast to the large collections of arabidopsis cellulose and hemicellulose mutants, a limited number of pectin-related mutants have been isolated. These mutants often have pleiotropic phenotype, having many different changes, and are thus not specifically pectin mutants. An example of this is *mur1* where a mutation in the enzyme catalyzing the first step of *de novo* L-fucose synthesis, results in the complete deficiency of L-fucose, an important constituent of hemicellulose, pectic polysaccharides and many glycoproteins (Bonin *et al*., 1997).

The *quasimodo1-1* (*qua1-1*) mutant was identified from a systematic screen of a collection T-DNA transformants from the French National Institute for Agricultural Research (Samson *et al*., 2002, Bouton *et al*., 2002). In this approach, the random insertion of the T-DNA by

A. tumefaciens was used as the mutagen, rather than a chemical approach such as EMS mutagenesis. Thus the experiment is still an example of forward genetics. A second T-DNA insertion mutant allelic to *qua1-1* was subsequently identified, *qua1-2* (Bouton *et al*., 2002). Both *qua1* mutant lines were dwarfed and misshapen in stature, with an overall rough and lumpy appearance attributed to cells detaching from the surface of both above- and below-ground organs. Biochemical analyses of the cell wall sugars showed a 25% reduction in D-galacturonic acid content, a significant component of pectic polysaccharides. To further investigate this, pectic epitopes were probed with antibodies, specifically JIM5 and JIM7, which label homogalacturonan. Immunolabelling experiments corroborated the reduced pectin content, with reduced labelling in both the mutant lines (Bouton *et al*., 2002). This data strongly indicated that the disrupted gene is likely to be involved in the biosynthesis of pectin, and supports the link between pectins and cell adhesion. The T-DNA insertion sites of the *qua1* mutants were determined with PCR-based techniques since the insert itself allows the localization of the mutated gene, eliminating the need for mapping, and found to disrupt a gene which encoded a putative membrane-bound glycosyltransferase, a member of a large glycosyltransferase family 8 (Campbell *et al*., 1997). This discovery suggests that the other family members may also be important for pectin biosynthesis.

A typical forward genetic approach lead to the isolation of *qua2*, an EMS mutant which was isolated in a screen for cell wall alterations using Fourier transform infrared microspectroscopy (Mouille *et al*., 2003, Mouille *et al*., 2007). The *qua2* mutant had a very similar phenotype to that of *qua1*, with a deformed dwarfed stature and reduced cell adhesion (Mouille *et al*., 2007). Biochemical analyses of the cell wall showed that *qua2* was specifically affected in pectin with a 50% reduction in homogalacturonan content. The PAM1 antibody, which recognizes homogalacturonan, also had significantly reduced labelling in *qua2* (Mouille *et al*., 2007). The *QUA2* gene was shown to encode a putative membrane-

bound pectin methyltransferase. Complementation of the *qua2* mutant with a QUA2-fusion protein confirmed that the mutation was responsible for the phenotype and demonstrated that QUA2 localized to the Golgi apparatus. The same observations were made with a QUA1-fusion protein in the *qua1* mutant (Mouille *et al*., 2007).

Thanks to an extensive knowledge of the arabidopsis genome, the investigation of T-DNA insertion mutants in putative pectin-related genes have often compensated for the lack of isolated pectin-specific mutants. The *ectopically parting cells1* (*epc1*) T-DNA insertion mutants in arabidopsis were identified using previously generated transcript profiling data derived from poplar (Hertzberg *et al*., 2001, Singh *et al*., 2005). The detailed transcript profiling data was used as a starting point to search for important glycosyltransferases during development in poplar and resulted in the identification of a poplar glycosyltransferase 64 family member, related to the animal exotosins from the glycosyltransferase 64 family. (Singh *et al*., 2005). Comparison of the poplar and arabidopsis genomes identified a glycosyltransferase 64 homolog in arabidopsis, *EPC1* (named after subsequent mutant analysis), predicted to be membrane-bound, Golgi-localized glycosyltransferase (Singh *et al*., 2005). The *epc1* mutants were dramatically reduced in size and exhibited defects in root and shoot development and vascular patterning, as well as reduced cell adhesion in the hypocotyl and cotyledon tissues (Singh *et al*., 2005). The predicted Golgi-localization along with the cell adhesion defect was consistent with EPC1 playing a possible role in pectin biosynthesis. However, the identification of a new mutant allele of the gene, *epc1-2*, has called into question the validity of the cell separation phenotype observed in *epc1* since reduced cell adhesion was neither observed in *epc1-2* nor *epc1-1* under different laboratory conditions (Bown *et al*., 2007). Thus, it was suggested that EPC1 may be involved in some other processes affecting plant growth and development, rather than cell adhesion directly.

A reverse genetic approach to study the function a putative membrane-bound glycosyltransferase identified in the arabidopsis genome lead to the characterization of the *arabinan deficient1* (*arad1*) T-DNA insertion mutant (Harholt *et al*., 2006). Although the disruption of the *ARAD1* gene had no impact on the visible phenotype of the plant, biochemical analyses of the cell wall monosaccharide composition determined that the content of arabinose, an important component of pectic side chains, was drastically reduced. This was corroborated with immunolabelling. The LM6 antibody, which recognizes arabinan, had reduced labelling, however no differences were seen with the LM5 and LM2 antibodies, which recognize galactan and arabinogalactan, respectively. The specific cell wall changes in arabinan indicated that ARAD1 is a putative arabinosyltransferase involved in the biosynthesis pectin.

From this brief review of a selection of cell wall mutants, it is clear that the effective use of forward genetic screens have proven incredibly successful in the identification of essential components require for the biosynthesis and metabolism of the plant cell wall

1.4 Hypothesis and objectives

The primary objective of this project is to map the mutated gene responsible for the *sloughy* phenotype. The mutation will be fine mapped utilizing high resolution melt point analysis of DNA to detect recombination events in a mapping population. Once all recombinants have been exhausted and the location of the mutation refined, all candidate genes will be sequenced to detect the mutation. The conventional approach could then be complementation analysis to rescue the mutant phenotype with the wild-type gene, an approach to demonstrate that the gene is indeed responsible for the *sloughy* phenotype.

Since *sloughy* displays a cell adhesion defect, the working hypothesis is that the mutated gene is associated with the biosynthesis or deposition of pectin. Indeed, the similarity of the cell detachment phenotypes between the qua*1* and *2* pectin mutants and *sloughy* provides strong support for this (Bouton *et al*., 2002, Mouille *et al*., 2007). Furthermore, the separating epidermal cells appear morphologically reminiscent to border-like cells in the root cap.

The maturation and developmental processes that give rise to the separation of border and border-like cells have been closely linked to pectin regulating enzymes, in particular pectin methylesterases, again providing strong support for the working hypothesis. Up to sixty putative pectin methylesterase genes, as well as 50 putative polygalacturonase genes, have been identified in arabidopsis (Driouich *et al*., 2007). However, initial analysis of the genomic location of these known pectin-related enzymes indicates that none of the genes encoding these proteins lie within the suggested map range of *sloughy* (see section 3.1.1 for the earlier crude mapping of *sloughy*). It is therefore possible that the mutated gene may not be directly involved with pectin biosynthesis or deposition, and that the altered cell wall

properties may be caused by an unanticipated downstream effects. This has often been the case in the forward genetic screens of cell wall mutants, with varied genes such as β-tubulin-3 (Collings and Baskin, Unpublished), DRP1A (Collings *et al*., 2008), ribose 5-phosphate isomerase (Howles *et al*., 2006) and an RNA helicase (Howles *et al*., submitted) that give rise to other *rsw* mutants.

Complementary to the molecular characterization of *sloughy* will be an in-depth phenotypic characterization of the mutant. This will include a range of growth experiments, as well as imaging with confocal microscopy. In addition to potentially revealing previously unidentified phenotypes, further phenotypic characterization will aid in linking exactly how the mutation effects plant growth and developmental processes. Furthermore, a fundamental aim of this study is to determine how the sides of the cell wall differ to the ends of the cell wall in the separating epidermal cells. An initial way to test for any biochemical differences between wild-type and *sloughy* will be to probe cell wall epitopes in the roots of seedlings with a range of cell wall antibodies.

Once the *sloughy* mutation has been mapped to a gene, and altered phenotypic and biochemical properties identified, the genotype may then be linked back to the phenotype, ultimately inferring functionality to a potentially novel gene.

Chapter 2

Phenotypic Characterization of *sloughy*

"If I have seen further it is by standing on the shoulders of giants."

- Isaac Newton (The correspondence of Isaac Newton, 1959)

2.1 Introduction

2.1.1 The isolation of *sloughy*: an arabidopsis cell separation mutant

To further understand the underpinning mechanisms of cell expansion and growth anisotropy, the Williamson research group at the Australian Nation University initiated a mutational analysis of root morphogenesis in arabidopsis. This screen was initially described by Baskin and colleagues (Baskin *et al*., 1992), and used a temperature-sensitive screening protocol to identify mutants with altered root morphology (see section 1.3.3). This screen resulted in the collection of approximately 40 *radial swelling* (*rsw*) mutants. During the screening of these mutants, emphasis was placed on identifying mutants in which the content of cellulose was markedly lower. Accordingly, the roots of the entire *rsw* mutant collection were screened for reduced cellulose content using fractionation assays that separate, characterise, and quantify the major polysaccharides in the cell wall (Peng *et al*., 2000). Those in which the cellulose levels were reduced, were pursued for further analysis. The *rsw* mutants in which the levels of cellulose remained normal were shelved.

In the late 1990s, an associated group at the Australian National University lead by Geoff Wasteneys also used a similar temperature-sensitive screen to look for microtubule-related mutants. This lead to the identification of *mor1*, a mutant in an ancient family of microtubule-associated proteins (Whittington *et al*., 2001). As a part of this project, thought was given to the identification of mutants associated with actin microfilaments. Just like microtubule disruption and cellulose disruption, microfilament disruption also results in the radial swelling of root cells rather than proper elongation (Baskin and Bivens, 1995, Collings *et al*., 2006). Thus, the plan was to screen for mutants with hypersensitivity to microfilament

disruption, as it had been shown that microtubule mutants were hypersensitive to both microtubule and microfilament disruption (Collings *et al*., 2006), and because various microtubule-related mutants had been isolated through similar approaches (Vaughn *et al*., 1987, Anthony *et al*., 1999, Furutani *et al*., 2000, Paredez *et al*., 2008). As a proof of concept, the collection of unidentified *rsw* mutants in which cellulose production was not down-regulated were screened for sensitivity to microfilament disruption. From this screen, only one further *rsw* mutant, provisionally called *unk14* (*unknown 14*) showed hypersensitivity to microfilament disruption, although it also showed hypersensitivity to microtubule disruption. The *unk14* mutant was successfully mapped and identified as a novel mutation in β-tubulin-3 (Collings, unpublished). The identical mutation had also been identified by Tobias Baskin's lab in *rsw6* (Bannigan *et al*., 2006), working from the same initial pool of *rsw* mutants.

It was during this screen for sensitivity to microfilament disruption, that the striking phenotype of the J22.11 line from the *rsw* collection was also noted. This mutant displayed aberrant cell separation of the epidermal cells in the elongation zone and was later renamed *sloughy*. Although apparently unrelated to either cellulose synthesis or the cytoskeleton, the *sloughy* phenotype appeared to be novel and intriguing, and was simultaneously mapped during the mapping process of *unk14.* Unfortunately, the attempted mapping of *sloughy* in 2004 to 2006 did not yield success, in part due to the limitation in approaches that could be used for fine mapping. This study aims to reinvestigate the *sloughy* mutant, beginning with an in-depth phenotypic characterization of the mutant phenotype.

2.1.2 Objectives

An in-depth investigation of the growth and development of a mutant is fundamental to understanding the function of the mutated gene(s). A thorough investigation and understanding of the phenotypic differences between the mutant and wild-type will later aid

in inferring the biochemical role(s) that the mutated gene may play within the cell. Thus, the aims of the work described in this chapter were numerous.

- The growth and development of *sloughy* plants was compared wild-type plants grown on agar or soil media to identify any developmental differences.

- Measurements of root growth, including length, width, and the number of lateral roots were calculated for wild-type and *sloughy* seedlings to further understand the changes in the development of the root.

- Root growth measurements were made at a range of temperatures to investigate the temperature sensitivity of *sloughy*.

- Agar plates containing different agar concentrations and different growth nutrients were tested to determine whether the *sloughy* phenotype was linked to its growth medium.

- The roots of *sloughy* seedlings were further investigated with confocal microscopy at the cellular level, including reconstructed cross sections of the root, to reveal any additional phenotypes that may otherwise have been hidden.

Together, these experiments will shed light on the extent to which the mutation present in *sloughy* impacts the growth and development of the plant.

2.2 Methods

2.2.1 *Arabidopsis* seed planting, growth conditions and harvesting seed

Arabidopsis seeds were surface sterilized in a Eppendorf tube (1.5 ml) with 1mL of a sterilizing solution containing 50% ethanol (v/v) and 3% hydrogen peroxide (v/v) (90 s) and washed extensively with sterile distilled water (3 x 1 min). Under sterile conditions, the seeds were planted on 1.2% (w/v) agar (Bacto-agar, Difco Laboratories, Franklin Lakes, NJ, USA) plates containing Hoaglands solution and 3% sucrose (w/v). The Hoaglands solution contains 2 mM KNO_3, 5 mM $Ca(NO_3)_2$, 2 mM $MgSO_4$, 1 mM KH_2PO_4, 90 μM iron-EDTA complex, 46 μM H_3BO_3, 9.1 μM $MnC1_2$, 0.77 μM $ZnSO_4$, 0.32 μM $CuSO_4$, and 0.11 μM $NaMoO_3$ (modified from Baskin *et al*., 1992).

As an alternative to Hoaglands solution, seeds were planted on agar plates containing 0.5x Murashige and Skoog (MS) basal salt mixture (MP Biomedicals, Santa Ana, CA, USA), 1% sucrose (w/v), and 0.5 g/L 2-(N-morpholino) ethanesulfonic acid (MES)(w/v) (modified from Sabatini *et al*., 2003). In addition, seeds were planted on media containing Hoaglands solution or half-strength MS at a range of agar concentrations including 0.8%, 1.0%, 1.2% and 1.4% (w/v).

Planted seed plates were wrapped with parafilm and incubated at 4°C for 48 h to synchronise seed germination. The plates were transferred to plant growth cabinet and grown vertically at 21°C (unless otherwise stated) with 24 h light (100 $\mu E.m^{-2}.s^{-1}$). Five day-old seedlings were transferred to pots containing potting mix (Black Magic seed raising mix, Yates, Auckland, New Zealand). These pots were placed in a large, clear plastic container and covered with

plastic wrap to ensure high humidity (1 week) and grown at 21°C with a 24 h light regime to promote early flowering.

Since arabidopsis is a self-pollinating species, the plants were surrounded with rolls of overhead transparency film to prevent out-crossing, and also to comply with regulations concerning the containment of pollen and seed. Once the plants had developed siliques, watering was ceased which allowed the plants to dry out and the siliques to turn a golden-brown colour. To harvest the seed, the inflorescences were cut off at the base and placed in a large envelope to dry out completely (1 week) and the seeds were sieved (400 µm pore size) from the remaining plant material and stored at 4°C.

2.2.2 Temperature-sensitive growth experiments

Wild-type and *sloughy* seeds were planted as described in section 2.2.1 and grown in a 21°C growth cabinet for 5 days, then transferred to growth cabinets at a range of different temperatures. Once the seedlings were transferred to their respective growth cabinets, the seedlings were scanned once a day for the following 5 days using transmitted light with an Epson Perfection V700 scanner (Suwa, Nagano, Japan). Root growth was measured using the ruler tool in Adobe Photoshop CS6 (Adobe, San Jose, CA, USA) to calculate to the total length of the primary root's daily growth. Lateral roots were counted by eye in the scanned seedlings of the final day of the experiment (9 days old). To calculate root widths, the 9 day old seedlings were also photographed with a Leica MZ10F stereomicroscope (Leica, Wetzlar, Germany) coupled to a Leica DFC310 FX Camera. Root width was measured using the ruler tool in Adobe Photoshop CS6 to calculate to the width of the primary root.

2.2.3 Confocal microscopy

Fluorescent and concurrent transmitted light images were recorded with a Leica SP5 confocal microscope with 20x and 63x glycerol immersion lenses. To aid in visualising the cell walls,

arabidopsis seedlings were incubated in propidium iodide at a concentration of 20 µM in distilled water (5 min) and immediately viewed with the confocal microscope. The laser excitation wavelength used for propidium iodide was 514 nm and the emitted fluorescence was captured from 565 nm to 723 nm. For imaging with the 20x lens, line averaging was set at 4 and z-sections step size at 2 µm. For generating reconstructed cross sections with the 63x lens, line averaging was set at 4 and z-sections step size at 0.5 µm. Images were processed with Leica Microsystems LAS AF Version 2.6.0 Build 7266, ImageJ Version 1.48r (NIH, Bethesda, MD, USA) and Adobe Photoshop Version CS6. To generate the reconstructed cross sections of the 63x root images, ImageJ was used to generate a hyperstack of the fluorescent output and the contrast was enhanced. The hyperstack was then re-sliced in the Z-plane, a narrow band of 6 slices kept, and an average intensity projection image calculated and saved. This image is equivalent to a cross-section through the root.

2.3 Results

2.3.1 Basic characterization of the *sloughy* phenotype

Wild-type and *sloughy* seedlings were grown on agar medium to observe any abnormalities and to measure root growth, and subsequently planted on soil to investigate any phenotype present in the aerial parts of mature plants. When seedlings were grown for 9 days on agar, the roots of *sloughy* were significantly shorter than that of wild-type, being on average only 30% of the length (Figure 2.1D). The *sloughy* seedlings also appeared to form more lateral roots. To test this, lateral roots, were counted on 9 day old seedlings. Although the average number of lateral roots per seedling showed no significant difference between wild-type and *sloughy* (Figure 2.2A), when root length was taken into account, *sloughy* seedlings produced significantly more lateral roots (Figure 2.2B).

When the plants were grown on soil on a 12 h light regime to promote vegetative growth, the aerial parts of the *sloughy* plants were slightly reduced in size compared to wild-type (Figure 2.3). Despite this slight reduction in size, there were no other discernible phenotypes in the above-ground organs of the *sloughy* plants. The rosette leaves, inflorescence stems, flowers, siliques and seeds all developed as would be expected during their life cycle. Since this project was primarily focused on the aberrant cell separation present in the roots of *sloughy*, an in-depth investigation of the above-ground organs was not pursued.

To further investigate the phenotype of the root, *sloughy* seedlings were labelled with propidium iodide and imaged by confocal microscopy. Propidium iodide is a DNA-intercalating agent that does not pass through the intact cell membrane of living cells but

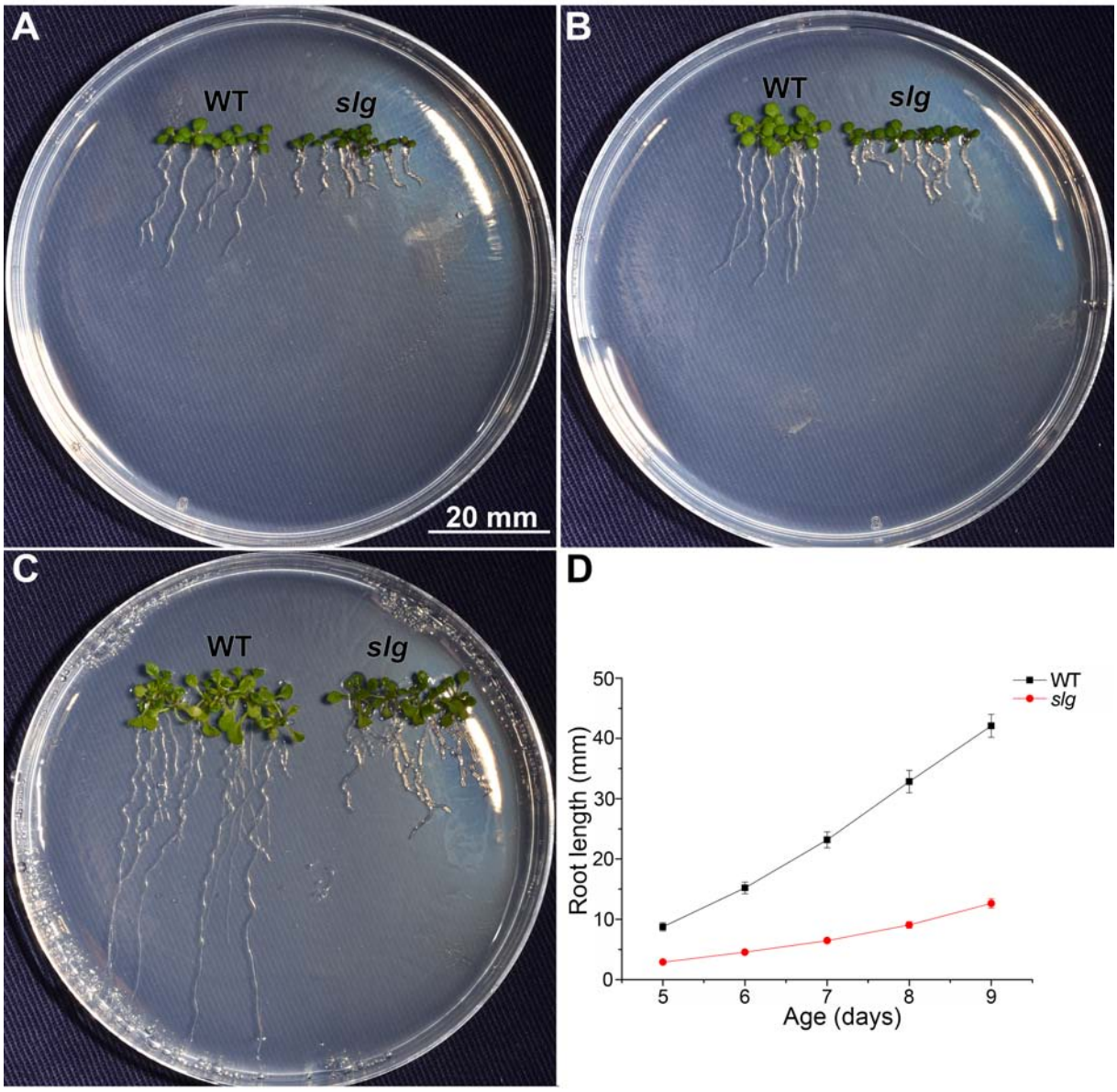

Figure 2.1 Reduced root length in *sloughy* (*slg*) seedlings compared to wild-type (WT) seedlings grown 21°C on agar medium. Scale bar in **A** = 20 mm.

A Five days.

B Seven days.

C Fourteen days.

D Primary root length measurements of wild-type and *sloughy* seedlings grown at 21°C. Data are averages ± standard errors; n = 36 replicate plants.

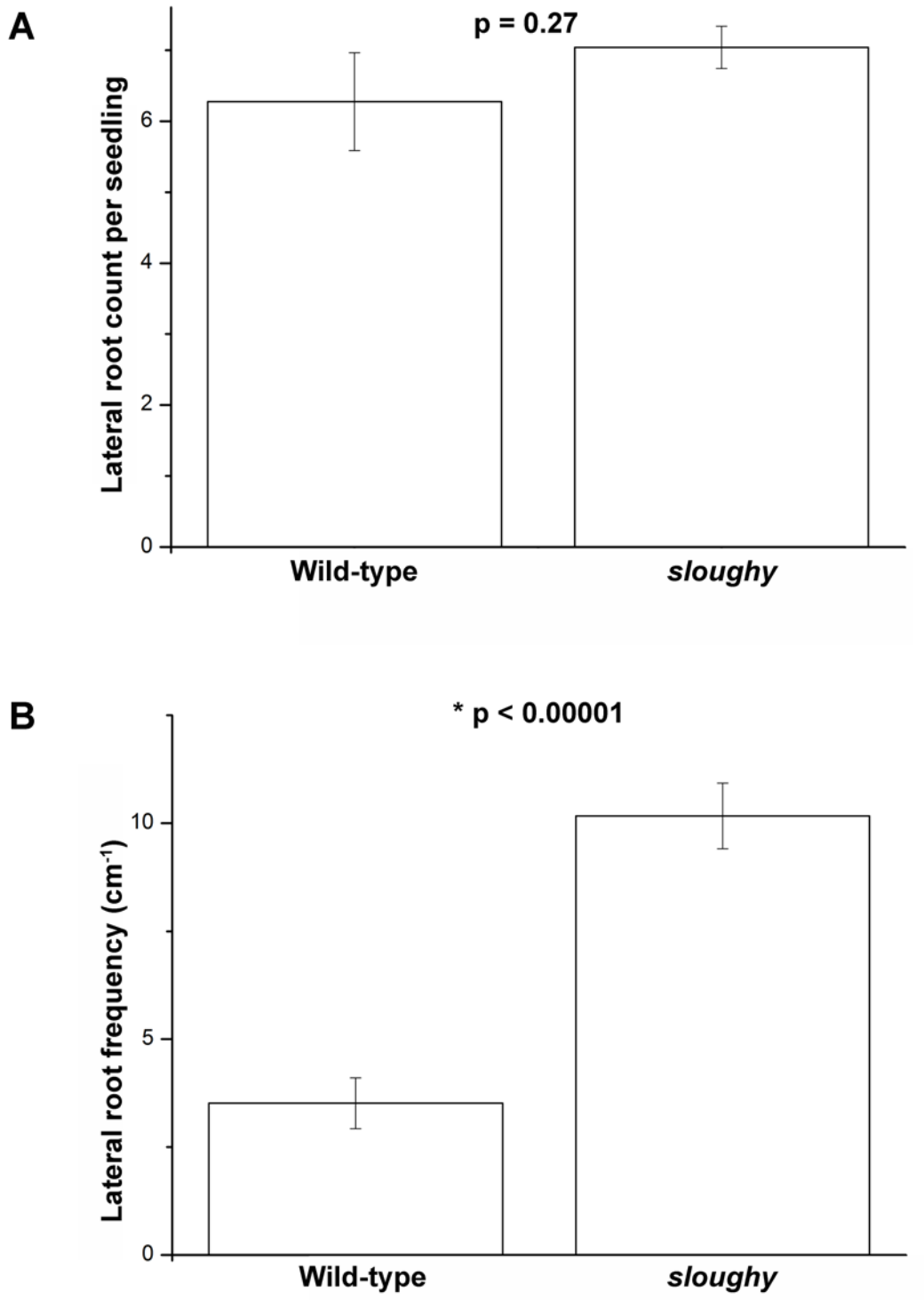

Figure 2.2 Increased frequency of lateral roots in *sloughy*. Data are averages ± SEM; n = 24 replicate plants. P-values calculated with a two-tailed T-test with a significance level of 0.05.

A Lateral root count per seedling ($p = 0.27$).

B Lateral root frequency (cm^{-1}) ($p < 0.00001$).

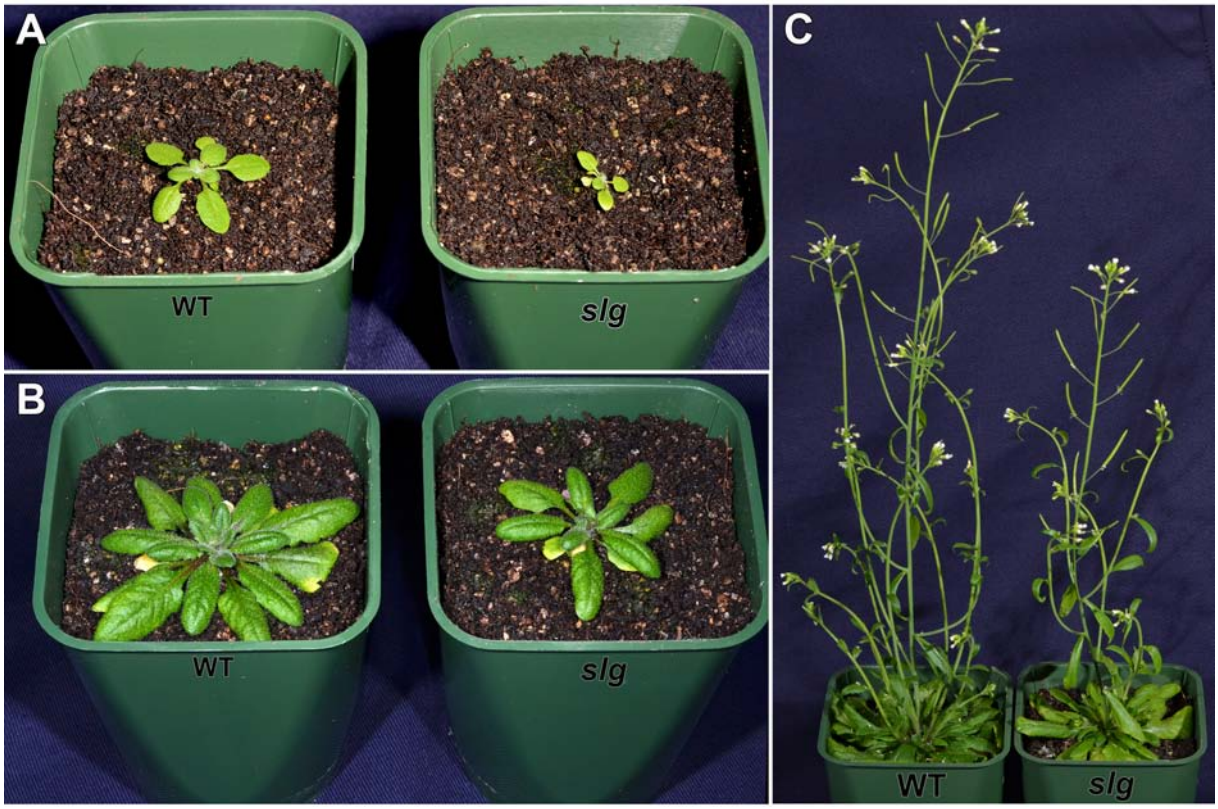

Figure 2.3 Comparative growth and development of wild-type (WT) and *sloughy* (*slg*) grown on soil at 21°C under a 12 h light regime.

A Twenty one days.

B Thirty five days.

C Forty nine days.

which also stains the cell wall. Thus, it has often been used to visualise the outline of plant cells with confocal microscopy (Rounds *et al*., 2011), notably as a cell wall counter-stain to Green Fluorescent Protein (GFP) as its emission wavelengths do not overlap with GFP (Truernit and Haseloff, 2008).

Confocal microscopy revealed the striking *sloughy* mutant phenotype. Files of elongating epidermal cells snaked away from the root surface, separating from adjacent epidermal cells and from the underlying cortex (Figure 2.4B). The epidermal cells detached along the side walls while remaining attached at the cell ends. It is for this phenotype that *sloughy* was named, since the epidermal cells appear to be sloughing away from the root.

The aberrant cell separation phenotype was most prominent in the elongation and differentiation zones of the primary root, but continued up the root until it reached the hypocotyl, upon which no further cell separation was observed. The number of root hairs in *sloughy* plant also appeared to be reduced, although this was not quantified due to technical limitations (Figure 2.4, arrows). In lateral roots, the cell separation phenotype was consistently reduced although altered cell morphologies (i.e. bean-shaped epidermal cells) were present in the laterals roots (Figure 2.5B, arrows).

To test whether the degree of the cell separation phenotype may be linked to the growth conditions, *sloughy* seedlings grown on agar plates with the standard Hoagland's solution were compared to half-strength MS salts (Murashige and Skoog, 1962) at a range of varying agar concentrations. Neither the concentration of the agar nor the alternative MS media had any observable effect on the classic cell separation phenotype (data not shown).

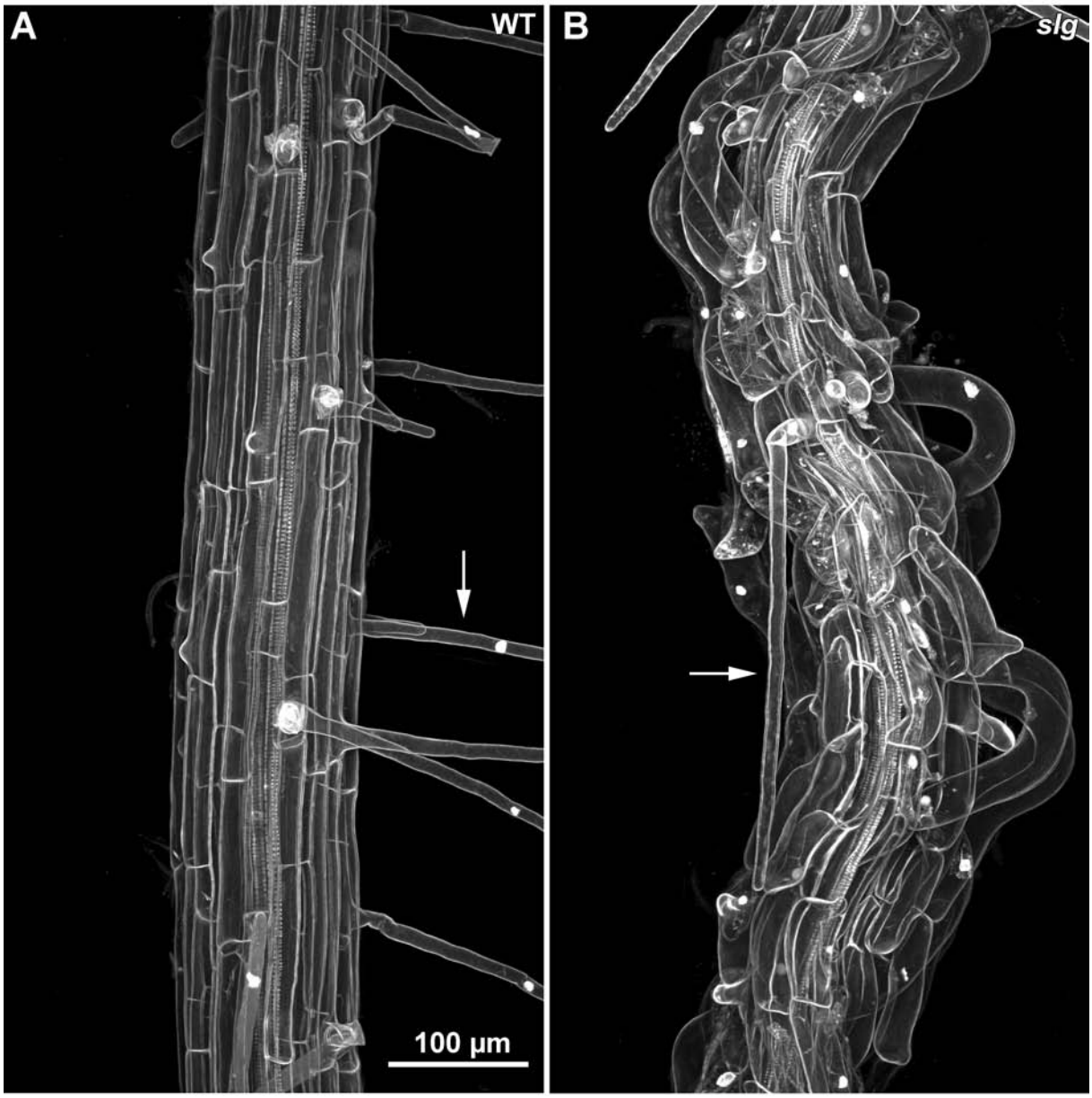

Figure 2.4 Cell separation phenotype in the roots of *sloughy*. Confocal maximum projections of roots stained with propidium iodide. The arrows indicate root hairs. Bar in **A** = 100 µm.

A Wild-type (WT).

B *sloughy (slg*).

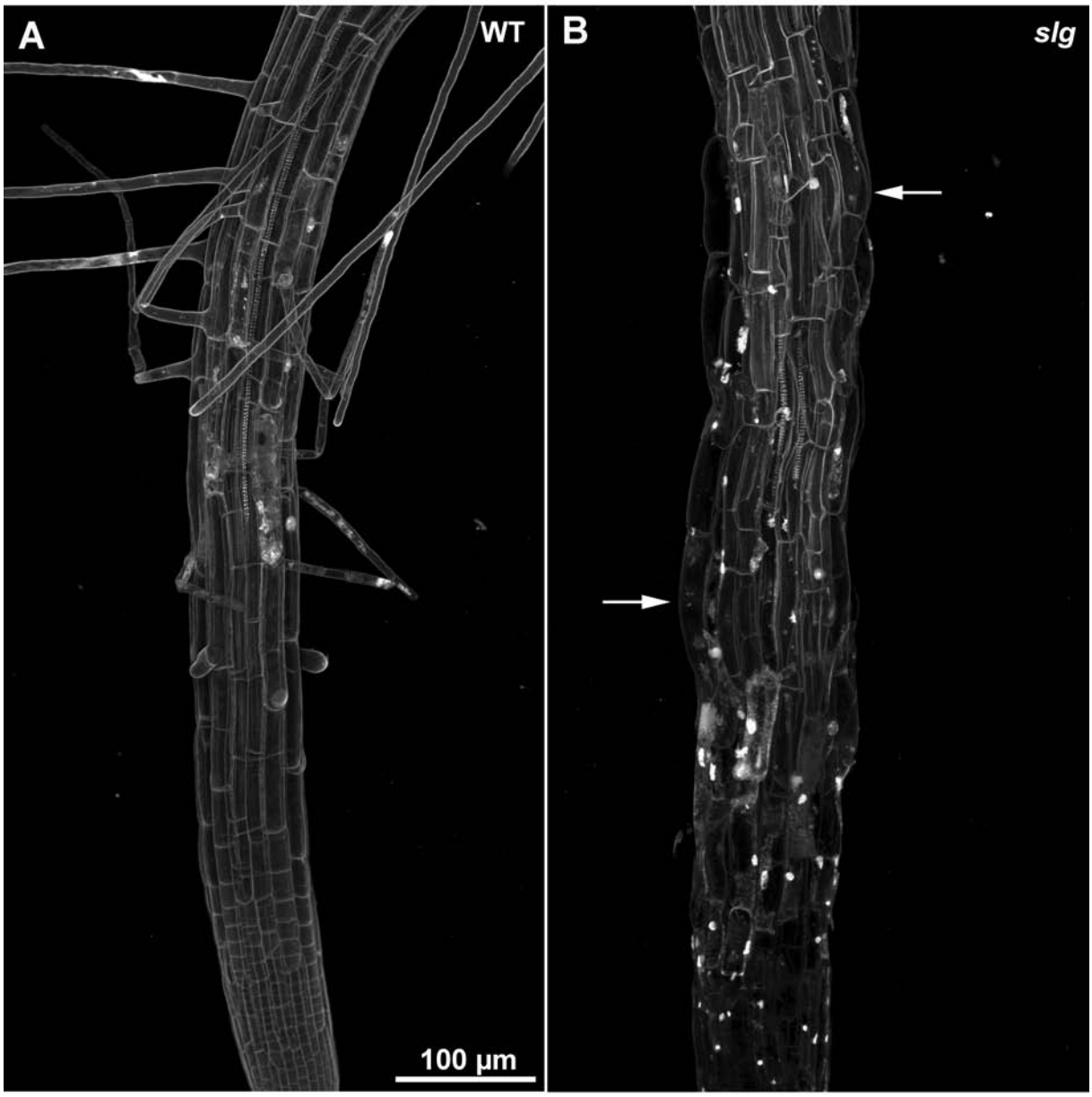

Figure 2.5 Reduced cell separation phenotype in the lateral roots of *sloughy*. Confocal maximum projections of roots stained with propidium iodide. The arrows indicate epidermal cells with abnormal morphology. Bar in **A** = 100 µm.

A Wild-type (WT).

B *sloughy* (*slg*).

2.3.2 Temperature-sensitive growth experiments

sloughy was isolated as an *rsw* mutant because of an apparent increase in root width following a temperature shift from 18°C to 31°C. Thus, it had always been assumed that *sloughy* was a temperature-sensitive mutant, with the mutation producing a severe effect on growth and development at higher temperatures. However, the degree of temperature sensitivity *sloughy* had never previously been explored.

Wild-type and *sloughy* seedlings were grown on agar plates in a 21°C growth cabinet for 5 days, before being transferred to a range of different temperatures, with root elongation measured over the course of the next 5 days. *sloughy* had significantly reduced root growth comparative to wild-type at all three temperatures (15°C, 21°C and 30°C) (Figure 2.6A), and displayed a similar optimal growth temperature to wild-type, with elongation greatest at 21°C and slower at 15°C and 30°C. This trend was also apparent when the ratio of *sloughy*-to-wild-type root length was calculated, with similar root elongation ratios at all three temperatures (Figure 2.6B). Thus, *sloughy* does not show a temperature-sensitive change in growth.

Lateral roots were also counted on 9 day old seedlings at all three temperatures. Both wild-type and *sloughy* had a similar temperature-sensitive increase in the number of lateral roots per seedling (Figure 2.7A). However, when the root of the length was taken into account, only *sloughy* seedlings display a temperature-sensitive increase in lateral root frequency (Figure 2.7B). *sloughy* produced significantly more lateral roots than wild-type at all three temperatures.

To measure the extent of any temperature-sensitive swelling present in *sloughy*, the widths of the 9 day-old primary roots were measured at 15°C, 21°C and 30°C. While wild-type roots averaged just under 140 μm in width at all 3 temperatures, *sloughy* roots increased in width at higher temperatures (Figure 2.8). Although there was no difference between the widths of

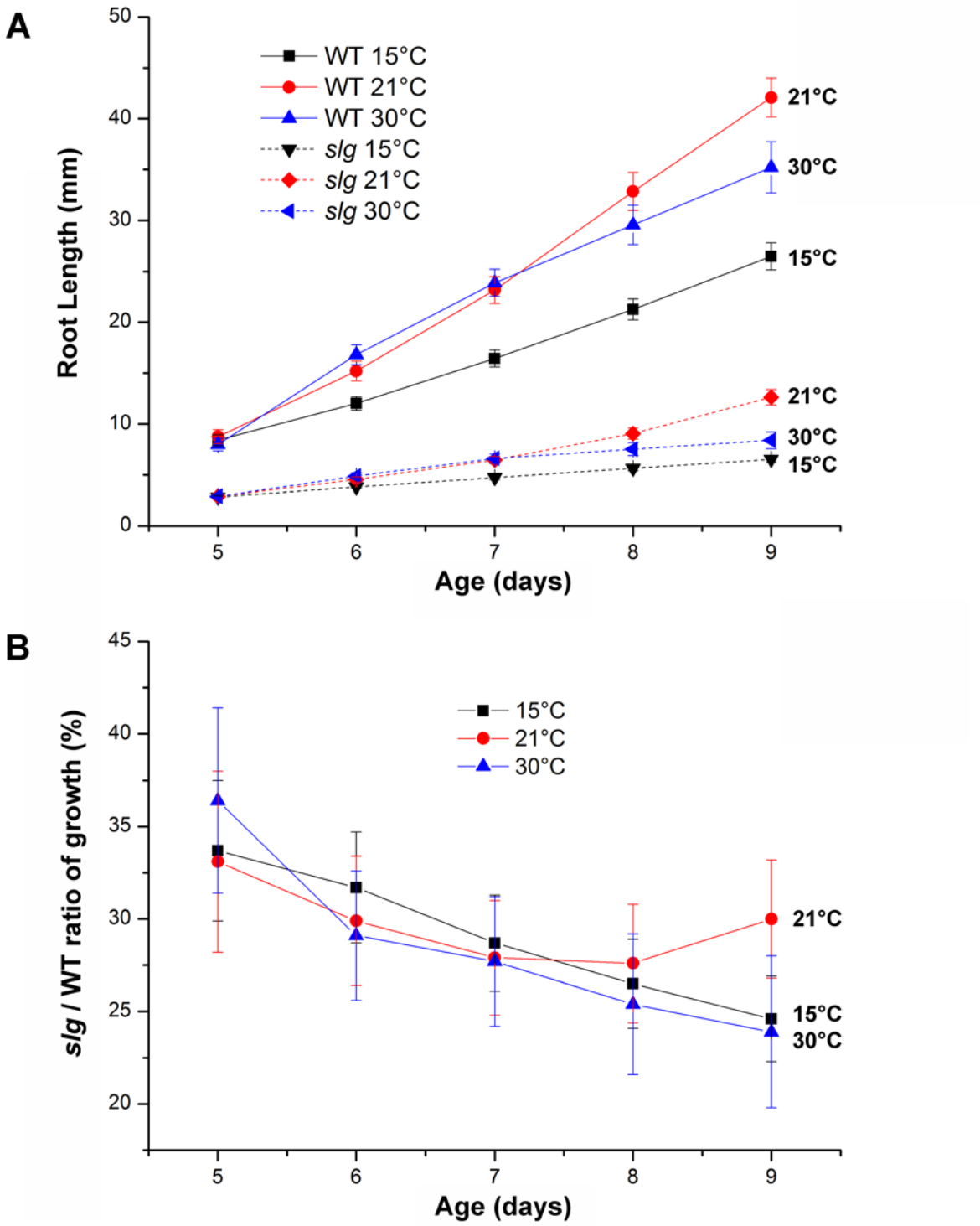

Figure 2.6 Temperature dependence of root elongation in wild-type (WT) and *sloughy* (*slg*) seedlings. Data are averages ± SEM; n = 36 replicate plants.

A Root lengths.

B Ratio of root growths (*slg* / wild-type).

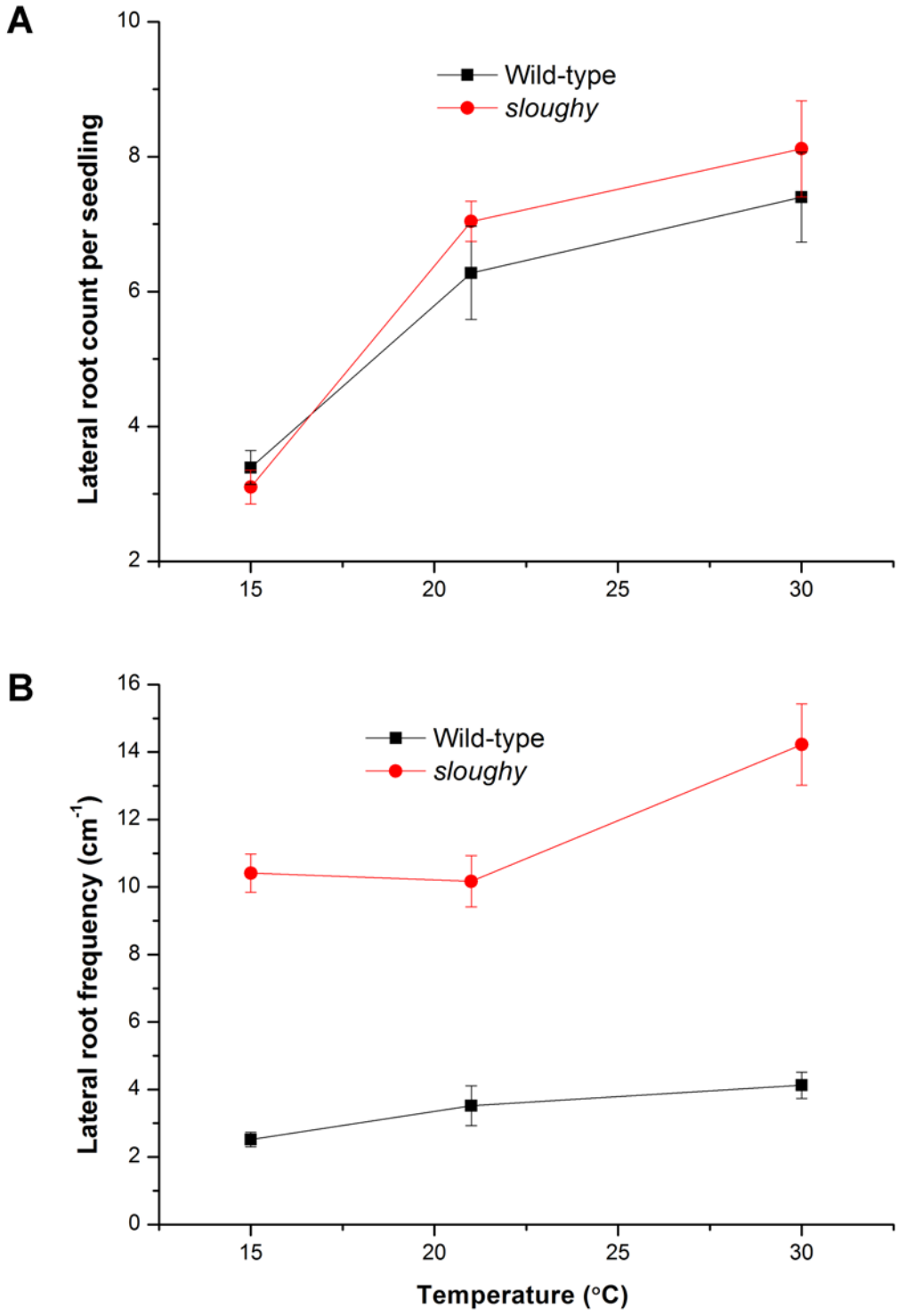

Figure 2.7 Temperature-dependence of lateral root formation in wild-type and *sloughy* seedlings. Data are averages ± SEM; n = 24 replicate plants.

A Lateral root count per seedling.

B Lateral root frequency (cm^{-1}).

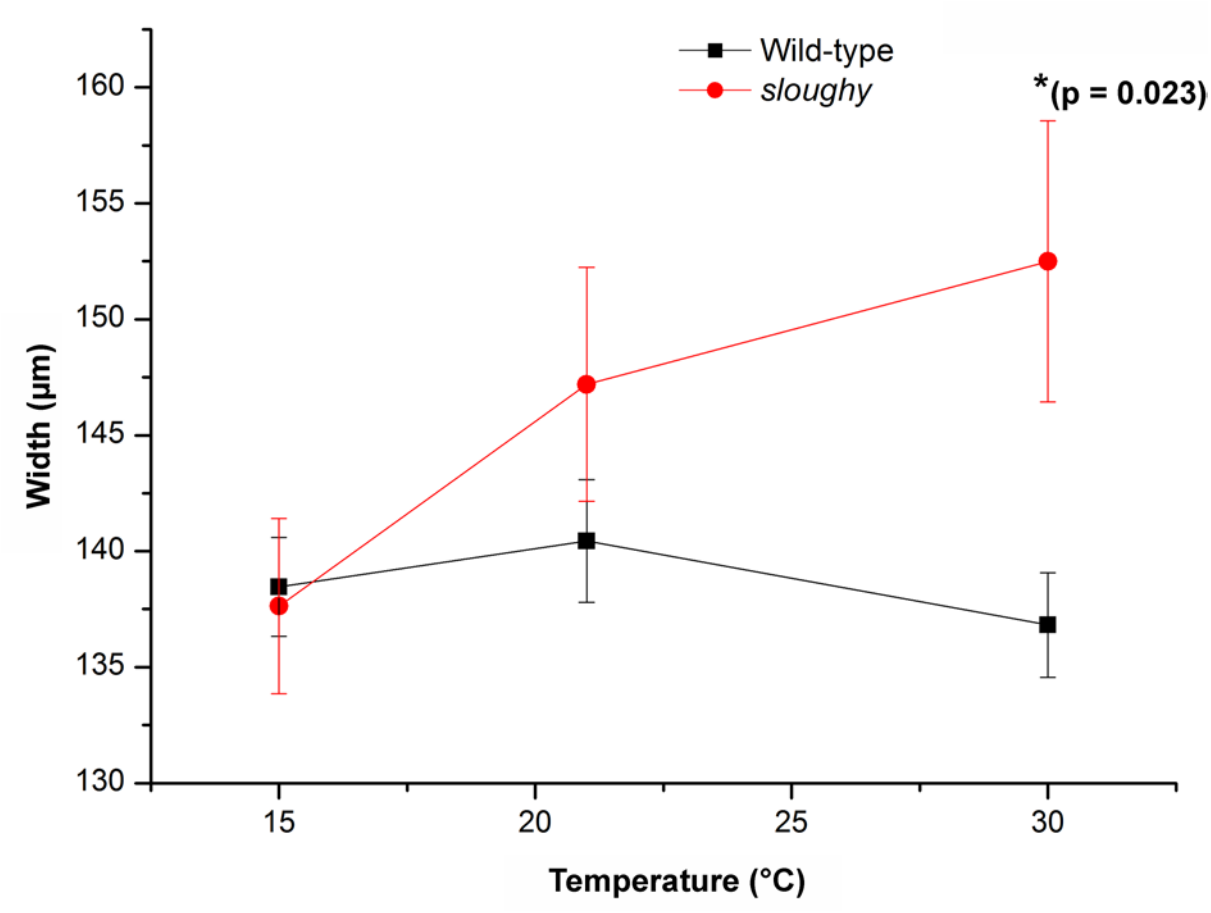

Figure 2.8 Primary root widths for 9 day-old wild-type and *sloughy* seedlings at different temperatures. Data are averages ± SEM; n = 12 replicate plants. P-values calculated with a two-tailed T-test with asterisk indicating a significant difference (significance level of 0.05).

wild-type and *sloughy* roots at 15°C and 21°C, the *sloughy* seedlings shifted to 30°C had a statistically significant increase in root width. It should be taken into account, however, that although wild-type plants have a very consistent phenotype, the *sloughy* cell separation phenotype is highly variable, not only from plant to plant, but also along an individual root (Figure 2.4) as reflected by their respective standard errors of root width (Figure 2.8).

To further investigate the sensitivity of the cell separation phenotype to temperature, *sloughy* seedlings were imaged with confocal microscopy at a range of temperatures. Although variable, there is a general trend of enhanced cell detachment at higher temperatures (Figure 2.9), with the degree of the cell separation phenotype being more pervasive at higher temperatures (i.e. greater at 21°C and 30°C compared to 15°C). By contrast, wild-type plants showed a similar phenotype at all three temperatures (data now shown). This result is consistent with the increase in root width in *sloughy* seedlings, confirming the presence of a temperature-sensitive root swelling phenotype in *sloughy*, the initial reason for its detection within the mutant screen.

2.3.3 Supernumerary cell layers and subepidermal root hairs in the *sloughy* roots

As an alternative to mechanically sectioning plant material, confocal microscopy was employed to reconstruct cross sections of the propidium iodide-stained roots of living wild-type and *sloughy* seedlings. Confocal microscopy uses a pinhole to eliminate out of focus light and generates thin optical sections. Scanning multiple optical sections through the sample at different depths (Z-stack collection) enables the reconstruction of a three-dimensional image of the sample, and cross sections through the living root (Pawley, 2010).

Optical sections were collected. A 63x lens was used giving the thinnest sections, and greatest resolution in the Z direction through propidium iodide-stained roots of *sloughy* and

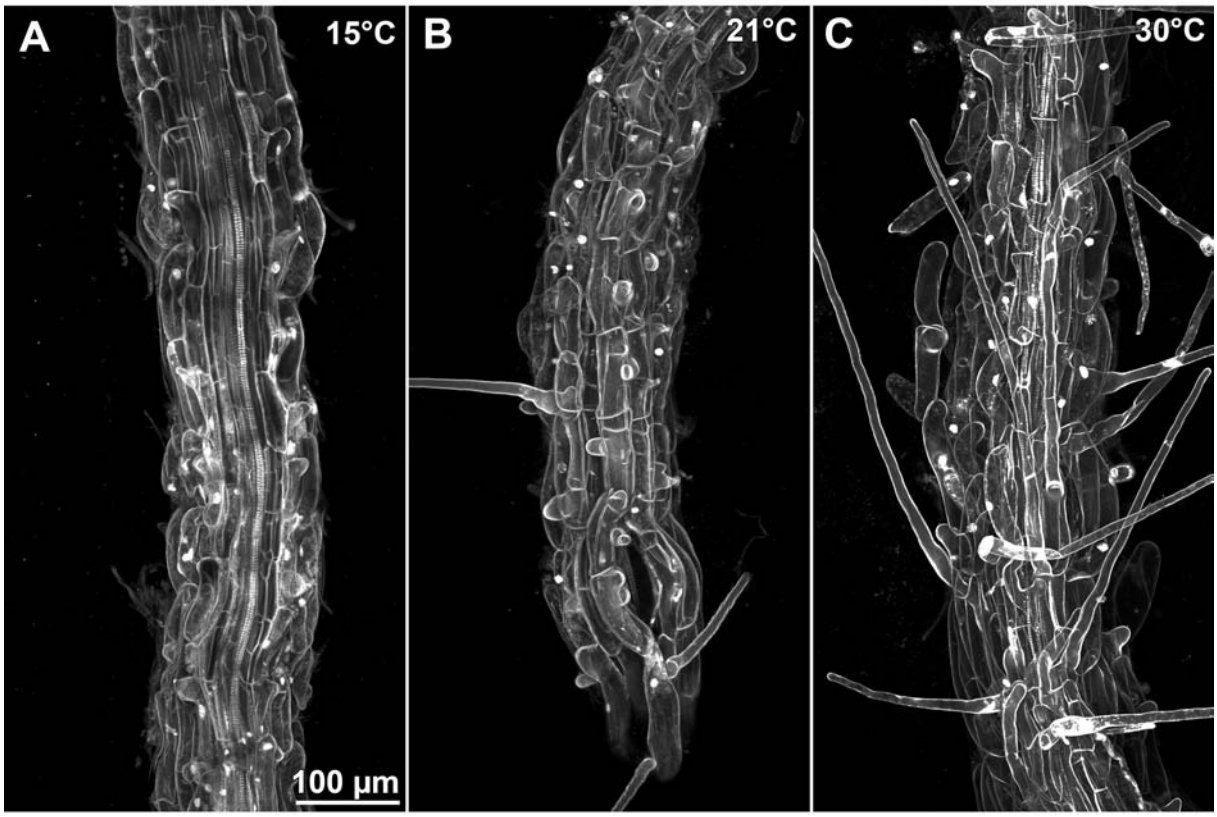

Figure 2.9 The cell separation phenotype of *sloughy* roots at different temperatures. Confocal maximum projections of roots stained with propidium iodide. Bar in **A** = 100 µm.

A 15°C.

B 21°C.

C 30°C.

wild-type seedlings as this aided in reconstructing root cross sections (see section 2.2.3). These were generated in the zone of differentiation. These reconstructed cross sections revealed that the cell layers of the root were altered in *sloughy* with the presence of an extra cell layer, often referred to as a supernumerary layer (Figure 2.10). In wild-type arabidopsis roots, three radial cell layers surrounded the vascular tissue, the stele (see section 4.1.1 for a discussion on cell layers) (Dolan *et al*., 1993). These are the endodermis, cortex and epidermis, all of which were visible in wild-type (Figure 2.10A). In *sloughy*, four radial cell layers surrounded the stele. Labelling of the casparian strip identified the endodermis (Figure 2.10B, arrow) (Naseer *et al*., 2012), and the epidermis (flattened against the cover slip) was also visible. Between these, however, were two cell layers, instead of the single cortex layer found in wild-type. Cell separation was also clearly visible in the epidermis, and possibly also the subepidermal layer, of *sloughy* (Figure2.10B, asterisks).

In addition to revealing a supernumerary cell layer, the reconstructed cross sections detected the development of root hairs from the subepidermal layer of the root (Figure 2.11). In wild-type roots, the development of root hairs are restricted to trichoblasts, epidermal cells that produce root hairs (Figure 2.11A, arrow). These trichoblasts form over the junction between underlying cortical cells, whereas atrichoblast epidermal cells lie over only a single cortical cells (Dolan *et al*., 1993). In *sloughy*, root hairs were formed developed from the cell layer below the epidermis (Figure 2.11B, asterisk). Since the formation of root hairs is indicative of epidermal identity, this subepidermal layer may then be hypothesized to possess epidermal identity (Figure 2.10B). On the assumption that the roots have at least one functional layer of cortex, the remaining cell layer may then be hypothesized to possess cortex identity (Figure 2.9B).

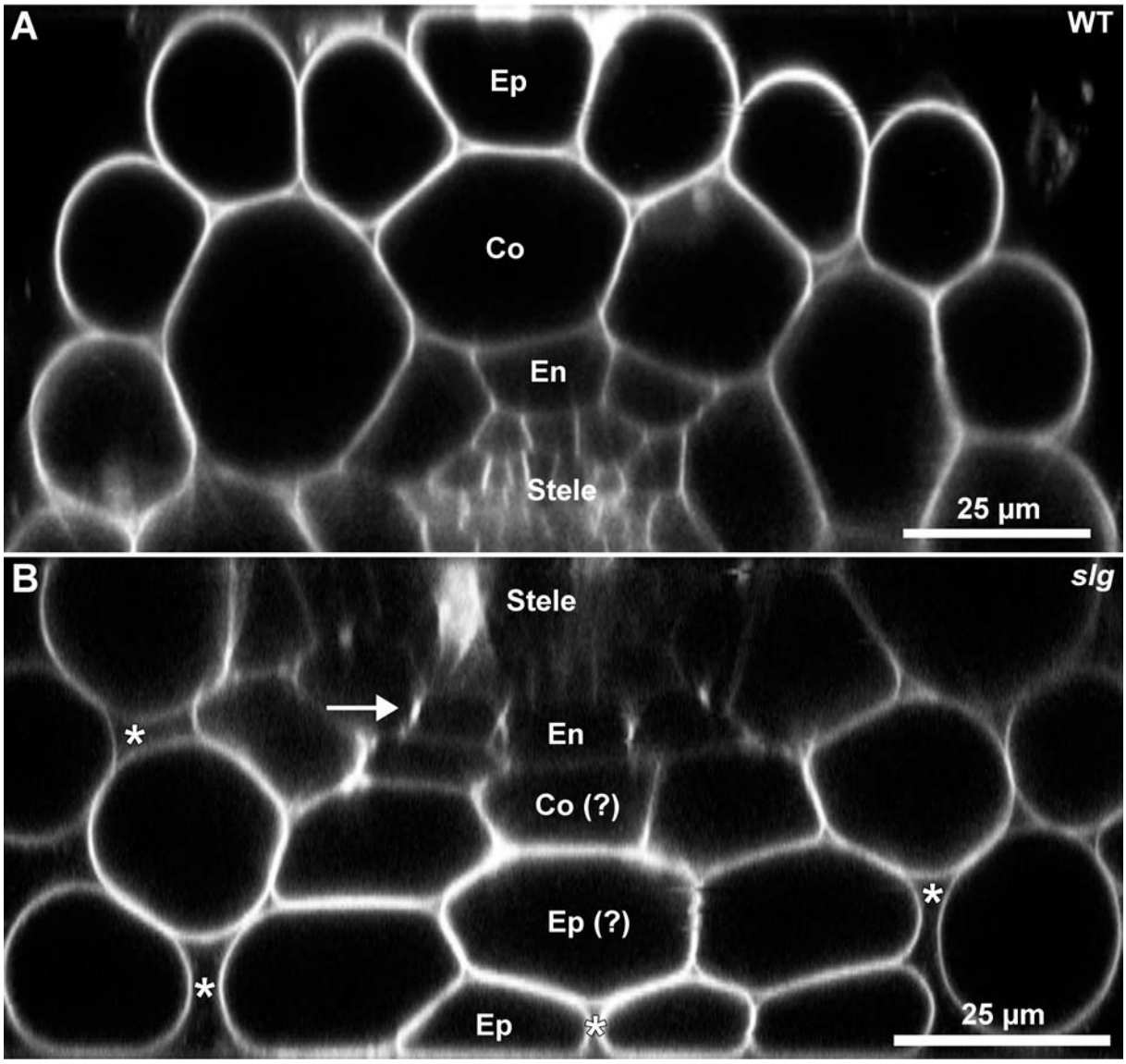

Figure 2.10 Supernumerary layer detected in *sloughy* roots. Reconstructed cross sections of wild-type (WT) and *sloughy* (*slg*) roots stained with propidium and imaged by confocal microscopy. Endodermis = En, cortex = Co and epidermis = Ep. Question marks indicate unknown, but hypothesized, identity. Arrow indicates labelling of casparian strip, while asterisks indicate evidence of cell separation in the epidermal and subepidermal layers. Bar in **A** and **B** = 25 µm.

A Wild-type (WT).

B *sloughy* (*slg*).

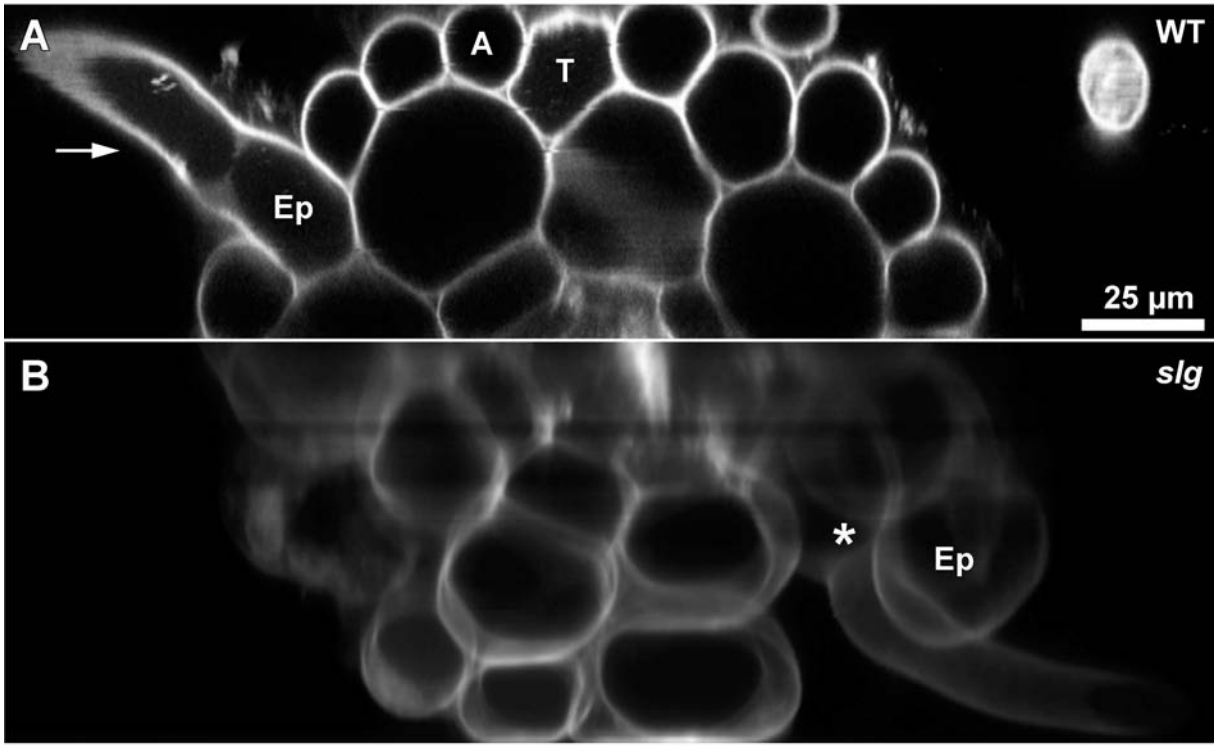

Figure 2.11 Subepidermal root hairs detected in *sloughy.* Reconstructed cross sections of wild-type (WT) and *sloughy* (*slg*) roots stained with propidium and imaged by confocal microscopy. Epidermis = Ep. Bar in **A** = 25 µm.

A Wild-type (WT). The arrow indicates the development of a root hair from the epidermal layer, while T and A indicate trichoblast and atrichoblast epidermal cells.

B *sloughy* (*slg*). The asterisk indicates the development of a root hair from the subepidermal layer.

2.4 Discussion

2.4.1 Growth and development of *sloughy*

The *sloughy* mutation had a profound impact on the rate of root growth of seedlings. At the age of 9 days, the primary roots of *sloughy* were approximately one-third the total length of wild-type, representing a significant reduction in root growth. The *sloughy* seedlings also had increased development of lateral roots. Although wild-type and *sloughy* had a similar number of lateral roots per seedling, when the size of the primary root is taken into account, *sloughy* produced significantly more lateral roots. Several possible explanations for this may exist. One may be that the seedlings simply produce more lateral roots to compensate for the reduced size of the primary root to increase the uptake of water and nutrients. Another may be a link between the levels of the hormone auxin and the initiation of lateral root formation. For example, treating roots with auxin has long been known to trigger the formation of lateral roots (Torrey, 1950), and in the arabidopsis mutant *superroot* (*sur1*), which overproduces auxin, a significant increase in lateral roots is observed (Boerjan *et al*., 1995). Due to the laborious nature of measuring hormone levels and time constraints of this project, the link between *sloughy* and hormone levels such as auxin was not pursued further.

Although the growth and development of the roots were severely impacted, the *sloughy* mutation had little effect on the aerial part of the plant. When grown on soil under 12 h lighting to induce vegetative growth, there was a slight reduction in the growth of the above-ground organs compared to wild-type. This reduced above-ground growth was, perhaps, a consequence of the reduced root growth, reflecting the root:shoot ratio of the plant, rather than a direct consequence of the *sloughy* mutation (Wilson, 1988). Despite this reduction in

general above-ground growth, there were no obvious abnormalities of any of the above-ground organs, with the plants developing normally through numerous life cycles. This, however, by no means excludes the presence of subtle mutant phenotypes present in the above ground tissue or organs that were not investigated.

Since the aberrant cell separation of the root epidermal cells was the primary focus of this project, the above-ground organs of *sloughy* were not investigated further. This basic phenotypic characterization at the whole plant level indicates that the mutated gene may only be active in the root, with little or no activity in the above-ground organs.

2.4.2 The *sloughy* cell separation phenotype

Confocal imaging of the roots of *sloughy* reveal the striking cell separation phenotype for which *sloughy* was named. Files of elongating epidermal cells separate from the adjacent epidermal cells and from the underlying cortex, loosing contact from the side walls while remaining attached at the cell ends. This cell separation phenotype is reminiscent of border-like cells in the root cap of arabidopsis (see section 1.2.4) (Vicré *et al*., 2005). Multiple files of border-like cells detach along the sides of the cell walls but remain attached at the cell ends. It is possible that similar cell wall modifications that occur in the root cap may also be occurring in the epidermal cells of *sloughy*. Studying the effect of these modifications may be one line of investigation to determine why the epidermal cells detach along the sides of their cell walls, while remaining attached at the ends. The aberrant cell separation phenotype appears to be constrained to the epidermal cells in the elongation and differentiation zones of the root with no observable cell separation in the hypocotyl or above-ground tissues. These observations suggest that mutated gene leads only to aberrant cell separation of the epidermal cells in developing roots. The degree of cell separation also appeared to be reduced in the lateral roots, although why this may be the case is not yet clear. Further characterization of

the lateral roots may reveal whether the *sloughy* gene is predominantly active in the developing primary root (i.e. during embryogenesis) or also in lateral root development. Again, since the aberrant cell separation of the root epidermal cells was the primary focus of this project and due to time constraints, lateral root phenotypes were not investigated in further detail.

Neither the concentration of the agar nor the alternative MS media had an effect on the cell separation phenotype present in the root, confirming that the aberrant cell separation is a *bona fide* phenotype, independent of its growth conditions. It is remarkable, given such an extreme phenotype, that the rest of the plant's development is not significantly altered in any other negative way. Since the abnormal epidermal cells in the root remain viable, this indicates that they are capable of carrying out their normal functions in root growth and development, despite their significantly altered morphology.

2.4.3 *sloughy* is not a true temperature-sensitive mutant

Although *sloughy* had been assumed to be a temperature-sensitive mutant, being isolated in a screen for radial swelling temperature-sensitive mutants (Baskin *et al*., 1992), its sensitivity to temperature had not been explored. The root growth measurements conducted at temperatures of 15°C to 30°C demonstrate that *sloughy* does not possess a temperature-sensitive mutation. At all temperatures tested, *sloughy* has significantly reduced root growth and displays similar growth temperature optima when compared to wild-type. Typical temperature-sensitive mutants only display the mutant phenotype at restricted higher temperatures, and upon being returned to permissive lower temperatures, gradually return to a wild-type growth habit and phenotype. This is not the case with *sloughy*, with significantly reduced root growth at all temperatures tested. Thus, by definition, *sloughy* is not a temperature-sensitive mutant.

Nonetheless, the degree of cell separation appeared to be partially sensitive to temperature. Although variable, there is a general trend of enhanced cell separation at higher temperatures. This result is consistent with the increase in root width in *sloughy* seedlings, since an increase in the detachment of epidermal cells from the underlying tissue layers would result in a detectable increase in root width. The enhanced cell separation phenotype observed at higher temperatures may simply be due to biochemical or physical effects, rather than a temperature-sensitive effect of the mutation. Several explanations could exist for this. For example, the chemical bonds in the cell walls may be loosened, the activity of cell wall modifying enzymes may be increased, or a greater mechanical shearing of epidermal cells due to an enhanced rate of cell expansion or root growth. Despite not being a true temperature-sensitive mutation, this data confirms that *sloughy* does have a temperature-sensitive root swelling phenotype, the initial reason for its detection within the mutant screen.

Both wild-type and *sloughy* seedlings produced a similar increase in the number of lateral of roots per seedling in response to temperature. Increased initiation of lateral root development in response to higher temperatures has been linked to increased auxin levels leading to the promotion and early initiation of lateral roots (Gray *et al*., 1998, Rogg *et al*., 2001). This indicates that *sloughy* has normal auxin signalling in response to temperature. When the length of the root was taken into account, only *sloughy* appears to have a temperature sensitive increase in the frequency of lateral roots. However, this increase may be a consequence of the enhanced lateral root initiation coupled to a shorter primary root at 30°C, giving the impression of a temperature-sensitive response. Again, *sloughy* produced significantly more lateral roots than wild-type at both 15°C and 30°C, corroborating the data collected at 21°C.

2.4.4 A putative supernumerary epidermal layer in *sloughy* roots

Further unanticipated phenotypes in the roots of *sloughy* were revealed from reconstructed cross sections. In wild-type roots, three radial layers surround the stele: the endodermis, cortex and epidermis (Dolan *et al*., 1993). However, in *sloughy* a supernumery layer is present, with a total of four cell layers surrounding the stele. This is indicative of an ectopic cell division occurring in the meristematic initial cells of the root apical meristem, which control the differentiation and development of tissue layers within the root. The significance of this result, and a discussion surrounding the root apical meristem and cell layers in general, is explored in greater detail in Chapter 4.

In addition to revealing a supernumery layer, the reconstructed cross sections also detected the development of subepidermal root hairs emerging from the roots of *sloughy*. In wild-type, the development of root hairs are restricted to trichoblasts, epidermal cells that border two cortical cells when viewed in cross section (Dolan *et al*., 1993). However in *sloughy*, root hairs develop from both the underlying subepidermal layer in addition to the epidermal layer. This indicates that both of these two outermost cell layers possess epidermal, or at least partial epidermal, identity. Thus, in addition to the endodermis which was identified by propidium iodide staining of the casparian strip and a hypothesized remaining cortex layer, *sloughy* possess two epidermal layers, resulting in the four radial cell layers surrounding the stele. Although, the exact identity of these cell layers cannot be determined by microscopy alone, cell-specific-GFP lines crossed to *sloughy* to determine their true cellular identity will be investigated in Chapter 4.

These results provide strong evidence for confused cell identity within the roots of *sloughy*. Thus, in contrary to what was previously hypothesized, the mutated gene in *sloughy* may be responsible for cell identity within the developing root, rather than the direct biosynthesis or

modification of the cell wall. The cell separation phenotype may be a result of incorrect signalling from surrounding ectopic tissues or a downstream effect of confused cell identity.

2.5 Summary

- The activity of the mutated gene severely impacts the growth and development of the root, with little or no effect on the above-ground organs of the plant.
- An extreme, aberrant cell separation phenotype is present in, and restricted to, the epidermal cell layers in the elongation and differentiation zone of roots.
- *sloughy* is not a temperatures-sensitive mutant, although the degree of cell separation may be partially sensitive to temperature.
- The development of subepidermal root hairs were detected from a supernumery cell layer with putative epidermal identity in the roots of *sloughy*.
- The mutated gene may play a role in controlling cell identity within the developing root, from which the cell separation phenotype may be a downstream effect, rather than a gene directly involved in the biosynthesis or modification of the plant cell wall.

Chapter 3

The Molecular Characterization of *sloughy*

"Mutation is random; natural selection is the very opposite of random."

- Richard Dawkins (The Blind Watchmaker, 1986)

3.1 Introduction

3.1.1 Fine mapping the *sloughy* mutation

In work conducted by Collings and colleagues at the Australian National University in Canberra between 2004 and 2006, the mutation responsible for *sloughy's* phenotype was localized near the middle of chromosome I. To do this, a mapping population was generated by crossing *sloughy*, a recessive mutant in the Columbia background, to Landsberg *erecta*. The progeny of this *sloughy* x Landsberg *erecta* cross, which would be heterozygous for the *sloughy* mutation, was then selfed to generate the F2 mapping population. Seed from this F2 generation separated with classical Mendelian genetics in a 3:1 ratio for wild-type against the recessive *sloughy* phenotype. F2 *sloughy* plants were grown, and DNA was isolated from these plants to look for linkage between the *sloughy* phenotype and DNA markers that differentiate Columbia and Landsberg *erecta*. Since *sloughy* is a recessive mutant in the Columbia background, all plants exhibiting the *sloughy* phenotype from the mapping population have a homozygote Columbia genotype at the mutated locus. Thus, the exchange of DNA between homologous chromosomes during meiosis I, known as genetic recombination, in the heterozygous F1 plants will be extremely limited near this locus, but will increase in frequency as the distance from *sloughy* locus increases. By testing molecular markers for recombination events, it is possible to map the genomic location of the mutation since molecular markers come in proximity to the mutation will have a reduced frequency of recombination. Once all recombinants have been exhausted, the two molecular markers with lowest frequency of recombination (excluding 0%) then provide the co-ordinates between

which the mutation must lie. This rationale provides the basis of both the previous fine mapping approach and in this project.

The previous mapping strategy was based on the standard methodology at the time. Recombination events were detected using restriction fragment length polymorphism analysis (Chang *et al*., 1988) with simple sequence length polymorphisms (Bell and Ecker, 1994), cleaved amplified polymorphic sequences (CAPs) (Konieczny and Ausubel, 1993) and dCAPs (Neff *et al*., 1998) as molecular markers. This approach had previously been used to successfully map other *radial swelling* (*rsw*) mutants that had been isolated from the same temperature-sensitive screen as *sloughy*, including *rsw9* (Collings *et al*., 2008) and *rsw10* (Howles *et al*., 2006). This attempt at mapping *sloughy* localized the mutation within the co-ordinates of 17,030 kb and 17,283 kb (markers SNP10400 and SNP293, respectively) on chromosome I, although the final step in this fine mapping was based on a single plant. This represented a 253 kb region encompassing a total of 62 genes. At the time, no genes in this region were identified as being likely candidates, and the genes that were sequenced showed no changes. Despite an effort to systematically transform the *sloughy* mutant with fragments of genomic DNA containing the 62 wild-type genes, no complementation of the phenotype was visible, with *sloughy* never reverting to wild-type growth. Due to these negative outcomes, it was assumed that a mistake may have been made during the fine mapping, with this generating a misleading result.

This project has, therefore, aimed to repeat the fine mapping of the *sloughy* mutation, this time utilizing high resolution melt point (HRM) analysis of DNA and single nucleotide polymorphisms (SNPs) as molecular makers. It has used the same *sloughy* mapping population that had previously been used and recombination frequencies have been calculated to look for linkage between the *sloughy* phenotype and molecular markers.

3.1.2 High resolution melt point analysis of DNA

Advances in quantitative PCR (qPCR) required the development of fluorescent reporter molecules that allow measurement of DNA amplification during PCR to be captured in real time. Typically, two types of fluorescent reporter molecules have been employed in qPCR:

i. Sequence specific probes that are labelled with a fluorescent reporter and which only emit fluorescence upon hybridization to their complementary sequences (Heid *et al*., 1996).
ii. Intercalating fluorescent dyes that specifically bind to double-stranded DNA (dsDNA), and which only fluoresce on binding (Wittwer *et al*., 1997).

In the absence of dsDNA, both types of reporter molecule fluoresce at a low level. Thus, when these dyes are incorporated into a PCR reaction, a negligible level of fluorescence occurs during the early cycles of the PCR due to the low concentration of dsDNA to which the reporter molecules can bind. As the PCR progresses, however, the concentration of dsDNA increases exponentially and high levels of florescence are emitted as the reporters bind the dsDNA. This fluorescence can be measured in real time and forms the basis of qPCR.

The recent developments in intercalating dyes used in qPCR have given rise to HRM analysis of DNA. This is a powerful molecular technique for fast, high-throughput analysis of nucleotide variation in dsDNA that works by detecting real-time fluorescence in a similar fashion to qPCR (Gundry *et al*., 2003). Following a qPCR run, a melt step is introduced in which the temperature is increased in small typically 0.1ºC. As the temperature increases, the dsDNA dissociates, releasing the intercalating dye and reducing the fluorescence. This reduction in fluorescence is measured and generates a melt curve from which the melting temperature (*T*m), the temperature at which 50% of the DNA dissociates, can be calculated.

As the *T*m of the PCR amplicon depends upon its nucleotide sequence, a sequence change of even a single nucleotide (e.g. a point mutation or a SNP), will result in a shift in the *T*m. Therefore, *T*m can be utilized to accurately differentiate between amplicons that vary in sequence. Melt curves can also be converted into melt peak profiles, allowing the discrimination of nucleotide sequence variation not only by the *T*m, but also by the shape of the melt peaks. For instance, discrimination of heterozygotes from homozygotes is possible based on the shape of the peaks, since homozygotes will display one smooth melt peak while heterozygotes will typically display a two-humped melt peak (Gundry *et al*., 2003).

Although HRM analysis is a very powerful and sensitive technique that can detect melting temperature changes as low as ~0.5ºC, HRM analysis has a limit with sequence variations that result in changes less than 0.4ºC being difficult to calculate and often indistinguishable (Liew *et al*., 2004, Croxford *et al*., 2008).

HRM analysis has demonstrated great utility in a wide range of applications including screening for heterozygosity (Gundry *et al*., 2003), mutation discovery (Gady *et al*., 2009), detecting polymorphisms (Reed and Wittwer, 2004), DNA mapping (Croxford *et al*., 2008), rapid species identification (Odell *et al*., 1985), and viral/bacterial population diversity measures (Cheng *et al*., 2006, Towler *et al*., 2010). It has also been used for SNP genotyping, mapping, and mutation detection in plants (Croxford *et al*., 2008, Gady *et al*., 2009, Bush and Krysan, 2010, Kazama *et al*., 2011, Han *et al*., 2012)

3.1.3 Objectives

The primary objective of this chapter is the identification of the mutation responsible for the cell separation phenotype observed in *sloughy* roots. This will build on the progress previously made into mapping the *sloughy* mutation and will follow the typical steps used to identify and clone a gene during a forward genetic screen.

- HRM analysis primers will be designed and tested to genotype the mapping population based on SNPs between Columbia and Landsberg *erecta*, thereby determining whether a recombination event has occurred.

- Numerous iterative rounds of HRM analysis, spanning the centre of chromosome I, will be undertaken to calculate the frequency of recombination, allowing the degree of linkage of between the mutation and known SNPs to be tested.

- Once all recombinants have been exhausted, and the genomic location of the mutation refined, all genes in the fine mapping region will be treated as candidate genes, and will be sequenced to detect any sequence variations.

- Once the mutated gene is successfully identified, *sloughy* may then be transformed with the cloned wild-type gene. Reverting *sloughy* back to a wild-growth habit would act as the most compelling evidence that the mutated gene is indeed responsible for the observed cell separation phenotype.

When coupled with the phenotypic data presented in Chapter 2, as well as the subsequent cellular analysis to be undertaken (Chapter 4), the functionality of the mutated gene may then be inferred, and the causative link between the genotype and the cell separation phenotype of *sloughy* identified.

3.2 Methods

3.2.1 The *sloughy* mapping population

Approximately 1600 seeds of the F2 *sloughy* mapping population were plated on agar (see section 2.2.2), grown at 21°C (5 days) and then transferred to a 30°C growth cabinet (4 days) to enhance the *sloughy* phenotype. The seedlings were screened for the *sloughy* phenotype using a stereomicroscope (Olympus, Tokyo, Japan) and all seedlings exhibiting the *sloughy* phenotype (398 plants in total) were transferred to and grown on soil (see section 2.2.2).

3.2.2 DNA extraction and purification

One or two leaves (~100 mg of plant tissue or less) were clipped into an Eppendorf tube (1.5 ml) that contained two small metal ball bearings. A Retsch Bead Mill (Retsch, Haan, Germany) was used to homogenise the fresh plant tissue (60 s). Immediately after milling, high purity genomic DNA was purified using a GenCatch Plant Genomic DNA Purification Kit (Epoch Life Sciences, Sugar Land, TX, USA) according to the manufacturer's instruction. The purified plant genomic DNA was eluted with 200 µl of preheated (65°C) TE buffer (10 mM Tris pH 7-9, 1 mM EDTA) and stored at -20°C.

3.2.3 Control plasmid preparation and sequencing

To guarantee that the correct region of chromosome I was being mapped, primers were designed to amplify, clone and sequence regions of Chromosome I that spanned the internal HRM analysis primer binding sites (Table A1.1). PCR reactions were run to amplify the genomic fragments of interest using KAPA Taq 2X ready-mix (KAPA Biosystems, Madison,

WI, USA) according to the manufacturer's instructions. A standard 20 µl PCR reaction consisted of 10 µl Taq ready mix (KAPA Biosystems), 1 µl primer (10 pmole/µl), 6 µl H_2O and 3 µl of genomic DNA. PCR reactions were carried out on an Eppendorf Mastercycler Gradient Thermal Cycler (Eppendorf, Hamburg, Germany). A typical PCR protocol involved 94°C activation (4 min), followed by 25 cycles of 94°C denaturation (30 s), 50 to 60°C annealing (30 s) and 72°C elongation (30 to 240 s).

PCR products were resolved on a 0.7% (w/v) agarose gel stained with SYBR Safe DNA (Life Technologies, Carlsbad, CA, USA) (110 V, 25 min). The DNA bands were visualised using a Dark Reader transilluminator (Clare Chemical Research, Dolores, CO, USA), excised with a scalpel, and cleaned with a Mega-Spin Agarose Gel Extraction Kit (Intron Biotechnology, Seongnam, South Korea) according to the manufacturer's instructions. Cleaned DNA was cloned into the TA Cloning Kit (Life Technologies) (24 h, room temperature) and the resulting recombinant plasmid was used to transform chemically-competent *Escherichia coli* produced in the laboratory via heat shock (37°C, 90 s). Plasmid from a transformed *E. coli* colony was isolated using a DNA-spin Plasmid DNA Purification Kit (Intron Biotechnology) according to the manufacturer's instructions and sequenced by primer walking at Macrogen (Seoul, South Korea). All sequences were edited and aligned in MEGA 5.10 (Tamura *et al*., 2011). For the control plasmids, serial dilutions were performed and quantified on a Rotor-Gene Q thermo cycler (Qiagen, Venlo, The Netherlands) to match relevant concentrations found in the DNA extractions.

3.2.4 qPCR and high resolution melt point analysis

HRM analysis to identify SNPs in the mapping population was carried out on a Rotor-Gene Q thermo cycler (Qiagen) using a 72-well carousel. For accurate detection of DNA sequence

variation, the KAPA HRM FAST PCR Kit (KAPA Biosystems) with the saturating dye EvaGreen was used.

Individual DNA samples extracted from the *sloughy* mapping population were run as 10 µl reactions consisting of 5 µl HRM FAST 2X ready mix (KAPA Biosystems), 1 µl $MgCl_2$, 0.5 µl primer (1 pmole/µl), 2.5 µl molecular grade H_2O and 1 µl of genomic DNA. Columbia, Landsberg *erecta* and a 50/50 mix of Columbia and Landsberg *erecta* DNA were used as positive controls, while molecular grade water samples were used as no-template negative controls.

A typical qPCR and HRM analysis involved a 95°C enzyme activation (3 min), followed by 40 cycles of 95°C denaturation (5 s) and 60°C annealing and extension (30 s), followed by a final 95°C denaturation (1 min). Following the qPCR, a high resolution melt step raised the temperature from 65°C to 90°C in 0.1°C steps. The temperature was held at each step (2 s) to detect fluorescence. During this melt step, fluorescence data was converted into melt curve profiles using the Rotor-Gene Q Pure Detection software (Qiagen). Melt curve profiles were then converted into distinct melt peak profiles with the software by plotting the first negative derivative of the fluorescence as a function of temperature (-dF/dT). The exact melt peak temperatures were determined with the software output listing the melt peak temperatures.

The HRM analysis primers for detecting recombination events were designed for 11 SNP locations spanning the centre of chromosome I that were predicted to cause a melt temperature change (Table 3.1). The SNP sequence differences between Columbia and Landsberg *erecta* had been identified at TAIR (www.arabidopsis.org). The primers were designed using the software program DNAMAN (Lynnon Biosoft, Point-Claire, QC, Canada) to minimise potential primer dimers, hairpin structures and false priming. Primers were

designed with lengths of 18 and 25 nucleotides, melting temperatures between 58°C and 60°C, and a target amplicon size between 80 to 220 bp.

3.2.5 Candidate gene sequencing

Primers were designed to amplify, clone and sequence five genes that were identified within the eventual fine mapping co-ordinates (Table A1.2). The protocol for sequencing the candidates genes followed that described in section 3.2.3 with slight modifications. KAPA HiFi HotStart 2X ready-mix (KAPA Biosystems) for high-fidelity amplification of large fragments was used in place of KAPA Taq 2X ready-mix, and the CloneJET PCR Cloning Kit (Fermentas, Glen Burnie, MD, USA) for cloning blunt ended fragments was used according to the manufacturer's instructions, in place of the TA Cloning Kit (Life Technologies). Sequencing was conducted at Macrogen (South Korea) (see section 3.2.3) and at Canterbury Sequencing and Genotyping (School of Biological Sciences, University of Canterbury). Bioinformatic analysis consisted of editing and aligning the sequences in MEGA 5.10 to identify any mutations or amino acid changes that may have been present in *sloughy* compared to Columbia and Landsberg *erecta*.

3.2.6 RNA extraction

To assess the levels of gene expression for the candidate gene, qPCR was run on RNA extracted from the roots of *sloughy* and control plants. Total RNA was extracted from the roots of Columbia, Landsberg *erecta* and *sloughy* seedlings that had been grown on agar at 21°C for 14 days (section 2.2.2). In RNase free conditions, 100 mg of root tissue (~160 seedlings) was dissected from the seedlings with a scalpel, placed immediately in liquid nitrogen and ground to a powder in an Eppendorf tube (1.5 ml) with a pestle. To the frozen ground tissue, 1 mL of TRIzol (Life Technologies) was added, quickly vortexed, incubated at room temperature (5 min) and then centrifuged at 11,000 rpm (5 min, 4°C). The supernatant

was transferred to a new Eppendorf tube (1.5 ml) and 200 µl of chloroform was added, shaken vigorously (15 s), incubated at room temperature (10 min) and centrifuged at 11,000 rpm to phase separate the RNA from the DNA and protein precipitates (15 min, 4°C). The top, aqueous phase that contained the RNA was carefully removed and transferred to a new Eppendorf tube (1.5 ml) to which an equal volume of 70% ethanol was added. The RNA/ethanol mix was loaded into a RNeasy Mini Kit spin column (Qiagen) and the RNA was purified according to the manufacturer's instructions. The RNA was eluted with 30 µl of RNase free H_2O and stored at -20°C. All RNA extractions were resolved on a 1% agar gel to ensure the quality of the RNA to demonstrate that no genomic DNA contamination or significant RNA degradation had occurred. To measure the quantity and purity of the RNA samples, a NanoDrop spectrophotometer (Thermo Fisher Scientific, North Shore City, New Zealand) was used. The NanoDrop spectrophotometer utilises the absorbance peak of RNA (260 nm) to calculate concentrations (ng/µl) and to estimate the purity of samples by assessing the 260/280 nm and 260/230 nm ratios. In addition to this, qPCR primers were tested against the RNA extractions to check for amplification of contaminating genomic DNA (no-reverse transcription control). In all cases, no DNA was detected in the RNA extractions, demonstrating that this protocol was effective at preventing genomic DNA contamination.

3.2.7 Measuring gene expression by reverse transcription qPCR

To normalize the RNA extractions, exactly 500 ng of total RNA was used for complementary DNA (cDNA) synthesis. cDNA synthesis was carried out with the QuantiTect Reverse Transcription Kit (Qiagen) allowing simultaneous DNase treatment and cDNA synthesis. Although no genomic DNA was detected in any of the RNA extractions, this simultaneous

DNase treatment is included in the QuantiTect Reverse Transcription Kit, and this helped to ensure the absence of contaminating DNA sources.

Quantification can take the form of absolute quantification, based on absolute copy number, or relative quantification compared to a reference gene and/or treatment group (Livak and Schmittgen, 2001). Absolute quantification of the candidate gene transcript copy number was performed on the cDNA synthesized from the Columbia, Landsberg *erecta* and *sloughy* seedlings. Absolute quantification is based on generating a standard curve to quantify the absolute copy number of the gene transcript, in place of comparing the relative expression to a reference gene. In order to generate a standard curve, a 665 bp genomic fragment that spanned the internal qPCR primer binding sites (see Table A1.3) was amplified, cloned into a plasmid, and sequenced (see section 3.2.3). The DNA concentration of the eluted plasmid was calculated using a NanoDrop spectrometer allowing the copy number of the plasmid to be calculated (5.75×10^{10} copies per µl) knowing the molecular weight of the plasmid containing the insert. Two independent, 12-fold serial dilutions were performed on the plasmid from 5.75×10^{10} copies per µl down to 0.06 copies per µl on the Rotor-Gene Q (Qiagen), with each series run in triplicate. A standard curve was produced using the Rotor-Gene Q Pure Detection software (Qiagen).

cDNA and the plasmid serial dilutions were amplified as described in section 3.2.4 with slight modifications. The SYBR FAST qPCR Kit (KAPA Biosystems) designed for qPCR was used in place of the HRM FAST PCR Kit (KAPA Biosystems) designed for HRM analysis. The RT-qPCR protocol involved a 95°C enzyme activation (3 min), followed by 40 cycles of 95°C denaturation (3 s) and 60°C annealing and extension (20 s), followed by a high resolution melt step (65°C to 90°C at 0.1°C increments, each held for 2 s). Post-PCR, the standard curve was imported using the Rotor-Gene Q Pure Detection software (Qiagen) and used to calculate the absolute copy number of the gene transcript.

3.3 Results

3.3.1 Fine mapping the *sloughy* mutation

Approximately 1600 seedlings from the F2 mapping population were screened on agar for the *sloughy* phenotype. All seedlings exhibiting the *sloughy* phenotype (398 plants in total) were grown on soil, and subsequently had their DNA extracted for the fine mapping analysis. All plants exhibiting a wild-type phenotype were discarded. It was possible to determine whether a recombination event had occurred in a selected *sloughy* individual by using HRM analysis to discriminate between the three genotypes which could exist at each locus being tested:

i. A Columbia homozygote genotype (no recombination events).
ii. A Columbia/Landsberg *erecta* heterozygote genotype (one recombination event).
iii. A Landsberg *erecta* homozygote (two recombination events).

Following HRM analysis, melt curve profiles were produced by the Rotor-Gene Q Pure Detection software (Figure 3.1A). A melt curve is a representation of the relative fluorescence in the sample captured in real time. As the temperature increases, the dsDNA dissociates releasing the intercalating dye, and the fluorescence is reduced. It is possible to distinguish each of the three possible genotypes based on the slight differences between the melt curve profiles. A shift in melting temperature is indicative of sequence variation between two homozygote individuals, whereas a change in shape is indicative of a heterozygote (Figure 3.1A).

However, instead of discriminating plants based on melting curves, distinct melt peak profiles, derived from the melting curve data by plotting the first negative derivative of the

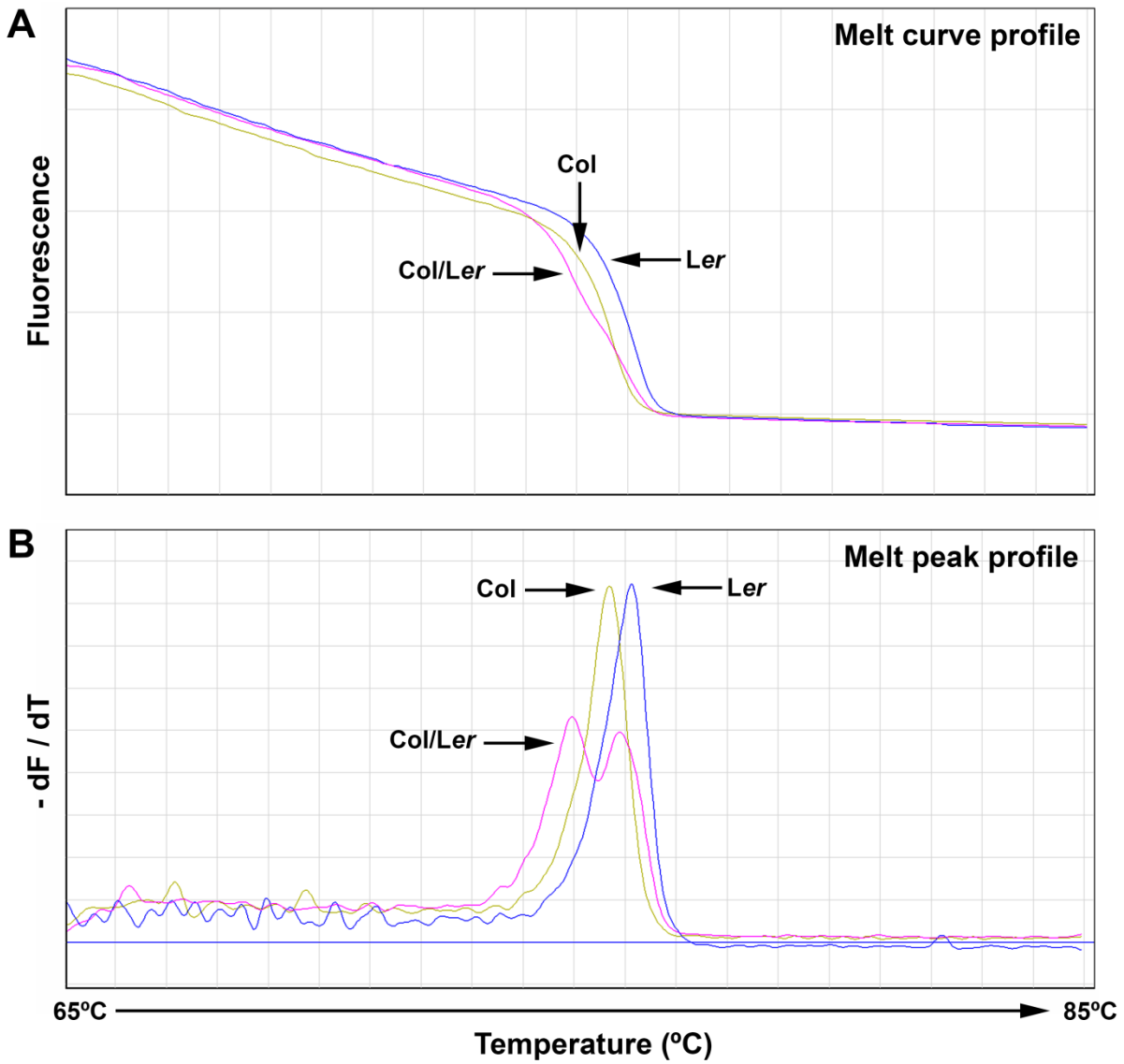

Figure 3.1 Utilizing HRM analysis to genotype the *sloughy* mapping population based on SNPs between Columbia (Col) and Landsberg *erecta* (L*er*). In this example, an adenine to guanine SNP exists between Columbia and Landsberg *erecta*, resulting in Landsberg *erecta* having a higher *T*m. The heterozygote (Col/L*er*) can be identified as having a differently shaped melt curve and melt peak profile. -dF/dT is the first negative derivative of the fluorescence as a function of temperature.

A Melt curve profiles.

B Melt peak profiles.

fluorescence as a function of temperature (-dF/dT), were used to rapidly genotype individuals (Figure 3.1B). Homozygote genotypes resulted in melt peak profiles with consistent peaks and a shift in temperature was indicative of a sequence variation. Heterozygote genotypes resulted in readily distinguishable melt peak profiles with lower double peaks (Figure 3.1B). The height of the peaks is a quantitative measure of DNA abundance, but was not relevant to this study. HRM analysis was able to detect single base pair changes resulting in a temperature change as low as 0.5ºC allowing the accurate and consistent genotyping between the Columbia and Landsberg *erecta* homozygotes. This approach was considerably faster and more accurate than the previous mapping procedure used because:

i. Gels were not required, and up to 72 samples could be processed in one run.
ii. Restriction enzyme digests were not required, making the approach faster, and less subject to variation.
iii. More use could be made of the extensive number of SNPs present when the Columbia and Landsberg *erecta* sequences are compared.

Iterative sets of primers were designed to detect SNPs spanning 11 locations on chromosome I, starting first with the SNPs PERL0133085 and SGCSNP10406, which were the last markers between which *sloughy* was rough mapped from 2004 to 2006 (Table 3.1). Plasmid positive controls were used for the outermost SNPs to ensure the primers were indeed amplifying their correct genomic target, guaranteeing that the correct region of chromosome I was being mapped. Melt peak profiles were used to rapidly genotype up to 72 plants at a time at each SNP location (Figure 3.2), and from this, the frequency of recombination (%) calculated. If no recombination events were detected in a plant at either of the outer locations, meaning that the plant was a Columbia homozygote across the entire range of being tested, then the plant was no longer pursued with further primer sets.

Table 3.1 Summary of the SNPs used as molecular markers and the respective primers to detect them using HRM analysis.

Name	SNP	Location (bp)	Forward Primer (5' - 3')	Reverse Primer (5' - 3')	Fragment (bp)
PERL0133085	G to T	16,231,163	GGT CTT GGT GAG GAG TGA GTC	TGA CTA AAC CAG ACG AAG AAC CA	111
SGCSNP10403	G to T	17,029,922	TGA GAG TTG AGC GAA TGG TAA CG	CCT CCA CAC CAA CTA CCT GTT	141/142*
PERL0143562	G to A	17,183,805	TGA TGA TGA TGA ATG AGG CAG	CAA GGC ACA CAG TTT CAT CG	141
PERL0143983	C to A	17,220,713	GAG ATG TTA CAA AGT ATG CC TCC C	GCC AGA ACA AAG AAG AGA AAC AG	83
PERL0144015	A to G	17,224,184	ACC GCA AGT GAT AAT CCG	CGC AAT GCC GTA TCC TAA C	95
PERL0144125	A to G	17,237,371	TCT TCT GCT TCT GTC TCT CGC	ACC CGA CTC AAG AAC AGA TAG G	180
PERL0144205	C to T	17,247,997	CTT GCT CTG TTG TAG AAA TGT GC	ATC TCG GTT CAT TGT GAC AGT C′	154
MASC07205	C to T	17,283,616	TCG CCA TTC TTT ATC GGG	GGA GAG AGT GGA TAC CTA AGG ATG	98
PERL0146587	A to G	17,379,237	CGA GTA AGA TGG CTA ATG AAA GAG G	TGT GCC AGA AGA TGA CGA AAC	119
PERL0148220	T to C	17,497,019	CCG AAA CGC CAA CAC AAG G	TGG ATT ATC GCT TGC GTG GC	136
SGCSNP10406	G to A	17,823,908	TGT GTA TCC GCT TTC CTT CTA CC	GAT GTA GTC GGT GGT GGA GC	110

Adenine = A, cytosine = C, guanine = G and thymine = T.

*The primers spanning SGCSNP10403 include a T insertion.

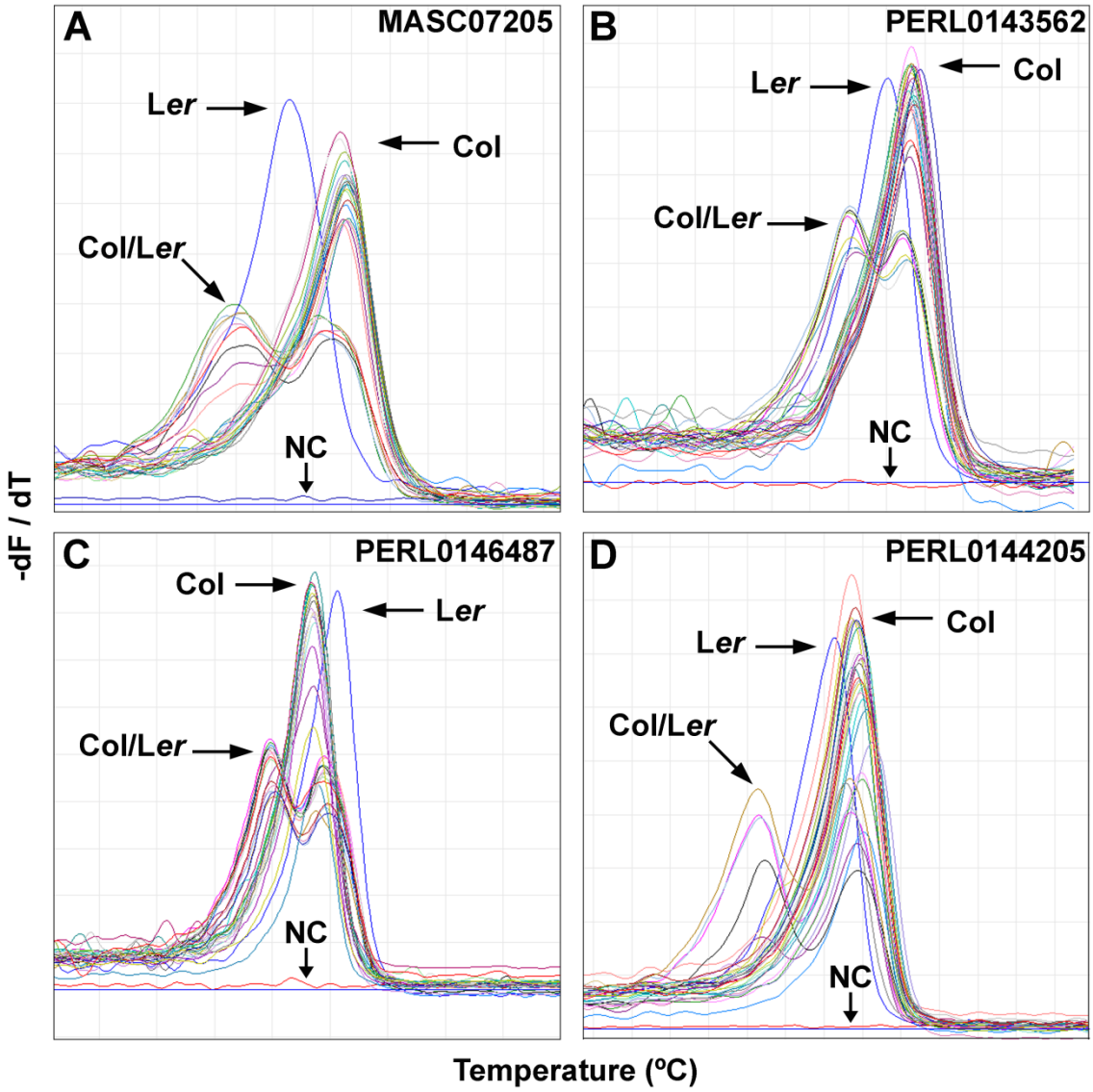

Figure 3.2 Genotyping the *sloughy* mapping population with HRM analysis. Columbia homozygote = Col, Landsberg *erecta* homozygote = L*er*, Columbia/Landsberg *erecta* heterozygote = Col/L*er* and negative control = NC. Y-axis (-dF/dT) represents the first negative derivative of the fluorescence as a function of temperature.

A MASC07205, cytosine to thymine polymorphism.

B PERL0143562, guanine to adenine polymorphism.

C PERL0146487, adenine to guanine polymorphism.

D PERL0144205, cytosine to thymine polymorphism.

However, plants in which a recombination was detected (either a Columbia/Landsberg *erecta* heterozygote or a Landsberg *erecta* homozygote) were kept for analysis with further primer sets. With this approach, the different primer sets were iteratively used to refine the location of the mutation to the co-ordinates 17,220,713 bp to 17,247,997 bp on chromosome I, representing a 27,284 bp region where the mutation responsible for *sloughy* must lie (Figure. 3.3). Only one plant had a heterozygote genotype at the location 17,220,713 bp (PERL0143983) and one other at location 17,247,997 bp (PERL0144205) (Figure 3.3). These two plants represented the limit of the fine mapping experiment, with no further additional recombination events detected with further primer sets. In arabidopsis, with a genome size of ~134,635 kb, this 27.28 kb fine mapped region represents approximately 0.0002% of the total genome.

Despite some concerns with the original fine mapping data produced in 2006, this second round of fine mapping agrees with original data, with the final co-ordinates lying within the previous round of fine mapping (Figure 3.3). This time, however, the mapping has been refined to a much smaller region of chromosome I (compare 253 kb to 27.28 kb).

3.3.2 Candidate gene sequencing

Once the genomic location of the mutation was refined with fine mapping, the next step in the forward genetic approach was to investigate the candidate genes located within the fine mapping co-ordinates. In the small, 27.28 kb fine mapping region there were only five genes present (Table 3.2). Of these, four were protein coding genes and one a transposable element which, as it was only partially within the mapping region, was not a strong candidate.

To identify the mutation, primers were designed to amplify, clone and sequence all five genes from *sloughy*, as well as from both Columbia and Landsberg *erecta*. Of the five candidate genes, only a single sequence variation was detected between *sloughy* and Columbia. This

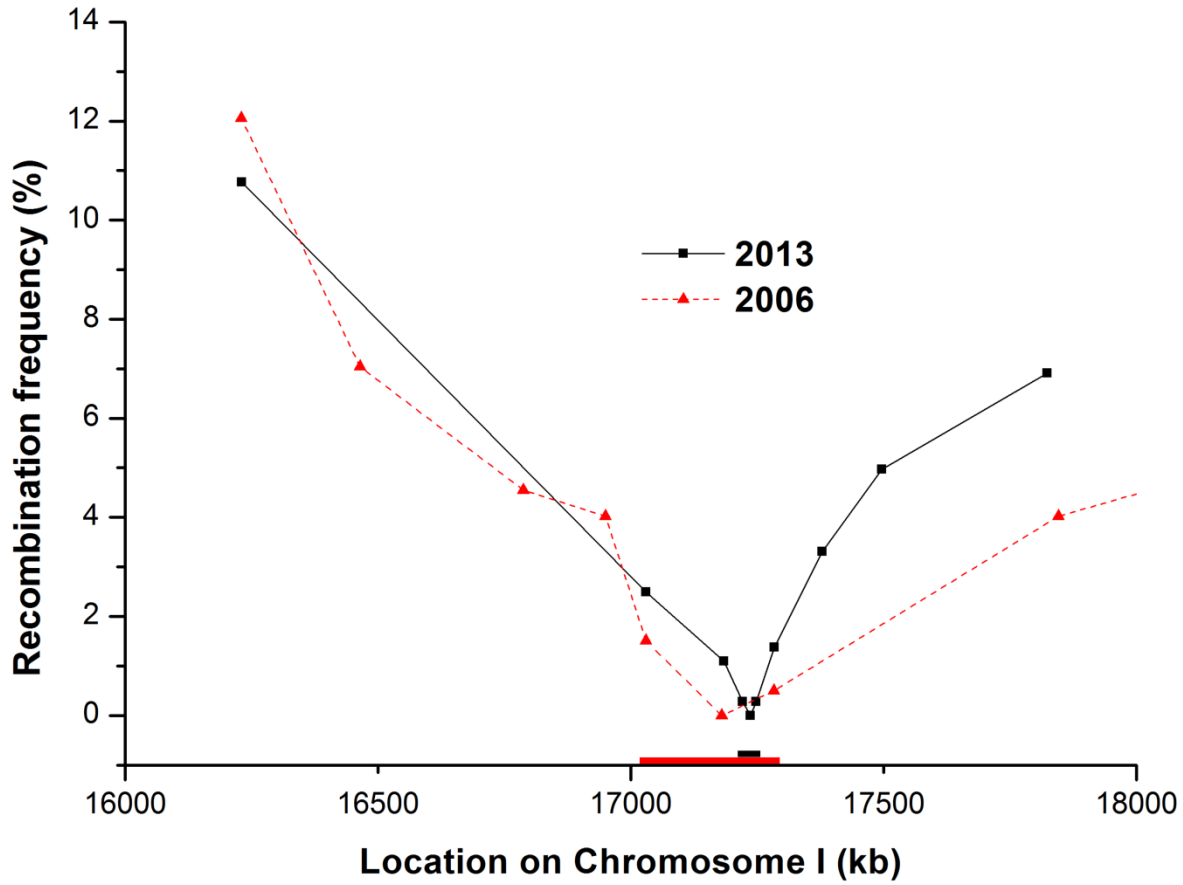

Figure 3.3 Recombination frequencies of the *sloughy* mapping population. Data from 2006 appears courtesy of Dr David Collings who utilised restriction length polymorphisms and 250 plants to generate the data. Data from 2013 comes from this project in which HRM analysis and 398 plants were used to generate the data. Coloured bars at bottom of graphs represent the fine mapped region in which the *sloughy* mutation must lie. Red bar = ~253 kb and the black bar = ~27 kb.

Table 3.2 Detailed list of candidate genes within the fine mapping region.

Locus	Name	Location (bp)	Amino acid length	Brief description[1]
AT1G46264	*SCHIZORIZA*	17,224,842 - 17,226,280	348 (1280 bp)	Encodes SCHIZORIZA, a member of the Heat Shock Transcription Factor (Hsf) family. Functions as a nuclear factor regulating asymmetry of stem cell divisions.
AT1G46336	unknown protein	17,230,411 - 17,230,653	80 (243 bp)	An unknown protein.
AT1G46408	*AGAMOUS-like 97*	17,232,135 - 17,232,935	266 (795 bp)	Encodes AGAMOUS-like 97, a sequence-specific DNA binding transcription factor activity.
AT1G46480	*WUSCHEL RELATED HOMEOBOX 4*	17,236,678 - 17,238,053	251 (1045 bp)	Encodes a WUSCHEL-related homeobox gene family member with 65 amino acids in its homeodomain.
AT1G46552	copia-like retrotransposon family	17,247,859 - 17,252,452	N/A (4,594 bp)	A member of the copia-like retrotransposon family.

[1]Information provided from TAIR (www.arabidopsis.com).

was a cytosine to the thymine mutation at 789 bp in exon 2 of the previously-described gene *SCHIZORIZA* (AT1G46264) (Figure 3.4 and Figure A2.1) (Mylona *et al*., 2002, ten Hove *et al*., 2010, Pernas *et al*., 2010). This primer set was also designed to amplify, clone and sequence ~2200 bp upstream of the *SCHIZORIZA* gene, but no additional variations were detected. This mutation was independently detected in sequencing conducted by Macrogen and in house (University of Canterbury) sequencing using a different primer sets.

When this cytosine to thymine mutation is translated into a protein sequence, an early stop codon is introduced in place of a glutamine (Figure 3.4C and Figure A2.2). This early stop codon in the SCHIZORIZA protein results in a protein truncated from 349 in wild-type to 186 amino acids in *sloughy*. The molecular weight of the wild-type protein is 39.6 kDa.

To date, five conserved regions have been identified in SCHIZORIZA (Nover *et al*., 2001, Ikeda and Ohme-Takagi, 2009) (Figure 3.4A). The DNA-binding domain represents the most conserved region of heat shock transcription factors, and is required for the specific recognition of heat stress elements (palindromic binding motifs). The hyrdophobic heptad repeat region (HR-A/B) is required for correct oligomerization and interaction with other proteins, and thus essential for the proteins specific role and regulatory behaviour. The nuclear localization and the nuclear export signals are essential for the import and export of the protein to and from the nucleus (Nover *et al*., 2001). Finally, a recently identified conserved repressive motif was identified, despite SCHIZORIZA not exhibiting any repressive activity itself (Ikeda and Ohme-Takagi, 2009). Since the *sloughy* mutation lies one amino acid upstream of the oligomerization region (HR-A/B), the truncated SCHIZORIZA protein is missing several conserved domains essential for activity.

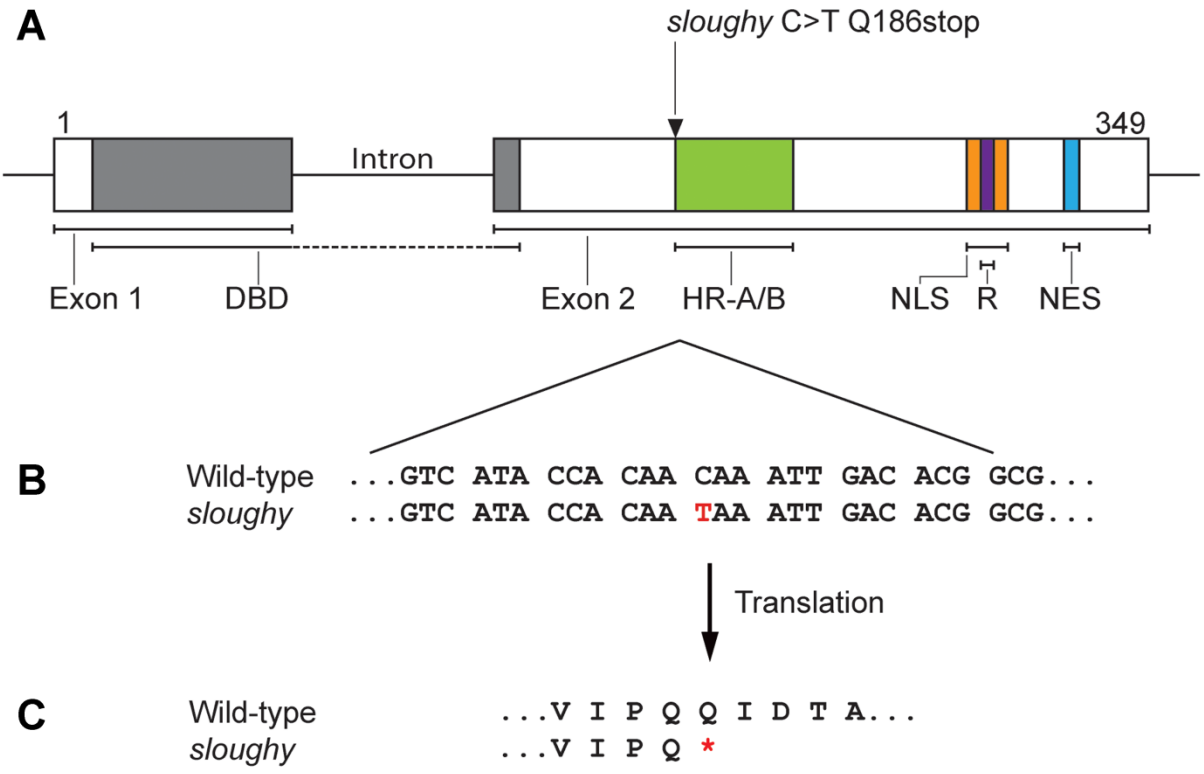

Figure 3.4 The *sloughy* mutation was detected in the *SCHIZORIZA* gene.

A. Diagram of the 1280 bp *SCHIZORIZA* gene demonstrating the two exons (279 bp and 786 bp, respectively), the intron (233 bp) and the conserved domains of the *SCHIZORIZA* gene. DNA-binding domain = DBD, oligomerization region = HR-A/B, nuclear localization signal = NLS, repression motif = R, and nuclear export signal = NES.

B. The cytosine to thymine point mutation detected in exon 2 (789 bp) of the *SCHIZORIZA* gene.

C. The glutamine to stop codon change (Q186stop) in the translated protein sequence of SCHIZORIZA. Asterisk denotes the stop codon and the end of protein translation.

3.3.3 Gene expression analysis

To identify whether misexpression of the *SCHIZORIZA* transcript may be contribute to the *sloughy* phenotype, expression analysis of the *SCHIZORIZA* gene was conducted. Total RNA was extracted from the roots of Columbia, Landsberg *erecta* and *sloughy* seedlings using a hybrid protocol of TRIzol and a QIAGEN RNeasy Mini Kit. When used by themselves, the QIAGEN RNeasy Mini Kit resulted in DNA contamination, whereas TRIzol resulted in poorer quality, degraded RNA. By combining the two protocols, TRIzol was utilized to phase separate the aqueous RNA layer from the DNA and protein precipitates, thereby eliminating DNA contamination, and then loaded onto QIAGEN RNeasy spin columns to quickly purify high quality RNA. When used concurrently, the RNA extracted was of a high quality and absent of any contaminating DNA.

Typically, two options are available in RT-qPCR. These are relative expression to reference (housekeeping) genes, or the absolute quantification of copy number. To determine if the *SCHIZORIZA* transcript was significantly altered in *sloughy* compared to that of wild-type (Columbia and Landsberg *erecta*), absolute quantification of copy number was performed on the cDNA syntheses of the RNA. Absolute quantification is based on generating a standard curve to quantify the absolute copy number of the gene transcript. To generate a standard curve, a fragment of the *SCHIZORIZA* gene, incorporating the internal RT-qPCR primers, was cloned into a plasmid. The DNA concentration of the eluted plasmid was calculated allowing the copy number of the plasmid to be calculated (5.75×10^{10} copies per µl) knowing the molecular weight of the plasmid containing the insert. Two independent, 12-fold serial dilutions were performed on the plasmid from 5.75×10^{10} copies per µl down to 0.06 copies per µl (effectively 0). Each series was amplified with qPCR in triplicates and a standard curve ($R^2 = 0.99229$) was produced (Figure 3.5). The standard curve was later imported to

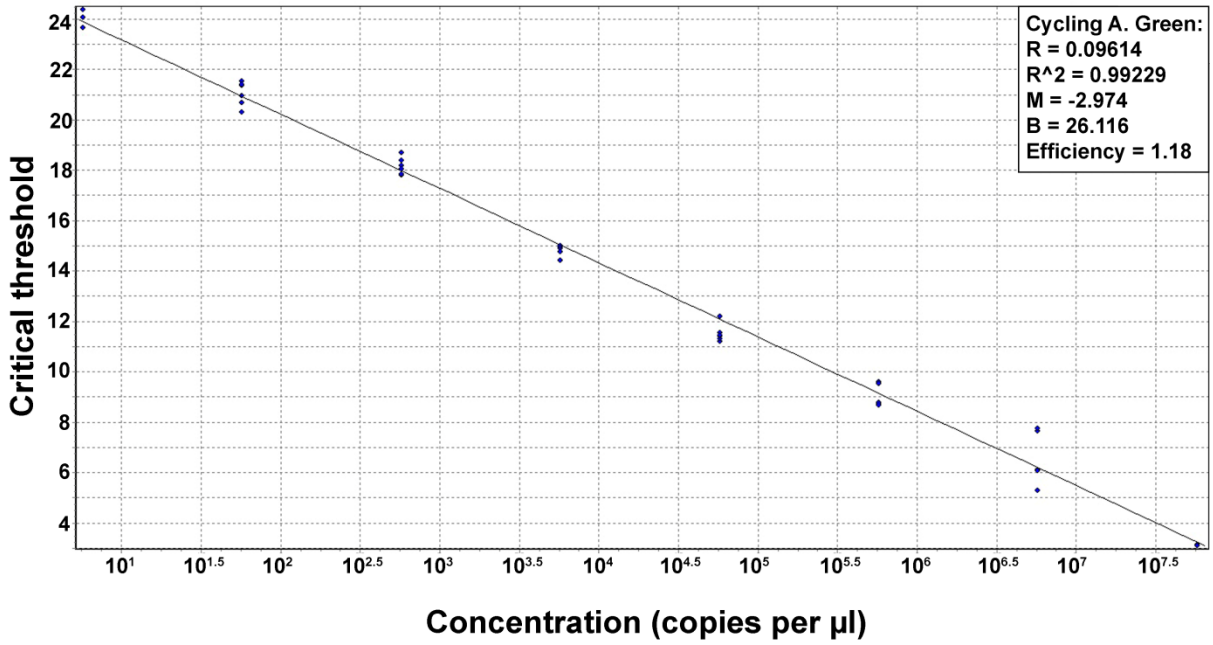

Figure 3.5 The standard curve generated with the Rotor-Gene Q Pure Detection software for absolute quantification of the *SCHIZORIZA* transcript from the roots of Columbia, Landsberg *erecta* and *sloughy* seedlings. R^2 = 0.99229. The critical threshold is an intersection between an amplification curve and a threshold line and represents a relative measure of the concentration of the amplicons in the PCR reaction.

calculate the absolute copy number of the *SCHIZORIZA* transcript from the root tissue of Columbia, Landsberg *erecta* and *sloughy* seedlings.

To normalize the cDNA, a consistent RNA extraction protocol was strictly followed and the exact same concentration of RNA for cDNA synthesis was always used. Four independent replicates of RNA extraction, cDNA synthesis, and RT-qPCR demonstrated that the expression *SCHIZORIZA* is not significantly different in *sloughy* roots comparative to wild-type Columbia or Landsberg *erecta* roots (Figure 3.6).

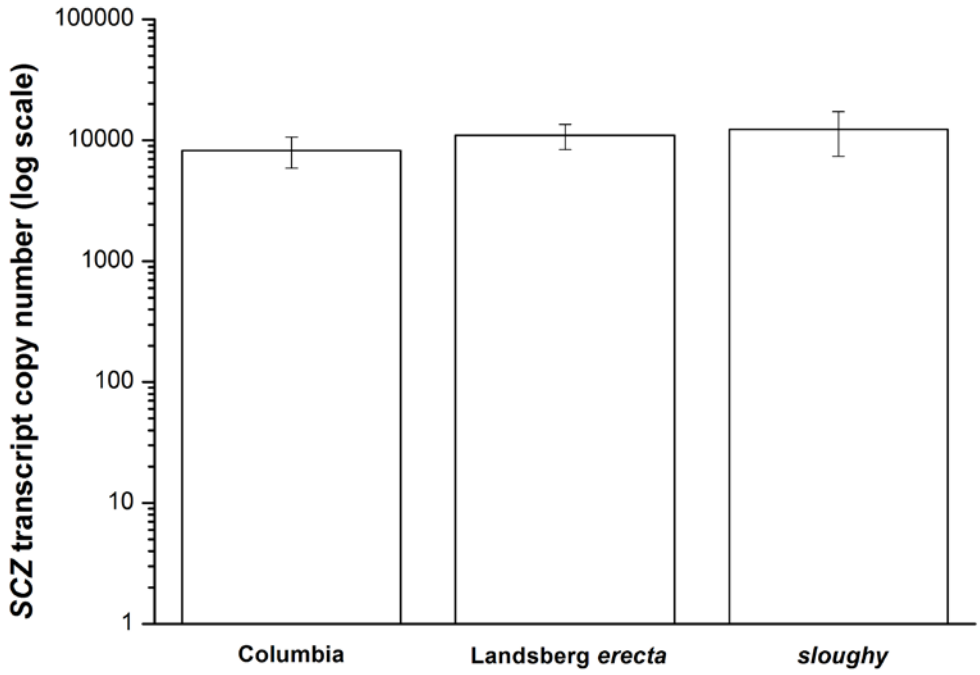

Figure 3.6 Absolute quantification of the *SCHIZORIZA* (*SCZ*) transcript copy number (log scale) from the roots of Columbia, Landsberg *erecta* and *sloughy* seedlings. Data are averages ± SEM; n = 4 independent replicate RNA extractions. No statistically significant difference (P = 0.712) was observed between any of the data sets; one-way analysis of variance (ANOVA) with a significance level of 0.05.

3.4 Discussion

3.4.1 Fine mapping the *sloughy* mutation

The mutation responsible for *sloughy's* phenotype was successfully fine mapped to a small 27,284 bp region of chromosome I (co-ordinates: 17,220,713 bp to 17,247,997 bp) using HRM analysis to detect recombination events in the *sloughy* mapping population. This region represents a very small fraction of the arabidopsis genome (approximately 0.0002%) and contains only five genes. This result demonstrates the ability of HRM analysis as an effective methodology to fine map a mapping population with high accuracy in a short period of time. This round of mapping was a significant improvement on the previous round of fine mapping in 2006, which mapped the mutation to a 253 kb region with 62 candidate genes.

Interestingly, this round of fine mapping was in agreement with the previous mapping attempt, with similar recombination frequencies observed. The low frequency of recombination observed at SGCSNP10406 in the previous round of fine mapping may have been because it was a particularly difficult marker to detect with restriction enzymes and gels. The original fine mapping co-ordinates did contain the *sloughy* mutation, despite the suspicion that a mistake had been made with misleading results. Thus, in contrast to what was previously thought, no mistake had been made in the previous round of fine mapping. This means that it was the later stages in indentifying the responsible mutation that did not yield success. It is also worth noting that although *schizoriza* mutants were first described in 2002 (Mylona *et al*., 2002), it was not until later in 2010 that the *SCHIZORIZA* gene was cloned (ten Hove *et al*., 2010, Pernas *et al*., 2010). This contributed to *SCHIZORIZA* not being identified as a strong candidate gene in the previous round of fine mapping. An analysis of

the gene's name would have ensured that this gene would have sequenced at the time, as schizoriza means "split root" (from Greek *schizein* meaning to split and *rhiza* meaning root).

3.4.2 Candidate gene sequencing

Four protein coding genes and one a transposable element were identified in the fine mapping co-ordinates. These were *SCHIZORIZA*, an unknown protein, *AGAMOUS-LIKE-97* and *WUSCHEL RELATED HOMEOBOX 4*, and a member of the copia-like retrotransposon family, respectively. On sequencing all five genes, only one sequence variation was detected between *sloughy* and Columbia. This was a cytosine to thymine point mutation in exon 2 of the previously-described *SCHIZORIZA* gene (Mylona *et al*., 2002, ten Hove *et al*., 2010, Pernas *et al*., 2010). Contrary the function that was originally hypothesized for the mutated gene, SCHIZORIZA is a member of the heat shock transcription family (HsfB4) which acts a cell fate determinate in the root meristem (Mylona *et al*., 2002, ten Hove *et al*., 2010, Pernas *et al*., 2010), and is not directly involved in the biosynthesis or metabolism of the plant cell wall. Although *SCHIZORIZA* encodes a member of the family of heat shock transcription factors, diverse microarray data has shown that HsfB4 is not involved in stress signalling (ten Hove *et al*., 2010). A full review of the literature on the *SCHIZORIZA* gene is provided in section 4.1.3.

This cytosine to thymine point mutation was independently sequenced by Macrogen and by in house (University of Canterbury) sequencing using different primers confirming that it was not a sequencing error. Furthermore, EMS predominantly induces cytosine to thymine point mutations randomly throughout the genome, supporting the successful identification of an EMS-induced mutation in *sloughy* (Gady *et al*., 2009). Together, these results are in strong support that the *sloughy* mutation has been successfully identified, one of the primary objectives this project.

Primers were also subsequently designed that detected the cytosine to thymine mutation in *sloughy* plants using HRM analysis (see section 4.3.1). These primers might be useful for tracking *SCHIZORIZA* heterozygote in crosses, but have not been specifically used for this purpose in this thesis.

When the *sloughy* mutation is translated into a protein sequence, an early stop codon is introduced in place of a glutamine, resulting in a protein truncated from 349 amino acids in wild-type to 186 amino acids in *sloughy*. This truncated SCHIZORIZA protein is missing several conserved domains essential for its activity, including the oligomerization region (HR-A/B), which is essential for the interaction with other proteins, and the nuclear localization and export signals, which are essential for the localization of the protein to the nucleus where it is active. The absence of these conserved domains would seriously impact the function of the SCHIZORIZA as a transcription regulator.

Typically, once a mutated gene has been identified in a forward genetic screen, the next step is to complement the mutant with the cloned wild-type gene, as this provides the most compelling evidence that the mutation does indeed cause the mutant phenotype. In this study, however, the complementation of *sloughy* with the wild-type *SCHIZORIZA* gene was not pursued for several reasons.

The fine mapping and sequencing data was already in strong support that the mutated gene had been successfully identified. Furthermore, the wild-type *SCHIZORIZA* gene has already been demonstrated to fully complement the *schizoriza* mutant, providing compelling evidence that the *SCHIZORIZA* gene is indeed responsible for the *schizoriza* mutant phenotype (ten Hove *et al*., 2010). Thus, as an alternative to complementation, a collection of *schizoriza* mutants were ordered for a phenotypic comparison to *sloughy*. This represented an economical approach, both in time and resources, to determine whether the SCHIZORIZA

gene was indeed responsible for the cell separation phenotype, as this was the primary motive at the time. This line of enquiry is presented as part of Chapter 4

Thought was also given to transform *sloughy* with a *SCHIZORIZA*-GFP fusion construct. The advantages of using a GFP fusion protein are that they can be used as a reporter of expression, and also allow for the cellular movement and localization of the protein to be tracked. However, it has been previously demonstrated that *SCHIZORIZA* is exclusively active in the ground tissue stem cells in the root meristem (see section 4.1.1) and it is thought that the protein itself does not travel between cells (ten Hove *et al*., 2010). Thus, *SCHIZORIZA*-GFP fusion protein would likely not reveal any further novel information and were not pursued further.

It would also be necessary to complement *sloughy* with the native promoter of the *SCHIZORIZA* gene in place of the more traditional over-expression methodology with the cauliflower mosaic virus 35S promoter (Odell *et al*., 1985) as this approach would result in a an over-expression phenotype (Begum *et al*., 2013) rather than a wild-type phenotype. Analysis of these *SCHIZORIZA* over-expression plants are presented in section 4.3.1. Thus, complementing *sloughy* with the appropriate wild-type gene appeared more challenging than originally thought and was not pursued.

3.4.3 Gene expression analysis of *SCHIZORIZA*

To test whether the misexpression of the *SCHIZORIZA* transcript may be a casual factor to the *sloughy* phenotype, absolute quantification of the *SCHIZORIZA* transcript was carried out. One of the contributing reasons for this line of enquiry was the fact that *SCHIZORIZA* over-expressing plants had been reported to possess aberrant cell separation further up the root (Begum *et al*., 2013). Thus, one possibility to explain the cell separation phenotype observed in *sloughy* roots, would be that the *sloughy* mutation may possess a *SCHIZORIZA*

over-expression phenotype. Although analysis of *SCHIZORIZA* over-expression plants is documented in section 4.3.1, a simple phenotypic comparison of the plants to *sloughy* would not be conclusive. Accordingly, gene expression analysis was undertaken.

Using RT-qPCR, it was determined that *SCHIZORIZA* was not differentially expressed in the roots of *sloughy* compared to Columbia and Landsberg *erecta*. These results were based on four independent replicates of RNA extraction, cDNA synthesis, and RT-qPCR. In all of the independent runs performed, there was no indication that the expression levels of *SCHIZORIZA* in *sloughy* were significantly different. Since the mutation identified in *sloughy* should only affect the translation of the *SCHIZORIZA* transcript into a protein, by way of introducing of an early stop codon, and not the expression levels of the gene itself, these results were not surprising. Thus, the gene expression analysis confirmed that the *sloughy* phenotype is not a consequence of misexpression of the *SCHIZORIZA* gene. Instead, the *sloughy* phenotype is likely a result of the truncated *SCHIZORIZA* protein missing several conserved domains essential for its activity.

3.5 Summary

- The *sloughy* mutation was mapped to a small 27,284 bp region on chromosome I using HRM analysis and SNPs as molecular markers to calculate recombination frequencies.
- Four protein coding genes and one transposable element were identified within the fine mapping region and sequenced.
- A mutation introducing a stop codon was detected in exon 2 in the previously-described transcription factor *SCHIZORIZA*, resulting in a truncated protein missing several conserved domains essential for activity.
- SCHIZORIZA acts a cell fate determinate in the root meristem, and is not directly involved in the biosynthesis or modification of the plant cell wall.
- The *SCHIZORIZA* transcript is not differentially expressed in *sloughy*.

Chapter 4

Cellular Characterization of *sloughy*, an Allele of *SCHIZORIZA*

"The schizophrenic is supremely creative in an almost extra-human sense because he is furthest from the animal: he lacks the secure instinctive programming of lower organisms; and he lacks the secure cultural programming of average men. No wonder he appears to average men as "crazy": he is not in anything's world."

- Ernest Becker (The Denial of Death, 1997)

4.1 Introduction

Mutations in the *SCHIZORIZA* gene lead to confused cell identity within the developing root, and have been investigated, as described in this chapter, using tissue-specific markers. Before reviewing the literature on *SCHIZORIZA*, brief overviews will be provided on meristematic tissues, the use of tissue-specific markers to study cell fate, and root developmental mutants.

4.1.1 Root meristematic tissue in plant growth and development

Meristems can be defined as localized sites of continued cell division of undifferentiated tissue, and are found at specific sites in the plant body (Graham *et al*., 2000, McManus and Veit, 2002). Meristems contain undifferentiated (meristematic) cells, analogous to stem cells found in animals. Primary meristems are spatially separated into the shoot apical meristem and the root apical meristem, which are located at the tip of the shoot and root axis in plants, respectively. In addition to these main locations, apical meristems are also found in the tip of each axillary shoot and lateral root. The primary function of apical meristems is to give rise to the organs of a plant, and to enable their growth. Meristems can be viewed as output/input systems, where continued cell division by mitosis adds more cells into the meristem, while cells are removed from the meristem via elongation and differentiation (McManus and Veit, 2002).

Secondary meristems are also present in plants. These include the vascular cambium and the cork cambium, which enable plant organs (stems and roots) to increase in diameter. Secondary meristems are not discussed further in this thesis.

The arabidopsis root is organised into concentric layers of cells composing the three principal tissue systems:

i. Dermal tissue.
ii. Ground tissue.
iii. Vascular tissue.

The dermal tissue is composed of a single layer of epidermal cells which surrounds the ground tissue. The ground tissue is composed of two layers, the cortex and the endodermis, with the cortex located between the epidermis and the endodermis. The endodermis surrounds the vascular tissue (the stele) which contains the pericycle, xylem and phloem.

Each concentric cell layer in the root can trace its origins back to a particular domain of stem cells (also known as initials) laid down during embryogenesis of the root meristem (Mylona *et al*., 2002). These domains of stem cells surround an organising centre of mitotically inactive cells, the quiescent centre (Clowes, 1956). The quiescent centre likely maintains the stem cells by producing signals that inhibit their differentiation (van den Berg *et al*., 1997, Knauer *et al*., 2013). The stele arises from a set of vascular stem cells above the quiescent centre, while the cortex and endodermis arise from a cortical/endodermal stem cell which first divides anticlinally (new wall perpendicular to the root surface) to regenerate itself and to produce a cortex/endodermis daughter cell. This cortex/endodermis daughter cell then divides periclinally (new wall parallel to the root surface), with the inner cell forming the endodermal cell layer and the outermost cell forming the cortex cell layer (Dolan *et al*., 1993). The epidermal and lateral root cap layers originate from a domain of protodermal stem cells, the outermost tissue layer of the embryo, that divide periclinally to a form a pair of cells (Dolan *et al*., 1993, Cnops *et al*., 2000). The inner cell undergoes a number of anticlinal divisions to form the epidermal layer, while the outermost cell undergoes a series of divisions

to form the lateral root cap layers. The columella, a distinct tissue system that is found in the very tip of the root and which is responsible for gravitropism, is derived from a set of columella stem cells below the quiescent centre, and together with the lateral root cap cells compose the root cap. In the root tip, the lateral root cap cells surround the epidermal and columella cells, but as the root transitions into the elongation zone, these lateral root cap cells slough off and die (Cnops *et al.*, 2000).

4.1.2 Arabidopsis GAL4-GFP enhancer trap lines as tissue markers

The GAL4 enhancer trap line system was first developed in the fruit fly (Brand and Perrimon, 1993) and later adopted for arabidopsis by Haseloff and colleagues (Haseloff, 1999). The GAL4-GFP enhancer trap line system in arabidopsis uses a T-DNA vector which contains the gene for the yeast transcription activator protein GAL4 without any promoter and an endoplasmic reticulum-targeted GFP driven by a GAL4-responsive promoter. This vector was designed so that when it was randomly transformed into plants, the expression of *GAL4* would be dependent on the fortuitous proximity to an enhancer element, a short region of DNA that can activate the transcription of a gene (Haseloff, 1999). As a result, different tissue- or cell-specific patterns of *GAL4* would be expressed depending upon which tissues or cells the enhancer is active in. The GAL4 protein then activates the GAL4-responsive expression of GFP allowing for these patterns of expression to be detected, with the *GAL4*-expressing tissues or cells marked with an endoplasmic reticulum-targeted GFP that cannot leak from one cell to adjacent cells via plasmodesmata. Over 7500 arabidopsis plants were transformed with this vector and their roots screened for GAL4-dependent expression of GFP. From this, a collection of 250 arabidopsis lines with distinct and stable patterns of GFP expression in the root were selected, and these have been made available through the ABRC (Haseloff, 1999).

The original intention of these enhancer trap lines was to develop a system for the tissue-specific expression of genes. Individual plants would be transformed with a particular gene of interest coupled to a GAL4 promoter and crossed to enhancer trap lines to drive the expression of that gene in specific tissues or cell types. However, the primary use of arabidopsis GAL4-GFP enhancer trap lines has been as tissue- or cell-specific markers to track cell fate during morphogenesis and development. These marker lines have proven useful in characterizing mutants with defects in developmental processes. Since such mutations often impact cell fate within the developing plant, it can often be difficult to determine the identity of cells in which the mutation modifies cellular identity. By crossing the developmental mutant to a GAL4-GFP enhancer trap line, it is possible to determine cellular identity by observing the expression patterns of GFP. Thus, the available collection of the GAL4-GFP enhancer trap lines have proven particularly powerful in plant developmental research. One area that these enhancer trap line have been used to investigate cell identity are the root patterning mutants described in the next section.

4.1.3 Root patterning mutants in *Arabidopsis thaliana*

The isolation of arabidopsis mutants with defects in the formation and maintenance of the root meristem, and the cloning of their respective genes, has proven incredibly powerful in elucidating the molecular mechanisms underpinning root development (McManus and Veit, 2002). Of note are the root patterning mutants *scarecrow*, *shortroot* and *woodenleg* (Scheres *et al*., 1995), *tornado1* and *tornado2* (Cnops *et al*., 2000), *anthocyaninless2* (Kubo *et al*., 1999), and *argonaute1* (Miyashima *et al*., 2009).

The *scarecrow* (*scr*), *shortroot* (*shr*) and *woodenleg* (*wol*) mutants were isolated by Ben Scheres and colleagues (Scheres *et al*., 1995) at the University of Utrecht, The Netherlands in a forward genetic screen for mutations that cause pattern defects in the root. The *scr* and *shr*

mutants were identified among a T-DNA-mutagenized population, while the *wol* mutant was identified from an EMS-mutagenized population. Both the *scr* and *shr* mutants contain only a single layer of ground tissue instead of the two distinct layers (cortex and endodermis) present in wild-type (Scheres *et al*., 1995). This shows that that SHR and SCR are required for the periclinal division of the cortex/endodermal daughter cell that give rise to the two distinct cortex and endodermal cell layers. The use of tissue-specific markers has shown that the single ground tissue cell layer in the *scr* mutant has both cortex and endodermal identity, demonstrating that SCR is important in the regulation of the periclinal division of the cortex/endodermal daughter cell, rather than specifying the cell fate of either the cortex or endodermis (Di Laurenzio *et al*., 1996). In the *shr* mutant, the single ground tissue layer has cortex identity, indicating that *shr* is not only necessary for the periclinal division of the cortex/endodermal daughter cell, but also for promoting the cell fate of the endodermis (Helariutta *et al*., 2000). In wild-type, *SCR* expression occurs in the cortex/endodermal daughter cells and the endodermis lineage, indicating that SCR is expressed and acts autonomously in the cells in which it required. In contrast, *SHR* expression is absent from ground tissue, but present in the adjacent stele tissue. This shows a non-cell-autonomous mode of action in which the SHR protein is produced in one cell type but active in another (Helariutta *et al*., 2000). The generation of *scr/shr* double mutants has also shown that SCR and SHR act in a common pathway, while *shr* mutants have a decreased amount of *SCR* transcript, suggesting that SHR acts upstream and is required for the transcription of SCR (Helariutta *et al*., 2000). *SCR* and *SHR* both encode related members of the GRAS family of transcription factors (Di Laurenzio *et al*., 1996, Helariutta *et al*., 2000).

The Scheres group (Aida *et al*., 2004) also identified the *PLETHORA1* (*PLT1)* and *PLT2* genes. These encode redundant AP2 class transcription factors which are required, and act in parallel with SCR- and SHR-mediated patterning, to define and maintain the quiescent centre

and stem cell positions in the root meristem. Whereas single T-DNA insertion mutants of *PLT1* or *PLT2* cause subtle defects in the quiescent centre and columella cells, the double mutant has a drastic impact on the organisation and maintenance of the root meristem. Root growth is extremely reduced with the columella containing significantly more cells and the number of meristematic cells significantly reduced. By the age of 6 - 8 days, all stem cells in the root meristem differentiate, and root hairs and xylem form all the way to the root tip. The double mutants also produce more lateral roots, resulting in a highly branched root system. *PLT1* and *PLT2* expression is stimulated by auxin and are hypothesized to be effectors of auxin accumulation patterns during organ development (Aida *et al*., 2004).

Scheres and colleagues (Welch *et al*., 2007) also identified the *SCR/SHR* interacting genes *JACKDAW* (*JKD*) and *MAGPIE* (*MGP*). JKD and MGP encode zinc finger proteins that directly interact with SHR and SCR to regulate stem cell divisions and tissue boundaries within the ground tissue. Recently, the SCR/SHR interacting protein SHRUBBY (SHBY) was also identified through yeast two-hybrid screening (Koizumi and Gallagher, 2013). T-DNA insertions in *SHBY* change both the longitudinal and concentric patterning of the arabidopsis root, decrease meristem activity and increase cell divisions in the ground tissue resulting in supernumerary ground tissue layers. In addition to SHR and SCR, SHBY was shown to regulate the levels of PLT1 and PLT2 (Koizumi and Gallagher, 2013).

Whereas the *scr* and *shr* mutants both specifically affect the development of the ground tissue, the *wol* mutant interferes with the organisation of the stele (Scheres *et al*., 1995). The *wol* mutants have fewer vascular stem cells, resulting in a vascular system comprised of only protoxylem, with metaxylem and phloem completely absent. This shows that WOL controls cell number in the stele, as well as phloem and metaxylem differentiation (Scheres *et al*., 1995, Mahonen *et al*., 2000). The *WOL* gene encodes a member of a family of two-component regulators that are thought to act as a receptor that controls asymmetric cell

divisions in the vascular stem cells. *CYTOKININ REPSONSE 1* (*CRE1*), which was identified as a cytokinin receptor, is allelic to *WOL* suggesting that cytokinin plays a role in the development of the stele (Inoue *et al*., 2001).

The *tornado1* (*trn1*) and *trn2* mutants, which cause severe dwarfism and twisted growth of all organs, were characterized by Liam Dolan and colleagues at the John Innes Centre, UK (Cnops *et al*., 1996, Cnops *et al*., 2000). The periclinal division of the protodermal stem cells which gives rise to the epidermal and lateral root cap layers are defective in the *trn1* and *trn2* mutants. In the root tip, a subset of epidermal cell files contain long, thin cells exhibiting lateral root cap-like features. These cells die upon transition to the elongation zone leaving gaps in the epidermis that runs along the length of the root (Cnops *et al*., 2000). A lateral root cap-specific marker line shows that the subset of lateral root cap-like cells in the epidermis exhibits partial lateral root cap identity. These results mean that TRN1 and TRN2 are required for the periclinal division of the protodermal stem cells and act as negative regulators of lateral root cap fate in the epidermis (Cnops *et al*., 2000). *TRN1* encodes a large, plant-specific protein of unknown function while *TRN2* is a transmembrane protein of the tetraspanin (TET) family (Cnops *et al*., 2006).

A forward genetic screen of EMS-mutagenized seeds based on the direct observation of aberrant root organization resulted in a collection of novel mutants containing three-layers of ground tissue that lack a concentric organisation (Miyashima *et al*., 2009). The mutants were found to be allelic to *ARGONAUTE1* (*AGO1*), which encodes a catalytic component of the RNA-induced silencing complex that plays a central role in RNA interference. The action of AGO1 on ground tissue patterning is independent of SCR and SHR action. Thus, the organisation and maintenance of the ground tissue is mediated by two independent pathways, one post-transcriptional pathway mediated by AGO1 and the other with SCR/SHR acting as transcriptional regulators (Miyashima *et al*., 2009).

This brief review demonstrates the ability of forward genetic screens to elucidate the complex genetic framework which controls the development of the root meristem. Complementing this work has been the characterization of the *schizoriza* mutant, which was first isolated during a screen for root mutants with defects in root epidermal development (Mylona *et al*., 2002). Research on *schizoriza* has revealed a novel mechanism for the specification of ground tissue and epidermal cell fate in the developing root.

4.1.4 SCHIZORIZA plays a crucial role in the development and maintenance of the root meristem

The *shizoriza* mutant that was initially described by the Dolan group (Mylona *et al*., 2002) as having hairier roots than wild-type plants, with the development of root hairs from a subepidermal layer.

In wild-type, the cortex/endodermal daughter cell undergoes a single periclinal division to produce two layers, the cortex and the endodermis. In *schizoriza*, however, an additional round of periclinal cell division takes place, resulting in a root with three ground tissues layers. The location of the epidermis and lateral root cap daughter cells in the root meristem is difficult to define, and the quiescent centre is displaced upwards (Mylona *et al*., 2002).

Crosses of *schizoriza* to the epidermal-specific GAL4-GFP enhancer trap line J0481, which expresses GFP solely in the root epidermis, show that both the epidermal and subepidermal layers have epidermal identity in the *schizoriza* root meristem. However, crosses to the cortex/endodermis-specific marker line J0571 and the endodermis-specific lines J3611 and J2672 did not show expression in the subepidermal layer. This demonstrates that although the subepidermal layer derives from an extra ground tissue division, it has epidermal and not ground tissue identity. This accounts for the development of subepidermal root hairs, and

suggests that SCHIZORIZA may act as a suppressor of epidermal cell fate in the ground tissue (Mylona *et al*., 2002).

Double mutants of *schizoriza* with either *scr* or *shr* suppressed the extra periclinal divisions, resulting in plants with a single ground tissue layer. This indicated that these genes act in the same pathway in the regulation of cell division in the root meristem. In this initial description of the *schizoriza* mutant, the gene responsible for the *schizoriza* phenotype was not identified (Mylona *et al*., 2002).

It was not until 2010 that the *SCHIZORIZA* gene was located and the mutant described in significantly greater detail by both the Scheres and Dolan groups (ten Hove *et al*., 2010, Pernas *et al*., 2010). To find novels genes involved in the maintenance of the root meristem, Scheres and colleagues mutagenized homozygous lines expressing quiescent centre-specific markers, and the F2 progeny were screened for altered expression patterns. A collection of independent, allelic mutants to *schizoriza* with reduced root growth, a disorganized meristem and hairier roots were isolated. SCHIZORIZA encodes for *HEAT SHOCK TRANSCRIPTION FACTOR B4* (*HsfB4*) (AT1G46264), a member of the arabidopsis heat shock transcription factor family (ten Hove *et al*., 2010, Pernas *et al*., 2010), albeit one that is not recruited to stress response. The identical phenotypes of the collection of mutants, including two *schizoriza* TILLING mutants obtained from the ABRC (lines CS88021 and CS93157 respectively) indicated that they are all likely to be HsfB4 null mutants (ten Hove *et al*., 2010).

The analysis of cortex and endodermal specific markers, taken in account with cell morphological characteristics, demonstrated that both the innermost layer next to the stele and next layer out represent endodermis, with cortex identity abolished in the ground tissue.

These results are consistent with SCHIZORIZA also playing an essential role in the specification of cortex cell fate (ten Hove *et al*., 2010).

The expression patterns of *WEREWOLF* (*WER*)-*GFP*, a lateral root cap and epidermal-specific marker (Lee and Schiefelbein, 1999), and *SOMBRERO* (*SMB*)-*GFP*, a lateral root cap-specific marker (Willemsen *et al*., 2008), were analyzed in *schizoriza*. The two markers were expressed in both of the epidermal and subepidermal layers, demonstrating that the epidermal and subepidermal layers in *schizoriza* root meristems possess mixed epidermal and root cap identity. The identity of these cells in regions of that root above the meristem were not provided. Since the nearest tissue expressing *SCHIZORIZA* is the cortex, it is likely that SCHIZORIZA acts non-cell-autonomously in regulating epidermal and lateral root cap fate, being expressed in specific cells but taking effect in adjacent cells (ten Hove *et al*., 2010).

The *SCHIZORIZA* gene was expressed under several different tissue-specific promoters in *schizoriza* and the complementation of the mutant phenotype examined. The *schizoriza* mutant was only complemented with cortex and endodermis specific expression. Since none of the other tissue specific promoters could complement *schizoriza*, the activity of SCHIZORIZA was determined to be specifically required in the ground tissue to specify correct cell fate in the developing root. The non-cell autonomous action of SCHIZORIZA is thought to be a through an unknown ground tissue-derived factor (ten Hove *et al*., 2010).

Over-expression of SCHIZORIZA with the *35S* promoter introduces new cell fates in the developing root, with *SCHIZORIZA* over-expressing (*SCZ*-OE) plants having with extra cortex/endodermis, columella, epidermis and lateral root cap stem cells in the root meristem leading to supernumerary cell layers in the root (ten Hove *et al*., 2010, Pernas *et al*., 2010, Begum *et al*., 2013). This indicates that the ectopic expression of *SCHIZORIZA* is sufficient

to promote stem cell identity in the root meristem and to maintain these cells in an undifferentiated stem cell state (Pernas *et al*., 2010).

4.1.5 *schizoriza* phenotypes elsewhere within the plant

To date, published work on *SCHIZORIZA* has focused almost exclusively on the root meristem, with little documentation on the mature root or above-ground organs (Mylona *et al*., 2002, ten Hove *et al*., 2010, Pernas *et al*., 2010). In the original paper describing *schizoriza* (Mylona *et al*., 2002), no mention was made to an aberrant cell separation in the mature root, nor was there any mention in the subsequent paper from the Dolan group (Pernas *et al*., 2010). However, Scheres and colleagues described the epidermal cells in the mature root as long and flat, morphologically reminiscent of lateral root cap cells and indicative of mixed epidermal and lateral root cap identity. It was noted that

> "*whereas epidermal cell files are tightly connected in the wild-type, they separate as tissues mature in schizoriza, a feature that is restricted to root cap cells in the wild-type*"

This tissue separation was not explored further (ten Hove *et al*., 2010).

The roots of *SCZ*-OE seedlings have been reported to be significantly wider than wild-type, on the account of the numerous supernumerary layers. Interestingly, the roots were revealed to possess a rough surface, with the detachment of cells in the elongation and differentiation zones (Begum *et al*., 2013). The rough surface of the roots was linked to the proliferation of ectopic epidermal and lateral root cap layers further up in the root that detached after prolonged root growth. *WER*-GFP expression was reduced further up in the roots, indicating that the cells may have lost lateral root cap identity upon transition into the mature root (Begum *et al*., 2013).

In respect to the expression of the *SCHIZORIZA* gene in wild-type plants, expression is highest in the quiescent centre and ground tissue stem cells and their immediate daughter cells, as determined by in situ hybridization (ten Hove *et al*., 2010). Expression is absent in the columella and lateral root cap cells, and also absent in the subepidermal layer in *schizoriza* (ten Hove *et al*., 2010, Begum *et al*., 2013). Consistent with its function as a transcription factor, SCHIZORIZA localizes to the nucleus (ten Hove *et al*., 2010). Although no above-ground phenotypes have been reported for *schizoriza* or *SCZ*-OE plants, RT-qPCR has detected low levels of expression in the shoot apex and leaves, and GUS-staining has been detected in many above-ground, including the shoot apex, pistils, seeds, and the base of siliques plants organs in wild-type plants (Begum *et al*., 2013). No explanation has been provided for why *SCHIZORIZA* expression has been detected in these parts of the plants.

4.1.6 Objectives

Once the mutated gene had been identified in *sloughy*, the primary objective of this project shifted from the molecular characterization of *sloughy* to elucidating how this mutation results in the cell separation phenotype in *sloughy* roots. Several experiments were designed to explore this further.

- Growth and development in *sloughy* will be compared to a collection of EMS-generated *schizoriza* TILLING mutants and *SCZ*-OE plants to explore cell separation phenomena.
- *sloughy* will be crossed to GAL4-GFP enhancer trap lines to dissect cell identity in the elongation zone of *sloughy*, notably the cells displaying aberrant cell separation. These GAL4-GFP enhancer trap lines will include endodermal and cortex, epidermal, and root cap-specific marker lines.

- Cell wall biochemistry will be probed with a collection of antibodies to detect any biochemical changes that may be present in *sloughy* roots, and thus the cell wall modifications that may contribute to the reduced cell adhesion observed in the separating epidermal cells.

When combined with the previously collected data on the *schizoriza* mutants from the literature, these experiments should provide sufficient evidence to present a model on how the *sloughy* mutation leads to aberrant cell separation.

4.2 Methods

4.2.1 Analysis of *schizoriza* TILLING mutants and *SCZ*-OE lines

A collection of six *schizoriza* TILLING mutants were ordered from the ARBC (Table 4.1) and three independent *SCZ*-OE lines (*HsfB4*-OE5, *HsfB4*-OE7 and *HsfB4*-OE8) were donated by Friedrich Schöffl from Tübingen University, Germany. *SCHIZORIZA* expression levels are increased 75- to 434-fold in these *SCZ*-OE lines. Focus was placed on *HsfB4*-OE8 for comparative analysis, as this was the line that was reported upon by Schöffl and colleagues (Begum *et al*., 2013).

To confirm that that the reported mutations in the *schizoriza* TILLING mutants were present, primers were designed to clone, amplify and sequence the *SCHIZORIZA* gene in wild-type, *sloughy* and all six *schizoriza* TILLING mutant plants (Table A1.4). To sequence the gene, the plants were grown on soil (see section 2.2.1), their DNA extracted (see section 3.2.2) and prepared for sequencing (see section 3.2.5), and sequenced by primer walking (Macrogen, Seoul, South Korea). Primers were also designed to detect the mutations using HRM analysis in all of the *schizoriza* TILLING mutants and *sloughy*, which allowed for the easy and rapid genotyping of the mutant plants (Table A1.4). HRM analysis of wild-type, *sloughy* and the *schizoriza* TILLING mutant plants were carried out as described in section 3.2.4. All temperature-sensitive growth assays of wild-type, *sloughy*, *schizoriza* TILLING mutants and *SCZ*-OE seedlings were carried out as described in section 2.2.2.

4.2.3 GAL4-GFP enhancer trap line crosses

A collection of Arabidopsis GAL4-GFP enhancer trap lines were ordered form the ABRC (Table 4.2). Seed from the GAL4-GFP enhancer trap lines was grown on agar and screened for fluorescence with a Leica MZ10F stereomicroscope (Leica, Wetzlar, Germany), with plants expressing GFP being transferred to soil (see section 2.2.1).

The plants were crossed by hand using forceps aided by a dissecting microscope (Olympus, Tokyo, Japan). The microscope stage, forceps and hands were sterilised with 95% (v/v) ethanol and air dried to remove any contaminating pollen before handling parent plants. The GAL4-GFP enhancer trap lines were used as pollen donors, as expression of GFP in the progeny would confirm that the cross had been successful. A suitable pollen-donor for the cross was chosen by selecting flowers that had petals opened perpendicular to the main flower body, which is when the flowers would have anthers releasing pollen. The flowers were removed from the plant, the release of pollen grains confirmed, and the petals and sepals removed. For the female parent, a suitable pollen-acceptor was chosen by selecting young flower buds with white petals just beginning to emerge. These buds would contain short, immature stamens free of pollen grains but which would have receptive stigmas. A female parent plant that had several young flower buds located near the top of the inflorescence was pinned down to the stage of the dissecting microscope using blu-tack. All other flower buds and flowers that were not in the correct stage of development were removed from the inflorescence. The sepals and petals of the young flower buds were gently opened with forceps, and the immature stamens were removed. The stigma was then pollinated with the male anthers. Once pollination was completed, a paper cover was put on the pistil to protect it from other pollen sources. Following successful pollination, the pistil elongated as the seeds developed. Once the silique had fully elongated and dried to a golden-brown colour, it was removed from the plant and dried in an Eppendorf tube for a week

before harvesting. The seeds were then stored in 4°C for several days to increase frequency of germination before planting.

The F1 progeny of the crosses, which would be heterozygous for the *sloughy* mutation, were grown on agar and screened to ensure a wild-type phenotype was present (*sloughy* is recessive) and for the expression of GFP with the Leica MZ10F stereomicroscope. Plants expressing GFP were transferred to soil and selfed to generate the F2 population. The F2 plants were screened for plants displaying both a *sloughy* phenotype (25%) and the presence of GFP and imaged by confocal microscopy, with F2 plants displaying both the wild-type phenotype (75and GFP as controls. Fluorescent and concurrent transmitted light images were recorded with a Leica SP5 confocal microscope with 20x and 63x glycerol immersion lenses. To visualise cell walls, arabidopsis seedlings were incubated in propidium iodide (20 µM in distilled water, 5 min) and immediately viewed with the confocal microscope. The laser excitation wavelength used for GFP was 488 nm and the emitted fluorescence was captured from 500 nm to 550 nm. The laser excitation wavelength used for propidium iodide was 514 nm and the emitted fluorescence was captured from 565 nm to 721 nm. For imaging with the 20x and 63x lens, line averaging was set at 4 and z-sections step size at 2 µm. For generating reconstructed cross sections with the 63x lens, line averaging was set at 4 and z-sections step size at 0.5 µm. Images were processed and the reconstructed cross sections were generated as described in section 2.2.3.

4.2.3 Immunolabelling of whole roots

The cell wall immunolabelling procedure is based on a modified protocol used to label the cytoskeleton in whole arabidopsis roots (Collings and Wasteneys, 2005) with the removal of a cell wall digestion step that was used to permeabilize the walls. Five to seven day old seedlings were fixed (40 min) in PME buffer (50 mM PIPES pH 7.2, 2 mM $MgSO_4$ and

2 mM EGTA) containing 3.7% (v/v) formaldehyde, 1.0% (v/v) dimethyl sulfoxide and 0.1% (v/v) Triton X-100 and washed in phosphate buffered saline (PBS; 131 mM NaCl, 5.1 mM Na_2HPO_4, 1.56 mM $KHPO_4$, pH 7.2) (2 x 5 min). After extraction in PBS buffer containing 1% Triton X-100 (1 h) and washing in PBS buffer (3 x 5 min), the seedlings were dehydrated in methanol (-20°C, 20 min) and rehydrated in PBS buffer (3x 5 min). The seedlings were then transferred to 30 mm diameter plastic Petri dishes layered with a piece of parafilm and blocked (15 min) in incubation buffer (PBS containing 1% bovine serum albumin and 0.1% Tween 20). Roots were then incubated in primary antibodies (Table 4.3) for 60 - 90 min (or overnight at 4°C) at 1/20 and 1/50 dilutions in incubation buffer. After washing in PBS buffer (3 x 10 min) the roots were incubated with secondary antibodies. These were a mixture of goat anti-rat conjugated to FITC and Cy5 (Jackson ImmunoResearch, West Grove, PA, USA) diluted 1:400 in incubation buffer (60 - 90 min or overnight at 4°C). One exception to this was that a mixture of goat anti-mouse conjugated to FITC and Cy5 (Jackson ImmunoResearch) was used for the BG1 antibody. Following the secondary antibody incubation, the seedlings were washed in PSB buffer (3 x 10 min), mounted in 40 µl of AF1 antifade agent (Citifluor, London, UK) on a regular slide and sealed with nail polish.

Fluorescent and concurrent transmitted light images were recorded with a Leica SP5 confocal microscope with the 20x glycerol immersion lens. The laser excitation wavelength used for FITC was 488 nm and the emitted fluorescence was captured from 503 nm to 533 nm. The laser excitation wavelength used for Cy5 was 633 nm and the emitted fluorescence was captured from 644 nm to 732 nm. Cy5 images are presented in the results due to a brighter signal. Line averaging was set at 4 and the z-section step size at 2 µm. Images were processed with Leica Microsystems LAS AF Version 2.6.0 Build 7266 and Adobe Photoshop Version CS6.

4.3 Results

4.3.1 Analysis of *schizoriza* TILLING mutants and *SCZ*-OE lines

As no T-DNA insertional mutants are available for the *SCHIZORIZA* gene, the phenotype of *sloughy* was compared to a collection of other EMS mutants. This collection of six *schizoriza* TILLING mutant lines were ordered from the ABRC (Table 4.1). The TILLING (for Targeting Induced Local Lesions IN Genomes) process is an established method for identifying EMS-mutagenized plants with mutations in a particular gene (McCallum *et al*., 2000, Bush and Krysan, 2010) and a large number of arabidopsis TILLING mutants are available for many arabidopsis genes through the ABRC.

To confirm that the reported mutations were present in the TILLING lines, the *SCHIZORIZA* gene was sequenced in wild-type, *sloughy* and all six TILLING mutants. With the exception of CS93177, the sequencing results corroborated with the reported mutations (Table 4.1). The reported mutations were also screened with HRM analysis. Again, with the exception of CS93177 which was not analyzed further, the HRM analysis results corroborated with the reported mutations (data not shown). These HRM analysis primers can, therefore, be used to rapidly genotype the mutant plants, and to screen for the mutations in crosses in further experiments.

CS931216 and CS93587 were catalogued as having synonymous mutations, with no change in the protein sequence, and would thus be predicted to have a wild-type phenotype. Growth experiments showed that both of these lines were indistinguishable from wild-type (data not shown). CS88971 has a non-synonymous mutations, introducing an amino acid change in the

Table 4.1 Sequencing results of the *schizoriza* TILLING mutants.

Line Name	Polymorphism[1]	bp[2]	Amino acid change[3]	Protein change	Mutation confirmed
CS93216	G to A	323	K111K	×	✓
CS88021	C to T	394	Q132stop	✓	✓
CS93157	C to T	574	Q192stop	✓	✓
CS93587	G to A	582	T194T	×	✓
CS88971	C to T	775	L259F	✓	✓
CS93177	C to T	854	S285F	✓	×
sloughy	C to T	556	Q186stop	✓	✓

[1]Adenine = A, cytosine = C, guanine = G and thymine = T.

[2]Base pair location of the mutation, which refers to exon sequence only, with intron removed.

[3]Lysine = K, glutamine = Q, threonine = T, leucine = L, phenylalanine = F, serine = S.

SCHIZORIZA protein that might result in a mutant phenotype (Figure 4.1). Again, however, the growth of CS88971 was indistinguishable from wild-type (data not shown). Since these three lines did not produce mutant phenotypes, they were not analysed further.

Investigation focused on CS88021 and CS93157, as both lines were confirmed to have non-synonymous mutations resulting in the introduction of an early stop codon at 132 amino acids and 192 amino acids, respectively (Figure 4.1). For reference, the *sloughy* mutation introduces a stop codon at residue 186. Both lines had severely reduced root growth comparative to wild-type. CS93157 appeared to have shorter, wider and hairier roots than *sloughy*, reminiscent of the previously-described *schizoriza* mutants (Mylona *et al*., 2002, ten Hove *et al*., 2010), whereas CS88021 was phenotypically identical to *sloughy*, including having aberrant cell separation in the mature roots (data not shown). Thus, an initial hypothesis was that *sloughy* and CS88021 may have slightly different phenotypes to CS93157 and the other reported *schizoriza* mutants in the literature. Focus was, therefore, placed on CS93157 for comparative analysis.

In addition to CS93157, the *sloughy* phenotype was also compared to *SCZ*-OE plants donated by Friedrich Schöffl since *SCZ*-OE plants had been reported to possess aberrant cell separation in the mature root (Begum *et al*., 2013).

When wild-type, *sloughy*, CS93157 and *SCZ*-OE seedlings were grown on agar for 9 days at 21°C, the roots of *sloughy* and CS93157 were significantly shorter than wild-type, being on average only 35% and 26% of the total length of wild-type, respectively (Figure 4.2). The roots of *SCZ*-OE seedlings were much longer than *sloughy*, being on average 76% of the length of wild-type.

When the plants were grown on soil at 21°C on a 12 h light regime to promote vegetative growth, both *sloughy* and *SCZ*-OE plants developed normally, displaying similar above

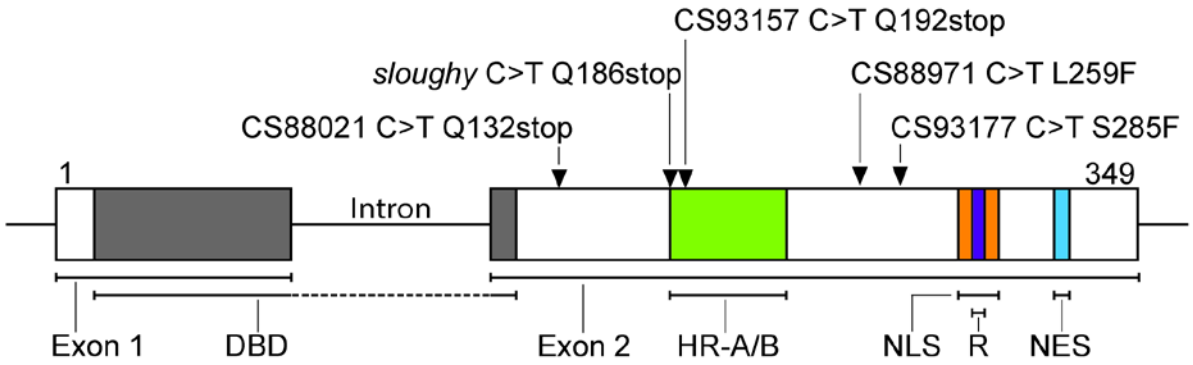

Figure 4.1 The mutations of the *schizoriza* TILLING lines CS88021, CS93157 and CS88971, and the putative but unconfirmed mutation in line CS93177, in relation to the *sloughy* mutation and the conserved domains of the *SCHIZORIZA* gene. DNA-binding domain = DBD, oligomerization region = HR-A/B, nuclear localisation signal = NLS, repression motif = R and nuclear export signal =NES.

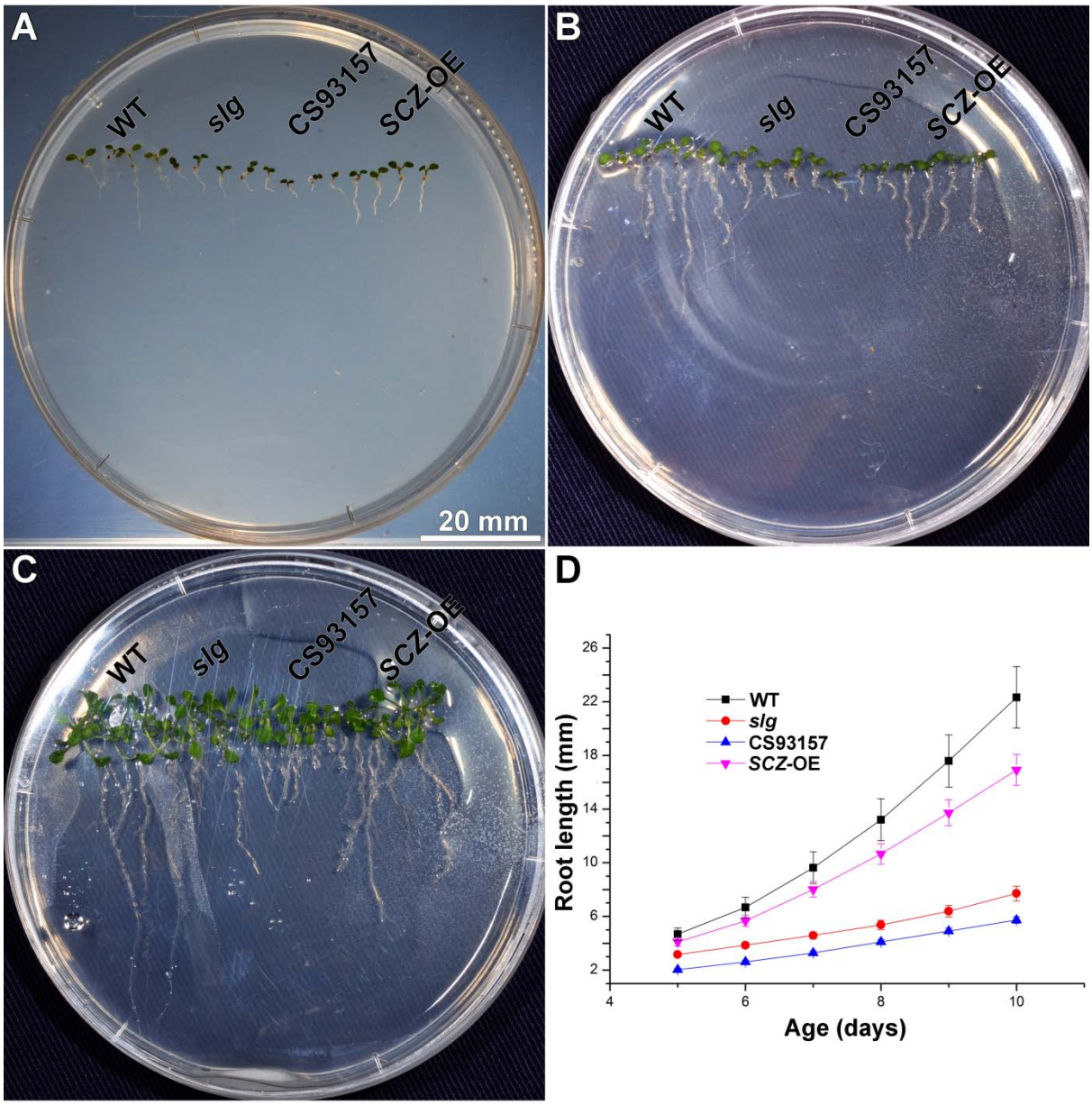

Figure 4.2 Comparative root growth of wild-type (WT), *sloughy* (*slg*), CS93157 and *SCZ*-OE seedlings grown at 21°C on agar. Scale bar in **A** = 20 mm.

A Five days.

B Seven days.

C Fourteen days.

D Primary root length measurements of WT, *slg*, CS93157 and *SCZ*-OE seedlings grown at 21°C. Data are averages ± standard errors; n = 36 replicate plants

ground growth to wild-type (Figure 4.3). In contrast, CS93157 plants were severely dwarfed in the above-ground growth, with the inflorescence stems, flowers and siliques all reduced in size (Figure 4.3C).

To test for temperature-sensitive growth responses, seedlings were grown on agar plates in a 21°C growth cabinet for 5 days, before being transferred to a range of different temperatures. *sloughy*, CS93157 and *SCZ*-OE seedlings all displayed similar optimal growth temperature to wild-type, with elongation greatest at 21°C and slower at 15°C and 30°C (Figure 4.4). *sloughy* and CS93157 had significantly reduced root growth comparative to wild-type at all three temperatures. The roots of *SCZ*-OE seedlings were much longer than *sloughy*, but shorter than wild-type at all three temperatures. *sloughy*, CS93157 and *SCZ*-OE, therefore, did not show a temperature-sensitive change in growth.

Lateral roots were counted on the 9 day old seedlings at all three temperatures. All seedlings had a similar temperature-sensitive increase in the number of lateral roots per seedling from 15°C to 21°C (Figure 4.5). However, in contrast to wild-type and *sloughy* seedlings, CS93157 and *SCZ*-OE seedlings did not display an increase in lateral roots per seedling from 21°C to 30°C. When root length was taken into account, there was an increase in the frequency of lateral roots in CS93157 and *SCZ*-OE seedlings from 15°C to 21°C. In contrast to *sloughy* seedlings, neither CS93157 nor *SCZ*-OE seedlings displayed a temperature sensitive increase in the frequency of lateral roots from 21°C to 30°C. Both *sloughy* and CS93157 had a significantly increased frequency of lateral roots compared to wild-type and *SCZ*-OE at all three temperatures. The frequency of lateral roots in *SCZ*-OE were similar to wild-type at all three temperatures.

To measure the extent of any temperature-sensitive swelling, the widths of 9 day-old primary roots were also measured. CS93157 and *SCZ*-OE seedlings were wider than wild-type at all

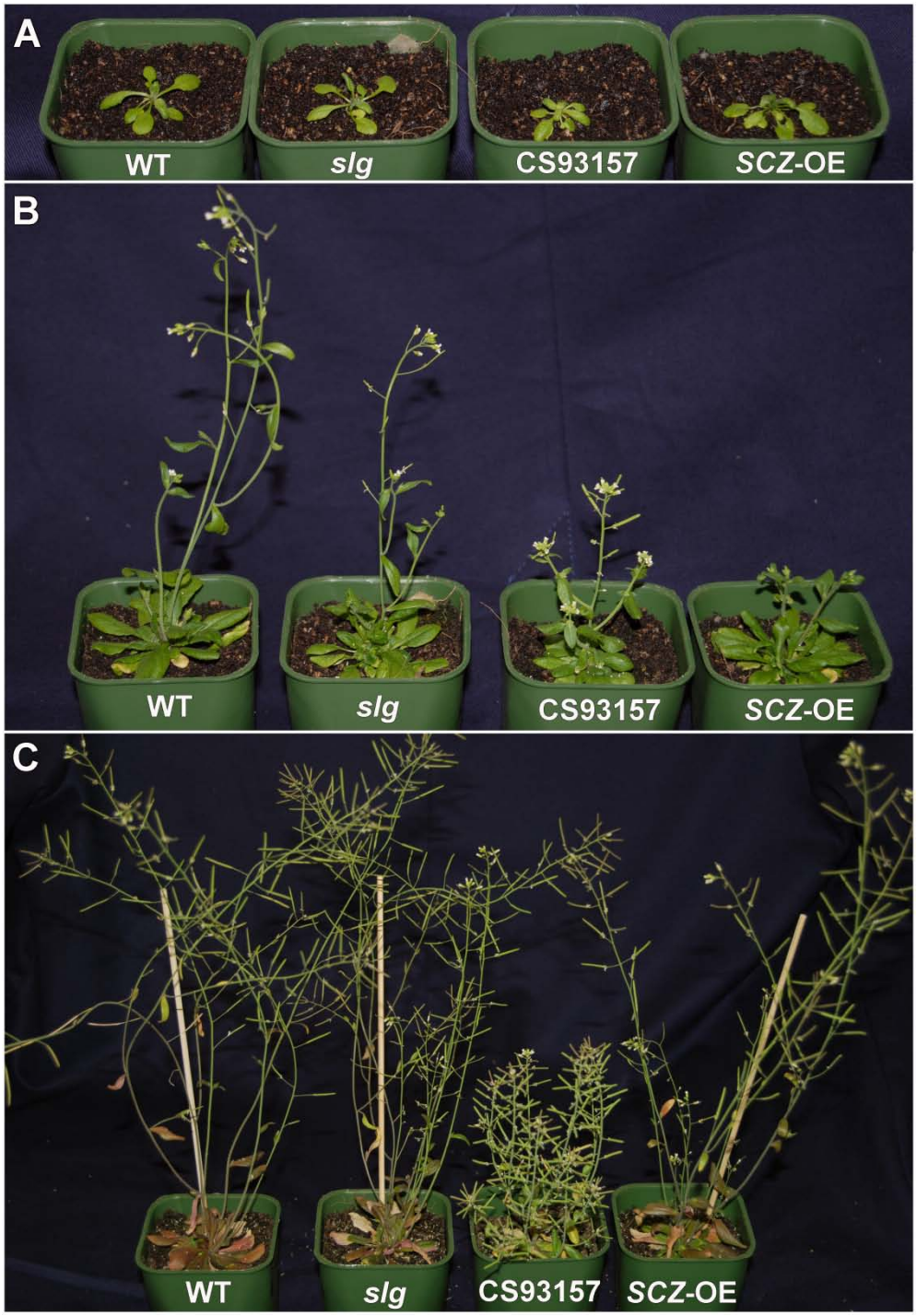

Figure 4.3 Comparative growth and development of wild-type (WT), *sloughy* (*slg*), CS93157 and *SCZ*-OE grown on soil at 21°C under a 12 h light regime.

A Twenty one days.

B Thirty five days.

C Forty nine days.

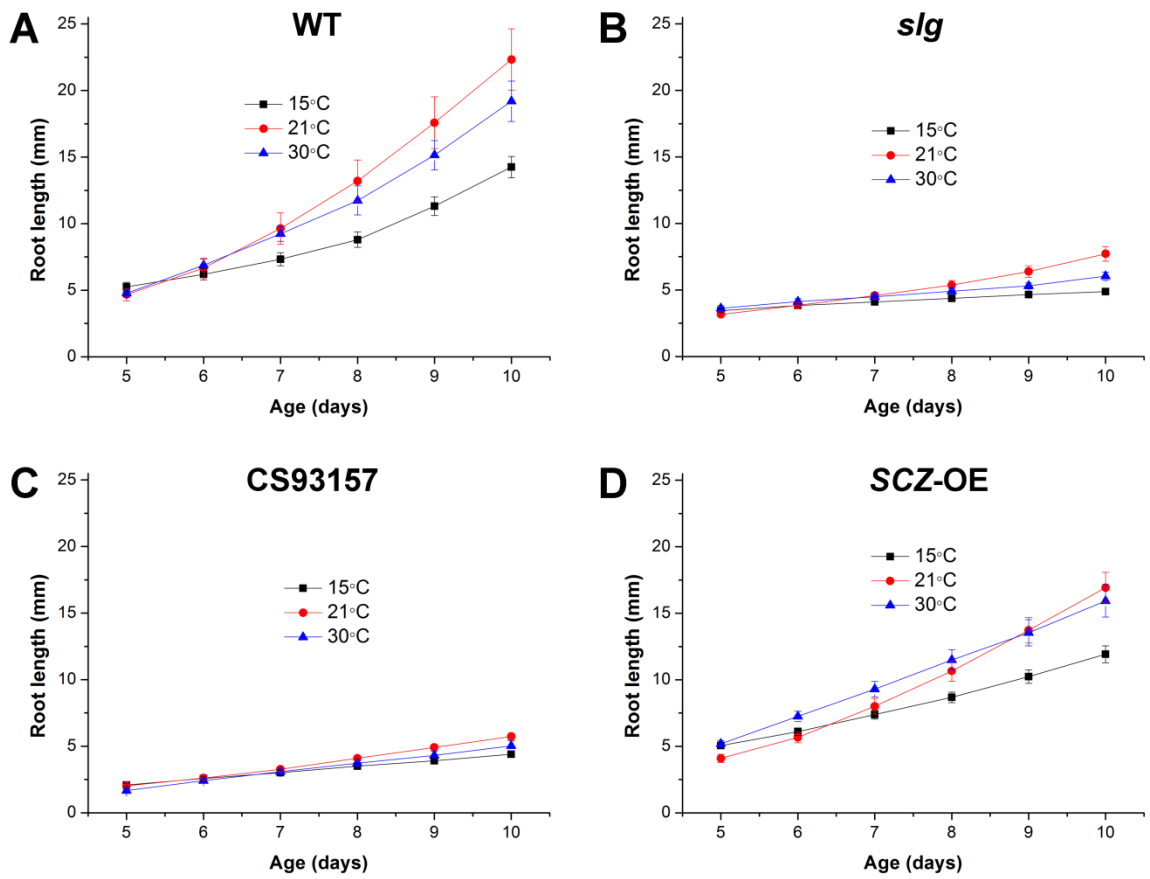

Figure 4.4 Temperature dependence of root elongation in wild-type (WT), *sloughy* (*slg*), CS93157 and *SCZ*-OE seedlings. Plants were germinated and grown at 21°C to day 5, and then transferred to the different temperatures. Data are averages ± SEM; n = 24 replicate plants.

A Wild-type (WT).

B *sloughy* (*slg*).

C CS93157.

D *SCZ*-OE.

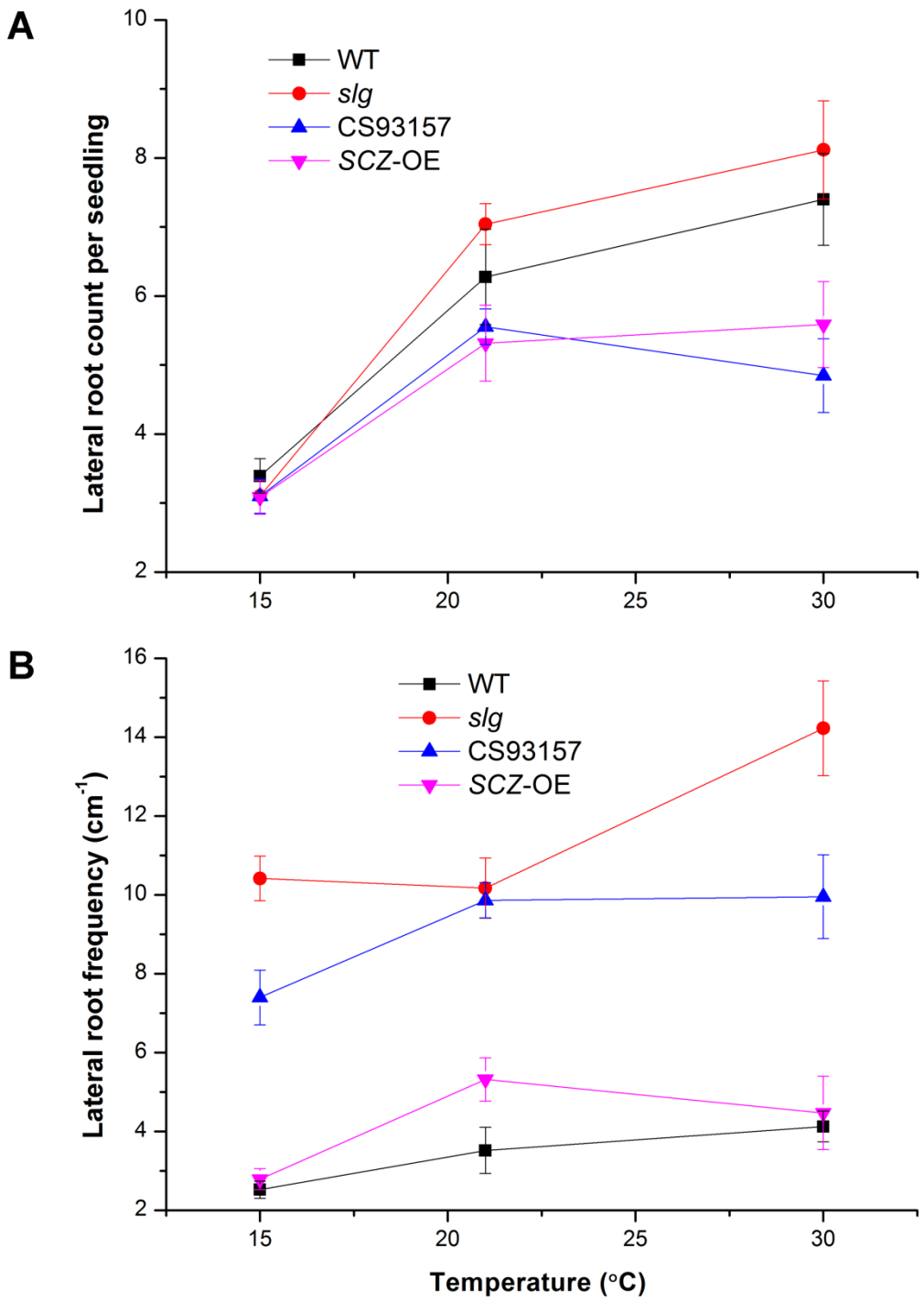

Figure 4.5 Lateral root formation in 10 day-old wild-type (WT), *sloughy* (*slg*), CS93157 and *SCZ*-OE seedlings at different temperatures. Data are averages ± SEM; n = 24 replicate plants.

A Lateral root count per seedling.

B Lateral root frequency (cm^{-1}).

three temperatures (Figure 4.6). Although CS93157 showed a similar temperature-sensitive response in root width to *sloughy*, the seedlings were on average wider than *sloughy* at all three temperatures. CS93157 showed similar root widths to *SCZ*-OE seedlings at 15°C and 21°C. The *SCZ*-OE seedlings displayed the most significant temperature-sensitive increase in root width from an average of 149 µm in width at 15°C to an average of 173 µm at 30°C. At 30°C, *SCZ*-OE seedlings were not only wider than wild-type, but also statistically significantly wider than *sloughy* and CS93157 seedlings. Thus, *sloughy*, CS93157 and *SCZ*-OE show a temperature-sensitive root swelling phenotype.

To explore cell separation phenomena present in the plants, whole seedlings grown at 21°C were labelled with propidium iodide and imaged by confocal microscopy (Figure 4.7). The roots of CS93157 seedlings often appeared shorter, hairier and wider, with evidence of reduced elongation of epidermal root cells. Despite these phenotypic differences, an aberrant cell separation phenotype similar to that observed in *sloughy* was also detected (Figure 4.7C). The roots of *SCZ*-OE seedlings were phenotypically distinct from that of *sloughy*, being noticeably wider, with an apparent increase in the formation of roots hairs (Figure 4.7D). Although the *SCZ*-OE seedlings often showed cells detaching from the mature root, the detaching cells did not appear to snake away from the surface of the root as seen in *sloughy*. Instead, they often detached at their cell ends and released as individual cells (data not shown).

4.3.2 Cell identity in *sloughy* roots

To investigate cell identity in the roots of *sloughy*, a collection of twelve GAL4-GFP enhancer trap lines for a variety of tissue-specific expression patterns were crossed to *sloughy* (Table 4.2). Nine of the enhancer trap line crosses were successful with GFP detected in both the F1 and F2 generations. However, lines J0671 and J0891 did not appear to express any

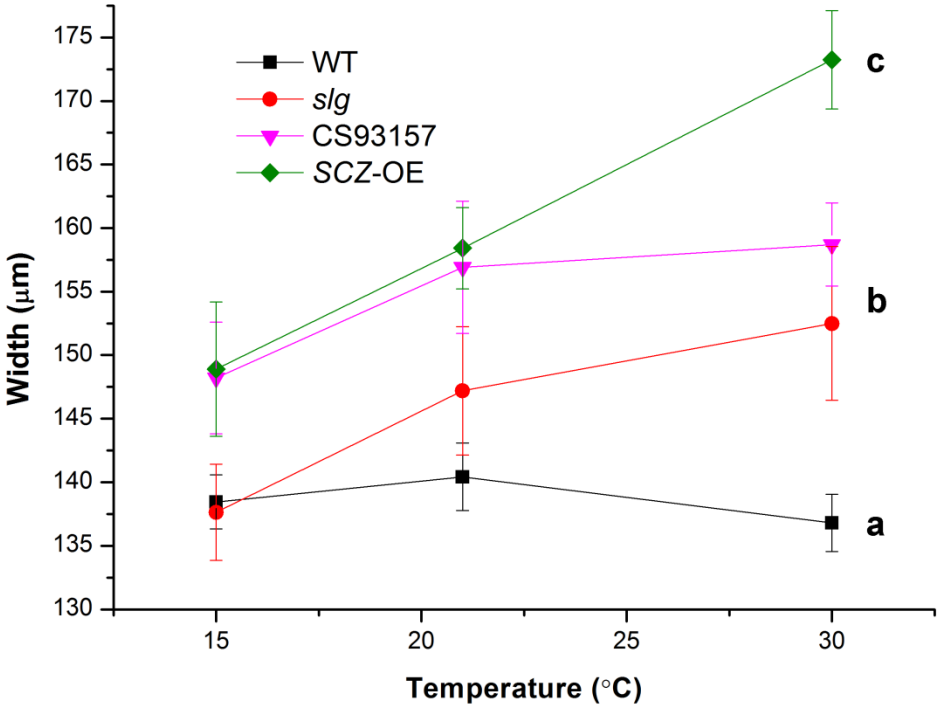

Figure 4.6 Primary root widths for 10 day-old wild-type (WT), *sloughy* (*slg*), CS93157 and *SCZ*-OE seedlings at different temperatures. Data are averages ± SEM; n = 12 replicate plants. a, b and c refer to statistically significant differences between the groups, calculated with a two-tailed T-test (significance level of 0.05).

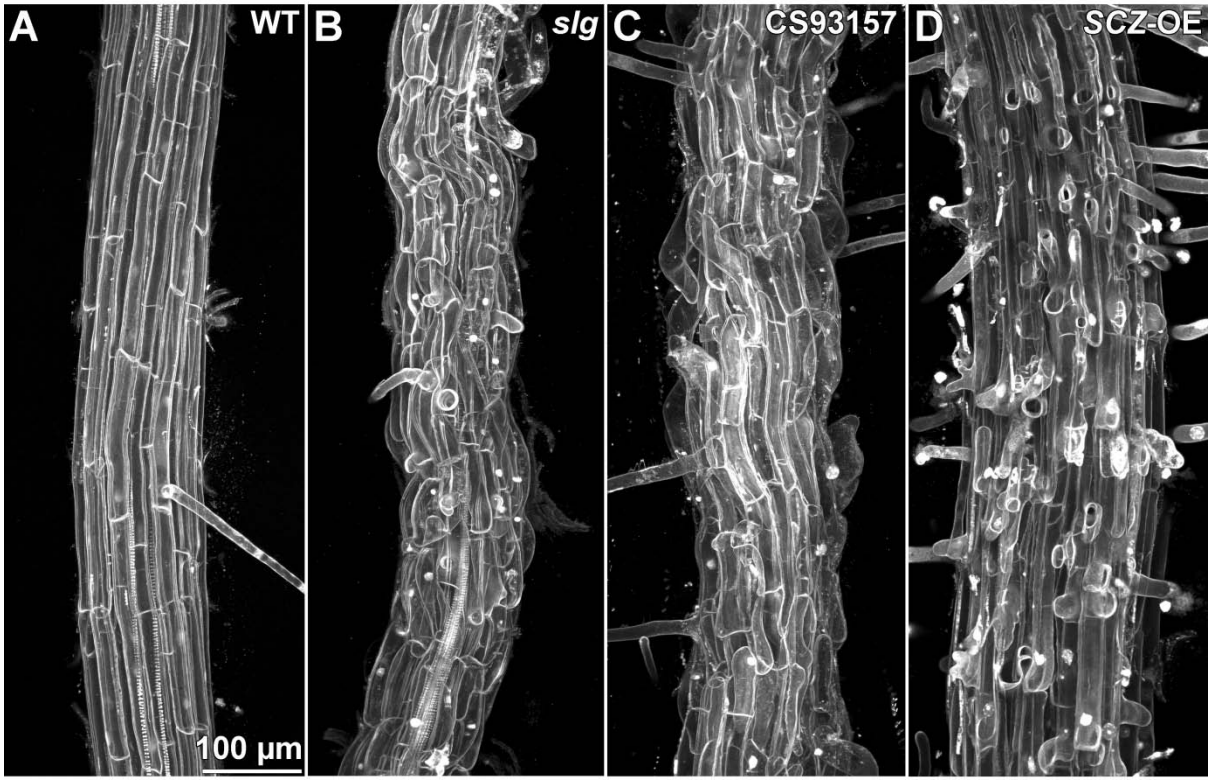

Figure 4.7 Phenotypic comparison of wild-type (WT), *sloughy* (*slg*), CS93157 and *SCZ*-OE seedlings grown at 21°C. Confocal maximum projections of roots stained with propidium iodide. Scale bar in **A** = 100 µm.

A Wild-type (WT).

B *sloughy* (*slg*).

C CS93157.

D *SCZ*-OE.

Table 4.2 Summary of GAL4-GFP enhancer trap lines crossed to *sloughy*.

ABRC code	Haseloff code[1]	GFP expression location[1]	Cross successful
CS9158	J1772	Cortex in mature root.	×
CS9142	J0671	Cortex in mature root.	×
CS1936	J0321	Epidermis and root cap in root tip. Epidermis in mature root.	✓
CS9093	J0481	Epidermis and root cap in root tip. Epidermis in mature root.	✓
CS9143	J0891	Atrichoblasts in mature root.	×
CS9146	J1071	Atrichoblasts in mature root.	✓
CS9162	J2092	Epidermis and root cap in root tip. Atrichoblasts in mature root.	✓
CS9094	J0571	Cortex and endodermis in root tip. Cortex and endodermis in mature root.	✓
CS9124	J2672	Endodermis and root cap in root tip. Endodermis in mature root.	✓
CS9157	J1731	Vascular tissue and root cap in root tip. Vasculature in mature root.	✓
CS9105	J1721	Vascular tissue and root cap in root tip. Vasculature in mature root.	✓
CS9156	J1701	Vascular tissue and root cap in root tip. Vasculature in mature root.	✓

[1]Details from a GAL4-GFP enhancer trap line catalogue dated from 1998 and downloaded from the Haseloff research group website (http://brindabella.mrc-lmb.cam.ac.uk; accessed 28/05/13, site no longer active).

GFP to begin with, while the offspring of the line J1772 cross failed to express any GFP. These three lines were not pursued further.

The cortex and endodermal-specific line J0571 revealed that ground tissue identity is restricted to two ground tissue cell layers in *sloughy* roots, with no expression detected in the subepidermal or epidermal cell layers (Figure 4.8). The layer surrounding the stele was identified as endodermis by propidium labelling of the casparian strip. Since line J0571 is a marker for both cortex and endodermal identity, it was not possible to differentiate between cortex or endodermal identity in the next cell layer out. Since no cortex-specific marker lines were successfully crossed to *sloughy*, the exact identity of this ground tissue cell layer surrounding the endodermis was not resolved. A closer inspection of the root cap and endodermis-specific line J2672 may reveal whether this ground tissue layer has partial endodermal identity.

The epidermal-specific J0481 line revealed that both the epidermal and the subepidermal cell layers possessed epidermal identity in *sloughy* roots (Figure 4.9). This line also displayed evidence of partial epidermal identity in the ground tissue layer surrounding the endodermis (Figure 4.9B, asterisk). Further investigation of epidermal-specific marker lines are required to resolve this finding. The epidermal and the subepidermal cell layers expressing epidermal identity was corroborated by line J0321 (data not shown). Due to time constraints, the expression of trichoblast identity with the lines J1071 and J2092 was not investigated in either wild-type or *sloughy* roots.

The root cap and vasculature specific line J1731 demonstrated that root cap identity was restricted to the root tip, with no evidence of ectopic root cap identity further up in the mature roots of *sloughy* (Figure 4.10). Imaging of the root meristem also demonstrated that there was

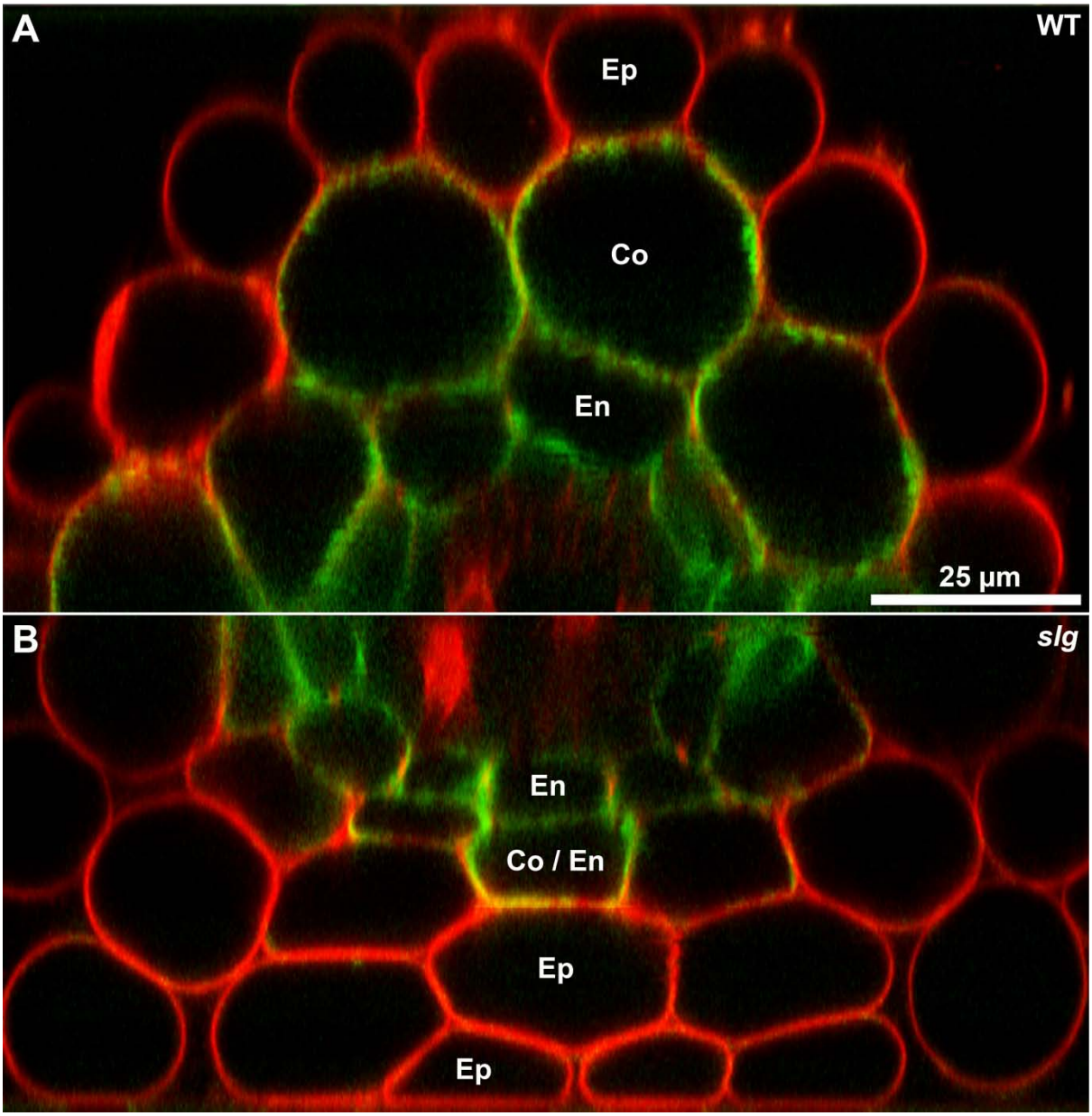

Figure 4.8 Endodermis and cortex identity are restricted to two ground tissue cell layers in *sloughy* roots. Reconstructed cross sections of line J0571 for endodermis and cortex identity (GFP shown in green) expressed in wild-type (WT) and *sloughy* (*slg*) roots stained with propidium iodide (red) and imaged with confocal microscopy. Endodermis = En, cortex = Co and epidermis = Ep. Scale bar in **A** = 25 µm.

A Wild-type (WT).

B *sloughy (slg*).

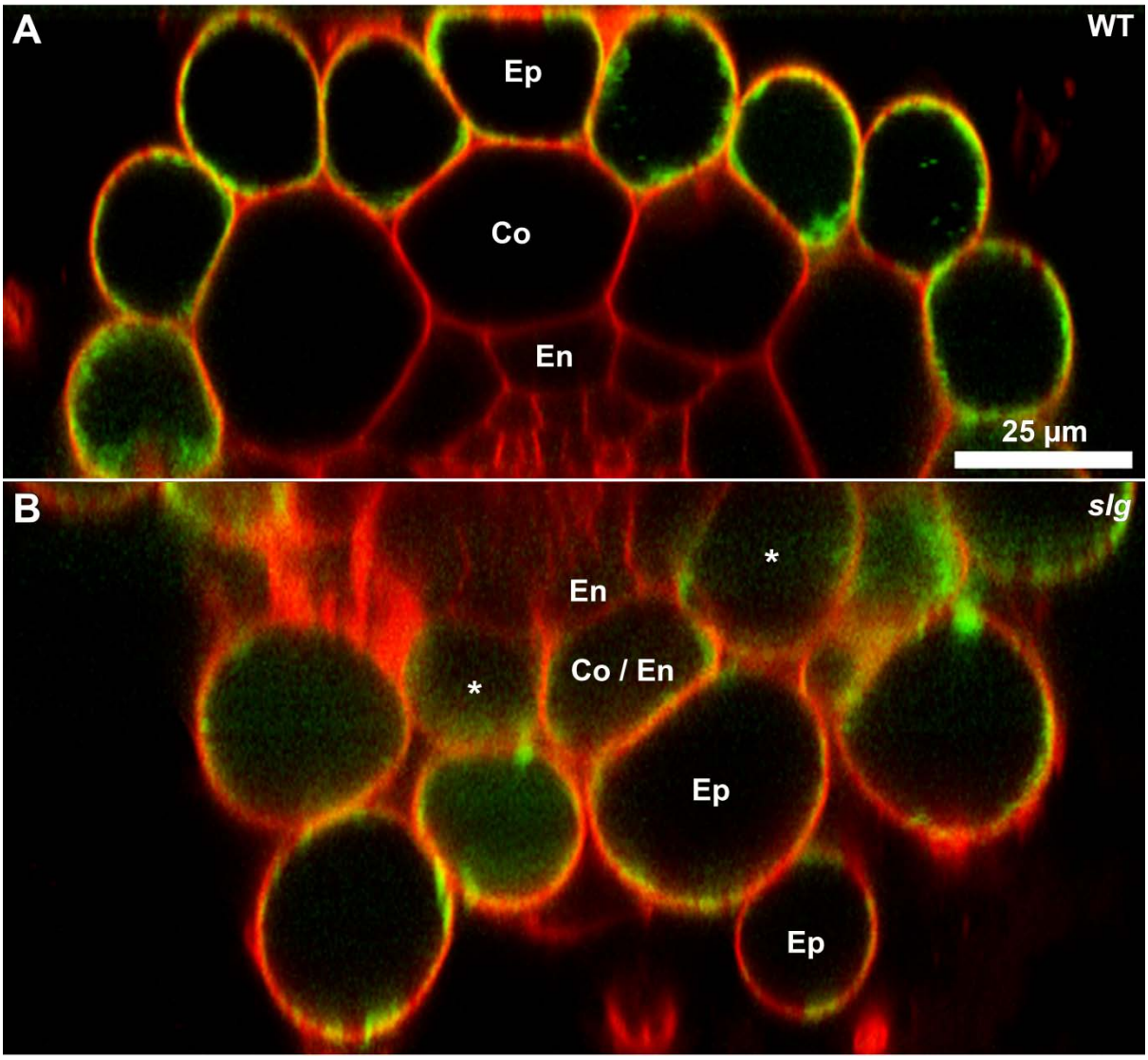

Figure 4.9 A supernumery layer with epidermal identity is present in *sloughy* roots. Reconstructed cross sections of line J0481 for epidermal identity (GFP shown in green) expressed in wild-type (WT) and *sloughy* (*slg*) roots stained with propidium iodide (red) and imaged with confocal microscopy. Endodermis = En, cortex = Co and epidermis = Ep. Scale bar in **A** = 25 µm.

A Wild-type (WT).

B *sloughy (slg*). Asterisks indicates ground-tissue derived cell layer surrounding the endodermis expressing epidermal identity.

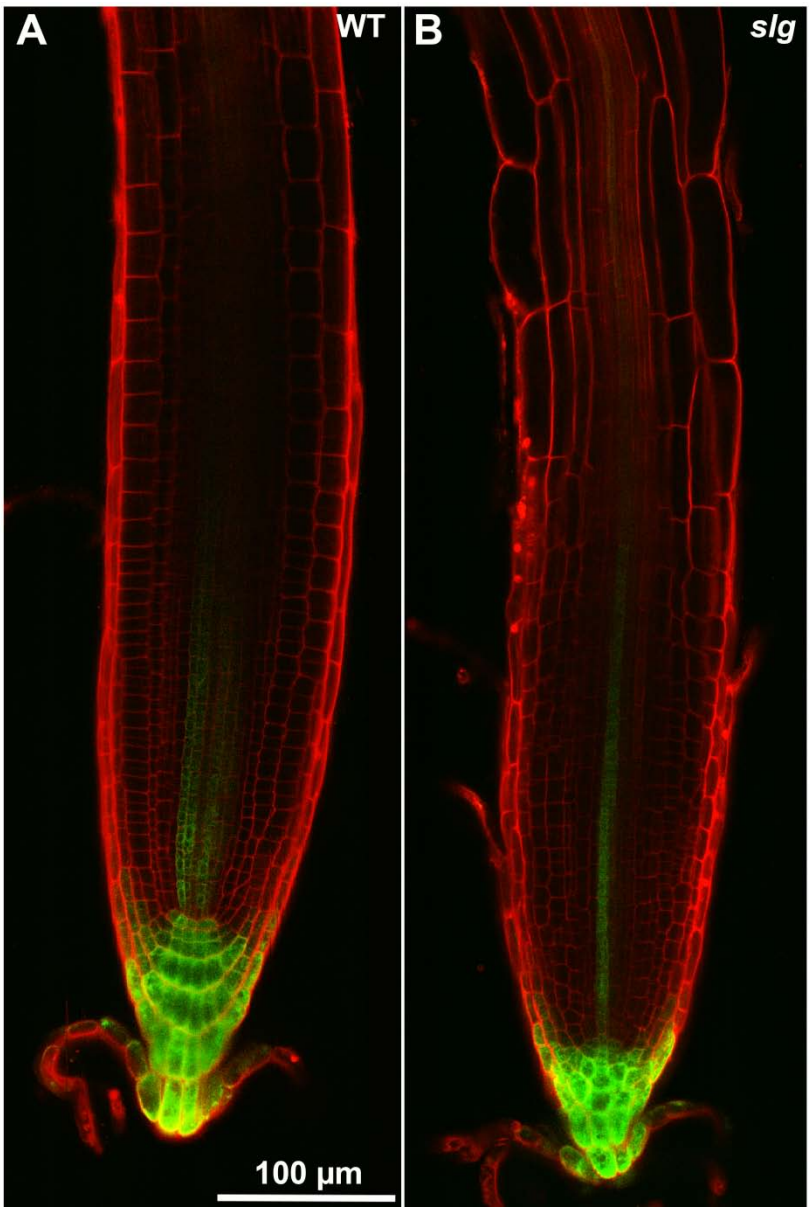

Figure 4.10 No ectopic root cap identity was detected in the elongation zone of *sloughy* roots. Maximum projection of line J1731 for root cap and developing vasculature identity (GFP shown in green) expressed in wild-type (WT) and *sloughy* (*slg*) roots stained with propidium iodide (red, single focal plane) and imaged with confocal microscopy. Scale bar in **A** = 100 µm.

A Wild-type (WT).

B *sloughy (slg*).

no ectopic expression of root cap identity detected in other cell layers (Figure 4.11). These results were corroborated by lines J1721, J1701 and J2672 (data not shown).

4.3.3 Immunolabelling of cell wall epitopes

A fundamental objective of this project had been to identify the altered biochemical properties in *sloughy*, and in particular the biochemical difference between the side walls and end walls of the separating epidermal cells. Although *sloughy* was originally hypothesized to be a cell wall mutant, *sloughy* is allelic to *SCHIZORIZA* and is instead defective in the development and maintenance of the root meristem. Therefore, the altered biochemical properties in *sloughy* are likely due to mixed cell fate leading to altered cell wall maturation processes. To investigate the cell wall properties that may have changed, a collection of twelve primary antibodies that target different cell wall epitopes were used to immunolabel whole roots of wild-type and *sloughy* seedlings and the results are summarised in Table 4.3. The screening protocol for altered cell wall properties was based on imaging the whole roots with confocal microscopy to detect changes in either the labelling intensity or ectopic patterns of labelling between wild-type and *sloughy*. Two antibodies showed possible different labelling patterns between wild-type and *sloughy*.

The JIM13 antibody specifically labels arabinogalactan proteins on the surface of border-like cells in the root cap of wild-type plants (Figure 4.12A) (Knox *et al*., 1991, Vicré *et al*., 2005). This strong labelling pattern was also observed in the root cap of *sloughy* (Figure 4.12B). However, in contrast to wild-type roots that showed no JIM12 labelling of the mature root, the JIM13 antibody often labelled the epidermal cells and surrounding mucilage in the mature roots of *sloughy* (Figure 4.13B).

The LM8 antibody recognises a specific epitope of a xylogalacturonan pectic polysaccharide that is found associated with the lateral root cap and mucilage of wild-type plants

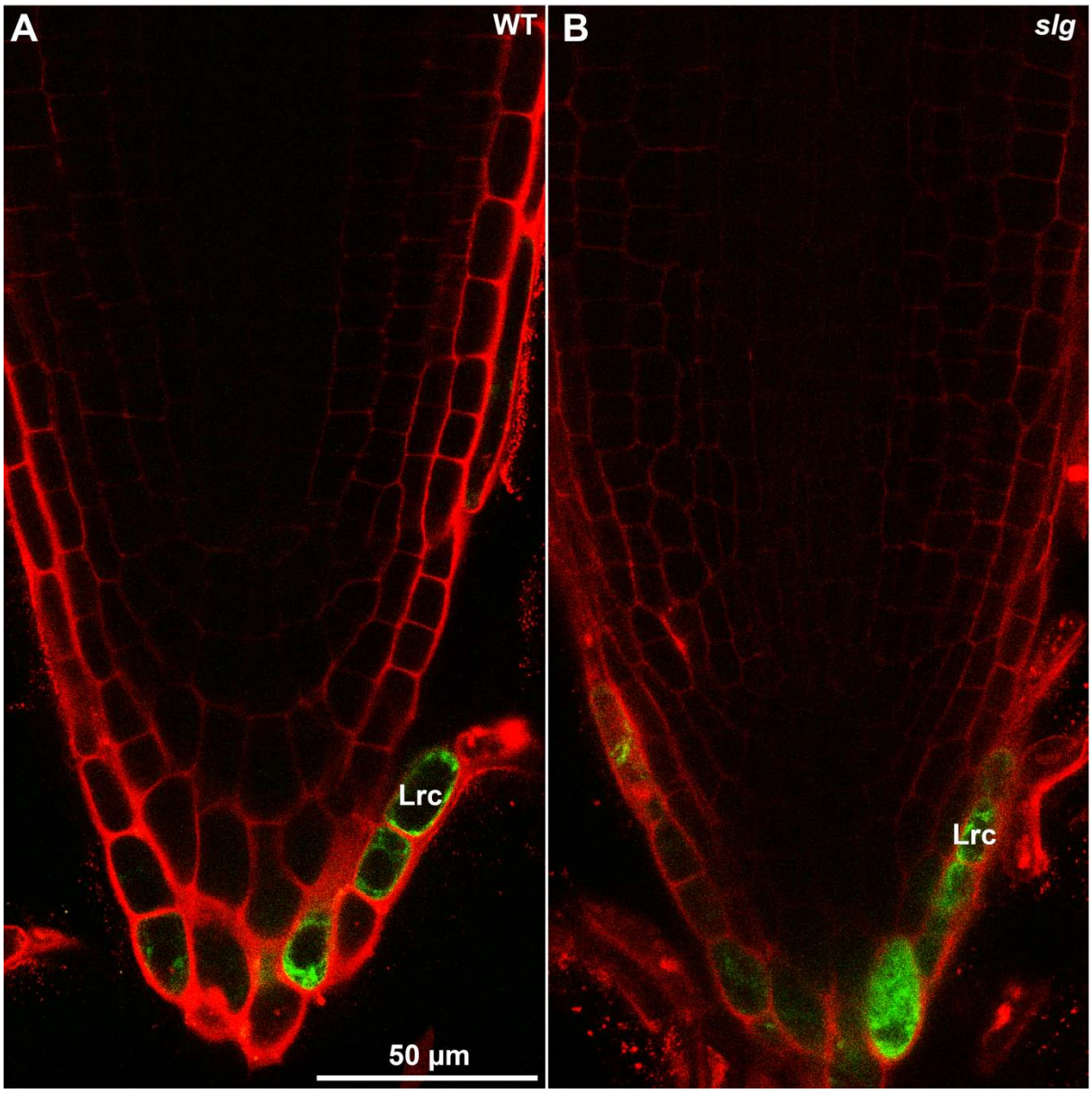

Figure 4.11 No ectopic root cap identity was detected in the root meristem of *sloughy*. Single focal plane of line J1731 for root cap and developing vasculature (GFP shown in green) identity expressed in wild-type (WT) and *sloughy* (*slg*) roots stained with propidium iodide (red) and imaged with confocal microscopy. Lateral root cap = Lrc. Scale bar in **A** = 50 µm.

A Wild-type (WT).

B *sloughy (slg*).

Table 4.3 Immunolabelling patterns of wild-type and *sloughy* whole roots with primary antibodies targeted against different cell wall epitopes.

Antibody name[1]	Antibody-target	Labelled whole roots	Differential labelling[2]	Reference
JIM5	Homogalacturonan	✓	×	Knox *et al*., 1990
JIM7	Homogalacturonan	×	×	Knox *et al*., 1990
JIM13	Arabinogalactan protein	✓	✓	Knox *et al*., 1991
JIM14	Arabinogalactan protein	✓	×	Knox *et al*., 1991
LM7	Homogalacturonan	×	×	Willats *et al*., 1999
LM8	Xylogalacturonan	✓	??	Willats *et al*., 2004
LM10	Xylan	×	×	McCartney *et al*., 2005
LM11	Xylan/Arabinoxylan	×	×	McCartney *et al*., 2005
LM18	Homogalacturonan	×	×	Verhertbruggen *et al*., 2009
LM19	Homogalacturonan	✓	×	Verhertbruggen *et al*., 2009
LM20	Homogalacturonan	✓	×	Verhertbruggen *et al*., 2009
BG1	(1-3,1-4)-β-D-glucan (callose)	✓	×	Meikle *et al*., 1994

[1]All antibodies (Plant Probes, Leeds, UK) were raised in rat with an exception to BG1 (BioSupplies, Clayton, Vic, Australia) which was raised in goat.

[2]Differential labelling patterning between wild-type and *sloughy* whole roots.

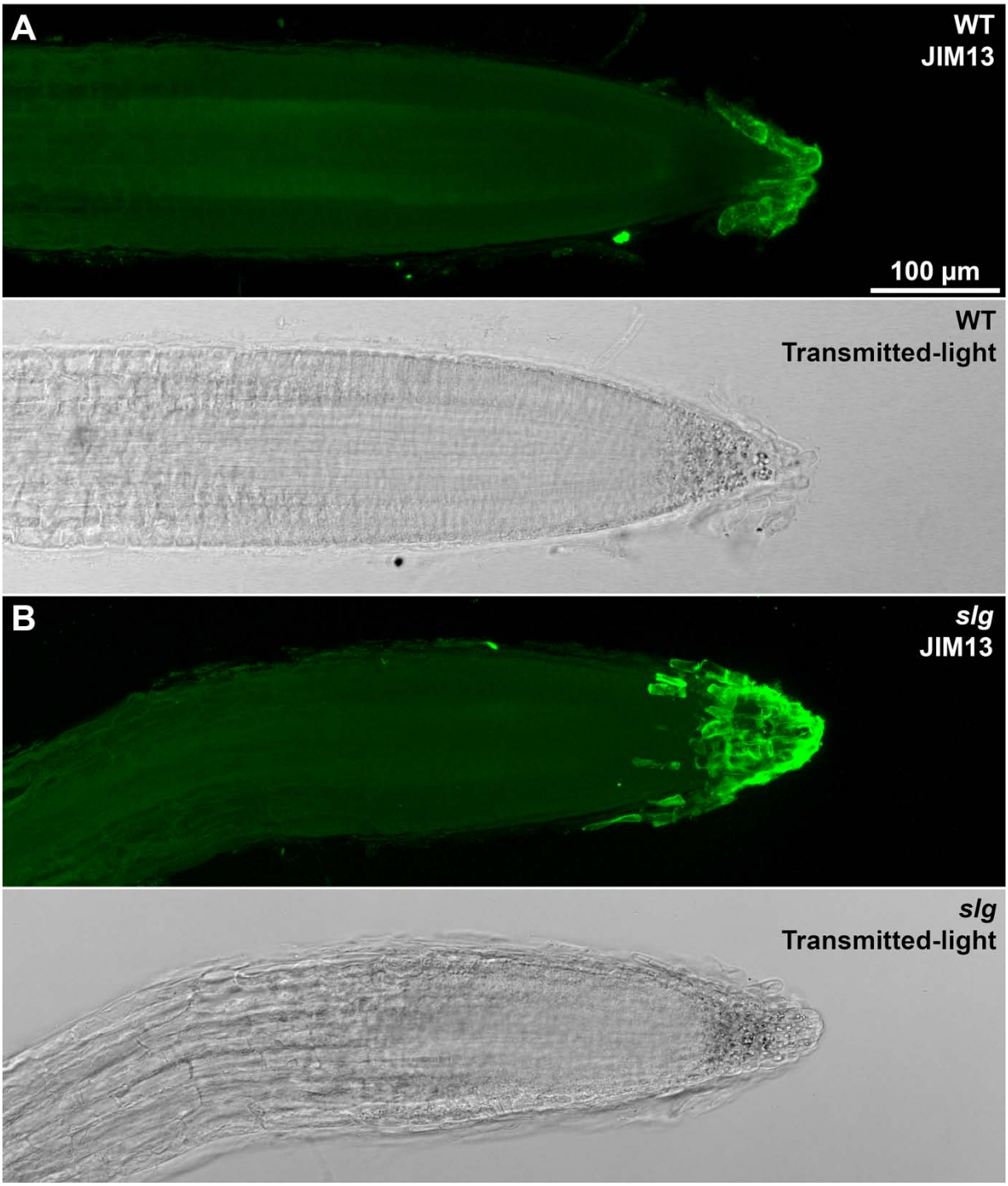

Figure 4.12 Root cap specific labelling of arabinogalactan proteins with the JIM13 antibody. Confocal maximum projections of roots labelled with JIM13 primary antibody and concurrent transmitted light image (single focal plane). Scale bar in **A** = 100 µm.

A Wild-type (WT).

B *sloughy (slg)*.

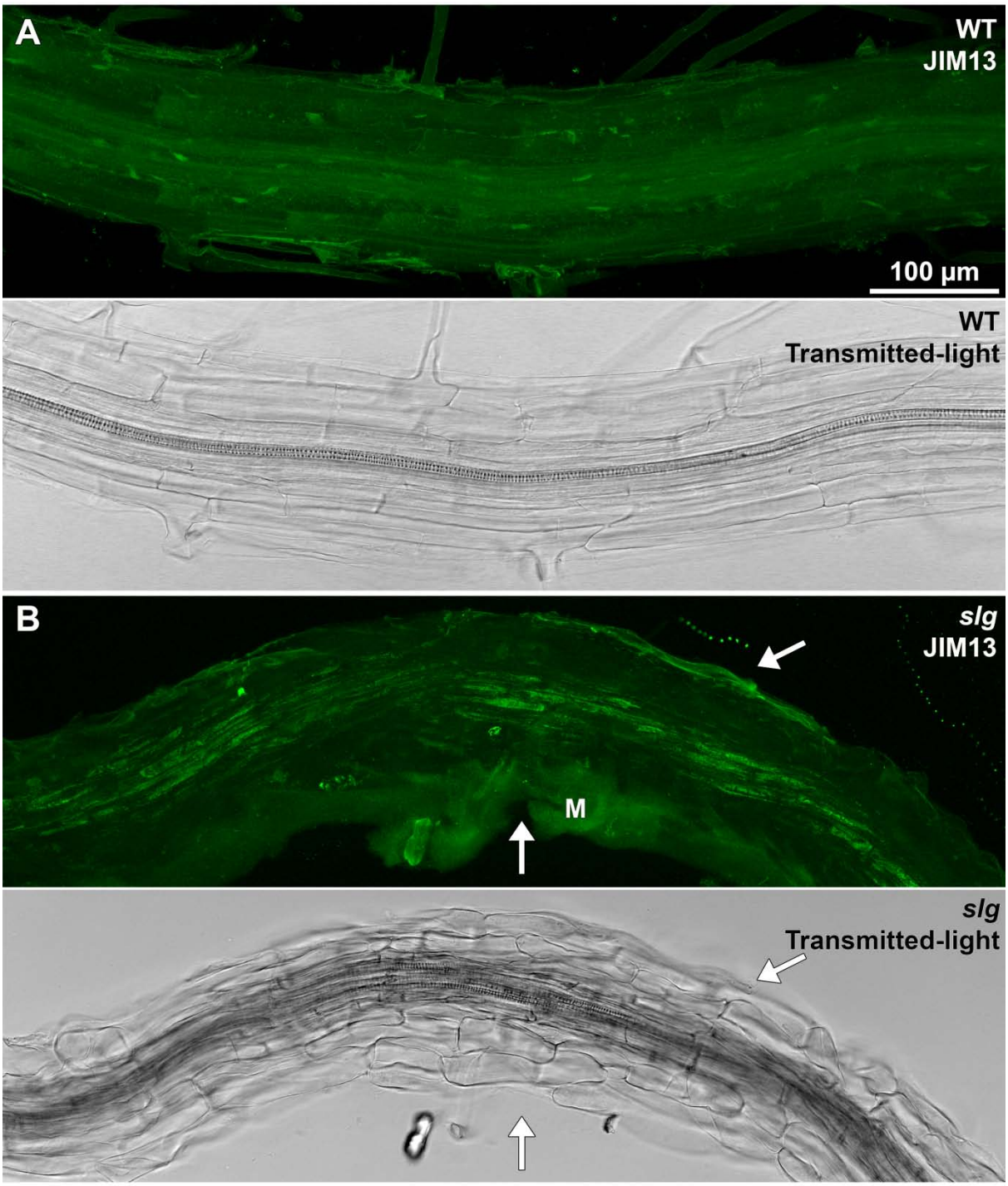

Figure 4.13 Ectopic arabinogalactan protein labelling with the JIM13 antibody in *sloughy* roots. Confocal maximum projections of roots labelled with JIM13 primary antibody and concurrent transmitted light image (single focal plane). Scale bar in **A** = 100 µm.

A Wild-type (WT).

B *sloughy (slg*). Arrows indicate ectopic labelling of JIM13 mucilage (M).

(Figure 4.14A) (Willats *et al*., 2004, Durand *et al*., 2009). Mucilage labelling was also detected in the root cap of *sloughy* (Figure 4.14B). The LM8 xylogalacturonan epitope showed equivalent labelling in the epidermal cells of wild-type and *sloughy* roots, but may also label ectopic mucilage in the mature roots of *sloughy* (Figure 4.15B). Further investigation with the LM8 antibody is needed to confirm this finding.

The JIM5 homogalacturonan epitope was equivalently labelled in wild-type and *sloughy* roots (Figure 4.16). The JIM5 antibody recognizes partially methyl-esterified or un-esterified epitopes of homogalacturonan (Knox *et al*., 1990). Another homogalacturonan epitope, LM19, was equivalently labelled in wild-type and *sloughy* roots (Figure 4.17). The LM19 antibody recognises a range of homogalacturonan epitopes, but appears to have a preference for un-esterified homogalacturonan (Verhertbruggen *et al*., 2009). A third homogalacturonan epitope, LM20, was also equivalently labelled in wild-type and *sloughy* roots (Figure 4.18). The LM20 antibody requires methyl-esterified homogalacturonan for recognition and does not bind to un-esterified homogalacturonan (Verhertbruggen *et al*., 2009).

The BG1 (1-3,1-4)-β-D-glucan (callose) epitope was equivalently labelled in wild-type and *sloughy* roots (Figure 4.19) (Meikle *et al*., 1994). The apparent reduced labelling of the *sloughy* roots seen in Figure 4.18B is likely an artefact of the stack of confocal images collected to create the maximum projection.

There was no evidence of epitope labelling in either wild-type or *sloughy* roots with the homogalacturonan antibodies JIM7, LM7 and LM18, the arabinogalactan protein antibody JIM14, the xylan antibody LM10, or the xylan/abrinoxylan antibody LM11. Troubleshooting the immunolabelling protocol for these antibodies was not pursued.

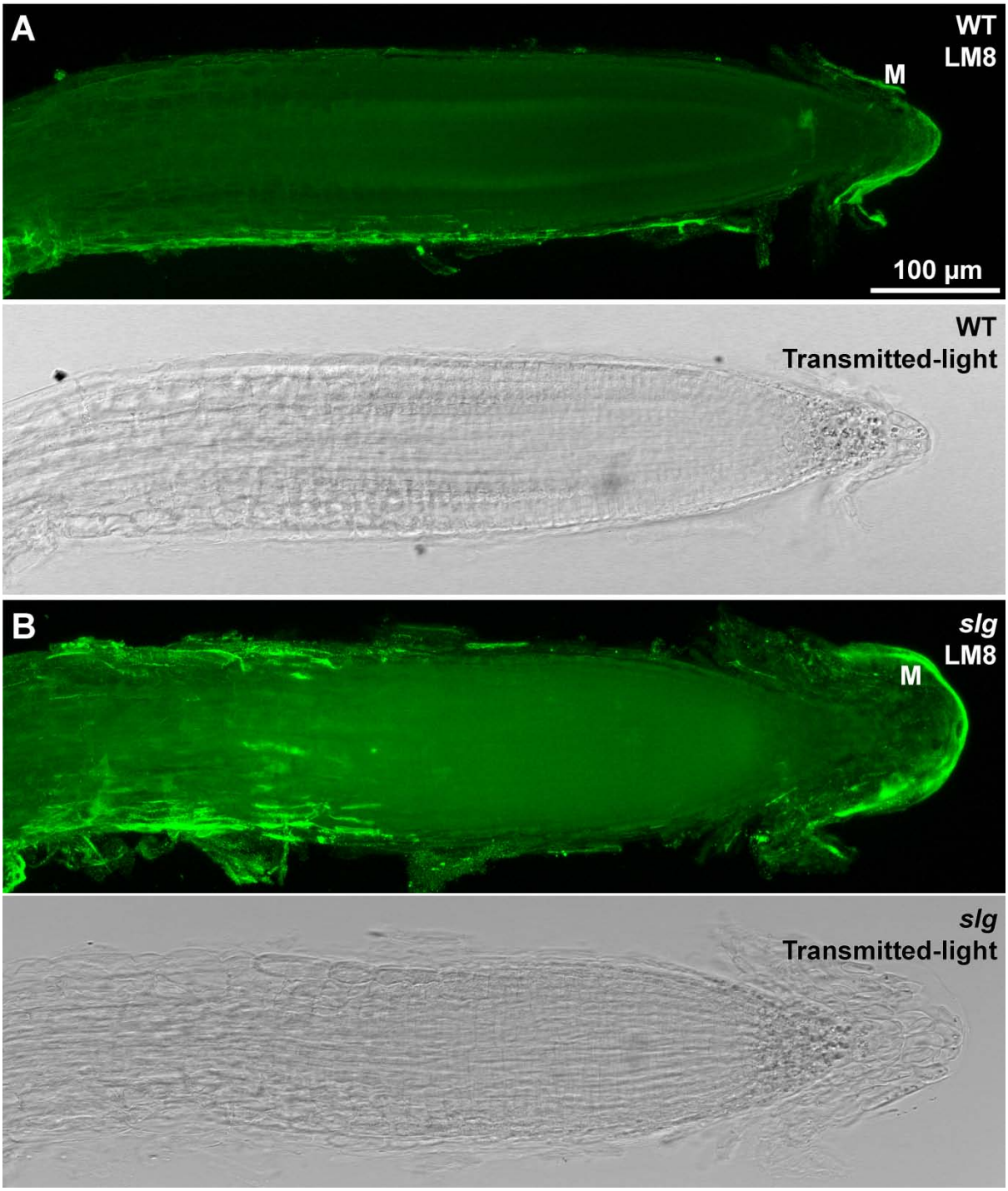

Figure 4.14 The LM8 xylogalacturonan epitope is associated with the lateral root cap and mucilage. Confocal maximum projections of roots labelled with the LM8 primary antibody and concurrent transmitted light image (single focal plane). Scale bar in **A** = 100 µm.

A Wild-type (WT). Mucilage = M.

B *sloughy (slg*). Mucilage = M.

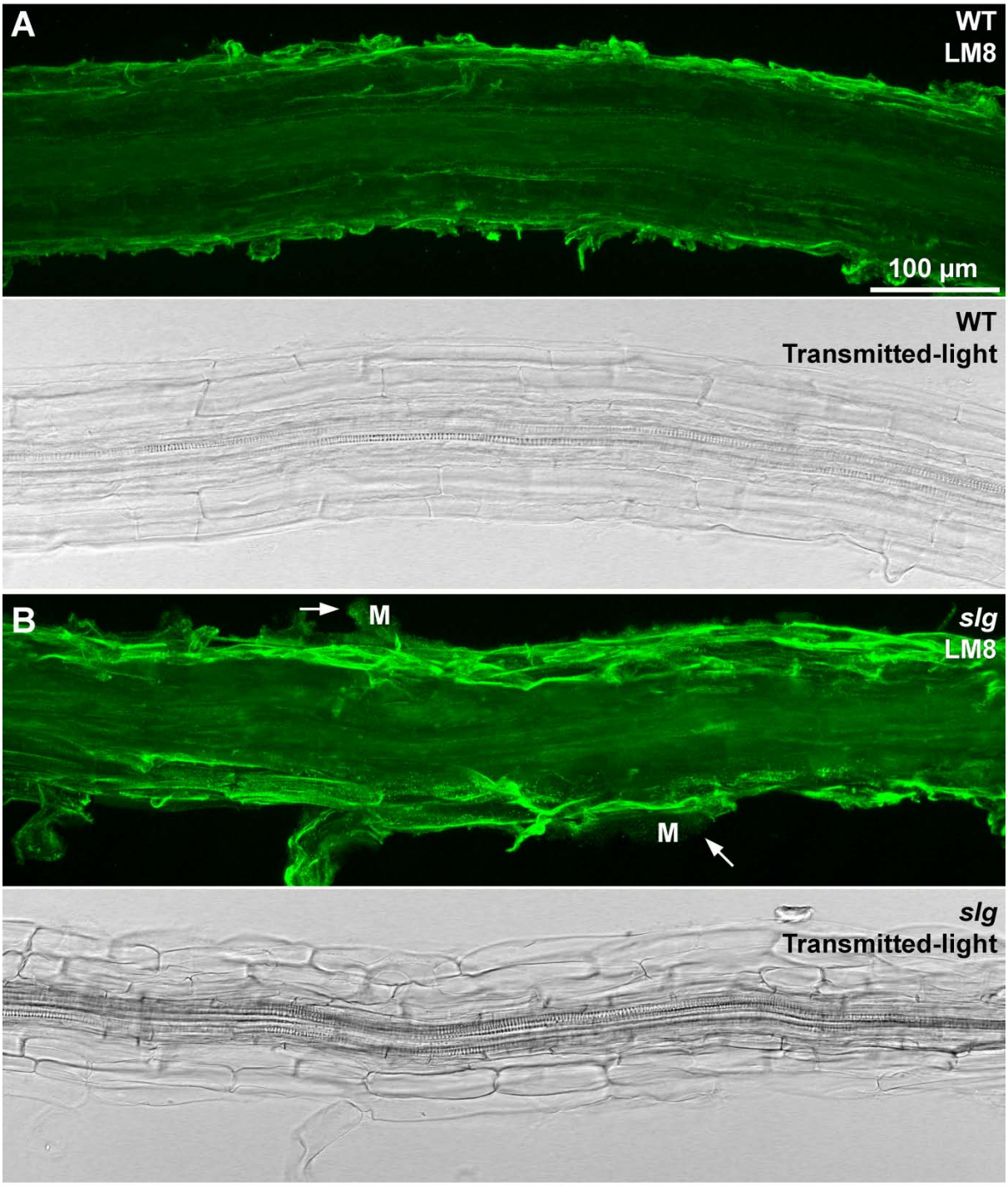

Figure 4.15 The LM8 xylogalacturonan epitope may label ectopic mucilage in *sloughy* roots. Confocal maximum projections of roots labelled with the LM8 primary antibody and concurrent transmitted light image (single focal plane). Scale bar in **A** = 100 µm.

C Wild-type (WT).

D *sloughy (slg*). Arrows indicate possible ectopic labelling of LM8. Mucilage = M.

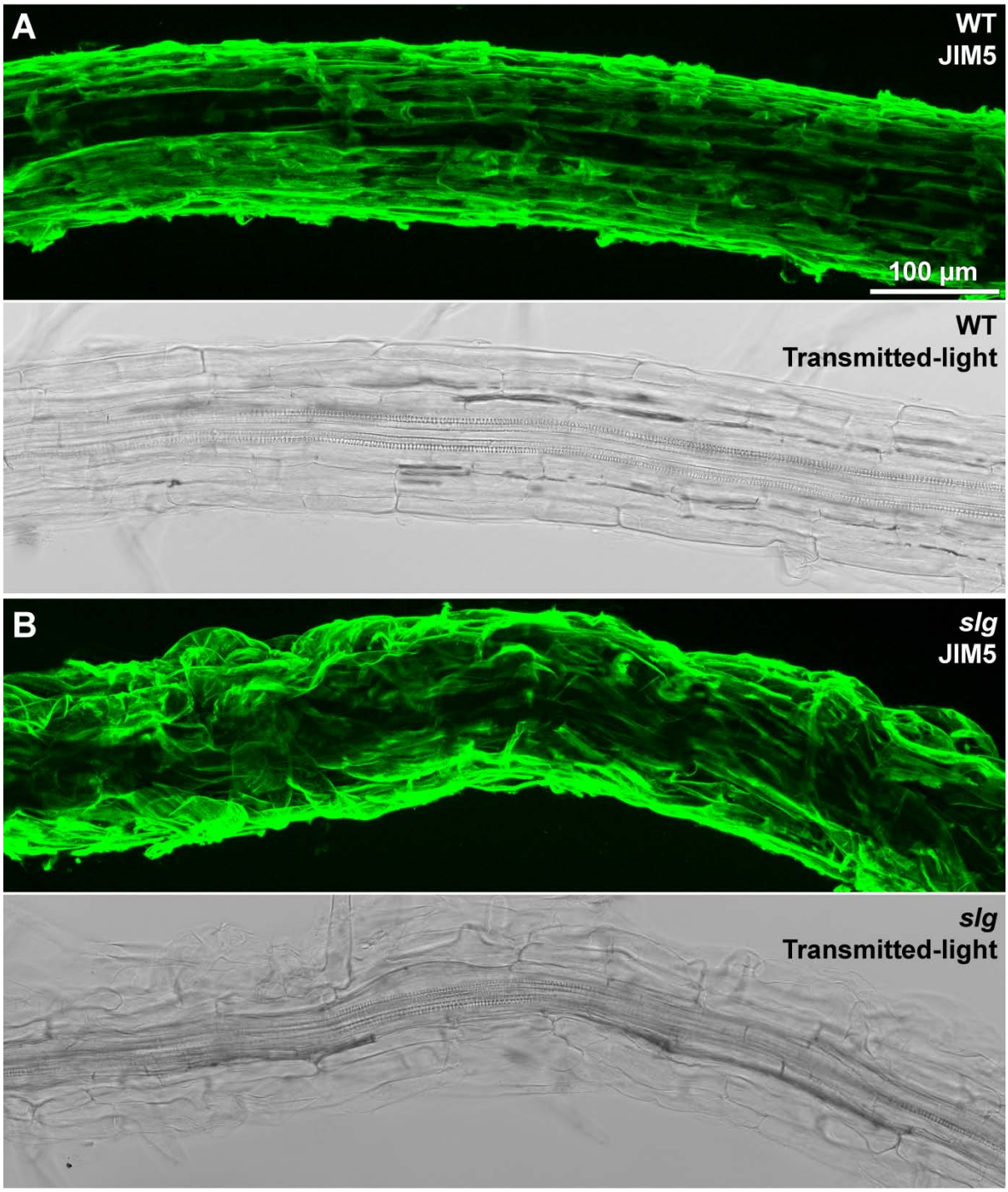

Figure 4.16 The JIM5 homogalacturonan epitope is not significantly altered in *sloughy* roots. Confocal maximum projections of roots labelled with JIM5 primary antibody and concurrent transmitted light image (single focal plane). Scale bar in **A** = 100 µm.

A Wild-type (WT).

B *sloughy (slg*).

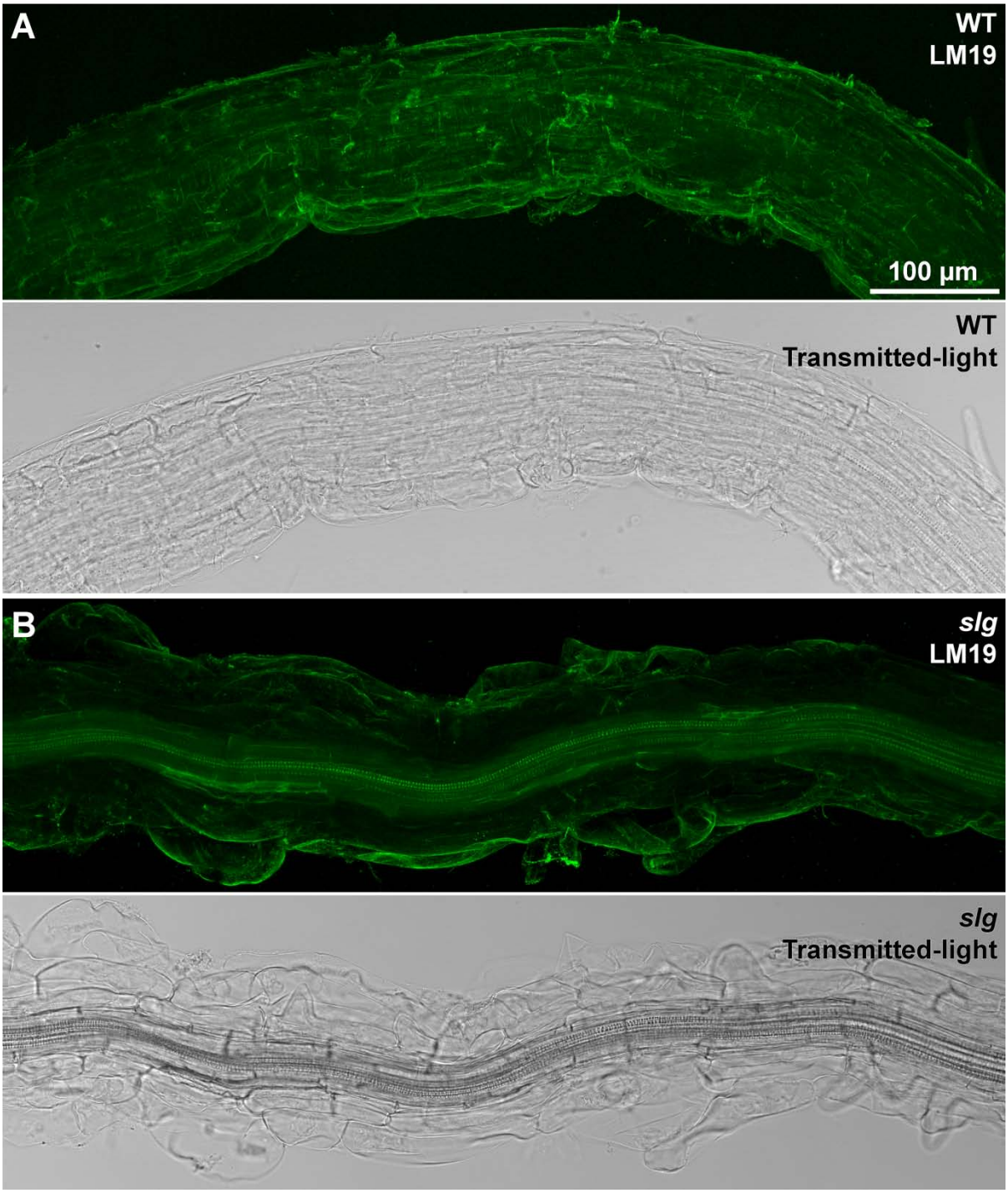

Figure 4.17 The LM19 homogalacturonan epitope is not significantly altered in *sloughy* roots. Confocal maximum projections of roots labelled with LM19 primary antibody and concurrent transmitted light image (single focal plane). Scale bar in **A** = 100 µm.

A Wild-type (WT).

B *sloughy (slg)*.

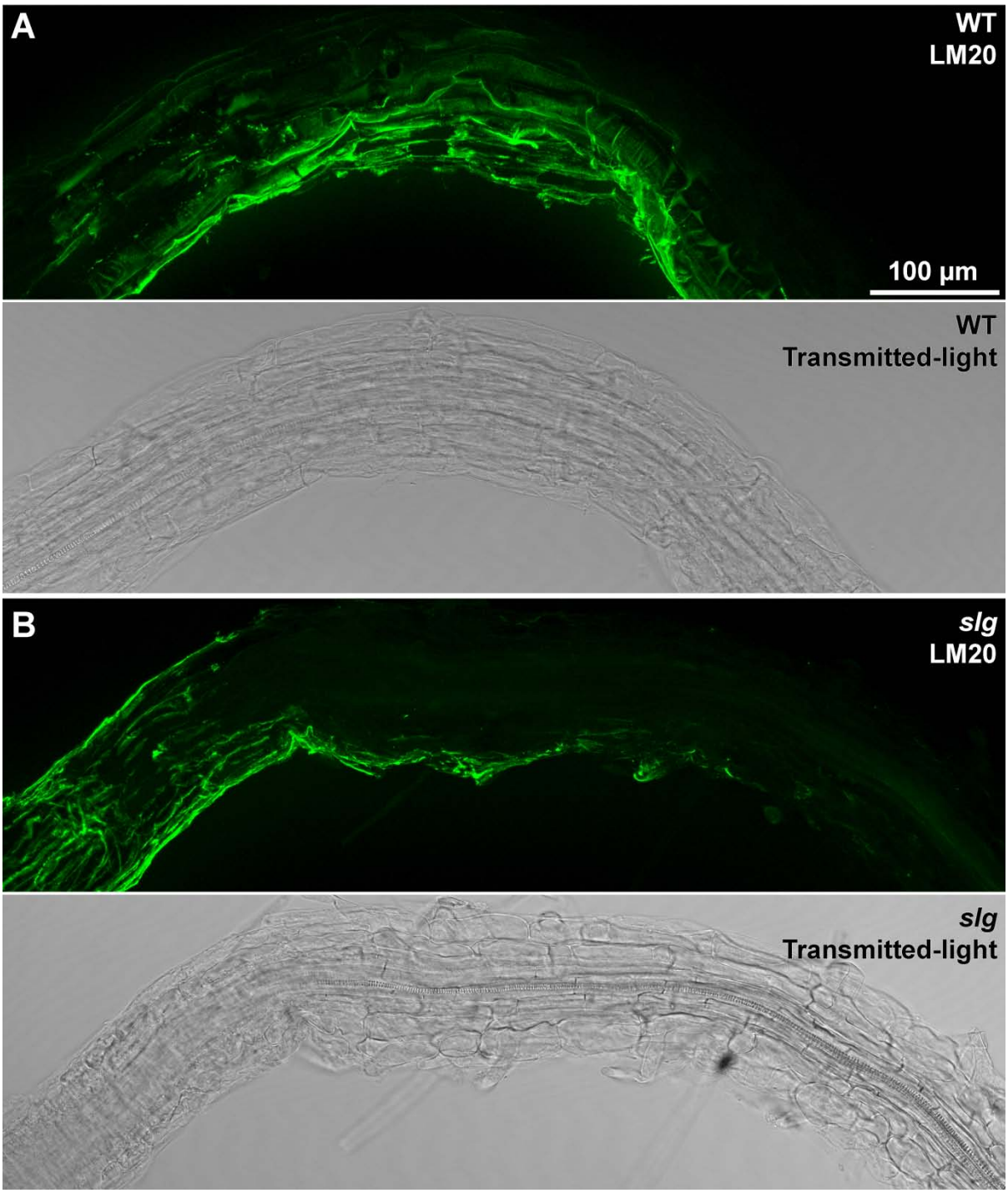

Figure 4.18 The LM20 homogalacturonan epitope is not significantly altered in *sloughy* roots. Confocal maximum projections of roots labelled with LM20 primary antibody and concurrent transmitted light image (single focal plane). Scale bar in **A** = 100 µm.

A Wild-type (WT).

B *sloughy (slg)*.

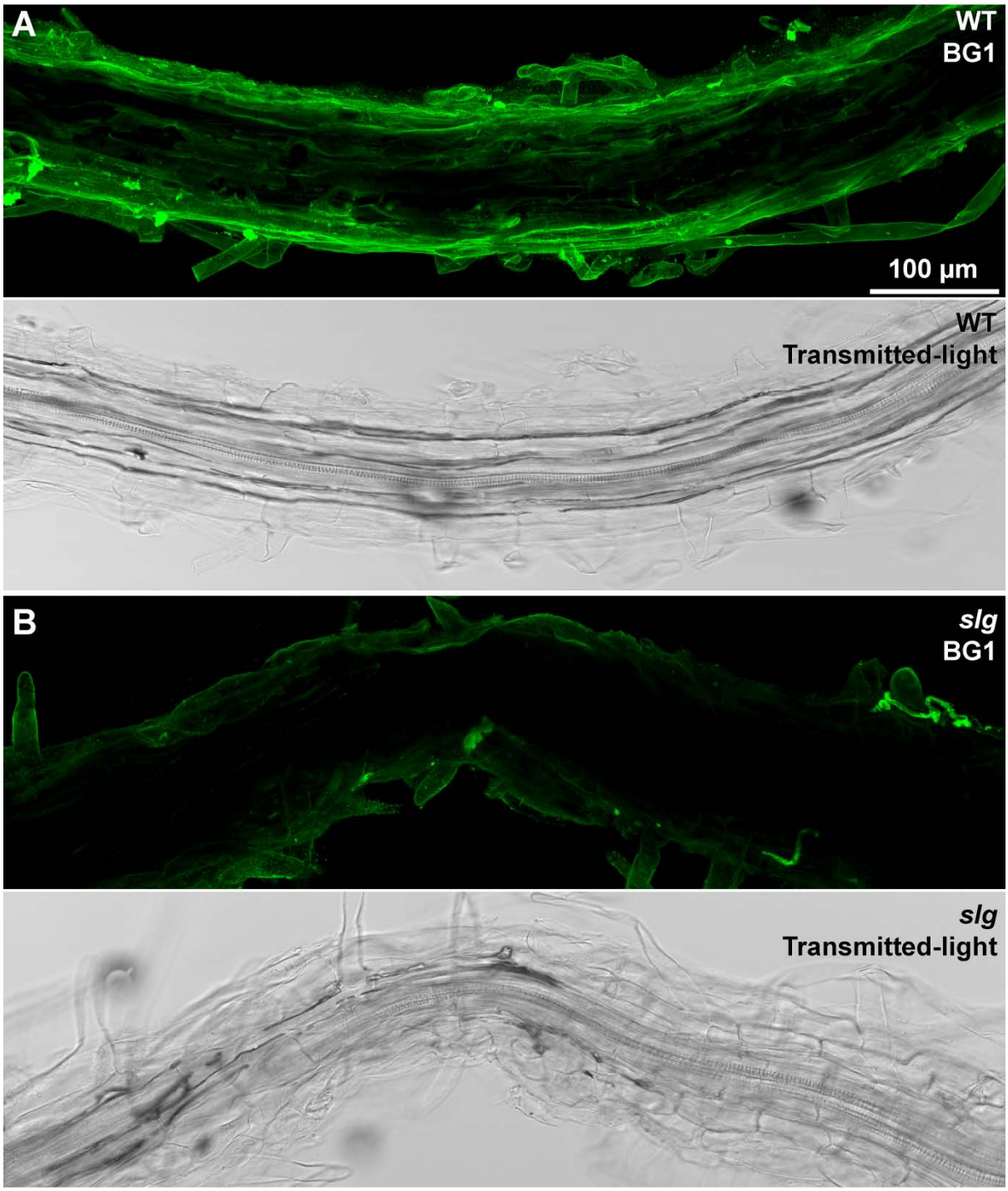

Figure 4.19 The BG1 callose epitope is not significantly altered in *sloughy* roots. Confocal maximum projections of roots labelled with the BG1 primary antibody and concurrent transmitted light image (single focal plane). Scale bar in **A** = 100 µm.

A Wild-type (WT).

B *sloughy (slg)*.

4.4 Discussion

4.4.1 Comparative analysis of the *schizoriza* TILLING mutants and *SCZ*-OE plants

Once the mutation in *sloughy* was mapped to the *SCHIZORIZA* gene, a collection of *schizoriza* TILLING mutants were ordered from the ABRC for comparative analysis. Focus was placed on lines CS88021 and CS93157 as both lines were confirmed to have non-synonymous mutations resulting in the introduction of an early stop codon. CS88021 produces a SCHIZORIZA protein of 132 amino acids, while CS93157 produces a protein of 192 amino acids, 6 residues longer than *sloughy*. Compared to the wild-type protein of 349 amino acids, all three mutants are missing several conserved domains that are required for full functionality, including the oligomerization region (HR-A/B), nuclear localisation signal and nuclear export signal. All three mutants are likely *SCHIZORIZA* null alleles.

CS88021 and CS93157 have reduced root growth comparative to wild-type, similar to that seen in *sloughy*, indicating that they did display mutant phenotypes. However, although CS88021 appeared phenotypically identical to *sloughy* seedlings, CS93157 had shorter and wider roots, and appeared to develop more root hairs comparative to *sloughy*, reminiscent of previously-described *schizoriza* mutants (Mylona *et al*., 2002, ten Hove *et al*., 2010). It was initially thought that *sloughy* and CS88021 may have possessed slightly different phenotypes compared to CS93157 and the other reported *schizoriza* mutants, with this explaining why the striking cell separation observed in *sloughy* and CS88021 has not been thoroughly documented.

However, the detailed comparisons of CS93157 and *sloughy* documented in this chapter suggest that the observed phenotypic difference in CS93157 may be a consequence of this line harbouring additional EMS-induced mutations. *sloughy* and CS93157 displayed similar patterns of reduced root growth and production of lateral roots on agar and both showed temperature sensitive increase in root width associated with cell separation. The primary differences between CS93157 and *sloughy* CS93157's shorter and wider roots and that when placed on soil, CS93157 was dramatically reduced in its above-ground growth. The above ground organs were severely dwarfed, with the inflorescence stems, flowers and siliques all reduced in size. Since neither *sloughy*, CS88021, nor any of the *schizoriza* mutants described in the literature possess above-ground phenotypes, this dwarfed phenotype in CS93157 indicates that the line may harbour additional EMS-induced mutations in the genome which impact its growth and development, both above- and below-ground. To test this, CS93157 needs to be crossed back to wild-type, selfed and the recessive *schizoriza* phenotype selected. Repeating this process several times, which time constraints in this project precluded, would 'clean up' the genome. If, after this series of crosses, CS93157 maintained the *schizoriza* root phenotype, but regained normal above-ground development, this would confirm that the dwarfed phenotype is due to the presence of an additional mutation(s). Since *sloughy* and CS88021 had identical phenotypes, and because CS93157 also displays evidence of cell separation, these results suggest that aberrant cell separation is prevalent in all *schizoriza* null mutants, and that the dwarfing phenotype observed in CS93157 is likely a red herring.

One possibility for the lack of documentation on the cell separation phenotype in the original *schizoriza* mutants (Mylona *et al*., 2002) is differences in growth conditions. In Chapter 2, for example, it was shown that the cell separation phenotype in *sloughy* is reduced at lower temperatures. Were plants only screen at lower temperatures, cell separation may have been overlooked. This is possible, for the Scheres group grew their *schizoriza* mutants at 22°C (ten

Hove *et al*., 2010). However, although temperature growth conditions were not detailed in the initial description of *schizoriza* (Mylona *et al*., 2002), the Dolan group subsequently grew their *schizoriza* plants at 25°C (Pernas *et al*., 2010) which suggests that a cell separation phenotype should have been seen. The different growth media used between the laboratories may have also been a confounding factor. However, neither the concentration of agar, nor an alternative growth medium based on the growth media used by the Scheres laboratory (ten Hove *et al*., 2010), modified the cell separation in *sloughy* roots (see Chapter 2). The simplest explanation for the lack of documentation on the cell separation phenotype in *schizoriza* mutants is that both the Dolan and Scheres research groups focus most strongly on root meristem development and the cell separation phenotype observed may have been overlooked or ignored.

The comparative analysis of *sloughy* to the collection of *schizoriza* TILLING mutants, in corroboration with the brief description on tissue separation by Scheres and colleagues (ten Hove *et al*., 2010), has established that aberrant cell separation is a *bona fide* phenotype in *schizoriza* null mutants. Although, the phenotype of CS93157 may be confounded by additional EMS-induced mutations in the genome, *sloughy* is a good representative of the *schizoriza* phenotype. Furthermore, the overwhelming evidence supporting that the *sloughy* mutation as the cause of the aberrant cell separation suggests that complementation analysis of *sloughy* with the wild-type *SCHIZORIZA* gene, which has not been attempted in this project, but which was reported by the Scheres group, might not be necessary.

A comparative analysis of *sloughy* to lines over-expressing *SCHIZORIZA* was also included since *SCZ*-OE plants had been reported to possess aberrant cell separation in the mature root (Begum *et al*., 2013). The growth experiments, however, demonstrated that the *SCZ*-OE plants were phenotypically distinct from *sloughy*, although they too show temperature-sensitive swelling.

In contrast to the shortened roots of *sloughy*, *SCZ*-OE roots were only slightly reduced in length, being on average 76% of that of wild-type. Moreover, although the frequency of lateral roots is significantly increased in *sloughy*, the frequency of lateral roots in *SCZ*-OE was similar to wild-type. Since this not a reciprocal phenotype to *sloughy*, this may call into question the hypothesis proposed in Chapter 2 linking the increased frequency of lateral roots in *sloughy* to altered auxin levels or responses. Further analyses of hormone levels and perception would be required to resolve this, but were not pursued.

The above-ground phenotype of *SCZ*-OE plants was similar to that seen in wild-type and *sloughy*. Clearly, neither the disruption of SCHIZORIZA function through the introduction of early stop codons, nor the ectopic over-expression of *SCHIZORIZA*, has a significant impact on the growth and development on the above-ground organs of a plant. However, the expression of *SCHIZORIZA* has previously been detected in many above-ground organs of wild-type plants, including the shoot apex, pistils, seeds, and the base of siliques (Begum *et al*., 2013).

The *SCZ*-OE roots were significantly wider and hairier than *sloughy*. In contrast to the single supernumerary layer present in *sloughy*, *SCZ*-OE seedlings have been reported to possess numerous supernumerary layers, including epidermal, in the roots accounting for their significantly wider appearance and increased frequency of root hair development (ten Hove *et al*., 2010, Pernas *et al*., 2010, Begum *et al*., 2013). It is not, however, clear why the *SCZ*-OE seedlings are significantly hairier than *sloughy* or *schizoriza*, which also have a supernumery epidermal layer. It is possible that trichoblast identity may be altered in the *SCZ*-OE seedlings, resulting in a higher frequency of epidermal cells developing root hairs. Trichoblast-specific enhancer trap lines crossed to *SCZ*-OE seedlings may be one line of investigation to determine whether this may be contributing factor. Although the *SCZ*-OE seedlings often showed evidence of cells detaching from the mature root, the cell detachment

phenotype was distinct from that of *sloughy*. In contrast to the epidermal cells in *sloughy*, which typically separate along the sides of the cells but remain attached at the cell ends, the cells detaching from *SCZ*-OE also detached at their cell ends, sloughing off as individual, isolated cells. The detachment of these cells in *SCZ*-OE seedlings has been linked to the proliferation of ectopic epidermal and lateral root cap cells further up in the root which detach after prolonged root growth (Begum *et al*., 2013).

4.4.2 Confused cell identity in *sloughy* roots

In chapter 2 *sloughy* was shown to possess a supernumery cell layer surrounding the stele. The development of subepidermal root hairs was also detected. This provided strong evidence for confused cell identity in the roots of *sloughy*. Indeed, the *sloughy* mutation was mapped to the *SCHIZORIZA* gene which encodes a transcription factor that plays a crucial role in the development and maintenance of the root meristem.

While the papers published on *SCHIZORIZA* have focused on cell fate within the developing meristem, in accordance with the research interests of the respective research groups and their data on where SCHIZORIZA is active (Mylona *et al*., 2002, ten Hove *et al*., 2010, Pernas *et al*., 2010), the identity of cells in the mature root has not previously been reported. Since this project was focused on the aberrant cell separation present in *sloughy* roots, and as the identity of these cells could not be determined by confocal microscopy alone, a collection of arabidopsis GAL4-GFP enhancer trap lines were crossed to *sloughy* to infer cell identity in the elongation zone, in particular the separating epidermal cells.

Mature, wild-type arabidopsis roots have three concentric cell layers surrounding the stele in the mature root with one layer of endodermis around the stele, one layer of cortex around the endodermis, and one layer of epidermis around the cortex. Together the endodermis and cortex compose the ground tissue, while the epidermis is dermal tissue. *sloughy* has a total of

four cell layers surrounding the stele. The cortex and endodermal-specific line J0571 showed two cell layers with ground tissue identity in *sloughy* roots. The innermost layer surrounding the stele morphologically resembles endodermis, with propidium iodide labelling of the casparian strip. The next outer layer also has ground tissue identity, but whether this is cortex or endodermis cannot be differentiated with the J0571 marker. Since no cortex-specific marker lines such as J1772 or J0671 were successfully crossed to *sloughy*, the exact identity of this ground tissue cell layer surrounding the endodermis could not be resolved. However, a closer inspection of the root cap and endodermis-specific line J2672, that has been successfully crossed to *sloughy*, may reveal whether this ground tissue layer has partial endodermal identity. As previously demonstrated for the root meristem (ten Hove *et al*., 2010), it would seem likely that these cell identities might be maintained in the more mature parts of *sloughy* roots, with two endodermal layers surrounding the stele and cortex identity abolished in the ground tissue.

Instead of a single layer of epidermis seen in wild-type, the epidermal-specific J0481 line revealed that both the epidermal and the subepidermal cell layers had epidermal identity in *sloughy* roots. This result is in corroboration with the previous data published on cell identity within the root meristem of *schizoriza* mutants (Mylona *et al*., 2002, ten Hove *et al*., 2010). Epidermal identity in the subepidermal identity accounts for the development of subepidermal root hairs from *sloughy* roots. However, the second layer out from the stele also appeared to have epidermal identity. This has not been reported on in the literature. Further investigation is required to confirm this finding. If confirmed, this cell layer might have mixed endodermal and epidermal identity.

These separating epidermal cells display morphological characteristics reminiscent of border-like cells in the root cap of arabidopsis and were hypothesized to display root cap identity. However, no ectopic root cap identity was detected in the root meristem or mature root of

sloughy with any of the root cap-specific enhancer trap lines used in this project. This result contrasts with previously published data on *schizoriza* mutants. *SMB-GFP*, a lateral root cap-specific marker (Willemsen *et al*., 2008), was expressed in both the epidermal and subepidermal layers of the root meristem in *schizoriza*, demonstrating that the epidermal and subepidermal layers in *schizoriza* mutants possess mixed epidermal and root cap identity (ten Hove *et al*., 2010). There are several possibilities as to why these root cap-specific enhancer trap lines may not have revealed ectopic root cap identity in *sloughy*. The simplest explanation is that the mixed identity cells are not capable of driving any of the enhancer trap lines used. The enhancer trap lines may require full root cap identity to drive GFP expression and since the cells may only possess partial root cap identity, the full expression patterns of root cap identity may not be activated, including the enhancer to drive GAL4-dependent expression of GFP. Another reason may be that these enhancer trap lines are for general root cap identity, and are not specifically lateral root cap identity. Thus, they would not be detected in the cells with mixed epidermal and lateral root cap identity. The failure of the enhancer trap lines may also explain why the lateral root cap-specific marker *SMB*-GFP has been used in *schizoriza* rather than root cap-specific GAL4-GFP enhancer trap lines (ten Hove *et al*., 2010).

Further crosses to *SMB*-GFP or *FEZ*-GFP, another lateral root cap marker (Willemsen *et al*., 2008), may reveal ectopic lateral root cap identity in the separating epidermal cells. However, if *SMB*-GFP and *FEZ*-GFP are only expressed in the root meristem, and not further up in the root, this would suggest that as the epidermal/lateral root cap cells leave the meristem and enter the elongation zone, lateral root cap identity is lost. This change has been previously demonstrated in the *trn* mutants (Cnops *et al*., 2000).

4.4.3 Cell wall epitope labelling in *sloughy* roots

To investigate the cell wall properties that may have changed in the epidermal cell layers of *sloughy*, a collection of twelve primary antibodies that target cell wall epitopes were used to immunolabel whole roots of wild-type and *sloughy*.

The JIM13 antibody specifically labelled the surface of root cap cells in both wild-type and *sloughy* seedlings, indicating that the JIM13 arabinogalactan protein epitope is not altered in the root cap cells of *sloughy*. In contrast to wild-type, however, the JIM13 antibody often labelled subsets of epidermal cells and surrounding mucilage in the mature roots of *sloughy*. This change in labelling pattern was not always consistent, with patches of labelling often running along an individual root.

The JIM13 antibody was raised against arabinogalactan protein enriched-fractions isolated from carrot suspension-cultured cell lines (Knox *et al*., 1991). Driouich and colleagues (Vicré *et al*., 2005) demonstrated that the JIM13 arabinogalactan epitope was associated with border-like cells and peripheral cells of the arabidopsis root cap, with no labelling detected in the meristematic, ground tissue or epidermal cells, and suggested that the maturation process of border-like cells is accompanied by the synthesis of significant amounts of arabinogalactan proteins. Driouich and colleagues (Durand *et al*., 2009) also demonstrated that although the cell walls of border-like cells in the *qua1* pectin mutant were weakly labelled with the JIM13 antibody compared to wild-type, the JIM13 antibody strongly labelled the thick, secreted mucilage of the *qua1* border-like cells. Their explanation was that the altered homogalacturonan content in the *qua1* mutant alters the cell wall architecture, thereby affecting cell wall porosity. This may limit the retention of arabinogalactan proteins in the cell wall and facilitate their secretion into the surrounding mucilage (Durand *et al*., 2009). This is supported by increased extracellular polymers detected in the medium of *qua1*

suspension cultured cells (Leboeuf *et al*., 2005). An alternative explanation was that the border-like cells in *qua1* compensate for the reduced homogalacturonan content by an increased production of arabinogalactan proteins (Durand *et al*., 2009).

The ectopic labelling pattern of the JIM13 arabinogalactan epitope in the epidermal cells and surrounding mucilage in the mature roots of *sloughy* provides biochemical evidence that the epidermal cell layers have border-like cell characteristics. This corroborates the cell identity data provided by Scheres and colleagues (ten Hove *et al*., 2010), who used *SMB-GFP* to demonstrate that the epidermal and subepidermal layer of *schizoriza* mutants have mixed epidermal and lateral root cap identity. The detection of the JIM13 arabinogalactan protein epitope in the secreted mucilage may also reflect altered cell wall porosity of the epidermal cells in *sloughy*, analogous to the *qua1* mutant.

Further experimentation with the JIM13 antibody will, however, be required. Apart from confirming JIM13 binding in cross sections of wax-embedded roots of *sloughy,* where JIM13 binding to the metaxylem would act as a positive control (Dolan *et al*., 1995), further investigation should include JIM13 immunolabelling of wild-type and *sloughy* roots that have been treated with Yariv reagents which specifically bind to and precipitate plant arabinogalactan proteins (Kitazawa *et al*., 2013). Reduced ectopic labelling of *sloughy* roots following Yariv reagent treatment due to the interference of the JIM13 epitope would confirm that the JIM13 antibody is specifically recognizing arabinogalactan proteins epitopes in the separating epidermal cells. The LM2 antibody which also label arabinogalactan proteins in arabidopsis roots, with similar labelling patterns to JIM13 labelling in *qua1* border-like cells (Durand *et al*., 2009), might also be tested to corroborate these findings.

The LM8 xylogalacturonan epitope showed a similar distribution in wild-type and *sloughy* roots, but may also be present in ectopic mucilage surrounding the mature roots of *sloughy*.

The LM8 antibody was raised against xylogalacturonan isolated from the seed coat of pea and recognises a specific epitope of a xylogalacturonan pectic polysaccharide that is associated with plant cell separation processes resulting in cell detachment in a wide range of species (Willats *et al*., 2004). The LM8 epitope is also associated with border-like cells and surrounding mucilage in wild-type arabidopsis plants, and the staining of the mucilage around isolated border-like cells of the *qua1* mutant appeared stronger than in wild-type (Durand *et al*., 2009, Driouich *et al*., 2010). The functional relationship between the LM8 xylogalacturonan epitope and cell separation processes is still not understood. Although this result needs to be repeated to confirm this finding, this may indicate that the LM8 xylogalacturonan epitope may be contributing to the cell separation observed in the epidermal cell layers, and corroborates with the ectopic labelling pattern seen with the JIM13 antibody.

In this study, which was limited to the labelling of whole roots, ten of the tested antibodies showed no differences in labelling patterns between wild-type and *sloughy* roots and several antibodies against pectin showed no differences despite pectin being important for cell adhesion.

The JIM5, LM19 and LM20 homogalacturonan epitopes were strongly labelled in both wild-type and *sloughy* roots. The JIM5 antibody recognizes partially methyl-esterified or un-esterified epitopes of homogalacturonan (Knox *et al*., 1990), while the LM19 and LM20 antibodies were isolated from a screen for binding to arabidopsis seed coat mucilage (Verhertbruggen *et al*., 2009). The LM19 antibody recognises a range of homogalacturonan epitopes, but appears to have a preference for un-esterified homogalacturonan, while the LM20 antibody requires methyl-esterified homogalacturonan for recognition and does not bind to un-esterified homogalacturonan. Together, these results provide strong evidence that the levels of a range of homogalacturonan epitopes remained unchanged on the surface of *sloughy* roots.

The BG1 (1-3,1-4)-β-D-glucan (callose) epitope showed equivalently labelling in wild-type and *sloughy* roots. The BG1 antibody was originally raised against a (1-3,1-4)-β-D-glucan coupled to bovine serum albumin (Meikle *et al*., 1994). As this antibody recognizes callose in plants, it identifies the location of plasmodesmata (Radford *et al*., 1998), pit fields (Orfila and Knox, 2000) and wounding sites (Nakashima *et al*., 2003). This results indicates that there is no change in the content or deposition of callose on the surface of *sloughy* roots.

There was no evidence of epitope labelling in either wild-type or *sloughy* roots with the homogalacturonan antibodies JIM7, LM7 and LM18, the arabinogalactan protein antibody JIM14, the xylan antibody LM10, or the xylan/abrinoxylan antibody LM11. Since the immunolabelling protocol was based on labelling and imaging whole roots, the cell wall epitopes for these particular antibodies may have not been exposed to these antibodies. To increase the rate of successful labelling, cross sections of roots might be immunolabelled in place of whole roots, as this might reveal changes in labelling patterns not previously detected with the JIM13, JIM5, LM19, LM20, LM8 and the BG1 antibodies. Immunolabelling cross sections of *sloughy* roots was originally planned for this project, but were not completed due to the laborious and time consuming nature of arabidopsis root sectioning. Higher magnification imaging of the roots, for example with 63x lens, may also reveal subtle biochemical differences that may have been overlooked with the screening protocol used.

4.5 Summary

- Investigation of a range of *schizoriza* TILLING mutants revealed that aberrant cell separation is ubiquitous to *schizoriza* null mutants.
- Plants over-expressing *SCHIZORIZA* are phenotypically distinct from *sloughy*, and although they also display evidence of ectopic cell detachment, this cell separation is morphologically distinct from *sloughy*.
- Cortex and endodermal-specific GAL4-GFP enhancer trap lines revealed that these two identities are restricted to the endodermal layer, and the next ground tissue layer that surrounds it in *sloughy* roots.
- Epidermal-specific GAL4-GFP enhancer trap lines revealed that the epidermal and subepidermal layers in *sloughy* roots have epidermal identity.
- No evidence for ectopic root cap identity was detected in the root meristem or mature roots of *sloughy* with any of the tested root cap-specific GAL4-GFP enhancer trap lines. This result contrasts with previously published data on *schizoriza*.
- The JIM13 antibody, which specifically labels arabinogalactan proteins in wild-type root caps, often labelled the elongated epidermal cells and surrounding mucilage in *sloughy*. The LM8 antibody may also label ectopic mucilage in the mature roots, supporting the concept that the epidermal cells have border-like cell characteristics.
- The JIM5, LM19 and LM20 homogalacturonan epitopes and the BG1 callose epitope were unchanged on the surface of *sloughy* roots.

Chapter 5

Discussion

"We believe that there is no structure in plants more wonderful, as far as its functions are concerned, than the tip of the radicle"

- Charles Darwin and Sir Francis Darwin (The Power of Movement in Plants, 1881)

5.1 Overview

The primary objective of this project was the identification and characterization of the *sloughy* mutation. Complementary to this was understanding a link between the mutation and the cell separation phenotype, as well as determining the nature of the altered cell wall properties of the epidermal cells. Since *sloughy* displayed a cell adhesion defect, the starting hypothesis was that the mutated gene may have been associated with the biosynthesis or deposition of pectic polysaccharides, or another related cell wall component implicated in cell adhesion.

Using HRM analysis to calculate recombination frequencies in the *sloughy* mapping population, the mutation was mapped to a small 27,283 bp region on chromosome I. On sequencing all five candidate genes in this region, a single nucleotide mutation introducing a stop codon was detected in the previously-described heat shock transcription factor *SCHIZORIZA* (Mylona *et al*., 2002, ten Hove *et al*., 2010, Pernas *et al*., 2010). While the rapid identification of the *sloughy* mutation was a significant outcome for this project, *SCHIZORIZA* plays a role in the development and maintenance of the root meristem, a result remarkably different to the initial hypothesis.

While identifying that the *sloughy* mutation is present in a previously characterized gene, this project has, nevertheless, been able to contribute novel information with regards to the activity of the *SCHIZORIZA* gene and protein. This is because the literature on *schizoriza* mutants has focused almost exclusively on the developing meristem, with little documentation on a cell separation phenotype. The investigation of *schizoriza* TILLING mutations, and from the brief descriptions of *schizoriza* mutants in the literature (ten Hove *et*

al., 2010), indicate that *sloughy* is a null allele of *SCHIZORIZA* and that the aberrant cell separation phenotype is ubiquitous to *schizoriza* null mutants.

GAL4-GFP enhancer trap lines were crossed to *sloughy* to investigate the identity of the separating epidermal cells that have undergone elongation after leaving the root meristem. A cortex and endodermal-specific line revealed that these identities are restricted to the endodermal layer and the next ground tissue layer out. The literature has indicated that both of these layers possess endodermal identity, with cortex identity abolished from the ground tissue (ten Hove *et al*., 2010), and thus, these two layers also likely represent endodermis in *sloughy*. Epidermal-specific lines revealed that both the epidermal and subepidermal layers of *sloughy* have epidermal identity. This result corroborates with the published data on *schizoriza* mutants and accounts for the development of subepidermal root hairs (Mylona *et al*., 2002, ten Hove *et al*., 2010). The supernumerary layer observed in *sloughy* roots is a result of an extra periclinal division in the cortex/endodermis daughter cells, resulting in a root with three ground tissues layers, with the subepidermal, ground-tissue derived layer assuming a dermal-layer identity (Mylona *et al*., 2002, ten Hove *et al*., 2010). There was no indication of ectopic root cap identity in either the root meristem or mature roots of *sloughy* with any of the four root cap-specific lines used. This result contradicts previously published data by Scheres and colleagues (ten Hove *et al*., 2010), who analyzed the expression patterns of *SMB-GFP*, a lateral root cap-specific marker, in *schizoriza*. They showed that *SMB-GFP* was expressed in both the epidermal and subepidermal layers of the root meristem, demonstrating that the epidermal and subepidermal layers in *schizoriza* mutants have mixed epidermal and lateral root cap identity (ten Hove *et al*., 2010).

The JIM13 antibody, which specifically labels arabinogalactan proteins in wild-type root caps, often labelled the epidermal cells and surrounding mucilage further up the root of *sloughy*. The LM8 antibody which is associated with the root cap and surrounding mucilage

in wild-type plants, may also label ectopic mucilage in mature roots of *sloughy*, supporting this finding. This immunolabelling data, taken in account with morphological characteristics of the epidermal cells, strongly support that the separating epidermal cell layers in *sloughy* have partial lateral root cap identity.

5.2 A model for aberrant cell separation in sloughy

Based on data from this study and the literature, a model linking the mutation in *sloughy* to the cell separation phenotype is proposed (Figure 5.1). Within this model, steps 1 to 3 have been fully or partially documented with this project, while steps 4 and 5 are speculated to lead to the observed phenotype.

A single nucleotide mutation in *sloughy* introduces an early stop codon in the transcription factor *SCHIZORIZA*, eliminating several conserved domains essential for activity. This change in SCHIZORIZA activity leads to confused cell identity in the developing roots, including mixed epidermal and lateral root cap identity in the epidermal and subepidermal layers of *sloughy*. This change in identity is accompanied by the expression of different cell wall proteins, including the JIM13 epitope. Border-like cells in the root cap of arabidopsis undergo specific cell wall modifications during development that allow for their detachment from the root. The cellulases CEL3 and CEL5 (del Campillo *et al*., 2004), the pectin glycosyltransferase QUA1 (Durand *et al*., 2009), the pectin methyltransferase QUA2, and pectolytic enzymes (Hawes and Lin, 1990) (see section 1.2.4) have all been implicated in these modifications. Moreover, because border-like cells release in files of cells attached end-on-end, these cell wall modifications must be highly specific, targeting certain cell walls but not others. Since the epidermal cell layers in *sloughy* separate in a similar fashion to border-like cells, detaching along the sides of the cell, while remaining attached at the cell ends, it is proposed that similar cell wall modifications take place in *sloughy* leading to the aberrant cell separation phenotype.

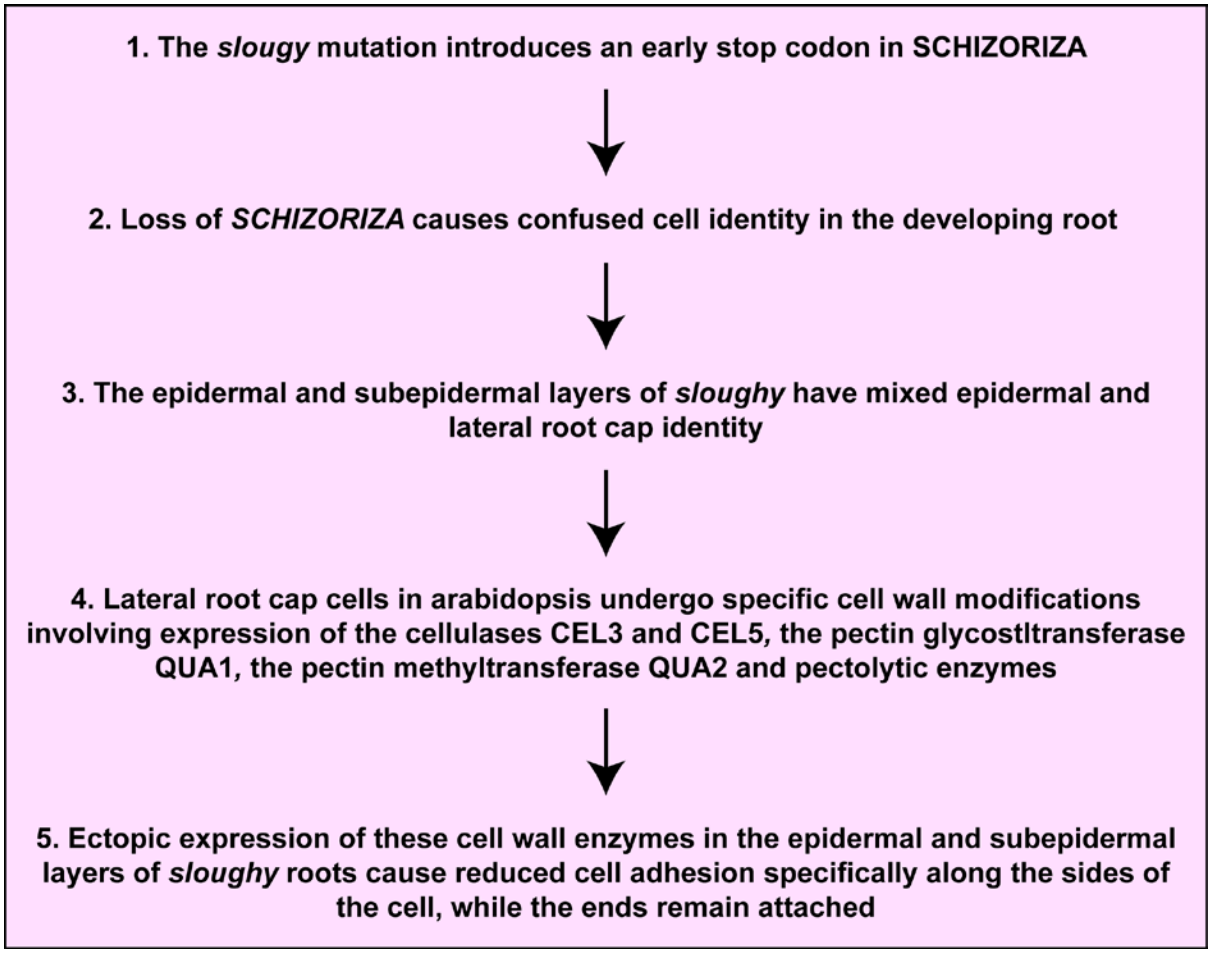

Figure 5.1 A proposed model for the cell separation phenotype observed in *sloughy* roots. Steps 1 through 3 have been confirmed, while steps 4 and 5 are suggested to cause the observed phenotype. CEL3 = CELLULASE3, CEL5 = CELLULASE5, QUA1 = QUASIDMODO1 and QUA = QUASIMODO2.

5.3 Experiments to test this model

The model proposed in Figure 5.1 contains a series of steps that are readably testable. In several cases, work on these experiments was started during the project, but time constraints prevented their completion.

5.3.1 Cell separation in the subepidermal layer

Since the model suggests that because both the epidermal and subepidermal layers in *schizoriza* mutants have epidermal and lateral root cap identity, both layers should exhibit characteristics of cell separation. Although a reconstructed cross section of the root (see Figure 2.9) indicated that the subepidermal layer may also separate in *sloughy*, this had previously not been identified nor has been confirmed. Further reconstructed cross sections of propidium iodide stained roots of *sloughy* seedlings grown at 30°C, as well as cross sections embedded in suitable resins or waxes, will be undertaken to resolve this.

5.3.2 Lateral root cap identity

Essential to this model is demonstrating that the separating epidermal cell layers in *sloughy* roots do possess partial lateral root cap identity. Although mixed epidermal and root cap identity has previously been described in the epidermal and subepidermal cell layers in the root meristem of *schizoriza* mutants (ten Hove *et al*., 2010), whether this lateral root cap identity is maintained further up in the root has not been documented. To confirm lateral root cap identity further up the roots, *sloughy* could be crossed to either *SMB*-GFP and *FEZ*-GFP, two NAC domain transcription factors exclusively expressed in the root cap that have been shown to control the activity of root cap stem cells (Willemsen *et al*., 2008). If the model is

correct, *sloughy* will express *SMB*-GFP or *FEZ*-GFP, identifiable by GFP localization to the nucleus, in the separating epidermal cell layers. However, if the epidermal cell layers do not express *SMB*-GFP or *FEZ*-GFP, this would indicate that the cells with mixed epidermal and lateral root cap identity within the meristem lose their lateral root cap identity upon entering the elongation zone, as this has been demonstrated in the *trn1* and *trn2* mutants (Cnops *et al*., 2000). Were this the case, the cell wall modifications that lead to the cell separation in the mature roots must have been initiated within the root meristem, before the cells enter the elongation zones.

5.3.3 Cell wall immunolabelling

Further cell wall epitope labelling of *sloughy* roots will be performed to reveal additional cell wall modifications involved in cell separation in *sloughy*. Transverse sections of *sloughy* roots embedded in suitable waxes will be immunolabelled with the collection of cell wall antibodies. Sectioning will allow the epitopes that were previously not exposed on the surface of roots to be labelled. Longitudinal sections will also be cut, at this would enable the differentiation between the cell wall properties of the side and end walls cells in *sloughy*.

Although twelve antibodies were tested during this project, additional cell wall antibodies will be ordered. For example, the LM2 antibody, which also recognizes arabinogalactan proteins with labelling patterns similar to JIM13 (Durand *et al*., 2009), would be predicted to also give ectopic labelling in mature *sloughy* roots. Similarly, the arabinogalactan epitope recognized by the CCRC-M7 antibody is present in the arabidopsis root epidermis, but is specifically reduced in the lateral root cap cells (Freshour *et al*., 1996). The model would predict that the labelling pattern of CCRC-M7 might be reduced or absent in the separating epidermal cells of *sloughy*. A plant cell wall antibody "Survey Kit", a collection of cell wall antibodies in a 96-well plate, is available from the Complex Carbohydrate Research Centre at

the University of Georgia (www.ccrc.uga.edu) and might also be used to compare immunolabelling of wild-type and *sloughy* roots.

As an alternative to immunolabelling, the altered cell wall properties of *sloughy* roots could be determined by biochemical analytical methods such as Fourier transform infrared microspectroscopy (McCann *et al*., 1992) or gas chromatography-mass spectrometry (Lisec *et al*., 2006). Such methodologies may provide significantly more insight into the altered cell wall properties of *sloughy*, but would require greater resources and expertise.

5.3.4 Transcription factors involved in lateral root cap development

Investigating the expression levels of genes implicated in the development of the lateral root cap may provide insight into the molecular dynamics occurring in the separating epidermal cells layers of *sloughy*. For example, the genes *FEZ*, *SMB*, *BEARSKIN1* (*BRN1*) and *BRN2* have all been shown to control the development of the root cap (Willemsen *et al*., 2008, Bennett *et al*., 2010). Furthermore, *SMB*, *BRN1* and *BRN2* have been shown to act redundantly to promote the cell wall modifications of the root cap that allow for the cell walls to detach (Bennett *et al*., 2010). Accordingly, the expression levels of *SMB*, *BRN1* and *BRN2* would be predicted to be up-regulated in the roots of *sloughy* comparative to wild-type.

5.3.5 The expression of cellulases and pectin-related enzymes in *sloughy*

The endo-1,4-β-D-glucanases CEL3 and CEL5 which hydrolyse cellulose have been proposed to function in the sloughing of the arabidopsis root cap (del Campillo *et al*., 2004). *CEL5* is expressed exclusively in root cap cells and a *cel5* T-DNA mutant had an increased retention of the root cap, thereby making sloughing less efficient. A paralog of *CEL5*, *CEL3*, was also identified in the arabidopsis genome. As the *cel5* T-DNA mutant has a modest phenotype, these two glucanases are thought to act redundantly in the sloughing of border-

like cells from the root tip by modifying cellulose content (del Campillo *et al*., 2004). Similarly, the pectin glycosyltransferase *QUA1* (Bouton *et al*., 2002) and the pectin methyltransferase *QUA2* (Mouille *et al*., 2007) have also been proposed to function in the separation of border-like cells from the root tip of arabidopsis (Durand *et al*., 2009). In contrast to wild-type border-like cells which separate as files of cell attached end-on-end, the border-like cells of the *qua1* and *qua2* mutants, both characterized as producing less homogalacturonan, release as isolated cells. This phenotype was more pronounced in *qua1* than in *qua2*. This suggests that the activity of QUA1 and QUA2 are essential for the adhesion of border-like cells at the cell ends (Durand *et al*., 2009).

This information is important, because it provides target genes and proteins that can be tested in *sloughy*.

Gene expression analysis of *CEL3*, *CEL5* and *QUA1* has already commenced to determine whether these genes are up-regulated in the roots of *sloughy* due to an increase in cells possessing lateral root cap identity. RT-qPCR primers (see section 3.2.7) were designed for the analysis of *CEL3*, *CEL5* and *QUA1*, and several actin reference genes (Table A1.5). Primers were also designed to clone, amplify and sequence genomic fragments of these genes spanning the internal RT-qPCR primer binding sites to generate standard curves for absolute quantification (see section 3.2.7). These control plasmids for each of the six genes were generated, sequenced by Macrogen (South Korea) and confirmed to contain the correct genomic inserts. Unfortunately, due to time constraints, the gene expression analysis of these three genes was not completed. However, since CEL3, CEL5 and QUA1 are all implicated in the cell wall modifications of border-like cells, an up-regulation of *CEL3*, *CEL5* and *QUA1* would be predicted in the roots of *sloughy* comparative to wild-type if the model were correct.

Crosses to *cel-3*, *cel-5*, *qua-1* and *qua2* mutants might also be conducted to confirm whether compounding phenotypes match the predictions generated by the model. T-DNA insertion mutants for *CEL3* and *CEL5* have been ordered from the ABRC and reciprocal crosses between *cel3* and *cel5* have been made. Although the seed from these crosses has been collected, the progeny of these crosses have not yet been investigated and isolation of the *cel3*/*cel5* double mutant will require screening the offspring with T-DNA insertion primers for a homozygous double T-DNA insertion. Since the *cel5* mutant lacks any other distinct phenotypic differences besides greater root cap retention, CEL3 and CEL5 were suggested to act redundantly in the process of border-like cell sloughing (del Campillo *et al*., 2004). Thus, it is predicted that the *cel3/cel5* double mutant will have an enhanced phenotype, with an even greater retention of the border-like cells. The double mutant will be crossed to *sloughy* to generate the *sloughy*/*cel3*/*cel5* triple mutant, which, after selfing, would be screened using the T-DNA insertional primers for CEL3 and CEL5, and the HRM analysis primers for *sloughy* (Table A1.4). If the model is correct, the *sloughy*/*cel3*/*cel5* triple mutant should greatly reduce the aberrant cell separation seen in *sloughy*.

An arabidopsis CEL5::GUS line has previously been generated by Sara Patterson and colleagues to identify where CEL5 is expressed (del Campillo *et al*., 2004). GUS-staining of this line demonstrated that CEL5 expression was exclusively expressed in the root cap. A request for this line CEL5::GUS has been made to Dr Patterson, who is currently in the process of germinating the old seed stock. By crossing the CEL5::GUS line to *sloughy*, CEL5 activity could be tracked during the development of *sloughy* roots. As an alternative to detecting CEL3 or CEL5, antibodies may be raised against arabidopsis root cap specific cellulases and tested by immunolabelling. This approach has previously been used to confirm a role for cellulases in leaf abscission in bean (Sexton *et al*., 1980). Labelling of whole roots could then determine where the cellulases are present in the roots of wild-type and *sloughy*

seedlings. In both instances, the model would predict the detection of ectopic cellulase activity in the separating epidermal cell of *sloughy*.

A similar approach will be taken with the pectin-related genes *QUA1* and *QUA2*. *qua1* or *qua2* mutants have not yet been sourced, although mutants are available for either gene from the ABRC or from the source laboratories (Bouton *et al*., 2002, Mouille *et al*., 2007). Both *qua1* or *qua2* will be crossed to *sloughy* to generate double mutants. As border-like cells in *qau1* and *qua2* detach as isolated, individual cells, it is predicted that the separating epidermal cells typically seen in *sloughy* will lose attachment at their cell ends and completely dissociate as isolated cells in either of the double mutants. There is, however, a strong possibility that such a phenotype might be seedling lethal since the seedlings may completely lack a dermal tissue system in the roots. Such a result, nonetheless, would still support the model.

5.4 The bigger picture

In addition to the research directions outlined in the preceding section, many questions remain unanswered in respect to the function of SCHIZORIZA. Several additional lines of investigation are proposed that would shed more light on the action of SCHIZORIZA on plant growth development.

5.4.1 Analysis of the *schizoriza* transcriptome

As an alternative to the gene expression analysis of target genes, a transcriptomic analysis of the roots of *sloughy* roots might be carried out (Mitsuda and Ohme-Takagi, 2009). By identifying differentially expressed transcripts in the roots of *sloughy* comparative to wild-type, not only could novel cell wall modifying genes implicated in the cell separation be identified, but a host of independent genes that are regulated by SCHIZORIZA would be identified, providing a transcriptional regulatory network of SCHIZORIZA.

5.4.2 Determining the link between *schizoriza* and auxin

The significant increase in the frequency of lateral roots observed in *sloughy* indicated that auxin levels may be altered the roots. Treating roots with auxin has long been known to trigger the formation of lateral roots (Torrey, 1950), and in the arabidopsis mutant *superroot* (*sur1*), which overproduces auxin, a significant increase in lateral roots is also observed (Boerjan *et al*., 1995). This hypothesis is corroborated by observations made by Dolan's group (Mylona *et al*., 2002). The displacement of cells expressing quiescent centre-specific markers suggested that the *schizoriza* mutant displayed a defect in the apical-basal axis of the plant, similar to seedlings that are exposed to auxin transport inhibitors (Sabatini *et al*., 1999).

Auxin response or auxin transport mutants also display defective organization in the root meristem, supporting the role for auxin in root patterning (Sabatini *et al*., 1999, Friml *et al*., 2002). However, the role that auxin may play in the defects seen in *schizoriza* mutants still remains to be tested. Several lines of investigation could be pursued to test for altered auxin levels or responses in *sloughy*/*schizoriza*. For example, the levels of auxin could be measured with gas chromatography-mass spectrometry (Liu *et al*., 2012), the transport of auxin tracked with radiolabelled auxin (Lewis and Muday, 2009), or the expression levels of auxin-related genes analyzed with RT-qPCR (Jones *et al*., 2010) or with a transcriptomic analysis (Paponov *et al*., 2008).

5.4.3 Identifying SCHIZORIZA-interacting proteins

Whereas SHR and SCR have been studied extensively, with the three interacting proteins JKD, MGP (Welch *et al*., 2007), and SHBY (Koizumi and Gallagher, 2013) identified and described in great detail, SCHIZORIZA-interacting proteins have not been reported. Identifying the proteins that interact with SCHIZORIZA is critical for understanding the regulatory role the protein may play on a cellular level. Indeed, protein-protein interactions were highlighted by Collette ten Hove in her PhD thesis (ten Hove, 2010) as an important line of research for SCHIZORIZA. The two most popular methodologies for identifying protein-protein interactions are yeast-two hybrid screening (Fields and Song, 1989) and tandem affinity purification (Rigaut *et al*., 1999). Using yeast two hybrid screening, ten Hove (ten Hove, 2010) determined that SCHIZORIZA does not interact with SHR (Helariutta *et al*., 2000), SCR (Di Laurenzio *et al*., 1996), PLT1 or PLT2 (Aida *et al*., 2004), despite the fact that SCHIZORIZA acts in parallel with SHR and SCR pathways for the development and maintenance of the root meristem. However, the yeast two hybrid screening did show a protein interaction between SCHIZORIZA and another heat shock transcription factor,

amongst others (ten Hove, 2010). This data has not yet been published. Other candidate targets for yeast two hybrid screening could include the transcription factors FEZ, SMB, BRN1 and BRN2 which have all been implicated in the development of the root cap (Willemsen *et al*., 2008, Bennett *et al*., 2010).

5.4.4 A role for SCHIZORIZA in above-ground tissue?

Despite the expression of *SCHIZORIZA* in above-ground organs (Begum *et al*., 2013), neither the disruption of SCHIZORIZA function, nor the over-expression of *SCHIZORIZA*, has a significant impact on the above-ground growth and development of the plant (ten Hove *et al*., 2010, Pernas *et al*., 2010, Begum *et al*., 2013). In addition to expression within the roots, expression of *SCHIZORIZA* has been detected in many above-ground organs of the plant, including the shoot apex, pistils, seeds, and the base of siliques (Begum *et al*., 2013). A gene expression map of arabidopsis development has also detected expression of *SCHIZORIZA* in the roots, stems, leaves, flowers, and seeds (Schmid *et al*., 2005). A proposed role for SCHIZORIZA in organs apart from the roots, however, has not been reported. The gene expression results suggest that SCHIZORIZA may be constitutively expressed throughout the plant, but only active under certain cellular conditions, for example specifically within the developing root meristem. The identification of SCHIZORIZA interacting genes or proteins may provide clues into such regulation of SCHIZORIZA action. A thorough phenotypic and molecular characterization of the above-ground organs in *sloughy*/*schizoriza* or *SCZ*-OE plants may also reveal subtle phenotypes not previously identified. Identifying novel phenotypes may allow additional roles for SCHIZORIZA on plant development to be inferred.

Although many significant challenges remain, the future research of *sloughy/schizoriza* mutants will not only further our knowledge on the development and maintenance of the root

meristem, but will also contribute to a greater understanding of cell adhesion and separation phenomena in plants.

References

Aida, M., Beis, D., Heidstra, R., Willemsen, V., Blilou, I., Galinha, C., Nussaume, L., Noh, Y.S., Amasino, R., and Scheres, B. (2004). The *PLETHORA* genes mediate patterning of the *Arabidopsis* root stem cell niche. Cell *119*, 109–120.

Albersheim, P., Darvill, A., Roberts, K., Sederoff, R., and Staehelin, A. (2010). Plant cell walls (Garland Science, New York).

Alonso, J.M., Stepanova, A.N., Leisse, T.J., Kim, C.J., Chen, H.M., Shinn, P., Stevenson, D.K., Zimmerman, J., Barajas, P., Cheuk, R., *et al*. (2003). Genome-wide insertional mutagenesis of *Arabidopsis thaliana*. Science *301*, 653–657.

Anthony, R.G., Reichelt, S., and Hussey, P.J. (1999). Dinitroaniline herbicide-resistant transgenic tobacco plants generated by co-overexpression of a mutant α-tubulin and a β-tubulin. Nat. Biotechnol. *17*, 712–716.

Arabidopsis Genome Initiative (2000). Analysis of the genome sequence of the flowering plant *Arabidopsis thaliana*. Nature *408*, 796–815.

Arioli, T., Peng, L.C., Betzner, A.S., Burn, J., Wittke, W., Herth, W., Camilleri, C., Höfte, H., Plazinski, J., Birch, R., *et al*. (1998). Molecular analysis of cellulose biosynthesis in *Arabidopsis*. Science *279*, 717–720.

Atmodjo, M.A., Sakuragi, Y., Zhu, X., Burrell, A.J., Mohanty, S.S., Atwood, J.A., Orlando, R., Scheller, H.V., and Mohnen, D. (2011). Galacturonosyltransferase (GAUT)1 and

GAUT7 are the core of a plant cell wall pectin biosynthetic homogalacturonan: galacturonosyltransferase complex. Proc. Natl. Acad. Sci. U. S. A. *108*, 20225–20230.

Bannigan, A., Wiedemeier, A.M.D., Williamson, R.E., Overall, R.L., and Baskin, T.I. (2006). Cortical microtubule arrays lose uniform alignment between cells and are oryzalin resistant in the *Arabidopsis* mutant, *radially swollen 6*. Plant Cell Physiol. *47*, 949–958.

Baskin, T.I., Betzner, A.S., Hoggart, R., Cork, A., and Williamson, R.E. (1992). Root morphology mutants in *Arabidopsis thaliana*. Aust. J. Plant Physiol. *19*, 427–437.

Baskin, T.I., and Bivens, N.J. (1995). Stimulation of radial expansion in *Arabidopsis* roots by inhibitors of actomyosin and vesicle secretion but not by various inhibitors of metabolism. Planta *197*, 514–521.

Baskin, T.I., Wilson, J.E., Cork, A., and Williamson, R.E. (1994). Morphology and microtubule organization in *Arabidopsis* roots exposed to oryzalin or taxol. Plant Cell Physiol. *35*, 935–942.

Becker, E. (1997). The Denial of Death (Free Press, New York).

Begum, T., Reuter, R., and Schöffl, F. (2013). Overexpression of AtHsfB4 induces specific effects on root development of *Arabidopsis*. Mech. Dev. *130*, 54–60.

Bell, C.J., and Ecker, J.R. (1994). Assignment of 30 microsatellite loci to the linkage map of *Arabidopsis*. Genomics *19*, 137–144.

Bennett, T., van den Toorn, A., Sanchez-Perez, G.F., Campilho, A., Willemsen, V., Snel, B., and Scheres, B. (2010). SOMBRERO, BEARSKIN1, and BEARSKIN2 regulate root cap maturation in *Arabidopsis*. Plant Cell *22*, 640–654.

Boerjan, W., Cervera, M.T., Delarue, M., Beeckman, T., Dewitte, W., Bellini, C., Caboche, M., Van Onckelen, H., Van Montagu, M., and Inzé, D. (1995). *superroot*, a recessive mutation in *Arabidopsis*, confers auxin overproduction. Plant Cell *7*, 1405–1419.

Bonin, C.P., Potter, I., Vanzin, G.F., and Reiter, W.-D. (1997). The *MUR1* gene of *Arabidopsis thaliana* encodes an isoform of GDP-d-mannose-4,6-dehydratase, catalyzing the first step in the de novo synthesis of GDP-l-fucose. Proc. Natl. Acad. Sci. U.S.A. *94*, 2085–2090.

Bosca, S., Barton, C.J., Taylor, N.G., Ryden, P., Neumetzler, L., Pauly, M., Roberts, K., and Seifert, G.J. (2006). Interactions between MUR10/CesA7-dependent secondary cellulose biosynthesis and primary cell wall structure. Plant Physiol. *142*, 1353–1363.

Bouton, S., Leboeuf, E., Mouille, G., Leydecker, M.T., Talbotec, J., Granier, F., Lahaye, M., Höfte, H., and Truong, H.N. (2002). *QUASIMODO1* encodes a putative membrane-bound glycosyltransferase required for normal pectin synthesis and cell adhesion in *Arabidopsis*. Plant Cell *14*, 2577–2590.

Bown, L., Kusaba, S., Goubet, F., Codrai, L., Dale, A.G., Zhang, Z., Yu, X., Morris, K., Ishii, T., Evered, C., *et al*. (2007). The *ectopically parting cells 1-2* (*epc1-2*) mutant exhibits an exaggerated response to abscisic acid. J. Exp. Bot. *58*, 1813–1823.

Brand, A., and Perrimon, N. (1993). Targeted gene-expression as a means of altering cell fates and generating dominant phenotypes. Development *118*, 401–415.

Bringmann, M., Li, E., Sampathkumar, A., Kocabek, T., Hauser, M.-T., and Persson, S. (2012). POM-POM2/CELLULOSE SYNTHASE INTERACTING1 is essential for the functional association of cellulose synthase and microtubules in *Arabidopsis*. Plant Cell *24*, 163–177.

Burget, E.G., and Reiter, W.-D. (1999). The *mur4* mutant of *Arabidopsis* is partially defective in the de novo synthesis of uridine diphospho 1-arabinose. Plant Physiol. *121*, 383–390.

Burn, J.E., Hurley, U.A., Birch, R.J., Arioli, T., Cork, A., and Williamson, R.E. (2002). The cellulose-deficient *Arabidopsis* mutant *rsw3* is defective in a gene encoding a putative

glucosidase II, an enzyme processing N-glycans during ER quality control. Plant J. Cell Mol. Biol. *32*, 949–960.

Busby, C.H., and Gunning, B.E.S. (1983). Orientation of microtubules against transverse cell walls in roots of *Azolla pinnata* R. Br. Protoplasma *116*, 78–85.

Bush, S.M., and Krysan, P.J. (2010). iTILLING: a personalized approach to the identification of induced mutations in *Arabidopsis*. Plant Physiol. *154*, 25–35.

Campbell, J.A., Davies, G.J., Bulone, V., and Henrissat, B. (1997). A classification of nucleotide-diphospho-sugar glycosyltransferases based on amino acid sequence similarities. Biochem. J. *326*, 929–939.

Carpita, N., and Gibeaut, D. (1993). Structural models of primary-cell walls in flowering plants: Consistency of molecular structure with the physical properties of the walls during growth. Plant J. *3*, 1–30.

Chang, C., Bowman, J.L., DeJohn, A.W., Lander, E.S., and Meyerowitz, E.M. (1988). Restriction fragment length polymorphism linkage map for *Arabidopsis thaliana*. Proc. Natl. Acad. Sci. U.S.A. *85*, 6856–6860.

Cheng, J.-C., Huang, C.-L., Lin, C.-C., Chen, C.-C., Chang, Y.-C., Chang, S.-S., and Tseng, C.-P. (2006). Rapid detection and identification of clinically important bacteria by high-resolution melting analysis after broad-range ribosomal RNA real-time PCR. Clin. Chem. *52*, 1997–2004.

Clark, R.M., Schweikert, G., Toomajian, C., Ossowski, S., Zeller, G., Shinn, P., Warthmann, N., Hu, T.T., Fu, G., Hinds, D.A., *et al.* (2007). Common sequence polymorphisms shaping genetic diversity in *Arabidopsis thaliana*. Science *317*, 338–342.

Clough, S.J., and Bent, A.F. (1998). Floral dip: a simplified method for *Agrobacterium*-mediated transformation of *Arabidopsis thaliana*. Plant J. *16*, 735–743.

Clowes, F.L. (1956). Nucleic acids in root apical meristems of *Zea*. New Phytol. *55*, 29–34.

Cnops, G., den Boer, B., Gerats, A., Van Montagu, M., and Van Lijsebettens, M. (1996). Chromosome landing at the *Arabidopsis TORNADO1* locus using an AFLP-based strategy. Mol. Gen. Genet. *253*, 32–41.

Cnops, G., Neyt, P., Raes, J., Petrarulo, M., Nelissen, H., Malenica, N., Luschnig, C., Tietz, O., Ditengou, F., Palme, K., *et al*. (2006). The *TORNADO1* and *TORNADO2* genes function in several patterning processes during early leaf development in *Arabidopsis thaliana*. Plant Cell *18*, 852–866.

Cnops, G., Wang, X., Linstead, P., Van Montagu, M., Van Lijsebettens, M., and Dolan, L. (2000). *TORNADO1* and *TORNADO*2 are required for the specification of radial and circumferential pattern in the *Arabidopsis* root. Development *127*, 3385–3394.

Cocuron, J.-C., Lerouxel, O., Drakakaki, G., Alonso, A.P., Liepman, A.H., Keegstra, K., Raikhel, N., and Wilkerson, C.G. (2007). A gene from the cellulose synthase-like C family encodes a β-1,4 glucan synthase. Proc. Natl. Acad. Sci. U. S. A. *104*, 8550–8555.

Collings, D.A., Gebbie, L.K., Howles, P.A., Hurley, U.A., Birch, R.J., Cork, A.H., Hocart, C.H., Arioli, T., and Williamson, R.E. (2008). *Arabidopsis* dynamin-like protein DRP1A: a null mutant with widespread defects in endocytosis, cellulose synthesis, cytokinesis, and cell expansion. J. Exp. Bot. *59*, 361–376.

Collings, D.A., Lill, A.W., Himmelspach, R., and Wasteneys, G.O. (2006). Hypersensitivity to cytoskeletal antagonists demonstrates microtubule-microfilament cross-talk in the control of root elongation in *Arabidopsis thaliana*. New Phytol. *170*, 275–290.

Collings, D.A., and Wasteneys, G.O. (2005). Actin microfilament and microtubule distribution patterns in the expanding root of *Arabidopsis thaliana*. Can. J. Bot. *83*, 579–590.

Cosgrove, D.J. (2005). Growth of the plant cell wall. Nat. Rev. Mol. Cell Biol. *6*, 850–861.

Coutinho, P.M., Deleury, E., Davies, G.J., and Henrissat, B. (2003). An evolving hierarchical family classification for glycosyltransferases. J. Mol. Biol. *328*, 307–317.

Croxford, A.E., Rogers, T., Caligari, P.D.S., and Wilkinson, M.J. (2008). High-resolution melt analysis to identify and map sequence-tagged site anchor points onto linkage maps: a white lupin (*Lupinus albus*) map as an exemplar. New Phytol. *180*, 594–607.

Darwin, C., and Darwin, F. (1881). The power of movement in plants (D. Appleton and Company, New York).

Dawkins, R. (1986). The Blind Watchmaker (W. W. Norton & Company, New York).

de Chalain, T.M.B., and Berjak, P. (1979). Cell death as a functional event in the development of the leaf intercellular spaces in *Avicennia marina* (Forsskål) Vierh. New Phytol. *83*, 147–155.

Del Campillo, E., Abdel-Aziz, A., Crawford, D., and Patterson, S.E. (2004). Root cap specific expression of an endo-β-1,4-D-glucanase (cellulase): a new marker to study root development in *Arabidopsis*. Plant Mol. Biol. *56*, 309–323.

Di Laurenzio, L., Wysocka-Diller, J., Malamy, J.E., Pysh, L., Helariutta, Y., Freshour, G., Hahn, M.G., Feldmann, K.A., and Benfey, P.N. (1996). The *SCARECROW* gene regulates an asymmetric cell division that is essential for generating the radial organization of the *Arabidopsis* root. Cell *86*, 423–433.

Doblin, M.S., Kurek, I., Jacob-Wilk, D., and Delmer, D.P. (2002). Cellulose biosynthesis in plants: from genes to rosettes. Plant Cell Physiol. *43*, 1407–1420.

Dolan, L., Janmaat, K., Willemsen, V., Linstead, P., Poethig, S., Roberts, K., and Scheres, B. (1993). Cellular organization of the *Arabidopsis thaliana* root. Development *119*, 71–84.

Dolan, L., Linstead, P., and Roberts, K. (1995). An AGP epitope distinguishes a central metaxylem initial from other vascular initials in the *Arabidopsis* root. Protoplasma *189*, 149–155.

Driouich, A., Durand, C., Cannesan, M.-A., Percoco, G., and Vicré-Gibouin, M. (2010). Border cells versus border-like cells: are they alike? J. Exp. Bot. *61*, 3827–3831.

Driouich, A., Durand, C., and Vicré-Gibouin, M. (2007). Formation and separation of root border cells. Trends Plant Sci. *12*, 14–19.

Durand, C., Vicré-Gibouin, M., Follet-Gueye, M.L., Duponchel, L., Moreau, M., Lerouge, P., and Driouich, A. (2009). The organization pattern of root border-like cells of *Arabidopsis* is dependent on cell wall homogalacturonan. Plant Physiol. *150*, 1411–1421.

Endler, A., and Persson, S. (2011). Cellulose synthases and synthesis in *Arabidopsis*. Mol. Plant *4*, 199–211.

Fields, S., and Song, O. (1989). A novel genetic system to detect protein-protein interactions. Nature *340*, 245–246.

Freshour, G., Clay, R.P., Fuller, M.S., Albersheim, P., Darvill, A.G., and Hahn, M.G. (1996). Developmental and tissue-specific structural alterations of the cell-wall polysaccharides of *Arabidopsis thaliana* roots. Plant Physiol. *110*, 1413–1429.

Friml, J., Benková, E., Blilou, I., Wisniewska, J., Hamann, T., Ljung, K., Woody, S., Sandberg, G., Scheres, B., Jürgens, G., *et al*. (2002). AtPIN4 mediates sink-driven auxin gradients and root patterning in *Arabidopsis*. Cell *108*, 661–673.

Furutani, I., Watanabe, Y., Prieto, R., Masukawa, M., Suzuki, K., Naoi, K., Thitamadee, S., Shikanai, T., and Hashimoto, T. (2000). The *SPIRAL* genes are required for directional control of cell elongation in *Arabidopsis thaliana*. Development *127*, 4443–4453.

Gady, A.L.F., Hermans, F.W.K., Van de Wal, M.H.B.J., van Loo, E.N., Visser, R.G.F., and Bachem, C.W.B. (2009). Implementation of two high through-put techniques in a novel application: detecting point mutations in large EMS mutated plant populations. Plant Methods *5: 13*.

Goff, S.A., Ricke, D., Lan, T.H., Presting, G., Wang, R.L., Dunn, M., Glazebrook, J., Sessions, A., Oeller, P., Varma, H., *et al*. (2002). A draft sequence of the rice genome (*Oryza sativa* L. ssp *japonica*). Science *296*, 92–100.

Graham, L.E., Cook, M.E., and Busse, J.S. (2000). The origin of plants: body plan changes contributing to a major evolutionary radiation. Proc. Natl. Acad. Sci. U.S.A. *97*, 4535–4540.

Green, P.B. (1962). Mechanism for plant cellular morphogenesis. Science *138*, 1404–1405.

Gu, Y., Kaplinsky, N., Bringmann, M., Cobb, A., Carroll, A., Sampathkumar, A., Baskin, T.I., Persson, S., and Somerville, C.R. (2010). Identification of a cellulose synthase-associated protein required for cellulose biosynthesis. Proc. Natl. Acad. Sci. U.S.A. *107*, 12866–12871.

Gundry, C.N., Vandersteen, J.G., Reed, G.H., Pryor, R.J., Chen, J., and Wittwer, C.T. (2003). Amplicon melting analysis with labelled primers: a closed-tube method for differentiating homozygotes and heterozygotes. Clin. Chem. *49*, 396–406.

Han, Y., Khu, D.-M., and Monteros, M.J. (2012). High-resolution melting analysis for SNP genotyping and mapping in tetraploid alfalfa (*Medicago sativa* L.). Mol. Breed. New Strateg. Plant Improv. *29*, 489–501.

Harholt, J., Jensen, J.K., Sorensen, S.O., Orfila, C., Pauly, M., and Scheller, H.V. (2006). ARABINAN DEFICIENT 1 is a putative arabinosyltransferase involved in biosynthesis of pectic arabinan in *Arabidopsis*. Plant Physiol. *140*, 49–58.

Harholt, J., Suttangkakul, A., and Scheller, H.V. (2010). Biosynthesis of pectin. Plant Physiol. *153*, 384–395.

Haseloff, J. (1999). GFP variants for multispectral imaging of living cells. Methods Cell Biol. *58*, 139–151.

Hauser, M.T., Morikami, A., and Benfey, P.N. (1995). Conditional root expansion mutants of *Arabidopsis*. Development *121*, 1237–1252.

Hawes, M., and Lin, H. (1990). Correlation of pectolytic enzyme activity with the programmed release of cells from root caps of pea (*Pisum sativum*). Plant Physiol. *94*, 1855–1859.

Hayashi, T. (1989). Xyloglucans in the primary cell wall. Annu. Rev. Plant Physiol. Plant Mol. Biol. *40*, 139–168.

Heid, C.A., Stevens, J., Livak, K.J., and Williams, P.M. (1996). Real time quantitative PCR. Genome Res. *6*, 986–994.

Helariutta, Y., Fukaki, H., Wysocka-Diller, J., Nakajima, K., Jung, J., Sena, G., Hauser, M.T., and Benfey, P.N. (2000). The *SHORT-ROOT* gene controls radial patterning of the *Arabidopsis* root through radial signaling. Cell *101*, 555–567.

Hertzberg, M., Aspeborg, H., Schrader, J., Andersson, A., Erlandsson, R., Blomqvist, K., Bhalerao, R., Uhlén, M., Teeri, T.T., Lundeberg, J., *et al*. (2001). A transcriptional roadmap to wood formation. Proc. Natl. Acad. Sci. U.S.A. *98*, 14732–14737.

Howles, P.A., Birch, R.J., Collings, D.A., Gebbie, L.K., Hurley, U.A., Hocart, C.H., Arioli, T., and Williamson, R.E. (2006). A mutation in an *Arabidopsis* ribose 5-phosphate isomerase reduces cellulose synthesis and is rescued by exogenous uridine. Plant J. *48*, 606–618.

Ikeda, M., and Ohme-Takagi, M. (2009). A novel group of transcriptional repressors in *Arabidopsis*. Plant Cell Physiol. *50*, 970–975.

Inoue, T., Higuchi, M., Hashimoto, Y., Seki, M., Kobayashi, M., Kato, T., Tabata, S., Shinozaki, K., and Kakimoto, T. (2001). Identification of CRE1 as a cytokinin receptor from *Arabidopsis*. Nature *409*, 1060–1063.

Jander, G., Norris, S.R., Rounsley, S.D., Bush, D.F., Levin, I.M., and Last, R.L. (2002). *Arabidopsis* map-based cloning in the post-genome era. Plant Physiol. *129*, 440–450.

Johnson, K.L., Jones, B.J., Bacic, A., and Schultz, C.J. (2003). The fasciclin-like arabinogalactan proteins of *Arabidopsis*. A multigene family of putative cell adhesion molecules. Plant Physiol. *133*, 1911–1925.

Jones, B., Gunnerås, S.A., Petersson, S.V., Tarkowski, P., Graham, N., May, S., Dolezal, K., Sandberg, G., and Ljung, K. (2010). Cytokinin regulation of auxin synthesis in *Arabidopsis* involves a homeostatic feedback loop regulated via auxin and cytokinin signal transduction. Plant Cell *22*, 2956–2969.

Kazama, Y., Hirano, T., Saito, H., Liu, Y., Ohbu, S., Hayashi, Y., and Abe, T. (2011). Characterization of highly efficient heavy-ion mutagenesis in *Arabidopsis thaliana*. BMC Plant Biol. *11*, 161.

Keegstra, K. (2010). Plant cell walls. Plant Physiol. *154*, 483–486.

Kimura, S., Laosinchai, W., Itoh, T., Cui, X., Linder, C.R., and Brown, R.M. (1999). Immunogold labeling of rosette terminal cellulose-synthesizing complexes in the vascular plant *Vigna angularis*. Plant Cell *11*, 2075–2085.

Kitazawa, K., Tryfona, T., Yoshimi, Y., Hayashi, Y., Kawauchi, S., Antonov, L., Tanaka, H., Takahashi, T., Kaneko, S., Dupree, P., *et al.* (2013). β-galactosyl Yariv reagent binds to the β-1,3-galactan of arabinogalactan proteins. Plant Physiol. *161*, 1117–1126.

Knauer, S., Holt, A.L., Rubio-Somoza, I., Tucker, E.J., Hinze, A., Pisch, M., Javelle, M., Timmermans, M.C., Tucker, M.R., and Laux, T. (2013). A protodermal miR394

signal defines a region of stem cell competence in the *Arabidopsis* shoot meristem. Dev. Cell *24*, 125–132.

Knox, J.P., Linstead, P.J., King, J., Cooper, C., and Roberts, K. (1990). Pectin esterification is spatially regulated both within cell walls and between developing tissues of root apices. Planta *181*, 512–521.

Knox, J.P., Linstead, P.J., Peart, J., Cooper, C., and Roberts, K. (1991). Developmentally regulated epitopes of cell-surface arabinogalactan proteins and their relation to root-tissue pattern-formation. Plant J. *1*, 317–326.

Koizumi, K., and Gallagher, K.L. (2013). Identification of SHRUBBY, a SHORT-ROOT and SCARECROW interacting protein that controls root growth and radial patterning. Development *140*, 1292–1300.

Konieczny, A., and Ausubel, F.M. (1993). A procedure for mapping *Arabidopsis* mutations using co-dominant ecotype-specific PCR-based markers. Plant J. *4*, 403–410.

Koornneef, M., and Meinke, D. (2010). The development of *Arabidopsis* as a model plant. Plant J. *61*, 909–921.

Kubo, H., Peeters, A.J., Aarts, M.G., Pereira, A., and Koornneef, M. (1999). *ANTHOCYANINLESS2*, a homeobox gene affecting anthocyanin distribution and root development in *Arabidopsis*. Plant Cell *11*, 1217–1226.

Lane, D.R., Wiedemeier, A., Peng, L., Höfte, H., Vernhettes, S., Desprez, T., Hocart, C.H., Birch, R.J., Baskin, T.I., Burn, J.E., *et al*. (2001). Temperature-sensitive alleles of *RSW2* link the KORRIGAN endo-1,4-β-glucanase to cellulose synthesis and cytokinesis in *Arabidopsis*. Plant Physiol. *126*, 278–288.

Leboeuf, E., Guillon, F., Thoiron, S., and Lahaye, M. (2005). Biochemical and immunohistochemical analysis of pectic polysaccharides in the cell walls of

Arabidopsis mutant *QUASIMODO 1* suspension-cultured cells: implications for cell adhesion. J. Exp. Bot. *56*, 3171–3182.

Lee, M.M., and Schiefelbein, J. (1999). WEREWOLF, a MYB-related protein in *Arabidopsis*, is a position-dependent regulator of epidermal cell patterning. Cell *99*, 473–483.

Lewis, D.R., and Muday, G.K. (2009). Measurement of auxin transport in *Arabidopsis thaliana*. Nat. Protoc. *4*, 437–451.

Li, S., Lei, L., Somerville, C.R., and Gu, Y. (2012). Cellulose synthase interactive protein 1 (CSI1) links microtubules and cellulose synthase complexes. Proc. Natl. Acad. Sci. U. S. A. *109*, 185–190.

Liepman, A.H., Wightman, R., Geshi, N., Turner, S.R., and Scheller, H.V. (2010). *Arabidopsis* - a powerful model system for plant cell wall research. Plant J. *61*, 1107–1121.

Liew, M., Pryor, R., Palais, R., Meadows, C., Erali, M., Lyon, E., and Wittwer, C. (2004). Genotyping of single-nucleotide polymorphisms by high-resolution melting of small amplicons. Clin. Chem. *50*, 1156–1164.

Lisec, J., Schauer, N., Kopka, J., Willmitzer, L., and Fernie, A.R. (2006). Gas chromatography mass spectrometry-based metabolite profiling in plants. Nat. Protoc. *1*, 387–396.

Liu, X., Hegeman, A.D., Gardner, G., and Cohen, J.D. (2012). Protocol: high-throughput and quantitative assays of auxin and auxin precursors from minute tissue samples. Plant Methods *8*, 31.

Livak, K.J., and Schmittgen, T.D. (2001). Analysis of relative gene expression data using real-time quantitative PCR and the 2(T)(-Delta Delta C) method. Methods *25*, 402–408.

Lu, P., Han, X., Qi, J., Yang, J., Wijeratne, A.J., Li, T., and Ma, H. (2012). Analysis of *Arabidopsis* genome-wide variations before and after meiosis and meiotic recombination by resequencing Landsberg *erecta* and all four products of a single meiosis. Genome Res. *22*, 508–518.

Lukowitz, W., Gillmor, C.S., and Scheible, W.R. (2000). Positional cloning in *Arabidopsis*. Why it feels good to have a genome initiative working for you. Plant Physiol. *123*, 795–805.

Madson, M., Dunand, C., Li, X.M., Verma, R., Vanzin, G.F., Calplan, J., Shoue, D.A., Carpita, N.C., and Reiter, W.D. (2003). The *MUR3* gene of *Arabidopsis* encodes a xyloglucan galactosyltransferase that is evolutionarily related to animal exostosins. Plant Cell *15*, 1662–1670.

Mahonen, A.P., Bonke, M., Kauppinen, L., Riikonen, M., Benfey, P.N., and Helariutta, Y. (2000). A novel two-component hybrid molecule regulates vascular morphogenesis of the *Arabidopsis* root. Genes Dev. *14*, 2938–2943.

McCallum, C.M., Comai, L., Greene, E.A., and Henikoff, S. (2000). Targeted screening for induced mutations. Nat. Biotechnol. *18*, 455–457.

McCann, M.C., Hammouri, M., Wilson, R., Belton, P., and Roberts, K. (1992). Fourier transform infrared microspectroscopy is a new way to look at plant cell walls. Plant Physiol. *100*, 1940–1947.

McCann, M.C., and Rose, J. (2010). Blueprints for building plant cell walls. Plant Physiol. *153*, 365–365.

McCartney, L., Marcus, S.E., and Knox, J.P. (2005). Monoclonal antibodies to plant cell wall xylans and arabinoxylans. J. Histochem. Cytochem. *53*, 543–546.

McManus, M.T., and Veit, B.E. (2002). Meristematic tissues in plant growth and development (Sheffield Academic Press, Shieffield).

McQueen-Mason, S., and Cosgrove, D. (1995). Expansin mode of action on cell walls. Analysis of wall hydrolysis, stress relaxation, and binding. Plant Physiol. *107*, 87–100.

Meikle, P.J., Hoogenraad, N.J., Bonig, I., Clarke, A.E., and Stone, B.A. (1994). A (1→3,1→4)-β-glucan-specific monoclonal antibody and its use in the quantitation and immunocytochemical location of (1→3,1→4)-β-glucans. Plant J. *5*, 1–9.

Mitsuda, N., and Ohme-Takagi, M. (2009). Functional analysis of transcription factors in *Arabidopsis*. Plant Cell Physiol. *50*, 1232–1248.

Miyashima, S., Hashimoto, T., and Nakajima, K. (2009). ARGONAUTE1 acts in *Arabidopsis* root radial pattern formation independently of the SHR/SCR pathway. Plant Cell Physiol. *50*, 626–634.

Mohnen, D. (2008). Pectin structure and biosynthesis. Curr. Opin. Plant Biol. *11*, 266–277.

Mouille, G., Ralet, M.-C., Cavelier, C., Eland, C., Effroy, D., Hematy, K., McCartney, L., Truong, H.N., Gaudon, V., Thibault, J.-F., *et al*. (2007). Homogalacturonan synthesis in *Arabidopsis thaliana* requires a Golgi-localized protein with a putative methyltransferase domain. Plant J. *50*, 605–614.

Mouille, G., Robin, S., Lecomte, M., Pagant, S., and Höfte, H. (2003). Classification and identification of *Arabidopsis* cell wall mutants using Fourier-Transform InfraRed (FT-IR) microspectroscopy. Plant J. *35*, 393–404.

Murashige, T., and Skoog, F. (1962). A revised medium for rapid growth and bio assays with tobacco tissue cultures. Physiol. Plant. *15*, 473–497.

Mylona, P., Linstead, P., Martienssen, R., and Dolan, L. (2002). *SCHIZORIZA* controls an asymmetric cell division and restricts epidermal identity in the *Arabidopsis* root. Development *129*, 4327–4334.

Nakashima, J., Laosinchai, W., Cui, X., and Brown, R.M. (2003). New insight into the mechanism of cellulose and callose biosynthesis: proteases may regulate callose biosynthesis upon wounding. Cellulose *10*, 369–389.

Naseer, S., Lee, Y., Lapierre, C., Franke, R., Nawrath, C., and Geldner, N. (2012). Casparian strip diffusion barrier in *Arabidopsis* is made of a lignin polymer without suberin. Proc. Natl. Acad. Sci. U. S. A. *109*, 10101–10106.

Neff, M.M., Neff, J.D., Chory, J., and Pepper, A.E. (1998). dCAPS, a simple technique for the genetic analysis of single nucleotide polymorphisms: experimental applications in *Arabidopsis thaliana* genetics. Plant J. *14*, 387–392.

Newton, I. (1959). The correspondence of Isaac Newton (Cambridge University Press, Cambridge).

Nguema-Ona, E., Vicré-Gibouin, M., Cannesan, M.-A., and Driouich, A. (2013). Arabinogalactan proteins in root-microbe interactions. Trends Plant Sci. *18*, 440–449.

Nicol, F., His, I., Jauneau, A., Vernhettes, S., Canut, H., and Höfte, H. (1998). A plasma membrane-bound putative endo-1,4-β-D-glucanase is required for normal wall assembly and cell elongation in *Arabidopsis*. EMBO J. *17*, 5563–5576.

Nover, L., Bharti, K., Doring, P., Mishra, S.K., Ganguli, A., and Scharf, K.D. (2001). *Arabidopsis* and the heat stress transcription factor world: how many heat stress transcription factors do we need? Cell Stress Chaperones *6*, 177–189.

Odell, J.T., Nagy, F., and Chua, N.-H. (1985). Identification of DNA sequences required for activity of the cauliflower mosaic virus 35S promoter. Nature *313*, 810–812.

Orfila, C., and Knox, J.P. (2000). Spatial regulation of pectic polysaccharides in relation to pit fields in cell walls of tomato fruit pericarp. Plant Physiol. *122*, 775–782.

Orfila, C., Sørensen, S.O., Harholt, J., Geshi, N., Crombie, H., Truong, H.-N., Reid, J.S.G., Knox, J.P., and Scheller, H.V. (2005). *QUASIMODO1* is expressed in vascular tissue

of *Arabidopsis thaliana* inflorescence stems, and affects homogalacturonan and xylan biosynthesis. Planta *222*, 613–622.

Page, D.R., and Grossniklaus, L. (2002). The art and design of genetic screens: *Arabidopsis thaliana*. Nat. Rev. Genet. *3*, 124–136.

Paponov, I.A., Paponov, M., Teale, W., Menges, M., Chakrabortee, S., Murray, J.A.H., and Palme, K. (2008). Comprehensive transcriptome analysis of auxin responses in *Arabidopsis*. Mol. Plant *1*, 321–337.

Paredez, A.R., Persson, S., Ehrhardt, D.W., and Somerville, C.R. (2008). Genetic evidence that cellulose synthase activity influences microtubule cortical array organization. Plant Physiol. *147*, 1723–1734.

Paredez, A.R., Somerville, C.R., and Ehrhardt, D.W. (2006). Visualization of cellulose synthase demonstrates functional association with microtubules. Science *312*, 1491–1495.

Pawley, J. (2010). Handbook of biological confocal microscopy (Springer Science & Business Media, New York).

Payen, A. (1838). Mémoire sur la composition du tissu propre des plantes et du ligneux. Comptes Rendus 7, 1052-1056.

Pear, J.R., Kawagoe, Y., Schreckengost, W.E., Delmer, D.P., and Stalker, D.M. (1996). Higher plants contain homologs of the bacterial *CelA* genes encoding the catalytic subunit of cellulose synthase. Proc. Natl. Acad. Sci. U. S. A. *93*, 12637–12642.

Peng, L., Hocart, C.H., Redmond, J.W., and Williamson, R.E. (2000). Fractionation of carbohydrates in *Arabidopsis* root cell walls shows that three radial swelling loci are specifically involved in cellulose production. Planta *211*, 406–414.

Peng, L., Kawagoe, Y., Hogan, P., and Delmer, D. (2002). Sitosterol-β-glucoside as primer for cellulose synthesis in plants. Science *295*, 147–150.

Peretto, R., Favaron, F., Bettini, V., Lorenzo, G.D., Marini, S., Alghisi, P., Cervone, F., and Bonfante, P. (1992). Expression and localization of polygalacturonase during the outgrowth of lateral roots in *Allium porrum* L. Planta *188*, 164–172.

Pernas, M., Ryan, E., and Dolan, L. (2010). *SCHIZORIZA* controls tissue system complexity in plants. Curr. Biol. *20*, 818–823.

Qu, L.-J., and Qin, G. (2014). Generation and identification of *Arabidopsis* EMS mutants. Methods Mol. Biol. *1062*, 225–239.

Radford, J.E., Vesk, M., and Overall, R.L. (1998). Callose deposition at plasmodesmata. Protoplasma *201*, 30–37.

Rédei, P. I. (1992). A heuristic glance at the past of *Arabidopsis* genetics. In Methods in Arabidopsis Research, World Scientific, pp. 1–15.

Reed, G.H., and Wittwer, C.T. (2004). Sensitivity and specificity of single-nucleotide polymorphism scanning by high-resolution melting analysis. Clin. Chem. *50*, 1748–1754.

Reiter, W., Chapple, C., and Somerville, C. (1993). Altered growth and cell walls in a fucose deficient mutant of *Arabidopsis*. Science *261*, 1032–1035.

Reiter, W.D., Chapple, C., and Somerville, C.R. (1997). Mutants of *Arabidopsis thaliana* with altered cell wall polysaccharide composition. Plant J. *12*, 335–345.

Rhee, S.Y., Beavis, W., Berardini, T.Z., Chen, G.H., Dixon, D., Doyle, A., Garcia-Hernandez, M., Huala, E., Lander, G., Montoya, M., *et al*. (2003). The Arabidopsis Information Resource (TAIR): a model organism database providing a centralized, curated gateway to *Arabidopsis* biology, research materials and community. Nucleic Acids Res. *31*, 224–228.

Rigaut, G., Shevchenko, A., Rutz, B., Wilm, M., Mann, M., and Séraphin, B. (1999). A generic protein purification method for protein complex characterization and proteome exploration. Nat. Biotechnol. *17*, 1030–1032.

Roberts, J.A., and Gonzalez-Carranza, Z. (2007). Plant cell separation and adhesion (Blackwell Publishing Ltd, New Jersey).

Rose, J.K.C. (2003). The plant cell wall (CRC Press, Florida).

Rounds, C.M., Lubeck, E., Hepler, P.K., and Winship, L.J. (2011). Propidium iodide competes with Ca^{2+} to label pectin in pollen tubes and *Arabidopsis* root hairs. Plant Physiol. *157*, 175–187.

Sabatini, S., Beis, D., Wolkenfelt, H., Murfett, J., Guilfoyle, T., Malamy, J., Benfey, P., Leyser, O., Bechtold, N., Weisbeek, P., *et al*. (1999). An auxin-dependent distal organizer of pattern and polarity in the *Arabidopsis* root. Cell *99*, 463–472.

Sabatini, S., Heidstra, R., Wildwater, M., and Scheres, B. (2003). *SCARECROW* is involved in positioning the stem cell niche in the *Arabidopsis* root meristem. Genes Dev. *17*, 354–358.

Sagan, C.S. (1985). Cosmos (Ballantine Books, New York).

Samson, F., Brunaud, V., Balzergue, S., Dubreucq, B., Lepiniec, L., Pelletier, G., Caboche, M., and Lecharny, A. (2002). FLAGdb/FST: a database of mapped flanking insertion sites (FSTs) of *Arabidopsis thaliana* T-DNA transformants. Nucleic Acids Res. *30*, 94–97.

Sato, S., Tabata, S., Hirakawa, H., Asamizu, E., Shirasawa, K., Isobe, S., Kaneko, T., Nakamura, Y., Shibata, D., Aoki, K., *et al*. (2012). The tomato genome sequence provides insights into fleshy fruit evolution. Nature *485*, 635–641.

Saxena, I.M., and Brown, R.M. (2005). Cellulose biosynthesis: current views and evolving concepts. Ann. Bot. *96*, 9–21.

Scheible, W.-R., and Pauly, M. (2004). Glycosyltransferases and cell wall biosynthesis: novel players and insights. Curr. Opin. Plant Biol. *7*, 285–295.

Scheller, H.V., and Ulvskov, P. (2010). Hemicelluloses. Annu. Rev. Plant Biol. *61*, 263–289.

Scheres, B., Dilaurenzio, L., Willemsen, V., Hauser, M., Janmaat, K., Weisbeek, P., and Benfey, P. (1995). Mutations affecting the radial organization of the *Arabidopsis* root display specific defects throughout the embryonic axis. Development *121*, 53–62.

Schmid, M., Davison, T.S., Henz, S.R., Pape, U.J., Demar, M., Vingron, M., Schölkopf, B., Weigel, D., and Lohmann, J.U. (2005). A gene expression map of *Arabidopsis thaliana* development. Nat. Genet. *37*, 501–506.

Schnable, P.S., Ware, D., Fulton, R.S., Stein, J.C., Wei, F., Pasternak, S., Liang, C., Zhang, J., Fulton, L., Graves, T.A., *et al*. (2009). The B73 maize genome: complexity, diversity, and dynamics. Science *326*, 1112–1115.

Sexton, R., Durbin, M.L., Lewis, L.N., and Thomson, W.W. (1980). Use of cellulase antibodies to study leaf abscission. Nature *283*, 873–874.

Showalter, A.M. (2001). Arabinogalactan-proteins: structure, expression and function. Cell. Mol. Life Sci. *58*, 1399–1417.

Singh, S.K., Eland, C., Harholt, J., Scheller, H.V., and Marchant, A. (2005). Cell adhesion in *Arabidopsis thaliana* is mediated by ECTOPICALLY PARTING CELLS 1 - a glycosyltransferase (GT64) related to the animal exostosins. Plant J. *43*, 384–397.

Sitrit, Y., Hadfield, K.A., Bennett, A.B., Bradford, K.J., and Downie, A.B. (1999). Expression of a polygalacturonase associated with tomato seed germination. Plant Physiol. *121*, 419–428.

Somerville, C. (2006). Cellulose synthesis in higher plants. Annu. Rev. Cell Dev. Biol. *22*, 53–78.

Stephenson, M., and Hawes, M. (1994). Correlation of pectin methylesterase activity in root caps of pea with root border cell separation. Plant Physiol. *106*, 739–745.

Sterling, J.D., Atmodjo, M.A., Inwood, S.E., Kumar Kolli, V.S., Quigley, H.F., Hahn, M.G., and Mohnen, D. (2006). Functional identification of an *Arabidopsis* pectin biosynthetic homogalacturonan galacturonosyltransferase. Proc. Natl. Acad. Sci. U. S. A. *103*, 5236–5241.

Sterling, J.D., Quigley, H.F., Orellana, A., and Mohnen, D. (2001). The catalytic site of the pectin biosynthetic enzyme α-1,4-galacturonosyltransferase is located in the lumen of the Golgi. Plant Physiol. *127*, 360–371.

Steudle, E., Zimmermann, U., and Lüttge, U. (1977). Effect of turgor pressure and cell size on the wall elasticity of plant cells. Plant Physiol. *59*, 285–289.

Stevens, R.A., and Martin, E.S. (1978). Structural and functional aspects of stomata. Planta *142*, 307–316.

Szyjanowicz, P.M.J., McKinnon, I., Taylor, N.G., Gardiner, J., Jarvis, M.C., and Turner, S.R. (2004). The *irregular xylem 2* mutant is an allele of *korrigan* that affects the secondary cell wall of *Arabidopsis thaliana*. Plant J. *37*, 730–740.

Taiz, L., and Zeiger, E. (2002). Plant physiology (Sinauer Associates, Sunderland).

Takahashi, J., Rudsander, U.J., Hedenström, M., Banasiak, A., Harholt, J., Amelot, N., Immerzeel, P., Ryden, P., Endo, S., Ibatullin, F.M., *et al*. (2009). *KORRIGAN1* and its aspen homolog *PttCel9A1* decrease cellulose crystallinity in *Arabidopsis* stems. Plant Cell Physiol. *50*, 1099–1115.

Tamura, K., Peterson, D., Peterson, N., Stecher, G., Nei, M., and Kumar, S. (2011). MEGA5: molecular evolutionary genetics analysis using maximum likelihood, evolutionary distance, and maximum parsimony methods. Mol. Biol. Evol. *28*, 2731–2739.

Taylor, N.G., Scheible, W.R., Cutler, S., Somerville, C.R., and Turner, S.R. (1999). The *irregular xylem 3* locus of *Arabidopsis* encodes a cellulose synthase required for secondary cell wall synthesis. Plant Cell *11*, 769–780.

ten Hove, C.A. (2010). Regulation of cell fate and meristem maintenance in *Arabidopsis* root development. PhD thesis; University of Utrecht, Utrecht.

ten Hove, C.A., Willemsen, V., de Vries, W.J., van Dijken, A., Scheres, B., and Heidstra, R. (2010). *SCHIZORIZA* encodes a nuclear factor regulating asymmetry of stem cell divisions in the *Arabidopsis* root. Curr. Biol. *20*, 452–457.

Thibault, J., Renard, C., Axelos, M., Roger, P., and Crepeau, M. (1993). Studies of the length of homogalacturonic regions in pectins by acid-hydrolysis. Carbohydr. Res. *238*, 271–286.

Torrey, J. (1950). The induction of lateral roots by indoleacetic acid and root decapitation. Am. J. Bot. *37*, 257–264.

Towler, W.I., James, M.M., Ray, S.C., Wang, L., Donnell, D., Mwatha, A., Guay, L., Nakabiito, C., Musoke, P., Jackson, J.B., *et al.* (2010). Analysis of HIV diversity using a high-resolution melting assay. Aids Res. Hum. Retroviruses *26*, 913–918.

Truernit, E., and Haseloff, J. (2008). A simple way to identify non-viable cells within living plant tissue using confocal microscopy. Plant Methods *4*, 15.

Tuskan, G.A., DiFazio, S., Jansson, S., Bohlmann, J., Grigoriev, I., Hellsten, U., Putnam, N., Ralph, S., Rombauts, S., Salamov, A., *et al.* (2006). The genome of black cottonwood, *Populus trichocarpa* (Torr. & Gray). Science *313*, 1596–1604.

van den Berg, C., Willemsen, V., Hendriks, G., Weisbeek, P., and Scheres, B. (1997). Short-range control of cell differentiation in the *Arabidopsis* root meristem. Nature *390*, 287–289.

Vanzin, G.F., Madson, M., Carpita, N.C., Raikhel, N.V., Keegstra, K., and Reiter, W.D. (2002). The *mur2* mutant of *Arabidopsis thaliana* lacks fucosylated xyloglucan because of a lesion in fucosyltransferase AtFUT1. Proc. Natl. Acad. Sci. U. S. A. *99*, 3340–3345.

Vaughn, K.C., Marks, M.D., and Weeks, D.P. (1987). A dinitroaniline-resistant mutant of *Eleusine indica* exhibits cross-resistance and supersensitivity to antimicrotubule herbicides and drugs. Plant Physiol. *83*, 956–964.

Venter, J.C., Adams, M.D., Myers, E.W., Li, P.W., Mural, R.J., Sutton, G.G., Smith, H.O., Yandell, M., Evans, C.A., Holt, R.A., *et al.* (2001). The sequence of the human genome. Science *291*, 1304–51.

Verhertbruggen, Y., Marcus, S.E., Haeger, A., Ordaz-Ortiz, J.J., and Knox, J.P. (2009). An extended set of monoclonal antibodies to pectic homogalacturonan. Carbohydr. Res. *344*, 1858–1862.

Vicré, M., Santaella, C., Blanchet, S., Gateau, A., and Driouich, A. (2005). Root border-like cells of *Arabidopsis*. Microscopical characterization and role in the interaction with Rhizobacteria. Plant Physiol. *138*, 998–1008.

Vorwerk, S., Somerville, S., and Somerville, C. (2004). The role of plant cell wall polysaccharide composition in disease resistance. Trends Plant Sci. *9*, 203–209.

Welch, D., Hassan, H., Blilou, I., Immink, R., Heidstra, R., and Scheres, B. (2007). *Arabidopsis* JACKDAW and MAGPIE zinc finger proteins delimit asymmetric cell division and stabilize tissue boundaries by restricting SHORT-ROOT action. Genes Dev. *21*, 2196–2204.

Wen, F., Celoy, R., Price, I., Ebolo, J.J., and Hawes, M.C. (2008). Identification and characterization of a rhizosphere β-galactosidase from *Pisum sativum* L. Plant Soil *304*, 133–144.

Wen, F.S., Zhu, Y.M., and Hawes, M.C. (1999). Effect of pectin methylesterase gene expression on pea root development. Plant Cell *11*, 1129–1140.

Whittington, A.T., Vugrek, O., Wei, K.J., Hasenbein, N.G., Sugimoto, K., Rashbrooke, M.C., and Wasteneys, G.O. (2001). *MOR1* is essential for organizing cortical microtubules in plants. Nature *411*, 610–613.

Willats, W.G.T., Gilmartin, P.M., Mikkelsen, J.D., and Knox, J.P. (1999). Cell wall antibodies without immunization: generation and use of de-esterified homogalacturonan block-specific antibodies from a naive phage display library. Plant J. *18*, 57–65.

Willats, W.G.T., McCartney, L., Steele-King, C.G., Marcus, S.E., Mort, A., Huisman, M., Alebeek, G.-J. van, Schols, H.A., Voragen, A.G.J., Goff, A.L., *et al*. (2004). A xylogalacturonan epitope is specifically associated with plant cell detachment. Planta *218*, 673–681.

Willemsen, V., Bauch, M., Bennett, T., Campilho, A., Wolkenfelt, H., Xu, J., Haseloff, J., and Scheres, B. (2008). The NAC domain transcription factors FEZ and SOMBRERO control the orientation of cell division plane in *Arabidopsis* root stem cells. Dev. Cell *15*, 913–922.

Williamson, R.E., Burn, J.E., Birch, R., Baskin, T.I., Arioli, T., Betzner, A.S., and Cork, A. (2001). Morphology of *rsw1*, a cellulose-deficient mutant of *Arabidopsis thaliana*. Protoplasma *215*, 116–127.

Wilson, J.B. (1988). A review of evidence on the control of shoot: root ratio, in relation to models. Ann. Bot. *61*, 433–449.

Wittwer, C.T., Herrmann, M.G., Moss, A.A., and Rasmussen, R.P. (1997). Continuous fluorescence monitoring of rapid cycle DNA amplification. Biotechniques *22*, 130–131, 134–138.

Xu, X., Pan, S., Cheng, S., Zhang, B., Mu, D., Ni, P., Zhang, G., Yang, S., Li, R., Wang, J., *et al*. (2011). Genome sequence and analysis of the tuber crop potato. Nature *475*, 189–194.

Zablackis, E., Huang, J., Muller, B., Darvill, A.G., and Albersheim, P. (1995). Characterization of the cell-wall polysaccharides of *Arabidopsis thaliana* leaves. Plant Physiol. *107*, 1129–1138.

Zimin, A., Stevens, K.A., Crepeau, M.W., Holtz-Morris, A., Koriabine, M., Marçais, G., Puiu, D., Roberts, M., Wegrzyn, J.L., de Jong, P.J., *et al*. (2014). Sequencing and assembly of the 22-Gb loblolly pine genome. Genetics *196*, 875–890.

Appendix

A1 Primers

Table A1.1 Primers used to clone the four genomic controls to guarantee that the correct region of chromosome I was being mapped.

SNP Code	Location (bp)	Forward Primer (5' - 3')	Reverse Primer (5' - 3')	Fragment (bp)
PERL0133085	16,231,163	TTC TCC GAA TCC AAC CCA AAC	CTG GAA TCC TTA TCT TAG TTG TC	958
SGCSNP10403	17,029,922	GCA AAC TCA AAG AGC AGC CTT	AGA ATC CAA CCA CCA ACT CCG	602
PERL0148220	17,497,019	AGT TGT TTG GCT TTG GCT TGC	TCT CGG CGT CCT ATT TGC G	769
SGCSNP10406	17,823,908	CCG ACC CGA ATA CCC ACA T	CTA CGC TTG ACT TTG TGT CGT	1097

Table A1.2 Primers used to clone, amplify and sequence the five candidate genes identified in the fine mapping region.

Gene	Forward Primer (5' - 3')	Reverse Primer (5' - 3')	Fragment (bp)
SCHIZORIZA (Macrogen Inc)	CTA GTT GCC CGA GGA AAG CAG AG	GAA GAA GAC GTG AAT GCA TTA AAT AAC TGG ATC	3947
SCHIZORIZA (University of Canterbury)	TGA TAC CAC AAC AAC ACT CTC C	GTT TGG TCT GAG AAA TGA TGT G	597
unknown protein	TAA TGC TCT AAC CGA ACG	CGA GTA GTG AAG ATG CCC	951
AGAMOUS-like 97	GGT GTT ATG GTT GGA GAT G	ATT AGA ACG AGA GTG AGT CC	1,152
WUSCHEL-related homeobox 4	ACA TTC CTA CAT ACC AAC G	GTT GAT ACA TTA CTA TGC CG	1,857
copia-like retrotransposon family	CAC GAG ATT GTA TTG GAC TTC	GCA CCA AAC ACA TAG AAT CC	613

Table A1.3 Primers used for absolute quantification of the *SCHIZORIZA* transcript.

Description	Forward Primer (5' - 3')	Reverse Primer (5' - 3')	Fragment (bp)
Standard curve and plasmid control	CAG AAA GAT TGT ACC AGA TCG ATG	TCT TAG AAG AAG GCA ACG AAA CTC	665
RT-qPCR	TTA CGA CGA AGC AAC ACA GTG	TGA AGT TGG TGG AGA TGA GTT C	204

Table A1.4. Primers used to sequence the *SCHIOZRIZA* gene and for HRM analysis of the mutations present in *sloughy* and *schizoriza* TILLING mutants.

Description	Forward Primer (5' to 3')	Reverse Primer (5' to 3')	Fragment (bp)
Sequencing *SCHIZORIZA*	CA CTC ACT ACT CAG TAC TAG ACT ACC	GAC ATT CTC ATC TTC TCT GGA CAA CAA G	1604
HRM analysis: CS93216 and CS88021	CGA TGG GAG TTC GCG AA	GGT GTG ACA TGA ACG GAG AGT	118
HRM analysis: *sloughy*, CS93157 and CS93587	TCA CCA CCG TCA AGA CCA C	TGC TTC GTC GTA ATC TCT CG	97
HRM analysis: CS88971	GTC GGA ACT AGC TCA CAT GAA GA	GCA TTG ACA GTG GCA GTA TTG T	174
HRM analysis: CS93177	GAA CTC ATC TCC ACC AAC TTC AC	TAG AAG AAG GCA ACG AAA CTC C	122

Table A1.5 Primers for gene expression analysis of *CEL3*, *CEL5* and *QUA1* and for plasmid preparation for absolute quantification of copy number.

Description	Forward Primer (5' to 3')	Reverse Primer (5' to 3')	Fragment (bp)
Target genes			
CEL3-qPCR	TTT GAT TCG GAC CTC CTA CG	TCG TTC TCA ATC GTT AGG CTG	104 bp
CEL3-plasmid	GGG TCC TTT AGT ATT GGG T	GTA ACC TCC ATA ACA TTC TTG C	602 bp
CEL5-qPCR	ATG TAG CCG CTG AAA CCG	CGC CTC GGT ATT GAA TGG	132 bp
CEL5-plasmid	AAG AAG ATG GGA CCC GAG	GCG TAT TTA TTG TCC CAA CTG	611 bp
QUA1-qPCR	TGA TGA AGG GAA AGA TAG ACC G	TTC ACA ACC ACC GAA GCC	99 bp
QUA1-plasmid	AGG CTG ATG GAA GAG AGG	CTC CAT TCA CTT TCC CAT C	565 bp
Reference genes			
ACT2 -qPCR	TCC TTT GTT GCT GTT GAC TAC G	CA ATC GTG ATG ACT TGC CC	103 bp
ACT2 -plasmid	CAG GTA TTG TGC TGG ATT CTG	GGA AGC AAG AAT GGA ACC AC	599 bp
ACT7 -qPCR	AGG AGA AAC TTG CTT ATG TCG C	GCT CCG ATG GTT ATG ACT TGT C	118 bp
ACT7 -plasmid	TTT CTC TCT ATG CCA GTG GTC	CTT TGC TCA TAC GGT CAG C	664 bp
ACT8 -qPCR	GCA GAC CGT ATG AGC AAA GA	GAA CCA CCA ATC CAG ACA CTG	104 bp
ACT8 -plasmid	GCT TTC CTT TGT CGC TGT C	TCT GTG GAC AAT GCC TGG	579 bp

A.2 Gene and protein sequences

aaacaaacacaaatctcttctcttttctctctctctgtctctctctttctcgaactctcta
ATGGCGATGATGGTCGAGAATAGCTACGGTGGTTACGGTGGTGGCGGCGGAGAGAGGATACA
ACTTATGGTCGAAGGTCAAGGCAAAGCTGTTCCGGCTCCGTTTTTGACAAAGACTTATCAAC
TTGTTGATGATCCTGCGACGGATCATGTCGTTTCTTGGGGTGATGATGATACTACTTTTGTC
GTTTGGCGTCCACCGGAGTTTGCTCGTGATCTTCTTCCTAATTACTTTAAACATAACAACTT
CTCTAGCTTCGTTCGTCAGCTCAATACTTATgtatgtagaataaagctctctcctttctctc
taaagttacgattttattaccaaaacgatttgggtatttgagattttggtctgttatacgt
ttttgtgattacccatctcttaaagttccaatctttataccaaaaacagaagaaaaaatgt
gttcttgagatttgggggttttgagtttttgtcttcttctacaagaaatctgatgttatga
tctttgattttgttagGGTTTCAGAAAGATTGTACCAGATCGATGGGAGTTCGCGAACGAGT
TTTTCAAGAGAGGAGAGAAACATTTACTCTGCGAAATCCACCGCCGTAAAACATCTCAAATG
ATACCACAACAACACTCTCCGTTCATGTCACACCACCACGCTCCGCCGCAGATTCCATTCTC
CGGCGGTTCTTTCTTCCCATTACCACCACCACGTGTCACCACTCCAGAAGAAGACCATTACT
GGTGCGACGACTCACCACCGTCAAGACCACGAGTCATACCACAATAAATTGACACGGCGGCG
CAAGTAACGGCATTGAGTGAAGACAACGAGAGATTACGACGAAGCAACACAGTGTTAATGTC
GGAACTAGCTCACATGAAGAAACTCTACAACGACATTATCTACTTTGTTCAAAACCATGTCA
AGCCTGTTGCTCCAAGTAACAACTCTAGTTATCTCTCTTCATTTCTCCAGAAGCAACAACAA
CAACAACCTCCAACACTTGATTATTACAATACTGCCACTGTCAATGCCACTAATCTCAATGC
TTTGAACTCATCTCCACCAACTTCACAAAGCTCTATTACAGTTCTTGAAGATGATCACACTA
ATCATCATGATCAGAGTAATATGAGAAAGACAAAGCTTTTTGGAGTTTCGTTGCCTTCTTCT
AAGAAGAGATCACATCATTTCTCAGACCAAACAAGCAAAACGAGACTTGTGTTGGATCAGTC
TGATCTTGCTTTGAATCTCATGACTGCTTCTACACGTTAAgagagtgtctttgttttatttt
tgataagtatctatcagcattattagcactaatgttgttatgatgaagatgaatattctggt
taaatctttactt

Figure A2.1 Nucleotide sequence of the *SCHIZORIZA* gene in *sloughy***.** Translational start/stop (highlighted blue), untranslated regions (red), exon (orange), intron (purple) & the C to T mutation detected in *sloughy* (highlighted green).

MAMMVENSYGGYGGGGGERIQLMVEGQGKAVPAPFLTKTYQLVDDPATDHVVSWGDDDTTFV
VWRPPEFARDLLPNYFKHNNFSSFVRQLNTYGFRKIVPDRWEFANEFFKRGEKHLLCEIHRR
KTSQMIPQQHSPFMSHHHAPPQIPFSGGSFFPLPPPRVTTPEEDHYWCDDSPPSRPRVIPQ*
IDTAAQVTALSEDNERLRRSNTVLMSELAHMKKLYNDIIYFVQNHVKPVAPSNNSSYLSSFL
QKQQQQQPPTLDYYNTATVNATNLNALNSSPPTSQSSITVLEDDHTNHHDQSNMRKTKLFGV
SLPSSKKRSHHFSDQTSKTRLVLDQSDLALNLMTASTR*

Figure A2.2 Translated protein sequence of SCHIZORIZA in *sloughy*. Translated protein sequence in *sloughy* only (light grey shaded) & the gluatmine (Q) to stop codon (*) amino acid change in *sloughy* (highlighted green).